Customized ammonia tolerant methanogenic inocula to alleviate ammonia toxicity in anaerobic digesters

Yan, Miao

Publication date:
2020

Document Version
Publisher's PDF, also known as Version of record

DTU Miljø

Customized ammonia tolerant methanogenic inocula to alleviate ammonia toxicity in anaerobic digesters

Miao Yan

PhD Thesis

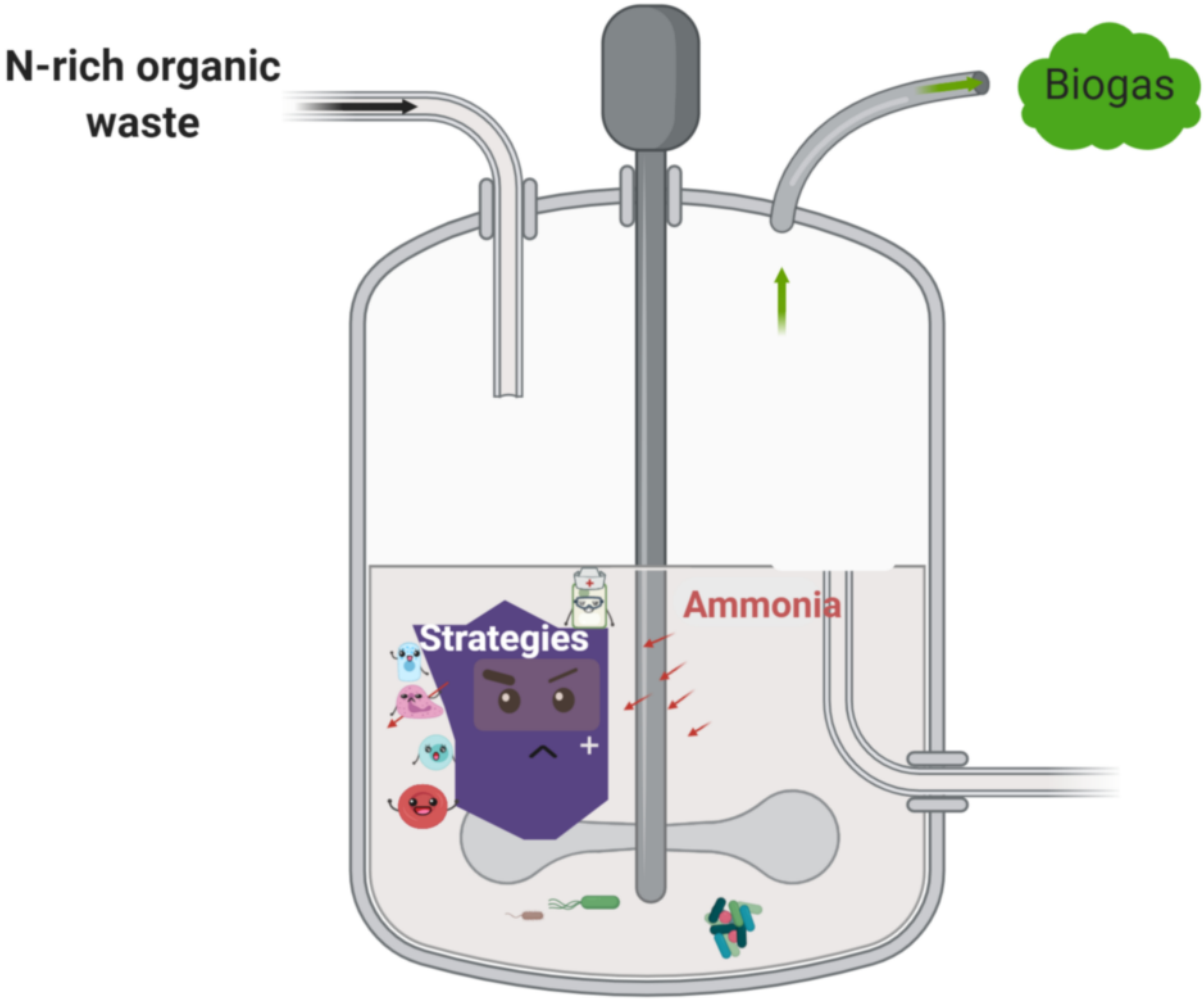

Customized ammonia tolerant methanogenic inocula to alleviate ammonia toxicity in anaerobic digesters

Miao Yan

PhD Thesis
October 2020

DTU Environment
Department of Environmental Engineering
Technical University of Denmark

Customized ammonia tolerant methanogenic inocula to alleviate ammonia toxicity in anaerobic digesters

Miao Yan

PhD Thesis, October 2020

Address: DTU Environment
Department of Environmental Engineering
Technical University of Denmark
Bygningstorvet, Building 115
2800 Kgs. Lyngby
Denmark

Phone reception: +45 4525 1600
Fax: +45 4593 2850

Homepage: http://www.env.dtu.dk
E-mail: reception@env.dtu.dk

Cover: STEP

Preface

This Ph.D. thesis, entitled “Customized ammonia tolerant methanogenic inocula to alleviate ammonia toxicity in anaerobic digesters” presents the research performed at the Department of Environmental Engineering, the Technical University of Denmark from November 1st, 2017 to October 31st, 2020. The research was co-funded by the China Scholarship Council and the Technical University of Denmark. Professor Irini Angelidaki was the main supervisor and Associate Professor Ioannis Fotidis was the co-supervisor.

The thesis is organized into two parts: the first part puts into context the findings of the Ph.D. in an introductive review; the second part consists of the papers listed below. These will be referred to in the text by their paper number written with the Roman numerals **I-VI**.

I **Yan, M**., Fotidis, I. A., Tian, H., Khoshnevisan, B., Treu, L., Tsapekos, P., & Angelidaki, I. (2019). Acclimatization contributes to stable anaerobic digestion of organic fraction of municipal solid waste under extreme ammonia levels: focusing on microbial community dynamics. Bioresource Technology, 286, 121376.

II **Yan, M**., Treu, L., Zhu, X., Tian, H., Basile, A, Fotidis, I. A., Campanaro S., Angelidakia I., (2020). Insights into ammonia adaptation and methanogenic precursor oxidation by genome-guided analysis. Environmental Science & Technology. 2020.

III **Yan, M**., Treu, L., Campanaro, S., Tian, H., Zhu, X., Khoshnevisan, B., Tsapekosa, P., Angelidakia, I., Fotidis, I. A., (2020) Effect of ammonia on anaerobic digestion of municipal solid waste: inhibitory performance, bioaugmentation and microbiome functional reconstruction. Chemical Engineering Journal, 126159.

IV **Yan, M**., Fotidis, I. A., Jéglot, A., Treu, L., Tian, H., Palomo, A., Angelidaki, I. (2020). Long-term preserved and rapidly revived methanogenic cultures: Microbial dynamics and preservation mechanisms. Journal of Cleaner Production, 121577.

In this online version of the thesis, paper **I-IV** are not included but can be obtained from electronic article databases, e.g. via www.orbit.dtu.dk or on request from DTU Environment, Technical University of Denmark, Miljoevej, Building 113, 2800 Kgs. Lyngby, Denmark, info@env.dtu.dk.

Besides, the following publications, not included in this thesis, were also concluded during this Ph.D. study:

V **Yan, M**., Zhu, X., Treu, L., Ravenni. G., Ferrigno. R., Goonesekera, M., Angelidaki, I., Fotidis, I.A. (2020) Assessment of multiple strategies to alleviate ammonia inhibition (Manuscript under preparation for submission)

VI Tian, H., **Yan, M**., Treu, L., Angelidaki, I. and Fotidis, I.A. (2019) Hydrogenotrophic methanogens are the key for a successful bioaugmentation to alleviate ammonia inhibition in thermophilic anaerobic digesters. Bioresource Technology 293, 122070.

Acknowledgements

I would like to thanks my supervisor Professor Irini Angelidaki, who has a profound knowledge of anaerobic digestion. You are always energetic and smiley, which inspires me a lot both in life and science. I appreciate my co-supervisor, Associate Professor Ioannis Fotidis. You encourage me to express my opinion on science and allow me to "fight with" you. In this case, if I finally convinced you, you were happier than me. Both you gave me the freedom to design and perform the experiments I wanted, which encouraged me to become scientifically independent. Meanwhile, thanks to the financial support from China Scholarship Council and "MicrobialStopNH_3" project supported by Energinet.dk.

My sincere appreciation goes to Associate professor Stefano Campanaro and Dr. Laura Treu. They gave me a lot of guidance for microbial analysis and paper writing. The precise and responsible attitude for science from you two will company with me for the rest of life. Besides, special thanks for your sweet care when I was at the University of Padua.

I am thankful that Thomas Fruergaard Astrup, Anne Harsting, Christina Pannach, and Kim are very helpful and supportive.

Thanks Dr. Xinyu Zhu for teaching me microbial analysis during these three years. Most importantly, we have great times together for delicious food, skiing, guitar learning, and skateboard.

Special thanks go to Dr. Hailin Tian. Your strict requirement and patience improved me a lot when I cooperated with you. Your encouragement meant a lot to me when I was frustrated.

Thanks all the master students who worked with me: Arnaud Jeglot, Dongdong Xie, Rosa Ferrigno, and Estelle Maria Goonesekera. Because of you, my research life was more joyful and productive.

Grateful thanks are due to the following people (Hector, Sin, Benyamin, Panagiotis, Yifeng, Hao, Zengshuai, Chunxing, Rusen, Xiaoyong, Alex, Ding etc.) for assisting my lab work.

I would like to thank my friends for all their support and company in Denmark: Alex, Carlos, Chuchu, Chunxing, Charlotte, Concetta, Cunsheng, Dan, Guan, Huihui, Junhao, Juan, Kai, Konstantinos, Minmin, Mingyi, Muyao, Na, Nanan, Paola, Qingxian, Rusen, Shanfei, Song, Xiaoyong, Yanyan + Qunbao, Xueer,

Yufeng, Yi, Yifeng, Yi Xin, Zengshuai, Zhenhan, and Zhibo. Thanks Enrico and Serena for your sincere care and friendship. I would never know how many surprises you gave to me, I'm touched beyond words”.

Thanks my officemate, Adam, Maria, and Na for creating a friendly working environment, your kindness and positive outlook on life will always light me.

Lastly, I would like to thank my family, you are always my motivation to be a better person.

Summary

Anaerobic digestion (AD) is a globally popular waste management technology where the organic matters are degraded into biogas (mainly CH_4 and CO_2) and digestate under oxygen-free conditions. To date, biogas has been widely promoted according to its following uses in electricity, other value-added products, transport, and heating. United Nations aims to achieve a greater share of the biogas in renewable energy for Sustainable Development Goals. The organic waste from industries and households are suitable feedstocks for biogas production, which is exactly following the important concept of "waste to energy". Despite the various benefits and great potential of AD, further development of AD is delayed by several difficulties, one of which is the sole degradation of N-rich substrates. The ammonia released from them (exceed 1.5 g NH_4^+-N/L) is an inhibitor to microorganisms in the AD, especially methanogens, which leads to less methane yield. Thus, approaches to recover methane production from ammonia inhibition are required. Furthermore, a balanced microbial composition is of utmost importance for the stable AD system process. Thus a deep insight into the microbial community provides the essential knowledge for process optimization. The continuous development of sequencing technology and bioinformatics methods is making it feasible to expand our understanding of complex microbial community composition and characteristics.

This Ph.D. project aimed to 1) develop methods to recover methane production from organic waste at high ammonia stress and 2) explore microbial synergistic networks and other functionalities determining stress resistance.

Firstly, to achieve an effective continuous anaerobic degradation of N-rich substrates, the stepwise acclimatization process was performed in mesophilic reactors fed with organic fraction of municipal solid waste (OFMSW). The results showed the acclimatization could increase the continuous stirring tank reactors (CSTRs) robustness up to 8.5 g NH_4^+-N/L and the methane yields fluctuated less than 10%. Meanwhile, the shift of dominant methanogens was observed from *Methanosaeta concilii* at low ammonia levels (1.1-5 g NH_4^+-N/L) to *Methanosarcina soligelidi* at high ammonia levels (6-9.5 g NH_4^+-N/L), respectively.

Secondly, to investigate the microbial synergistic networks and other functionalities that regulate ammonia tolerance, the initial microbial inoculum were cultivated into four groups (i.e., $G_{methanol}$, $G_{H2/CO2}$, $G_{formate}$ and $G_{acetate}$)

under increased ammonia levels in batch reactors. Synthetic basal anaerobic (BA) medium containing a single carbon source (either methanol, or H_2/CO_2, or formate, or acetate) was used as feedstock. After several generations' cultivation, the microbial consortia in $G_{methanol}$ and $G_{H2/CO2}$ were robust up to 7.25 g NH_4^+-N/L, followed by $G_{formate}$ (5.25 g NH_4^+-N/L) and $G_{acetate}$ (4.25 g NH_4^+-N/L), respectively. The metabolic pathways of dominant microbes were reconstructed based on the genomics analysis coupling with intermediates measurement during the degradation process, thereby a possible mechanism of ammonia tolerance was proposed. Briefly, the existence of genes responsible for osmotic regulators (K^+, N^{ε}-acetyl-L-lysine, glutamine, glutamate, and glycine betaine) and energy conservation complexes (i.e. Ech and Eha) was proposed to be the main reason to assist the consortia against ammonia stress. Besides, the syntrophy (e.g., catabolic complementarity) between bacteria and methanogens supported them in overcoming bioenergetic barriers caused by ammonia inhibition.

Thirdly, the bioaugmentation with acclimatized ammonia tolerant *Methanoculleus* sp. was implemented to stimulate the under-performing AD process. A 21% increase in methane yields and 10% reduction in volatile fatty acids confirmed that the addition of *Methanoculleus sp.* successfully alleviated ammonia stress. The genome-centric metagenomics revealed that multiple energy regulating complexes and osmolytes uptake systems in *Methanoculleus* sp. might contribute to its remarkable robustness to ammonia. Meanwhile, the bioaugmentation of *Methanoculleus* sp. triggered the change in bacterial community composition. Regarding dominant bacteria, the genes involved in parallel degradation pathways of glucose and acetate possibly provided them with enough flexibility to overcome ammonia stress. Therefore, the resume of electron transfer between the syntrophic bacterial community and methanogen led to the successful bioaugmentation.

Finally, the microbial consortia preservation technology was developed to provide the ready-to-use inocula for future full-scale bioaugmentation applications. The ammonia tolerant methanogenic consortia were preserved in two carriers, namely, liquid BA medium and agar gel, at two different temperatures of 4 °C and 24 °C, respectively. The best strategy for long-term preservation was in agar gel up to 168 days at 24 °C, followed by a liquid BA medium within 84 days at 24 °C. Besides, high methanogenic activities of *Methanosarcina soligelidi* and *Methanoculleus palmolei* were observed during the revival test, indicating their high potential as ready-to-use inocula.

Overall, this Ph.D. project offered feasible methods to improve methane yields from the ammonia-stressed anaerobic reactors. Besides, the knowledge regarding microbial composition and metabolic pathways had practical guidance for AD process optimization.

Dansk sammenfatning

Anaerob nedbrydning (AD) er en populær global affaldshåndteringsteknologi, hvor de organiske stoffer nedbrydes til biogas (hovedsageligt CH_4 og CO_2) under iltfrie forhold. Til dato er biogas blevet promoveret i henhold til følgende anvendelser: elproduktion, andre merværdiprodukter, transportbrændstof og opvarmningsformål. En større andel af biogas i vedvarende energi forventes at nå de Forenede Nationers mål for bæredygtig udvikling. Det organiske affald fra industrier og husholdninger er egnetsom råmateriale til produktion af biogas, hvilket er god i overensstemmelse med konceptet om "affald til energi". På trods af de forskellige fordele og det store potentiale ved AD forsinkes udviklingen af AD grundet en række udfordringer, hvoraf den ene er nedbrydningen af N-rige substrater. Den frigjorte ammoniak (over 1,5 g NH_4^+ -N/L) hæmmer vækst af mikroorganismer i AD, især methanogener, hvilket fører til mindre methanudbytte. Derfor er metoder til at opretholde metanproduktion på trods af ammoniakhæmning påkrævet. Desuden er en afbalanceret mikrobiel sammensætning af stor betydning for en stabil AD-proces. Således giver en dyb indsigt i den mikrobielle sammensætning væsentlig viden for procesoptimering. Udvikling af sekventeringsteknologi og bioinformatiske metoder gør det muligt at udvide vores forståelse af komplekse mikrobielle sammensætning og egenskaber.

Dette ph.d. projekt har til formål at 1) udvikle metoder til at opretholde metanproduktion fra organisk affald med højt ammoniakindhold og 2) udforske mikrobielle synergistiske netværk og andre funktioner, der påvirker den mikrobielle stressmodstand.

For at opnå en effektiv kontinuerlig anaerob nedbrydning af N-rige substrater blev den trinvise akklimatiseringsproces udført i mesofile reaktorer fodret med den organiske fraktion af husholdningsaffald (OFMSW). Resultaterne viste, at akklimatisering kunne øge procesrobustheden i fuldomrørte reaktorer (CSTRs), med en ammoniakbelastning op til 8,5 g NH_4^+-N/L. Methanudbyttet varrierede mindre end 10%. I mellemtiden var der et skift af methanogener, der var dominerende i processen, fra *Methanosaeta concilii* ved lave ammoniakniveauer (1,1-5 g NH_4^+-N/L) til *Methanosarcina soligelidi* ved høje ammoniakniveauer (6-9,5 g NH_4^+-N/L).

For at undersøge de mikrobielle synergistiske netværk og andre funktionaliteter, der regulerer ammoniak-tolerancen, blev podematerialet dyrket i fire grupper (dvs. $G_{methanol}$, $G_{H2/CO2}$, $G_{formiat}$ og G_{acetat}) under øgede

ammoniakniveauer i batchreaktorer. Syntetisk basalt anaerobt (BA) medium indeholdende en enkelt carbonkilde (methanol, H_2/CO_2, formiat og acetat) blev anvendt som råmateriale. Under akklimatiseringsprocessen var konsortierne i $G_{methanol}$ og $G_{H2/CO2}$ robuste op til 7,25 g NH_4^+-N/L efterfulgt af G_{format} og G_{acetat} til henholdsvis 5,25 og 4,25 g NH_4^+-N/L. Omsætningsveje for dominerende mikrober blev rekonstrueret baseret på en genomanalyse kombineret med målinger af mellemprodukter under nedbrydningsprocessen, hvorved den mulige mekanisme for ammoniak-tolerance blev foreslået. I korte træk skulle eksistensen af gener, der er ansvarlige for osmotiske regulatorer (K^+, Nε-acetyl-L-lysin, glutamin, glutamat og glycinbetain) og energibesparelseskomplekser (dvs. Ech og Eha), være hovedårsagen til at hjælpe konsortier mod ammoniak stress. Desuden understøttede syntrofi (fx katabolisk komplementaritet) mellem bakterier og methanogener dem i at overvinde bioenergiske barrierer forårsaget af ammoniakhæmning.

Derefter blev bioaugmenteringen med akklimatiseret ammoniak-tolerant *Methanoculleus* sp. implementeret for at stimulere den begrænsede AD-proces. En stigning på 21% i methanudbytte og 10% reduktion i flygtige fedtsyrer bekræftede, at tilsætningen af *Methanoculleus* sp. lykkedes med at lindre ammoniakstress. Metagenomics analysen viste, at flere energiregulerende komplekser og osmolytter optager systemer i *Methanoculleus* sp. og kan bidrage til dets bemærkelsesværdige robusthed over for ammoniak. I mellemtiden forårsagede bioaugmenteringen af *Methanoculleus* sp. ændringer i bakteriesamfundets sammensætning. Med hensyn til dominerende bakterier gav generne, der var involveret i parallelle omsætningsveje for nedbrydning af glucose og acetat, muligvis tilstrækkelig fleksibilitet til at overvinde ammoniakstress. Derfor førte genoptagelsen af elektronoverførsel mellem det syntrofiske bakteriesamfund og methanogen til en vellykket bioaugmentering.

Endelig blev den mikrobielle konserveringsteknologi udviklet til at give en klar-til-brug podning til fremtidige fuldskala bioaugmenteringsapplikationer. De ammoniak-tolerante metanogene konsortier blev konserveret i to medier, nemlig flydende basisk anaerobt medium og agargel ved to forskellige temperaturer på henholdsvis 4 °C og 24 °C. Den bedste strategi til langvarig konservering var i agargel op til 168 dage efterfulgt af et flydende basisk anaerobt medium inden for 84 dage ved 24 °C. Derudover blev der observeret høje metanogene aktiviteter af *Methanosarcina soligelidi* og *Methanoculleus palmolei* under genoplivningstesten, hvilket indikerer deres høje potentiale som inokula klar til brug.

Samlet set har dette Ph.D. projekt udviklet mulige metoder til forbedring af methanudbyttet fra ammoniak-stressede anaerobe reaktorer. Desuden har den nye viden om mikrobiel sammensætning og omsætningsveje under ammoniumstress givet ny forståelse, som kan anvendes til procesoptimering af ammonium belastede AD-processer.

Table of contents

Abbreviations

AD	Anaerobic digestion
SDGs	Sustainable Development Goals
LCFA	Long-chain fatty acids
EMP	Emben-Meyerhof-Parnas
ED	Entner Doudoroff pathway
VFA	Volatile fatty acid
FAN	Free ammonia nitrogen
TAN	Total ammonia nitrogen
OFMSW	Organic fraction of municipal solid waste
GHG	Greenhouse gas
BA	Basal anaerobic medium
VS	Volatile solid
PCA	Principal component analysis
TS	Total solid
MAG	Metagenome assembled genome
PTA-ACKA	Phosphotransacetylase-acetate kinase pathway
ACS	Forming acyl-CoA synthetase
acs	Acyl-CoA synthetase gene
ack	Acetate kinase gene
mcrA	Methyl coenzyme M reductase gene
Mta/b	Coenzyme M methyltransferase genes
coo	Carbon monoxide dehydrogenase gene
gcv	Glycine decarboxylase genes
grd	Glycine reductase gene
Vho	Methanophenazine-reducing hydrogenase
Frh	Coenzyme F420-reducing hydrogenase
Ech	Energy converting hydrogenase
Fpo	F420H2 dehydrogenase
hdr	Membrane-bound heterodisulfide reductase gene
Ehb	Energy-conserving hydrogenase B
WL	Wood-Ljungdahl
Rnf	Rhodobacter nitrogen fixation complex

1 Introduction

1.1 Background

The human population is predicted to reach over 9 billion by 2050; meanwhile, the demand for energy and food is expected to increase by over 50%. Consequently, the increasing amount of organic waste and disposal from the human is estimated as a global problem (Ferroukhi et al. 2015). If there is no proper treatment, the massive waste generated may worsen the water, soil, and air quality (Minelgaitė and Liobikienė 2019). To achieve the United Nations' Sustainable Development Goals (SDGs) by 2030, a circular economy concept should be performed by integrating organic waste treatment with bioenergy production and nutrients recovery (Schroeder et al. 2019, Favaro et al. 2019). European Union has banned the application of biodegradable organic wastes in landfills (Briassoulis et al. 2019). As a consequence, many countries have introduced incineration for waste treatment and energy production (Tozlu et al. 2016). However, incineration is not preserving nutrients and seems to be an unsustainable approach from economic and environmental perspectives (Tozlu et al. 2016, Tian et al. 2020).

Anaerobic digestion (AD) is a promising approach where involves varieties of microbes in converting organic waste (e.g., municipal solid waste, industrial wastewater, agriculture waste, algae waste, etc.) to biogas and digestate (Ambaye et al. 2020, Satchwell et al. 2018). Biogas, one of the essential renewable energy, is expected to partially substitute fossil fuels for the supply of electricity, heat, and transportation in Denmark (Figure 1) (McAnulty et al. 2017). Furthermore, the digestate is rich in various types of nutrients, which can improve soil quality in agriculture sector (Tambone et al. 2010). Thus over 163 biogas plants are widely implemented in Denmark to maximize the energy recovery from the organic waste (European biogas association).

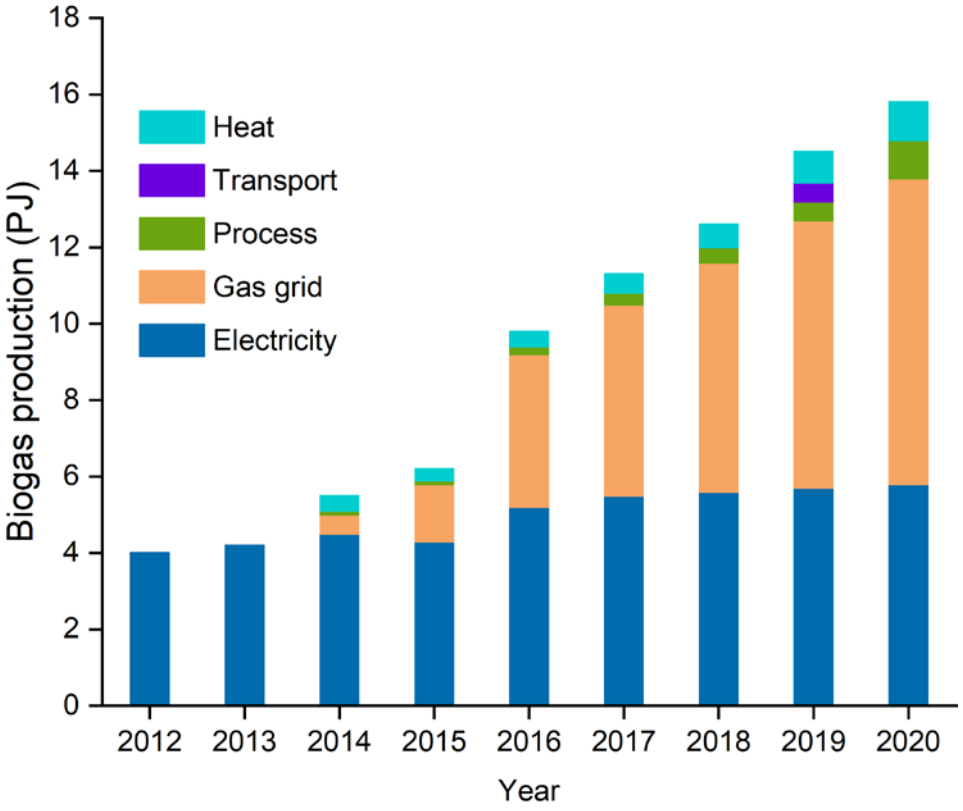

Figure 1. Biogas production and its application in Denmark 2012-2020. [Adapted from Danish Energy Agency]

1.1.1 Anaerobic digestion

The AD is a biological process, where organic matters are converted into methane (50-70%), carbon dioxide (30-50%), H_2 (0-1%), and H_2S (0-3%), etc., under oxygen-free conditions (Angelidaki et al. 2011a). However, the percentage of the biogas is determined by several factors, e.g., feedstock composition, digester retention time and temperature (Karube et al. 1980, Lin et al. 2019, Uçkun Kiran et al. 2016, Chen et al. 2008). AD process mainly occurs in four steps, namely hydrolysis, acidogenesis, acetogenesis, and methanogenesis (Ponsá et al. 2008) (Figure 2). Bacteria are involved in the first three steps, and archaea responsible for the final stage (Campanaro et al. 2018).

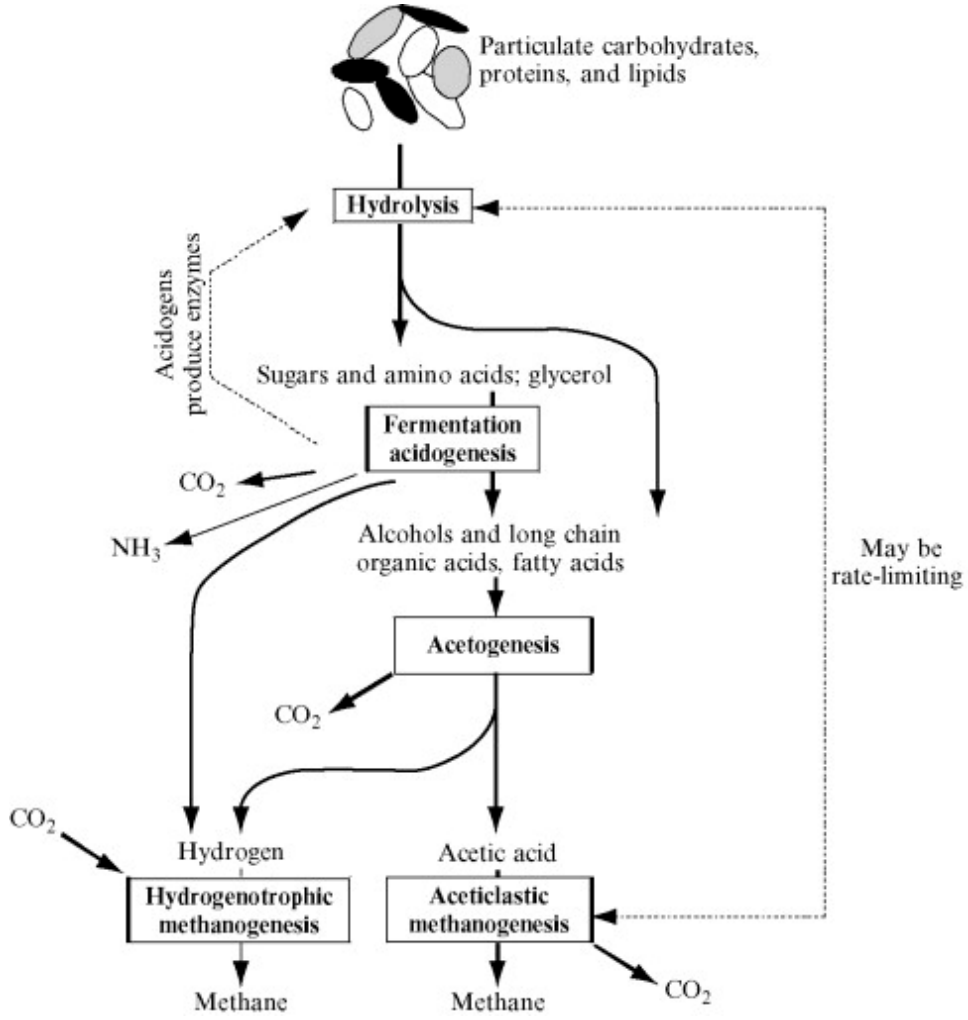

Figure 2. The main flow of the AD process in four steps [Adapted from Angelidaki et al. (2011b)]

1.1.2 Hydrolysis

The hydrolysis step is involved in the degradation of protein, carbohydrates, and lipids into amino acids, monosaccharides, and glycerol /long-chain fatty acids, respectively, through hydrolytic enzymes (Wilson 2011, Dimock and Morgenroth 2006, Chen and Chang 2017). The hydrolytic bacteria mainly belong to the phylum *Firmicutes* and *Bacteroidetes*, and they are more robust to environmental change (e.g., ammonia stress, and temperature), compared to the methanogen (Dimock and Morgenroth 2006, Chen and Chang 2017, Cazier et al. 2019).

1.1.3 Acidogenesis

During the acidogenesis step, the main products from hydrolysis, i.e., monosaccharides, amino acids, and glycerol/long-chain fatty acids (LCFA) are further degraded into smaller molecules (Myint et al. 2007).

The monosaccharides are converted into C3 products via Emben-Meyerhof-Parnas (EMP) pathway, and C2/C4/C6 products using Entner Doudoroff (ED) pathway, respectively (Zhu et al. 2019). C2/C4/C6 products (e.g., acetate, butyrate, caproate) are more commonly present in the AD process. In contrast, the C3 products (e.g., lactate) are rarely observed unless AD reactors are overloaded (Angelidaki et al. 2011a, Zhou et al. 2018a, Tian et al. 2019a).

The amino acid degradation commonly proceeds via the Stickland reaction where the paired amino acid is converted into organic acid (with one less carbon) and NH_3 in a coupled oxidation/reduction reaction (Chen et al. 2019). Most amino acids can be electron acceptors, donors, even both. In some cases, the acidogenesis of amino acid takes place via transamination, thereby pyruvic and oxaloacetic acids are formed (Tezel et al. 2011).

The LCFA is broken into shorter volatile fatty acids, acetate, and hydrogen following β-oxidation, and the shorter volatile fatty acids enter the next rounds of β-oxidation by the acetogenic-oxidizing bacteria (Tian et al. 2018a). So far, the known acetogenic β-oxidizing bacteria have been identified within the families of *Syntrophomonadaceae* and *Syntrophaceae* (Ziels et al. 2017). However, the LCFA is easily attached to the surface of microorganism, which limits the access of microorganism to the substrate (Zhou et al. 2018b). Generally, the biodegradation rate of LCFA is slower than the hydrolysis process, which causes the accumulation of LCFA quickly in the AD system. Meanwhile, the hydrogen, the by-product from the LCFA degradation, influences the distribution of the short-chain acid. Specifically, the higher hydrogen partial pressure inhibits short-chain acids production, leading to accumulation of LCFA due to the chemical equilibrium. As a consequence, it further reduces the activity of acetogenic β-oxidizing bacteria (Zhou et al. 2018b, Hao et al. 2016, Alves et al. 2001).

1.1.4 Acetogenesis

Acetogenesis refers to the process of acetate formation through two pathways, i.e., reduction of C1 units (e.g. CO_2) (Xu et al. 2011) and degradation of organic acids (Diekert and Wohlfarth 1994). The homoacetogens involved in the first pathway belong to the genera of *Acetoanaerobium*, *Acetogenium*, *Acetobacterium*, *Clostridium*, *Butyribacterium*, *Eubacterium*, and *Pelobacter* (Borja 2011). Most homoacetogens perform Wood-Ljundahl pathway for acetate generation, where H_2 and HCO_3^- are used as electron donor and acceptor, respec-

tively (Westerholm et al. 2016). Thus homoacetogens develop syntrophic co-operation with H_2-producing bacteria, while the competitive relationship with hydrogen-utilizing methanogens (Borja and Rincón 2017).

During the second pathway, the hydrogen-producing acetogens oxidize organic acids to acetate, from which the electrons produced are transferred to H^+ for H_2 and CO_2 generation (Zhu et al. 2019). However, these acetogenic bacteria can only grow in an efficient electron-removing environment. For example, the simplest co-culture involving syntrophic interaction comprises an acetogen and a hydrogen-scavenging microbe (e.g., hydrogenotrophic methanogen). Thus the presence of mutualistic co-culture is vital for the well-balanced anaerobic digestion (Angelidaki et al. 2011a, Borja 2011).

1.1.5 Methanogenesis

Methanogenesis takes place at the final stage of AD when the alternative electron acceptors (e.g., O_2, Fe^{3+}, and NO_3^-) are exhausted. Until now, all methanogens are classified into seven orders (*Methanococcales*, *Methanobacteriales*, *Methanosarcinales*, *Methanomicrobiales*, *Methanocellales*, *Methanopyrales*, and *Methanomassiliicoccales*) (Vanwonterghem et al. 2016). Due to their distinct metabolic traits, three different pathways are involved in methane production, i.e., the acetoclastic pathway, the hydrogenotrophic pathway, and the methylotrophic pathway (Angelidaki et al. 2011a, Lyu et al. 2018).

Firstly, acetoclastic methanogens enable the cleavage of acetate into CH_4 and CO_2. So far, only two genera of methanogens are identified for acetate utilization, namely, *Methanosarcina* and *Methanosaeta*. *Methanosaeta* is a specialist that uses acetate specifically within the range of 0-20 mM (Chen et al. 2017, Dyksma et al. 2020). Besides, *Methanosaeta* was reported as the primary methane producer on earth because it is widely present in the environment (e.g., rice paddies) and prevailed over *Methanosarcina* in nature with the low level of acetate (Smith and Ingram-Smith 2007, Rotaru et al. 2014). However, *Methanosarcina* is a metabolically versatile methanogen capable of producing methane from carbon dioxide, methanol, and methylamines as well (Smith and Ingram-Smith 2007). It is more abundant in the middle-high acetate and/or ammonia environment (Capson-Tojo et al. 2020).

Secondly, hydrogenotrophic methanogens (i.e., *Methanobacteriales*, *Methanomicrobiales*, *Methanococcales*, *Methanocellales*, and *Methanopyrales*) are capable of converting H_2 and CO_2 to CH_4. Their presence maintains the AD

system at a low H_2 partial pressure and makes stable acetogenesis process feasible (Zabranska and Pokorna 2018, Watkins et al. 2012, Tian et al. 2019b). Compared to acetoclastic methanogens, hydrogenotrophic methanogens are more robust to ammonia stress. Thus, they are of critical importance to stable methane production at high ammonia levels (Tian et al. 2019a).

Thirdly, methylotrophic methanogens (including some *Methanosarcinales* spp. and *Methanomicrobiales* spp.) can metabolize methylated C_1 compounds to methane (Vanwonterghem et al. 2016). Besides, formic acid, methanol, methyl sulfides, methylamines, and some methylated ethanolamines can serve as carbon sources (Zabranska and Pokorna 2018). Methylotrophic methanogens are significant contributors to methane production in marine sediments, and other extreme environments, e.g. hypersaline conditions and soda lake sediments (Vanwonterghem et al. 2016, Zhang et al. 2020)

1.1.6 Syntrophic network in the anaerobic digestion process

The complete conversion of various substrates to methane depends on the obligately mutualistic metabolism performed by archaea and bacteria in anaerobic bioreactors (Morris et al. 2013). For example, during the syntrophic degradation, the H_2 derived from some bacteria can directly feed hydrogen-utilizing microbes involved in the other steps. In turn, the hydrogen-utilizing microbes are crucial to maintaining the low partial pressure of H_2 that allows the H_2-producing reaction feasible (Stams and Plugge 2009).

This mutualistic metabolism is not only limited within the transfer of reducing agents, e.g., formate or hydrogen but also involves the exchange of organic compounds or the scavenging of toxic compounds (Morris et al. 2013). Due to these unique features, syntrophic partners take advantage of each other to catabolize the organic matter, which can not be driven by the individual microbes alone. Therefore, dedicated microbial studies will shed more light on the significance of unknown metabolic interactions between microorganisms.

1.2 Anaerobic digestion of N-rich waste

During the anaerobic digestion of N-rich waste (e.g., chicken manure, slaughterhouse waste, as well as industrial waste, etc.), ammonia (TAN) consisting of free ammonia nitrogen (FAN, NH_3) and ammonia ion (NH_4^+), is a by-product of acidogenesis step. Ammonia levels within the range of 0.05-0.2 g NH_4^+-N/L are necessary for microbial growth because ammonia serves as the N-source for amino acid and nucleic acids synthesis (Jiang et al. 2019). However, TAN being above 1.5 g NH_4^+-N/L has an adverse effect on microbial activities

due to FAN inhibition (Capson-Tojo et al. 2020, Rajagopal et al. 2013). The following explanations are provided:

1) FAN can freely permeate into cells and can be converted into ammonia ion due to protonation, thus leading to intracellular proton imbalance (Jiang et al. 2019).

2) High FAN levels suppress the uptake of potassium/magnesium/sodium that are required nutrients for microbial growth (Wittmann et al. 1995)

3) High FAN levels induce intense extracellular osmotic stress which disturbs microbial metabolic activity (Kadam and Boone 1996, Chang et al. 2020)

4) High ammonia levels lead to energy-intensive metabolic process (Wittmann et al. 1995)

Methanogens are widely reported more vulnerable to ammonia than bacteria because their cell walls lack peptidoglycan and the structure is "leaky" with S-layers (Capson-Tojo et al. 2020, Engelhardt 2007). Thus the inhibited methanogenic activity at high ammonia levels leads to a reduced consumption rate of acetate/H_2 (the critical precursors of methanogenesis) (Yang et al. 2019, Fotidis et al. 2013). Once this acetate / H_2 accumulated up to certain levels, the syntrophic acetogenic and acetate oxidizing reactions may become energetically unfavourable (Morris et al. 2013, Worm et al. 2010). Thus the conversion from organic waste to methane was suppressed entirely, evidenced by the lower total solid removal rate, VFA accumulation and methane yields (Chen et al. 2018, Dai et al. 2017).

1.2.1 Multiple strategies to recover methane production from under-performing AD process

To alleviate ammonia stress in AD, many techniques including air stripping, ammonia adsorption, hollow fibre membrane contactor, conductive materials addition (e.g., magnetite) have been developed (Liu et al. 2012, Wang et al. 2018, Yabu et al. 2011, Ho and Ho 2012, Lauterböck et al. 2012). However, their commercial applications are restricted by the high-cost and/or technical challenges. Biological treatments (e.g., acclimatization and bioaugmentation) have several advantages, e.g., easy operation, high efficiency, and negligible pollution to environment. Nevertheless, more dedicated studies are required for AD process optimization.

1.3 Objectives and thesis structure

1.3.1 Objectives

This Ph.D. project focuses on 1) developing efficient and sustainable strategies to recover methane production from ammonia inhibition; 2) deciphering the microbial characteristic and their syntrophic interaction. The specific objectives are listed as follows:

1) Acclimatize ammonia tolerant inocula to achieve stable methane production in continuous stirring tank reactors (CSTR) at high ammonia loads (Paper I).

2) Investigate the metabolic interaction of ammonia tolerant microbes grown on individual carbon source (i.e., acetate, formate, methanol, H_2/CO_2) (Paper-II).

3) Explore the mechanism of microbial tolerance to ammonia through genomics-centric analysis (Paper II).

4) Recover the methane yields from ammonia-inhibited reactors using bioaugmentation technology (Paper III).

5) Achieve the insights of microbial metabolic interaction triggered by the bioaugmentation with ammonia tolerant methanogen (Paper III).

6) Develop long-term microbial preservation methods to offer ready-to-use methanogenic cultures (Paper IV).

1.3.2 Structure of the thesis

In chapter 2, the stepwise acclimatization to extreme high ammonia levels is presented in mesophilic CSTR fed with organic fraction of municipal solid waste (OFMSW).

In chapter 3, the metabolic interactions among ammonia tolerant methanogenic culture fed with different single and simple carbon sources under thermophilic conditions are reconstructed using the genomics-centric analysis. The possible mechanism of microbial tolerance to ammonia is proposed.

In chapter 4, bioaugmentation with acclimatized ammonia tolerant inocula is performed to improve methane production from ammonia inhibition. Meanwhile, genomics-centric analysis shows the change in microbial composition induced by bioaugmentation.

In chapter 5, microbial preservation methods are assessed in order to provide the ready-to-use ammonia tolerant inocula. The methanogenic community composition after preservation is investigated.

In chapters 6 and 7, the main findings of the Ph.D. thesis are summarized, the future perspectives are presented.

2 Acclimatization as a method to achieve stable methane production of ammonia inhibited reactors

Acclimatization is a method where continuous exposure of microbial community to a specific environment improves its tolerance to this given environmental limitation. This bioremediation technology has been applied effectively in the AD field. For instance, microbial acclimatization successfully promoted the acidogenesis process (Saha et al. 2019), methane yield of AD from LCFAs stress (Kurade et al. 2020), and even resistance to metal toxicity (Bhakta 2016). Similar applications have been used to address ammonia inhibition which commonly occurs under AD of N-rich organic waste. The increased methane yields in batch reactors at TAN levels of 6.6 g NH_4^+-N/L (Tian et al. 2018b), and CSTR with TAN of 4.9 g NH_4^+-N /L (Dai et al. 2017) were observed. However, the ammonia threshold of acclimatization in CSTR is unclear, which may affect further technical application.

2.1 Acclimatization process

In the paper I, stepwise acclimatization to extreme ammonia levels (more than 7g NH_4^+-N /L) was performed in two mesophilic CSTRs (namely, R1 and R2) fed with OFMSW. The whole acclimatization process was divided into seven periods based on TAN levels (Table 1). Specifically, the average methane yield of P1 (no extra ammonia addition) was used as a baseline. Once anaerobic reactors reached a steady state with more than 85% of average methane yield of the P1, the TAN was increased (1-1.5 g NH_4^+-N /L each period). The mixture of urea and ammonium chloride was injected into feedstock and reactors simultaneously to achieve higher TAN levels.

Table 1. The experimental design of stepwise acclimatization in CSTR reactors. [Adapted from paper I]

Phase	Days	TAN	Extra added ammonia	
			$CO(NH_2)_2$	NH_4Cl
		(g NH_4^+-N/L)	(g NH_4^+-N/L)	(g NH_4^+-N/L)
P1	0-30	1.1	0	0
P2	31-51	4	1	1.9
P3	52-66	5	2	1.9
P4	67-74	6	2	2.9
P5	75-89	7	3	2.9
P6	90-127	8.5	4	3.4

P7	128-159	9.5	4.5	3.9

2.2 Reactor performance

The average methane yields, i.e., 345 ± 40 (R1) and 391 ± 59 (R2) mL CH_4/g VS during P1 were used as baseline references for evaluating inhibitory effect in the following phases (P2-P7) (Figure 4). Even though the two reactors experienced temporary inhibition (P2-P5) with an average reduction of 15% in methane yield compared to P1. Quick recovery with less than 6% loss was observed (Figure 3). When TAN of reactors was increased to 8.5 g NH_4^+-N/L (P7), the "inhibited steady-state" occurred with over 15% reduction in methane yields compared to P1. Meanwhile, the change in VFA from low levels (P3 to P5) to over 4000 mg /L (P6-P7) in both reactors were observed. Based on these results, 8.5 g NH_4^+-N/L was proposed as the threshold of acclimatization process in mesophilic anaerobic reactors of OFMSW. To be noticed, although the inhibitory effect of ammonia on the AD process was observed at P7, the methane yields were still higher than other acclimatization studies at the same ammonia levels (Capson-Tojo et al. 2020, Jiang et al. 2019).

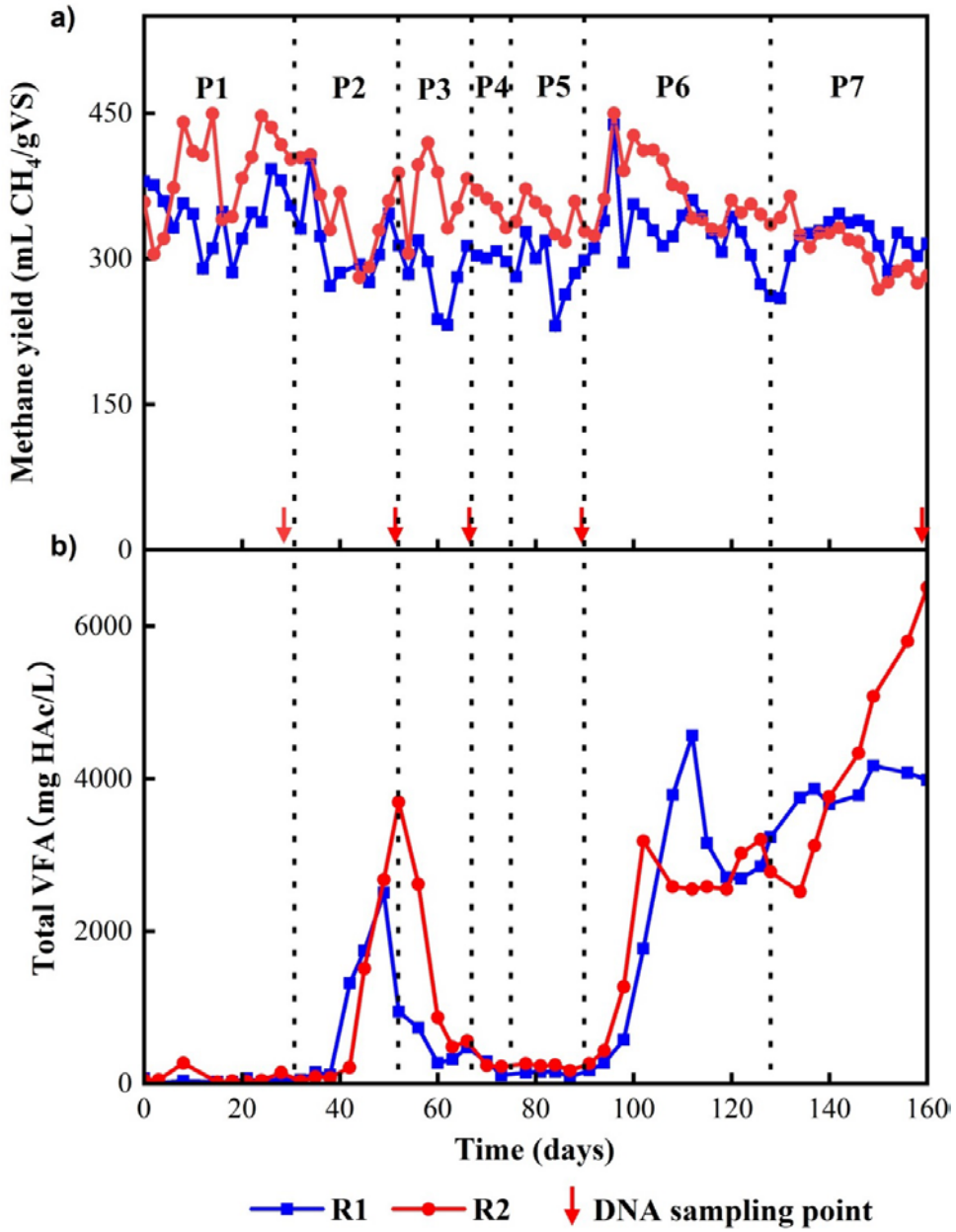

Figure 3. a) CH_4 production yields in R1 and R2, b) total VFA change from P1 to P7 [Adapted from paper I].

2.3 Microbial dynamicity

Ammonia effect on microbial shift was revealed using the 16S rRNA amplicon sequencing technology (Figure 4). Specifically, *Methanosaeta concilii* 2 was dominant methanogen with 50-70% of relative abundance of archaeal population during P1 to P2 (less than 5 g NH_4^+-N/L). As ammonia levels continuously increased, *Methanosarcina soligelidi* 1 gradually outcompeted *Methanosaeta concilii* 2 from P3 (40%) to P7 (90%). These findings agreed with other studies

that middle-high ammonia levels generally favored the growth of *Methanosarcina* spp. than *Methanosaeta* spp. in AD (Jiang et al. 2019, Tian et al. 2019c).

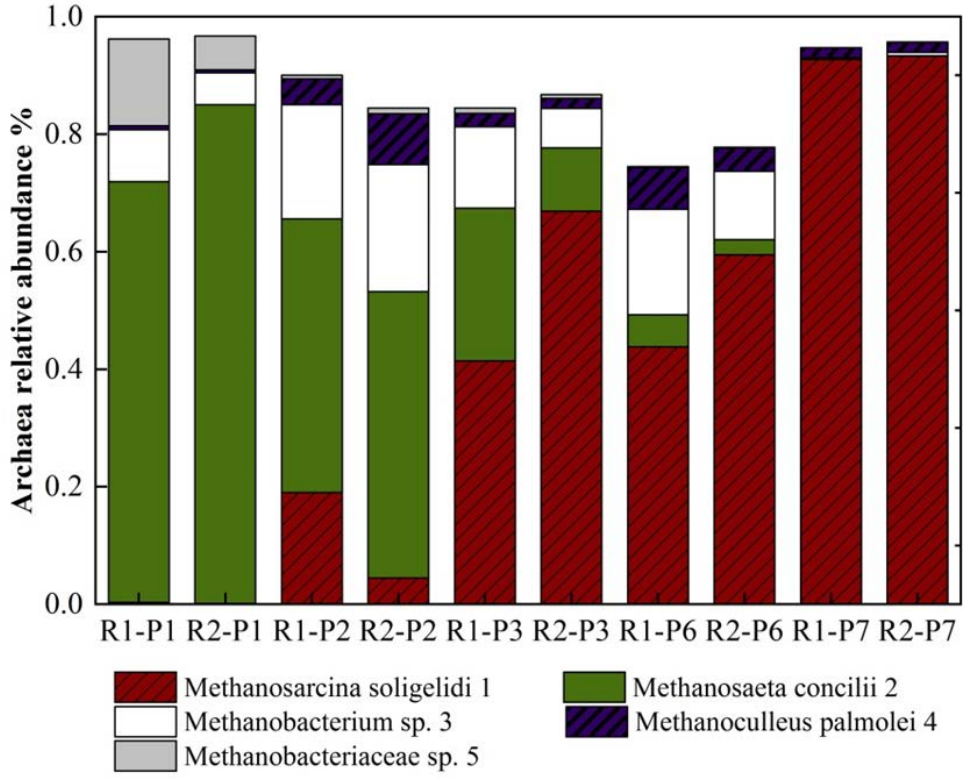

Figure 4. Archaeal relative abundance (%) in R1 and R2 at different periods. [Adapted from paper I].

In summary, successful acclimatization up to 8.5g NH_4^+-N/L was achieved to mitigate ammonia stress during AD of the OFMSW. Microbial analysis revealed that *Methanosarcina soligelidi* owned higher robustness to ammonia, which contributed to stable methane production at middle-high ammonia levels.

3 Insights into microbial tolerance to ammonia

Methanosarcina is generally more resilient to ammonia stress than *Methanosaeta* (Chen et al. 2018) and its capability to recover methane yields has been highly recognized at middle-high ammonia levels (Capson-Tojo et al. 2020, Zabranska and Pokorna 2018). Furthermore, hydrogenotrophic methanogens (e.g., *Methanothermobacter*, *Methanoculleus*, and *Methanobacterium*) can outcompete *Methanosarcina* for methanogenesis under extremely high ammonia levels in anaerobic digestors (Tian et al. 2019a, Westerholm et al. 2016, Jing et al. 2017). It seems that the distinct metabolic characteristics are linked to microbial tolerance to ammonia. Moreover, these methanogens mainly perform methanogenesis from acetate and/or H_2/CO_2, the knowledge about ammonia tolerance of methanogens grown on other methanogenic precursors (i.e., methanol and formate) is still absent. Understanding the metabolic characteristics and syntrophic interaction of ammonia tolerant microorganisms can help us to decipher the mechanisms of ammonia tolerance. In the last decades, microbial interaction and functionality were little known due to the limitation in microbial cultivation/isolation and biomolecular technology. Currently, the continuous development in metagenomics technology makes the cultivation-independent assessment feasible in terms of the most unexploited genetic reservoir of anaerobic microbial communities (Qin et al. 2010). It opens the door to the identification of unknown functional genes/pathways, and metabolic interaction. By now, most anaerobic microbial communities revealed by metagenomics were shaped by real organic waste (e.g., OFMSW, and industrial wastewater) containing complicated carbon sources (Forbes et al. 2017, Campanaro et al. 2019). A huge amount of Metagenome-Assembled Genomes (MAGs) achieved pose a challenge for the genomic metabolic analysis. Thus the ammonia tolerant microbiome grown on single carbon source (the common methanogenesis precursors: acetate, methanol, formate, and H_2-CO_2) would provide more clear insights of obligate mutualistic interactions and other functionalities.

3.1 Microbial interaction under four solely carbon sources

Four thermophilic batch reactors were inoculated with the same seed inocula that was collected from a thermophilic CSTR of cattle manure. The feedstock used in this experiment consisted of basic anaerobic medium, ammonia chloride

and single carbon source (methanol, acetate, formate, H_2/CO_2). During the acclimatization process, 5% (V/V) of fresh microbial samples were harvested to the next increased ammonia level (1g NH_4^+-N/L each step) when methane yields reached 80% of its maximal potential. The cultivation process was repeated under increased ammonia levels until the methanogenic consortia could not grow anymore (Table 2). The microbial DNA was taken from five sampling points: $G_{inocula}$, an initial inoculum (2.25 g NH_4^+-N/L); $G_{methanol}$, microbial community fed by methanol (7.25 g NH_4^+-N/L); $G_{acetate}$, microbial community fed by acetate (4.25 g NH_4^+-N/L); $G_{formate}$, microbial community fed by formate (5.25 g NH_4^+-N/L); $G_{H2/CO2}$, microbial community fed by H_2/CO_2 (7.25 g NH_4^+-N/L).

Table 2. Characteristics of the reactors. [Adapted from Paper II]

	Acetate	Formate	H_2/CO_2	Methanol	Organic loading range g.COD/L
Original ammonia level (N-NH_4^+g/L)	2.25±0.15				
pH	7.9±0.1	8.1±0.01	8.0±0.02	7.9 ±0.02	
Acclimatization process (N-NH_4^+g/L)	2.25	2.25	2.25	2.25	1
	3.25	3.25	3.25	3.25	1
	4.25	4.25	4.25	4.25	1
		5.25	5.25	5.25	1-2.5
			6.25	6.25	1-2.5
			7.25	7.25	1.7-2

* pH was maintained by NaOH solution (4 mol/L)

The microbial composition and their key functionalities in each group were unveiled using a genomics-centric approach. After the binning process, 81 MAGs were achieved. 52 out of 81 MAGs were high quality (contamination less than 5%; completeness over 90%), and the other 29 MAGs were medium quality (contamination ranging from 5% to 10%; completeness in the range of

50%-90%). The results showed that individual carbon source and ammonia shaped the common initial inocula into distinct four microbiomes (Figure 5).

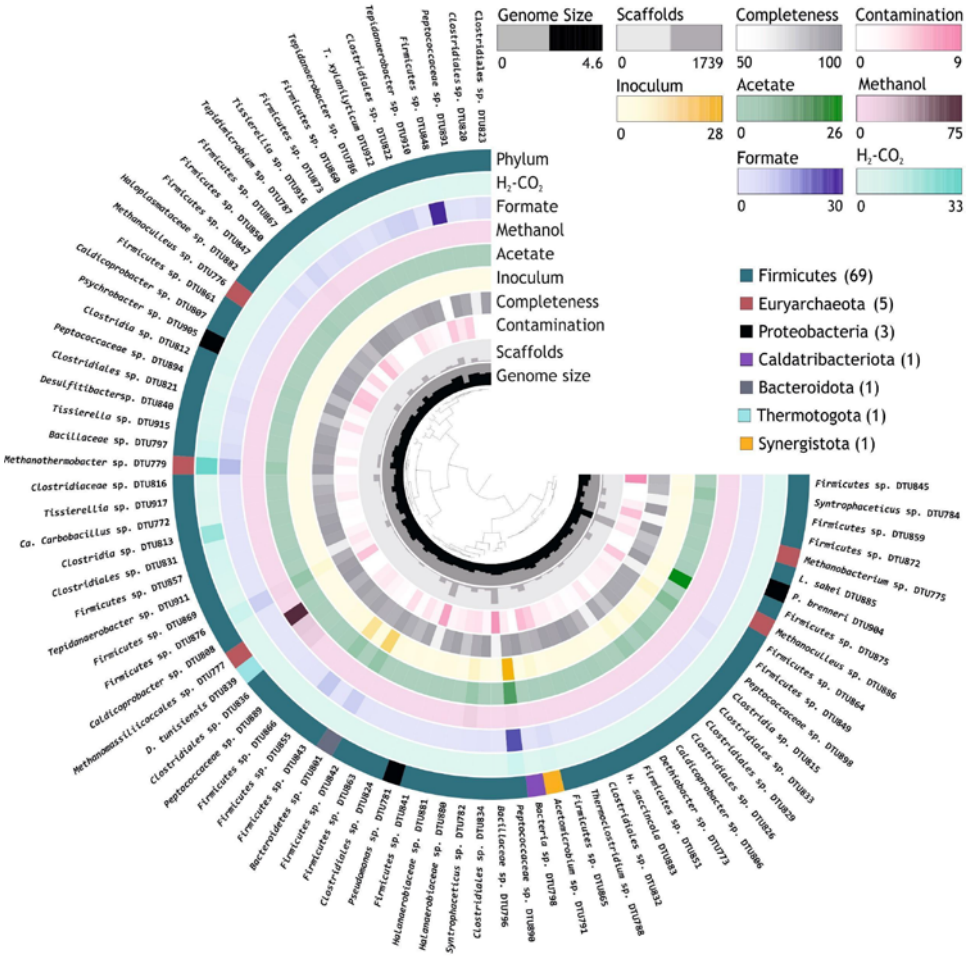

Figure 5. The characteristic (coverage, quality, and taxonomic assignment) of microbiome in $G_{inoculum}$, $G_{acetate}$, $G_{methanol}$, $G_{formate}$, and $G_{H2/CO2}$. The taxonomy at the phylum level, the relative abundance of each MAG in the different group (%), and a Pearson clustering of MAGs was listed in the outer, five middle, and inner layers. The genome size (Mbp), number of scaffolds, completeness (%), and contamination (%) are coloured in black, grey, green, and red, respectively. [Adapted from Paper II]

3.1.1 Microbiome in the $G_{inoculum}$

In $G_{inocula}$, the dominant bacterial MAGs consisted of *Peptococcaceae* sp. DTU890, *Bacteroidetes* sp. DTU801, *Firmicutes* sp. DTU855 and *Firmicutes* sp. DTU849 (Figure 5). They accounted for 58.95% of relative abundance and were assigned to sugar degraders (Table S5). The relative abundance of archaeal group was only 1.28% of the total microbial population, among them, *Methanoculleus* sp. DTU886, *Methanothermobacter* sp. DTU779, and *Methanomassiliicoccales* sp. DTU777 were 1.2%, 0.05% and 0.03% of relative

abundance, respectively. No acetoclastic methanogens were found, the possible explanation was that the TAN of 2.25 g NH_4^+-N/L in $G_{inocula}$ at 55°C suppressed their growth.

3.1.2 Ammonia tolerant microbiome in the $G_{acetate}$

$G_{acetate}$ at 4.25 g NH_4^+-N/L was mainly composed of *Methanoculleus* sp. DTU886 (26% of relative abundance), *Firmicutes* sp. DTU849 (7%) and *Peptococcaceae* sp. DTU890 (16%) (Figure 6). The syntrophic interactions in terms of the conversion of acetate to methane among these dominant MAGs were reconstructed. Specifically, the conversion of acetate to H_2/CO_2 (the precursor for methanogenesis) took place in *Firmicutes* sp. DTU849 through Wood-Ljungdahl (WL) and *Peptococcaceae* sp. DTU890 through coupling partial glycine cleavage system with the WL pathway, respectively (Zhu et al. 2019). The H_2/CO_2 was further converted to methane by *Methanoculleus* sp. DTU886, evidenced by the methane yields measurement and presence of genes (e.g. *fwd*, *mtr* and *mcr*) (Figure 6).

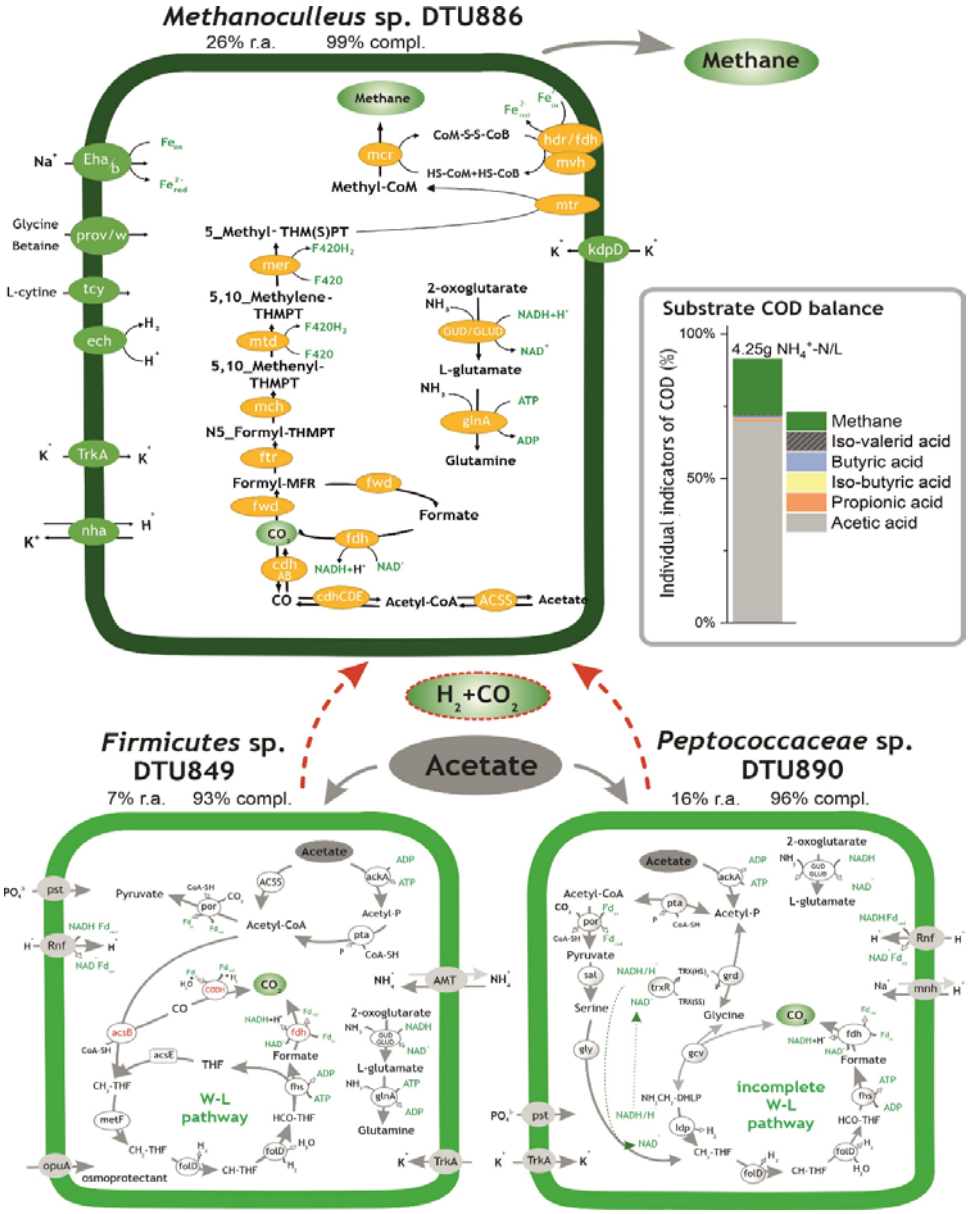

Figure 6. The figure on the right side represents the fate of acetate based on COD analysis in $G_{acetate}$. "R.a." and "compl." means "relative abundance" and "completeness", respectively. [Adapted from Paper II]

3.1.3 Ammonia tolerant microbiome in the $G_{methanol}$

$G_{methanol}$ at 7.25 g NH_4^+-N/L was dominated by *Methanomassiliicoccales* sp. DTU777, *Syntrophaceticus* sp. DTU782 and *Clostridiales* sp. DTU836 with 75%, 3%, and 5% of relative abundance, respectively (Figure 7). The complete methanogenesis pathway from methanol to methane in *Methanomassiliicoccales* sp. DTU777 suggested its methanogenic independence from other bacterial community. The co-occurrence of *acsE*, *acss*, and *metH* etc., in *Syntrophaceticus* sp. DTU782 and *Clostridiales* sp. DTU836 could be good indicators of

methanol degradation through two pathways. Briefly, the methylic group (in methanol) was firstly translocated to corrinoid Fe-S protein (CFeSP). Afterwards, CH_3-CFeSP was directly converted into acetate through acetate kinase pathway or was oxidized to acetate through partial WL pathway (Kremp et al. 2018) (Figure 7).

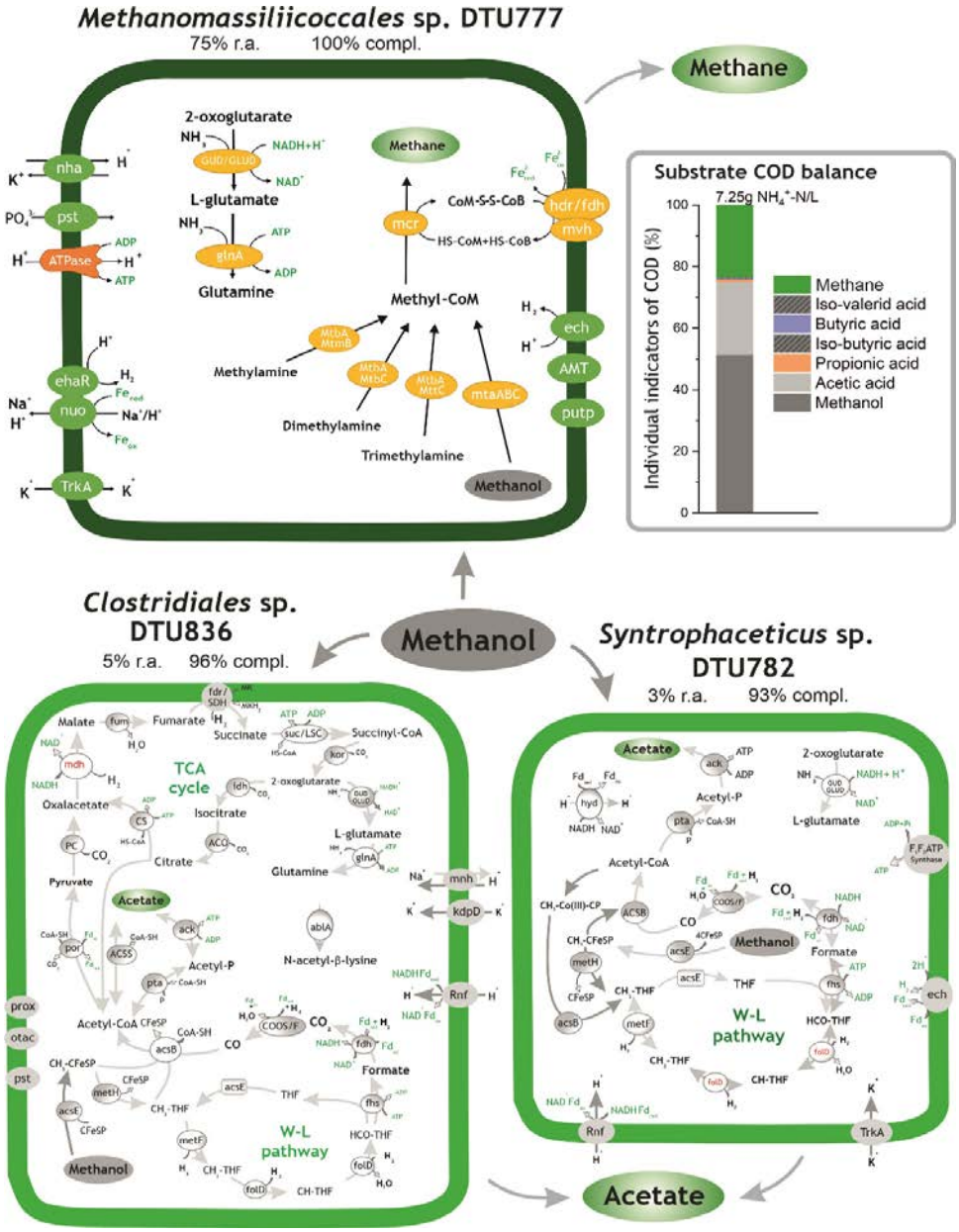

Figure 7. The figure on the right side represents the fate of methanl based on COD analysis in $G_{mehanol}$. "R.a." and "compl." means "relative abundance" and "completeness", respectively. [Adapted from Paper II].

3.1.4 Ammonia tolerant microbiome in the $G_{formate}$

The microbiome of $G_{formate}$ at 5.25 g NH_4^+-N/L was represented by *Firmicutes* sp. DTU848 (30%) and *Peptococcaceae* sp. DTU890 (22%), and *Methanothermobacter* sp. DTU779 (7%) (Figure 8). Based on the gene presence (*fdh*, *ftr*, *mch*, etc.) and methane yields, it was confirmed that *Methanothermobacter* sp. DTU779 performed hydrogenotrophic methanogenesis. Besides, incomplete reverse WL pathway and novel propionate generation pathway were detected in *Firmicutes* sp. DTU848 which explained the presence of acetate and propionate in $G_{formate}$. As mentioned before, *Peptococcaceae* sp. DTU890 possibly performed acetate oxidation using partial WL pathway coupled with the glycine cleavage system. Besides, *Peptococcaceae* sp. DTU890 and *Firmicutes* sp. DTU848 encoded formate dehydrogenase (*fdh*) and sodium ion pump (Rnf) that could be used as CO_2/H_2 sink for *Methanothermobacter* sp. DTU779 (Lins et al. 2012).

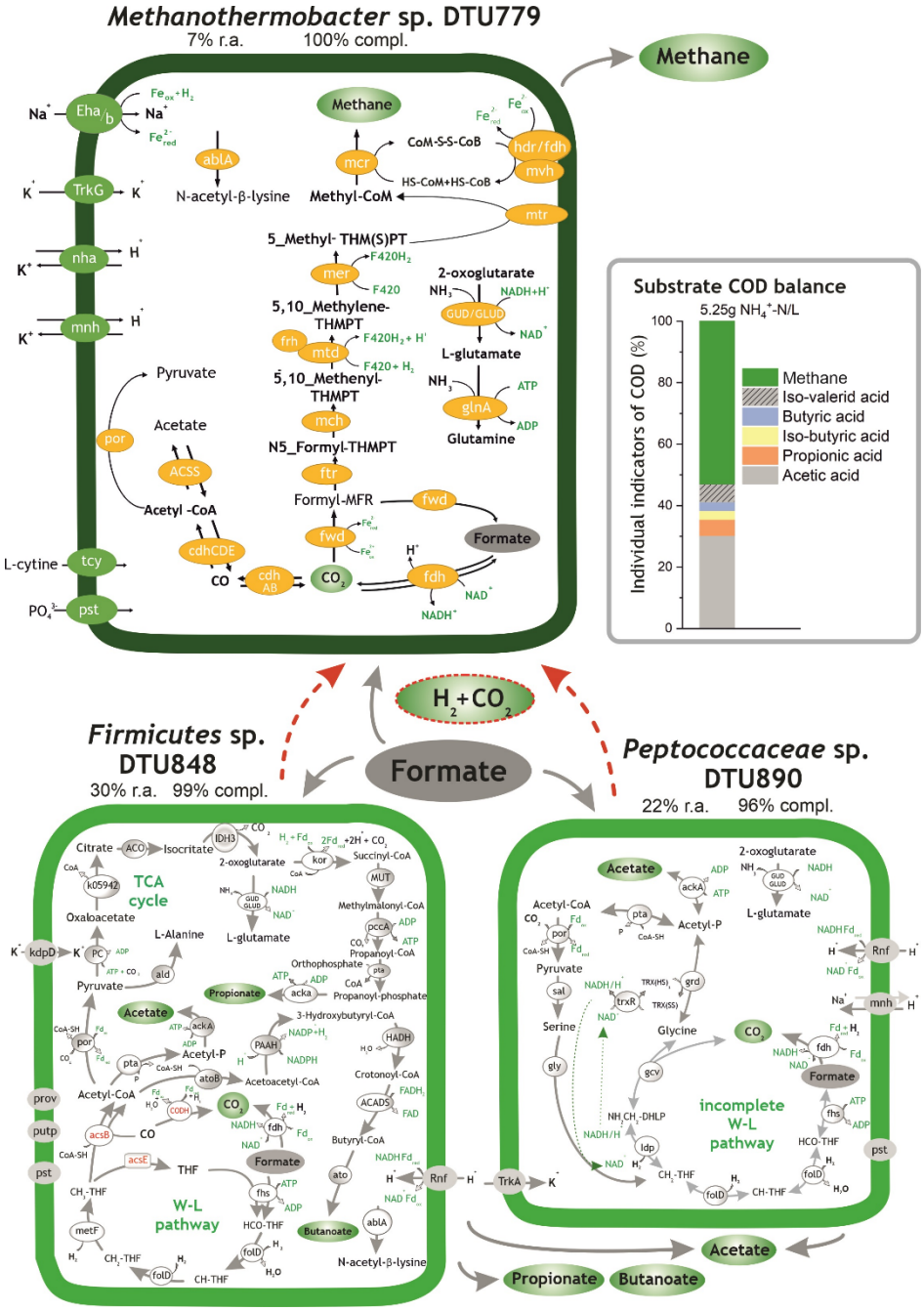

Figure 8. The figure on the right side represents the fate of formate based on COD analysis in $G_{formate}$. "R.a." and "compl." means "relative abundance" and "completeness", respectively. [Adapted from Paper II].

3.1.5 Ammonia tolerant microbiome in the $G_{H2/CO2}$

In the $G_{H2/CO2}$ at 7.25 g NH_4^+-N/L, *Methanothermobacter* sp. DTU779 showed higher ammonia tolerance to 7.25 g NH_4^+-N/L and accounted for an even higher relative abundance of 33% (5 times higher than in $G_{formate}$) (Figure 9). This finding confirmed *Methanothermobacter* sp. DTU779 preferred H_2 over formate as electron donor for methanogenesis (Lins et al. 2012). Additionally, the

bacterial community was dominated by *Pelotomaculum* sp. DTU813 (20% of relative abundance) and *Peptococcaceae* sp. DTU890 (6% of relative abundance). According to metabolic reconstruction, the parasitic relationship might develop between *Methanothermobacter* sp. DTU779 and *Pelotomaculum* sp. DTU813 where *Methanothermobacter* sp. DTU779 provided pyruvate as the substrate for *Pelotomaculum* sp. DTU813. This hypothesis was in agreement with other literature where the conversion of pyruvate to acetate and propionate occurred in *Pelotomaculum thermopropionicum* (Imachi et al. 2002). Since *Peptococcaceae* sp. DTU890 had versatile metabolic capabilities, it could produce or consume CO_2/H_2 and acetate depending upon metabolites' concentrations in the reactors. Thus the role of *Peptococcaceae* sp. DTU890 needed further investigation.

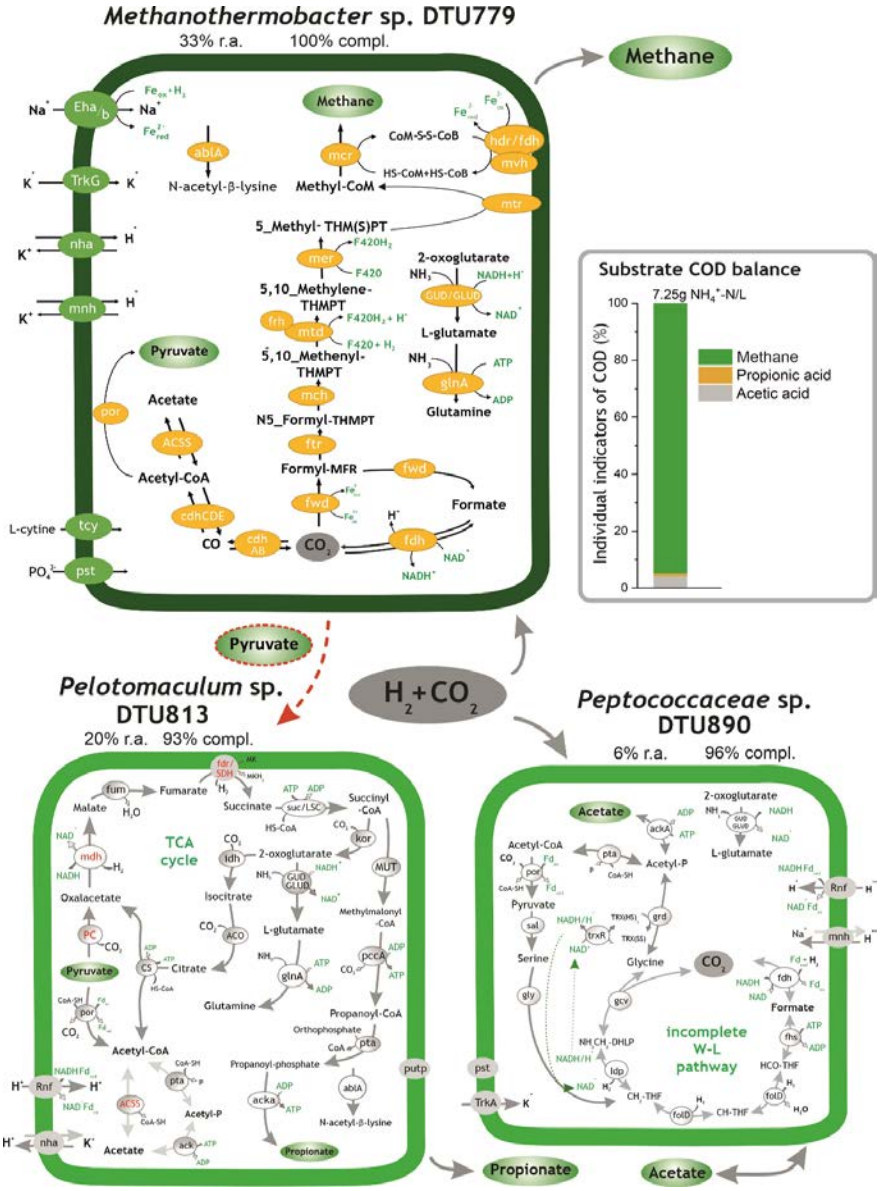

Figure 9. The figure on the right side represents the fate of H_2/CO_2 based on COD analysis in $G_{H2/CO2}$. "R.a." and "compl." means "relative abundance" and "completeness", respectively. [Adapted from Paper II].

3.2 Mechanism of microbial tolerance to ammonia

The single carbon source and stepwise increased ammonia concentrations drove the original inocula into four highly divergent communities with varied ammonia tolerance. The genes related to osmotic regulators, such as the K^+ uptake system (TrKA), sodium/proton antiporter (*nha*) system, osmoprotectant (glutamate, glycine betaine, and N^{ε}-acetyl-L-lysine, etc.), and energy converting complexes (e.g. Eha/b and Ech), might contribute microbes to counteract ammonia stress (Figure 10) (Kadam and Boone 1996, Sudmalis et al. 2018, Kraegeloh et al. 2005, Müller et al. 2005). Furthermore, the presence of distinct bacteria was linked to their role in supporting methanogen adaptation to ammonia through metabolic complementarity (Capson-Tojo et al. 2020, Zhu et al. 2020). This study expended the knowledge about the intricate syntrophic-supported food web among ammonia tolerant microbiomes grown on acetate, formate, H_2-CO_2, and methanol.

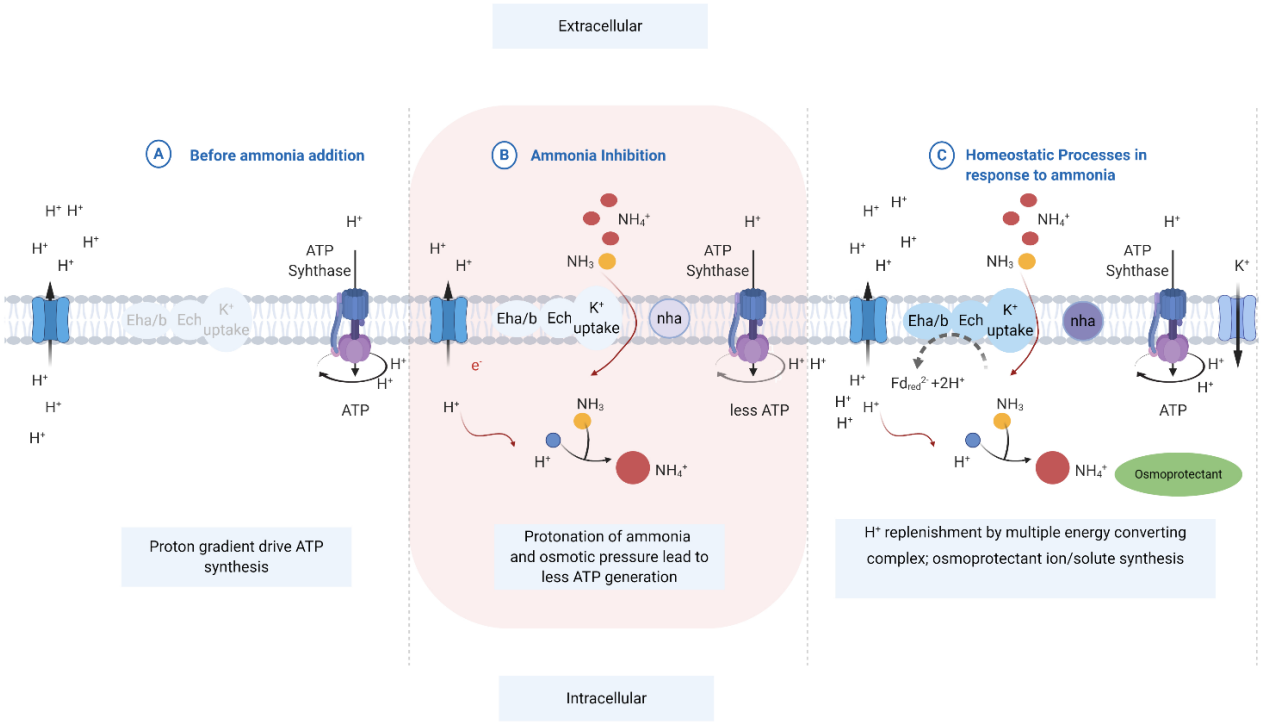

Figure 10. The response of methanogen to ammonia in different situations was proposed: a) before ammonia inhibition. b) under ammonia inhibition. c) homeostatic regulation to counteract ammonia stress. [Adapted from Paper II].

4 Bioaugmentation as an effective strategy to recover AD from ammonia inhibition

Bioaugmentation is the introduction of specialized microbial consortia into an under-performing system to speed up the degradation rate of organic matters. Bioaugmentation has been applied to increase methane yields from the N-rich substrate, reduce the recovery period of the AD process (Fotidis et al. 2014, Schauer-Gimenez et al. 2010), and decrease the total solid (TS) content (Tambone et al. 2010). Besides, discharged digestate containing bioaugmentation inocula can be used as a soil amendment or fertilizer, which is exactly following the circular economy (Favaro et al. 2019, Tambone et al. 2010). Conversely, the other technical attempts like magnetite and zeolite addition need extra separation steps before discharge, which poses technical challenges. Many researchers have proved that the bioaugmentation with ammonia tolerant methanogen promoted the conversion of organic matter to methane at middle-high ammonia levels (3-6 g NH_4^+-N /L) (Tian et al. 2019b, Yang et al. 2019, Town and Dumonceaux 2016, Li et al. 2017). Even though these findings provide good guidance on AD operation, the biological mechanisms behind bioaugmentation performance remains absent. It raises the doubt that why the bioaugmentation inocula own remarkble tolerance to ammonia and how they develop specific syntrophic networks, which awaits further discovery.

4.1 Bioaugmentation with pure *M. bourgensis* MS2 on two mesophilic CSTR reactors

To recover methane production from ammonia inhibition, bioaugmentation was applied in two identical mesophilic CSTRs (namely, R_{con} and R_{bio}) at an organic loading rate of 3.4 g VS/L/day. The whole process was divided into five periods, during which urea ($CO(NH_2)_2$) and ammonium chloride (NH_4Cl) were mixed into OFMSW as simulated N-rich feedstock. Ammonia levels in the CSTRs were increased stepwise from 9.5 g NH_4^+-N /L (P1) to 13.5 g NH_4^+-N /L (P3). During P4, ammonia acclimatized *M. bourgensis* MS2 strain with volatile suspended solids (VSS) of 67 mg/L was injected into the R_{bio} and the same volume of cultivation medium into the R_{con}. The experimental design was presented in Table 3.

Table 3. Details of the experimental process. [Adapted from Paper III]

Phase	Days	TAN	Extra added ammonia	
		(g NH_4^+-N/L)	$CO(NH_2)_2$ (g NH_4^+-N/L	NH_4Cl (g NH_4^+-N/L)
P1	0-5	9.5	4.5	3.9
P2	6-22	11.5	5.5	4.9
P3	23-50	13.5	6.5	5.9
P4 (Bioaugmentation)	51-54	13.5	-	-
P5	55-120	13.5	6.5	5.9

* "-": No extra ammonia addition

4.1.1 Reactor performance

Compared to the period without extra ammonia addition (described in section 2.1), the 25% reduction of methane yields in two reactors (P1 to P3) indicated severe inhibition occurring. While after bioaugmentation, a 21% increase in methane production yields (P5) was achieved in comparison to P3 (Figure 11). Correspondingly, VFA levels in R_{bio} reduced from 15,000 to 5,398 mg/L, and the VFA levels in R_{con} had been exceeding 7,500 mg/L revealing a severe ammonia inhibition occurring (Figure 11). The results were consistent with the previous research that bioaugmentation could alleviate the inhibitory effect of ammonia on AD performance (Capson-Tojo et al. 2020, Fotidis et al. 2017)

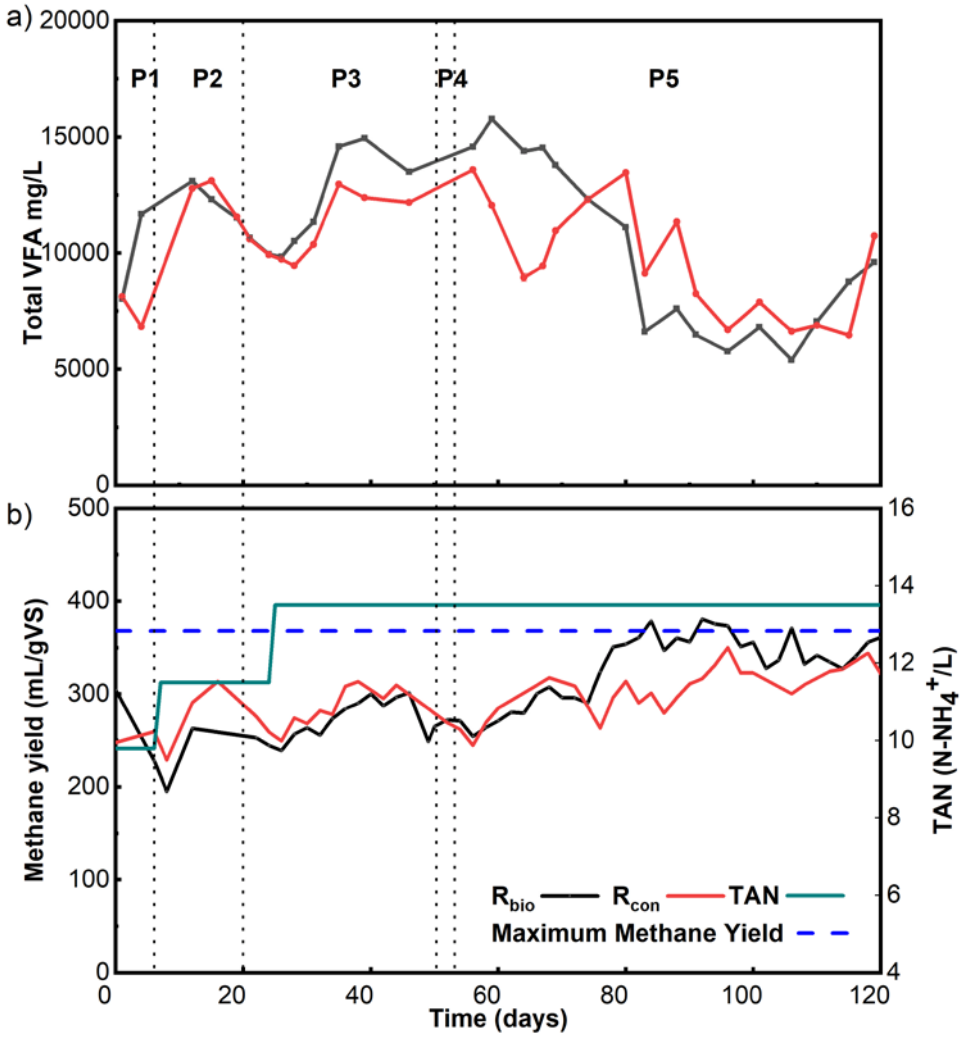

Figure 11. a) the VFA and b) methane production change through the experimental process.

4.1.2 Representative microbial metabolic interaction

The bioaugmentation with *M. bourgensis* triggered a 4.7, 2.4, and 1.5-fold increase in the relative abundance of *Peptococcaceae* spp. (DTU895, DTU900, and DTU 903), *Syntrophaceticus* sp. DTU 783 and *Tissierellales* sp. DTU879, respectively, between P3 to P5 (Figure 12).

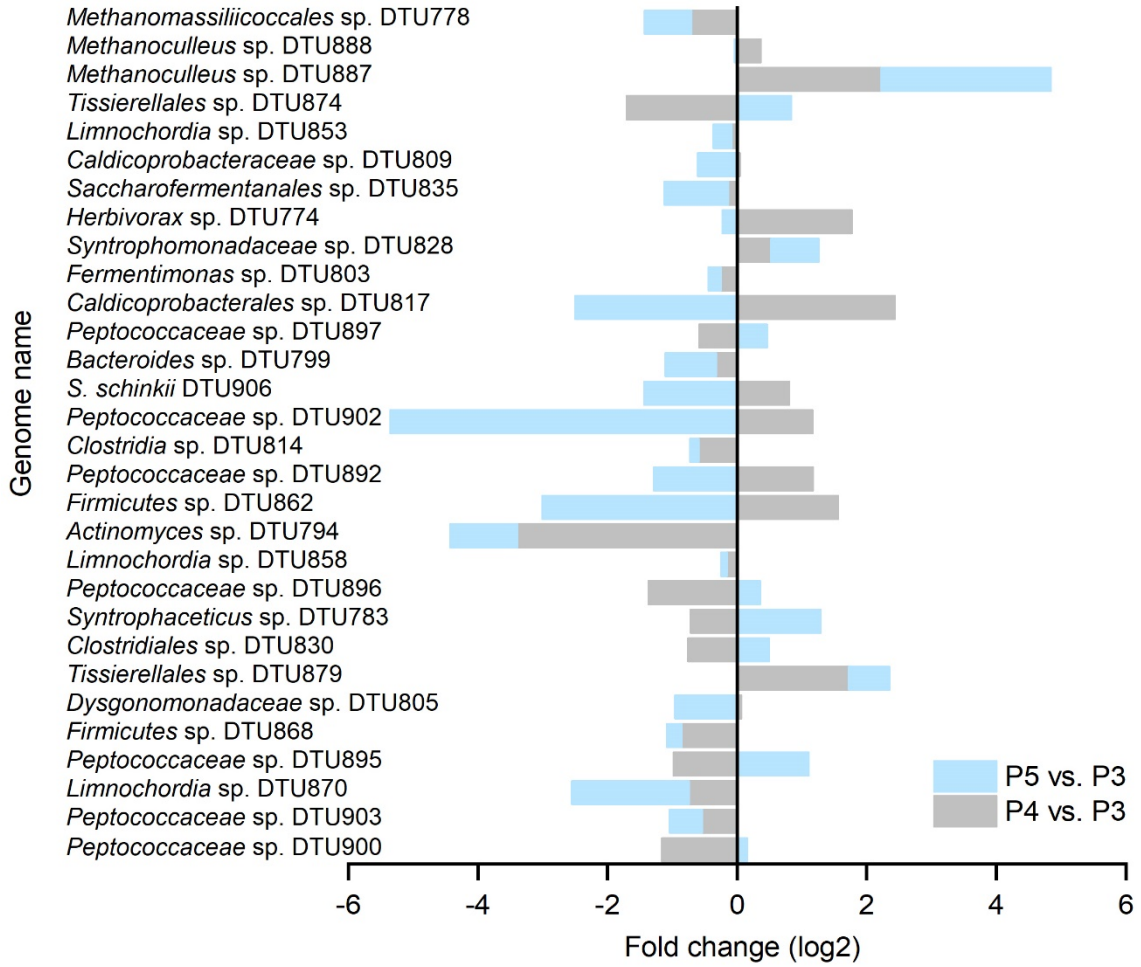

Figure 12. The shift of dominant MAGs was based on the fold change (log2) between the different periods. [Adapted from Paper III]

Correspondingly, the metabolic interactions among these dominant MAGS were reconstructed using metagenomics analysis (Figure 13). Two glucose catabolic pathways were detected in *Peptococcaceae* spp., and *Tissierellales* sp. DTU879, which might explain their dominant role in degrading carbohydrates-rich OFMSW. Specifically, pyruvate as intermediate, was derived from Embden-Meyerhof-Parnas (EMP) process. It was further converted to H_2/CO_2 through the first pathway coupling glycine cleavage system with tetrahydrofolate pathway. During the second pathway, the pyruvate was directly converted to acetate and H_2/CO_2, as evidenced by the presence of functional genes i.e., *kor*, *pta*, and *ackA* (Zhu et al. 2020).

Furthermore, the addition of *M. bourgensis* stimulated the 1.5-fold increase of *Syntrophaceticus* sp. DTU783 (Figures 12 and 13). Two acetate degradation pathways (i.e. WL pathway and glycine cleavage system coupling with the tetrahydrofolate pathway) were reconstructed in *Syntrophaceticus* sp. DTU783.

These multiple acetate degradation pathways possibly contributed its flexibility to varying environmental conditions or the absence of a syntrophic partner. The negative correlation between *Syntrophaceticus* sp. DTU783 and acetate suggested *Syntrophaceticus* sp. DTU783 played an essential role in scavenging acetate at elevated ammonia levels. However, the bioaugmentation with SAOB alone hardly affected the AD performance under ammonia inhibition (Yang et al. 2019, Westerholm et al. 2012).

Methanoculleus sp. DTU887 (the bioaugmentation inocula) contained the genes i.e., *putp*, *proW/V*, *kdp* and *mnhBCDE*, that were responsible for cells osmoregulation (Engelhardt 2007, Meury and Kohiyama 1992) (Figure 13). Besides, the multiple energy regulating complexes (Mtr, Eha, Ech and V/A type ATP synthase) could be the winning strategy to optimize its energy metabolism under severe environment (Vanwonterghem et al. 2016, Sapra et al. 2003). These genetic characteristics enabled its superior tolerance to ammonia stress and capability to perform stable methanogenesis process in ammonia-inhibited reactors. The establishment of *Methanoculleus* sp. DTU887 consumed the H_2 promptly, which stimulated the growth of *Syntrophaceticus* sp. DTU783, thus enhanced the acetate oxidizing rate. Like a domino effect, the complete chain of electron transfer between bacteria and methanogen was resumed. Eventually, the complete syntrophic substrate degradation was accelerated with a 21% increase in methane yield (Figure 11).

In summary, this study confirmed the feasibility of bioaugmentation as an efficient strategy to counteract high ammonia stress up to 13.5 g NH_4^+-N /L. Genome-centric analysis revealed that bioaugmentation inocula stimulated the growth of glucose degraders and acetate oxidizers in CSTR systems. The presence of parallel degradation pathways of both glucose and acetate in these increased bacteria might be their survival strategy under stressed conditions. Meanwhile, the exceptional ammonia tolerance of *Methanoculleus* sp. DTU887 might owe to its various complexes that were involved in energy conversion and osmoregulation.

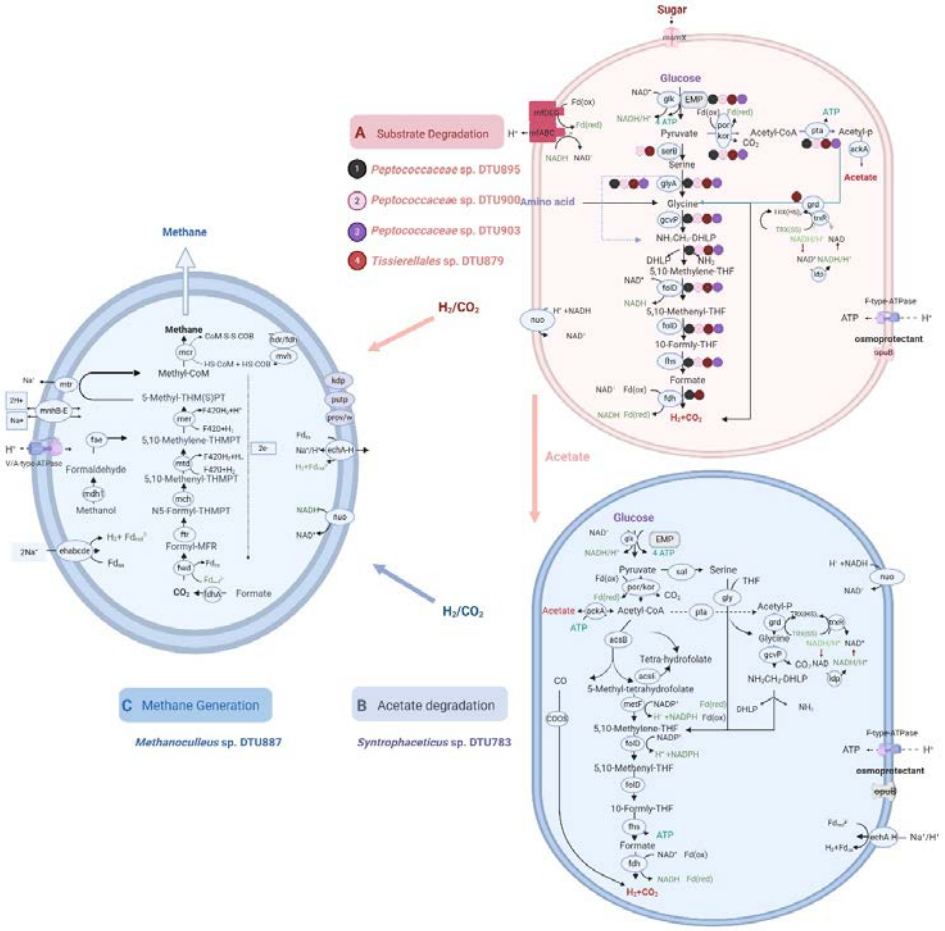

Figure 13. Metabolic reconstruction of the OFMSW degrading syntrophic community. Metagenomic data revealed pathways involved in substrate degradation, in the utilization of intermediates compounds (H_2/CO_2, acetate), and methanogenesis. [Adapted from Paper III]

5 Long-term preservation and fast recovery of ammonia tolerant methanogenic culture

Bioaugmentation effect to increase methane production in the AD system has been recognized (Fotidis et al. 2014, Tian et al. 2019d). However, methanogens are slow-growing, which means the period of cultivation is long (Imachi et al. 2002, Rincón et al. 2010, Cheng et al. 2008, Xue et al. 2006). It poses a technical challenge to perform timely bioaugmentation. The delay in recovering full-scale anaerobic digester from ammonia stress results in economic loss. Therefore, bioaugmentation with ready-to-use inocula is required for stable AD operation of N-rich organic waste. Until now, ready-to-use inocula have been rarely investigated to speed up bioaugmentation process (Massalha et al. 2015, Yarberry et al. 2019). Thus, it is crucial to develop a fast and easy method where ammonia tolerant consortia could be preserved. Several microbial preservation strategies have been explored, such as freeze-drying (Yarberry et al. 2019), heat-drying (Bhattad et al. 2017), liquid nitrogen storage (Rothrock et al. 2011), living cells entrapped in a gel or liquid medium (Banu et al. 2018, Iacobellis and DeVay 1986). In practice, there are many challenges in preserving anaerobic microorganism, due to their vulnerability to oxygen, operation cost, and transportation cost. However, agar gel and liquid medium seem to show tremendous potential as preservation carrier and their effectiveness for maintaining the metabolic activity of ammonia tolerant inoculum needs to be investigated.

5.1 Evaluation of microbial preservation method

In paper IV, two carriers (i.e. agar gel and liquid BA media) and storage temperatures of 4°C and 24°C were used, and ammonia tolerant enrichments were preserved with different time frames (i.e., 1, 7, 14, 28, 84, and 168 days). Specifically, the inocula collected from the previous research (Tian et al. 2019c) were cultivated with BA medium containing 4 g/L acetate and 9 g NH_4^+-N/L. The microbial enrichments were harvested for the preservation step when over 80% of the theoretical methane potential of acetate (373.33 mL CH_4/g VS) was achieved. Four different preservation strategies were performed as follows: 1) agar gel at 24°C ($PG_{(24°C)}$), 2) liquid BA medium at 24°C ($PL_{(24°C)}$), 3) agar gel at 4°C ($PG_{(4°C)}$), and 4) liquid BA medium at 4°C ($PL_{(4°C)}$). After 1, 7, 14, 28, 84, and 168 days of preservation, their efficiencies were evaluated based on

the methane production yields and lag phases. The detail of the whole process was presented in Table 4.

Table 4. Experimental setup. [Adapted from paper IV]

Strategy	Preservation medium	Preservation temperature °C	Reactivation
$PSG_{(24°C)}$	5 mL Inoculum + 2 mL Agar solution	24	33 mL BA medium+ 4g HAc/L+ 9.00 g NH_4^+-N/L
$PSG_{(4°C)}$	5 mL Inoculum + 2 mL Agar solution	4	33 mL BA medium+ 4g HAc/L+ 9.00 g NH_4^+-N/L
$PSL_{(24°C)}$	5 mL Inoculum	24	35 mL BA medium+ 3.77g HAc/L + 9.0 g NH_4^+-N/L
$PSL_{(4°C)}$	5 mL Inoculum	4	35 mL BA medium+ 3.77 g HAc/L+ 9.00 g NH_4^+-N/L

5.2 Methanogenic activity test after preservation

Among the four strategies, $PG_{(24°C)}$ showed advantages in maintaining microbial methanogenic activity for up to 168 days, and the lag-phase was less than 25 days during the revival test (Figure 14). The maximum time that microbes required to retain microbial metabolism in $PL_{(24°C)}$ were 84 days with a lag-phase of 41 days. Furthermore, when the preservation frame was within 14 days, $PL_{(24°C)}$ showed a shorter lag phase (less than 18 days) compared to $PG_{(24°C)}$. Conversely, both $PG_{(4°C)}$ and $PL_{(4°C)}$ were slow recovery or inactive after seven days of preservation, suggesting storage under 4°C was inefficient.

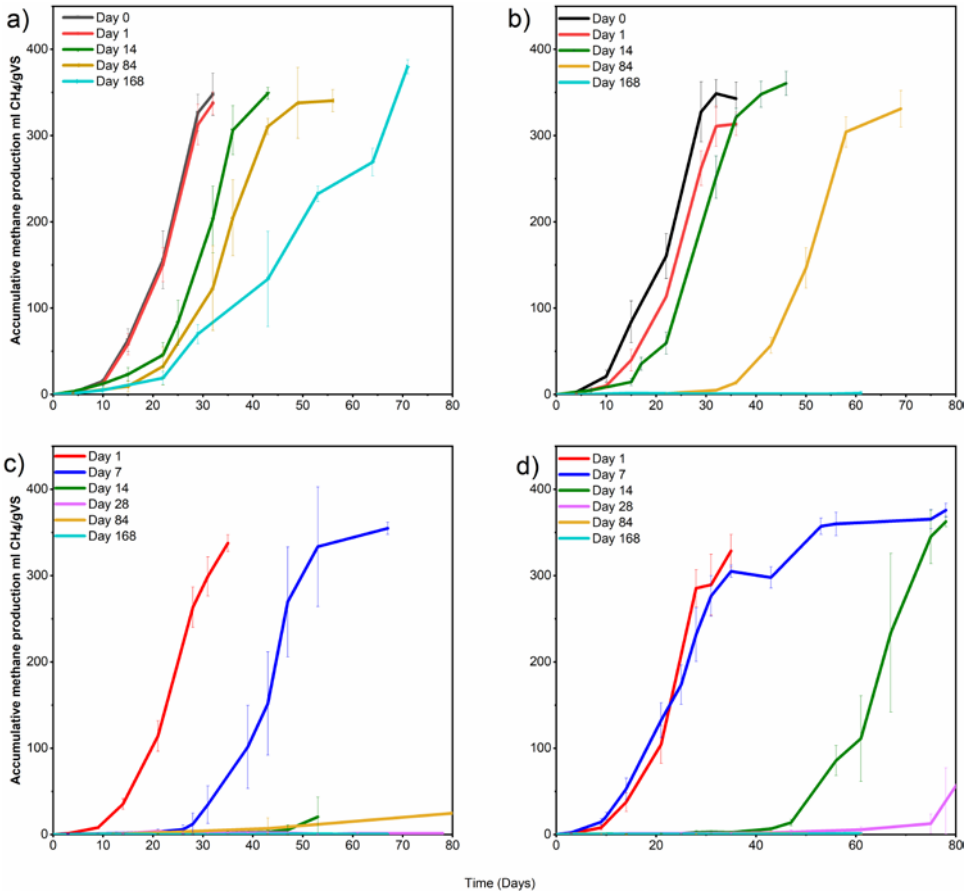

Figure 14. The accumulative methane production yield of the preserved ammonia-tolerant methanogenic enrichments during reactivation process: a) $PG_{(24°C)}$; b) $PL_{(24°C)}$; c) $PG_{(4°C)}$; d) $PL_{(4°C)}$. [Adapted from paper IV]

5.3 Microbial response to different preservation approaches

The microscopy using live/dead differential staining showed that alive cells were present in $PG_{(24°C)}$ and $PL_{(24°C)}$ after 84 days of preservation (Figures 15.a and b). When it was up to 168 days of preservation, the alive cells were only observed in $PG_{(24°C)}$ (Figure 16.a), which confirmed the cells entrapped in $PL_{(24°C)}$ were dead and not just under inactive state (Oliver 2010).

However, few alive cells were detected in $PG_{(4°C)}$ and $PL_{(4°C)}$ after 84 and 168 days of preservation which was consistent with their meagre methane yields (Figures 15.c, d, and Figures 16.c, d). Thus, 4°C was not appropriate temperature to maintain microbial viability in this study. These results agreed with other literature that carbon source addition could not stimulate microbial activity after 28 days of storage at 4±1°C (Scherer et al. 1981). Based on the results above, $PG_{(24°C)}$ was proposed as the most efficient long-term preservation method compared to others.

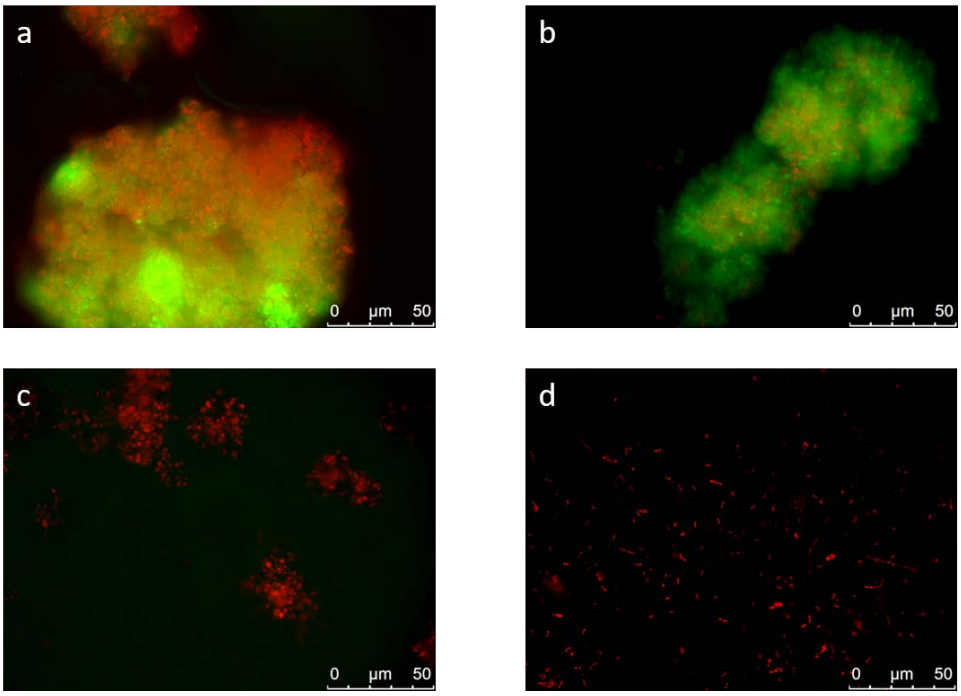

Figure 15. Identification of live or dead microorganisms in different preservation conditions: a) $PG_{(24°C)}$; b) $PL_{(24°C)}$; c) $PG_{(4°C)}$; d) $PL_{(4°C)}$ after 84 days preservation. DNA in dead or damaged microbial cell walls/membranes were stained with red fluorescence; DNA in alive microbial cell walls/membranes were stained with green fluorescence. [Adapted from paper IV].

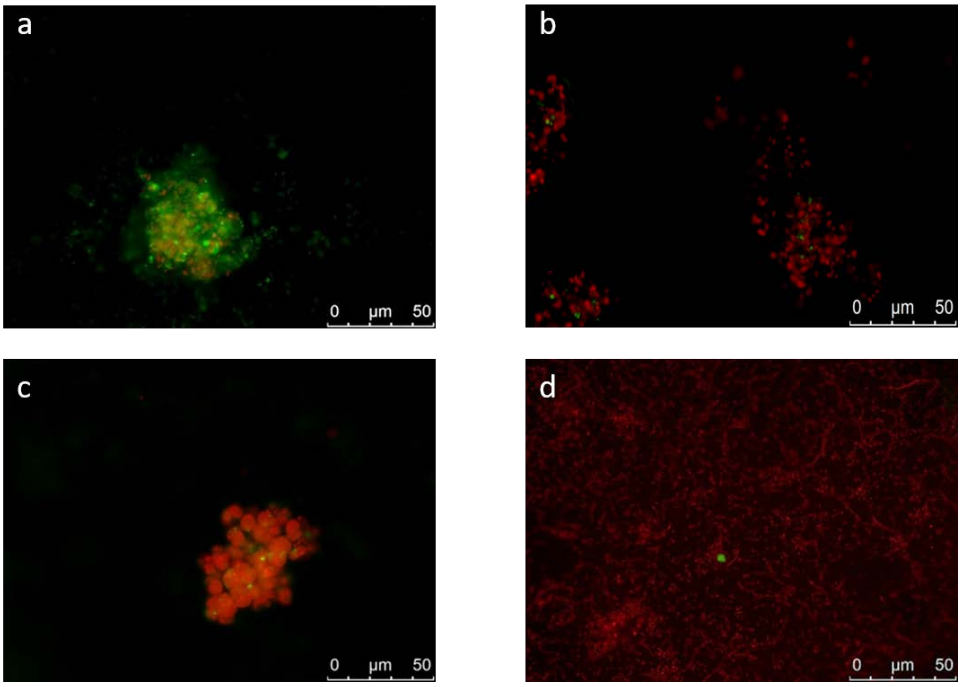

Figure 16. Identification of live or dead microorganisms in different preservation conditions: a) $PG_{(24°C)}$; b) $PL_{(24°C)}$; c) $PG_{(4°C)}$; d) $PL_{(4°C)}$ after 168 days preservation. DNA in dead or

damaged microbial cell walls/membranes were stained with red fluorescence; DNA in alive microbial cell walls/membranes were stained with green fluorescence. [Adapted from paper IV].

The initial inoculum was dominated by *Methanomassiliicoccus luminyensis* OTU18 (17.4% of relative abundance), *Methanosarcina soligelidi* OTU01 (12%), and *Methanoculleus palmolei* OTU12 (0.6%), respectively (Tian et al. 2019c). However, the preservation process changed the microbial community composition. In detail, the relative abundance of *M. luminyensis* OTU18 in all groups decreased significantly to less than 3% ($p < 0.05$) of the total population, revealing the sensitivity of *M. luminyensis* OTU18 to the preservation environment (Figure 17). Meanwhile, the increase in relative abundances of *M. soligelidi* OTU01, ranging from 21.6% to 33.7% suggested its high potential as long-term preserved methanogen. The other dominant methanogen was *M. palmolei* OTU12 with the 4.5-fold increase in $PL_{(24°C)}$-84 and $PG_{(24°C)}$-168 compared to the initial inocula, indicating its high robustness to long-term preservation.

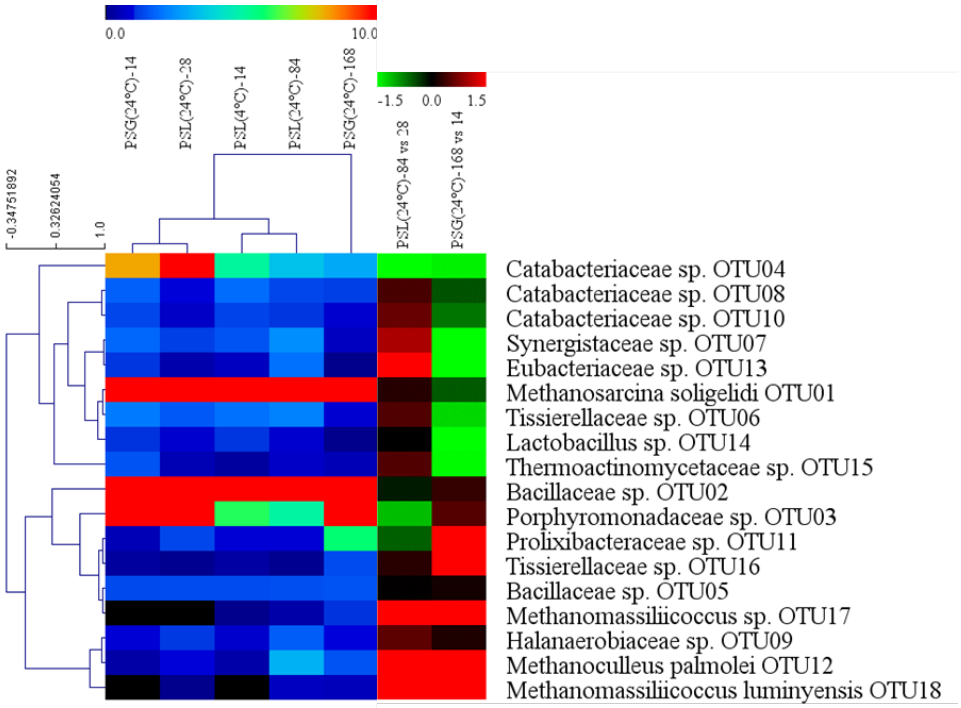

Figure 17. Hierarchical cluster analysis of the abundant microbes after preservation. Two right columns represent the fold change (log2) of each OTU between the two periods. [Adapted from paper IV].

Overall, paper IV assessed different approaches for the long-term preservation of ammonia tolerant methanogenic cultures and found that the $PG_{(24°C)}$ was the best preservation method, followed by the $PL_{(24°C)}$. The microbial analysis showed that *M. soligelidi* OTU01 and *M. palmolei* OTU12 were robust enough

to long-term preservation environments, including temperature and starvation shock. Thus this study developed successful and easy preservation methods and made the ready-to-use inocula possible for the timely bioaugmentation in full-scale biogas reactors.

6 Conclusions

This Ph.D. project mainly focused on developing methane recovery strategies to overcome ammonia inhibition and unveiling the microbial response to ammonia using high-throughput sequencing technology. Firstly, acclimatization and bioaugmentation approaches were applied to improve methane production during AD of N-rich substrate. Secondly, 16S rRNA amplicon sequencing technology and genome-centric analysis were used to decipher the effect of microbial composition on AD performance. Thirdly, the methods to preserve ammonia tolerant inocula were achieved. Specifically, the key findings of this Ph.D. project are listed:

1) Acclimatization up to 8.5 g NH_4^+-N /L was proved as an efficient approach to achieve stable methane yields with fluctuation less than 10% during AD of OFMSW.

2) During the stepwise increase of TAN, the dominant methanogen gradually shifted from *Methanosaeta concilii* to *Methanosarcina soligelidi*.

3) The different microbial tolerances to ammonia stress were observed: the consortia grown on methanol or H_2/CO_2 could adapt to ammonia levels up to 7.25 g NH_4^+-N/L, followed by formate group to 5.25 g NH_4^+-N/L and acetate group to 4.25 g NH_4^+-N/L.

4) The osmoprotectant synthesis/uptake (K^+, glutamate, glutamine, N^{ε}-acetyl-L-lysine, and glycine betaine, etc.) and energy regulating complexes (Ech and Eha/b), were proposed to improve microbial tolerance to ammonia stress.

5) The dominant bacteria in each microbiome was linked to their role in supporting the methanogens through catabolic complementarity.

6) Bioaugmentation with *Methanoculleus* sp. DTU887 remarkably improved the methane production yield by 21% and reduced VFA by 10% in CSTR at 13.5 g NH_4^+-N/L.

7) Genome-centric analysis revealed that the dominant bacteria (i.e., *Peptococcaceae* spp. and *Tissierellales* sp. DTU879) were important glucose degraders. The derived acetate was further degraded by *Tissierellales* sp. DTU879 and *Syntrophaceticus* sp. DTU783 at 13.5 g NH_4^+-N/L.

8) *Methanoculleus* sp. *DTU887* as an H_2 scavenger might play an essential role in supporting the growth of *Peptococcaceae* spp., *Tissierellales* sp.

DTU879 and *Syntrophaceticus* sp. DTU783 by complementary metabolic reactions at 13.5 g NH_4^+-N/L.

9) The presence of two parallel degradation pathways for both glucose and acetate possibly provided the dominant species (e.g., *Peptococcaceae* spp., *Tissierellales* sp. DTU879, and *Syntrophaceticus* sp. DTU783) enough flexibility against extremely high ammonia stress.

10) Ammonia tolerant methanogens could be well preserved in agar gel for168 days and liquid media for 84 days at 24°C, respectively.

11) *Methanosarcina soligelidi* and *Methanoculleus palmolei* showed robustness to long-term preservation, as evidenced by a high methanogenic activity after 168 days of preservation.

Overall, this PhD project proved the feasibility of stable methane production in the full-scale AD of N-rich organic waste. The knowledge about microbial tolerance to ammonia could be used to optimize AD process by controlling microbial composition. Based on these findings, the customized bioaugmentation method was provided according to the different conditions in AD, e.g, feedstock composition, ammonia levels.

7 Future perspective

This Ph.D. project provides sustainable approaches to improve biomethane production yields from N-rich organic waste. More insights into microbial tolerance to ammonia are revealed using high-throughput sequencing technology. To further optimize the biomethane process, the following suggestions are listed:

- Mathematical modelling can be applied to predict the timing point of bioaugmentation during AD of N-rich substrate to avoid the loss of methane.

- Metatranscriptomic analysis is vital to identify the real-time metabolic pathway that occurred under different ammonia levels when parallel pathways are present in critical microbes.

- The flux balance analysis is necessary to identify the microbial roles in the food web of AD, which can provide guidance for optimizing the microbial composition in the AD system.

- The possibility of gene transfer in terms of ammonia tolerance among anaerobic microorganisms could be tested to understand ammonia acclimatization further.

8 References

Ferroukhi, R., Nagpal, D., Lopez-Peña, A., Hodges, T., Mohtar, R., Daher, B., Mohtar, S. and Keulertz, M. (2015) Renewable energy in the water, energy & food nexus. IRENA, Abu Dhabi.

Minelgaitė, A. and Liobikienė, G. (2019) Waste problem in European Union and its influence on waste management behaviours. Science of the Total Environment 667, 86-93.

Schroeder, P., Anggraeni, K. and Weber, U. (2019) The relevance of circular economy practices to the sustainable development goals. Journal of Industrial Ecology 23(1), 77-95.

Favaro, L., Jansen, T. and van Zyl, W.H. (2019) Exploring industrial and natural Saccharomyces cerevisiae strains for the bio-based economy from biomass: the case of bioethanol. Critical Reviews in Biotechnology 39(6), 800-816.

Briassoulis, D., Pikasi, A. and Hiskakis, M. (2019) End-of-waste life: Inventory of alternative end-of-use recirculation routes of bio-based plastics in the European Union context. Critical reviews in environmental science and technology 49(20), 1835-1892.

Tozlu, A., Özahi, E. and Abuşoğlu, A. (2016) Waste to energy technologies for municipal solid waste management in Gaziantep. Renewable and Sustainable Energy Reviews 54, 809-815.

Tian, H., Wang, X. and Tong, Y.W. (2020) Waste-to-Energy. Ren, J. (ed), pp. 235-264, Academic Press.

Ambaye, T.G., Rene, E.R., Dupont, C., Wongrod, S. and van Hullebusch, E.D. (2020) Anaerobic Digestion of Fruit Waste Mixed With Sewage Sludge Digestate Biochar: Influence on Biomethane Production. Frontiers in Energy Research 8, 14.

Satchwell, A.J., Scown, C.D., Smith, S.J., Amirebrahimi, J., Jin, L., Kirchstetter, T.W., Brown, N.J. and Preble, C.V. (2018) Accelerating the deployment of anaerobic digestion to meet zero waste goals, ACS Publications.

McAnulty, M.J., Poosarla, V.G., Kim, K.-Y., Jasso-Chávez, R., Logan, B.E. and Wood, T.K. (2017) Electricity from methane by reversing methanogenesis. Nature Communications 8(1), 1-8.

Tambone, F., Scaglia, B., D'Imporzano, G., Schievano, A., Orzi, V., Salati, S. and Adani, F. (2010) Assessing amendment and fertilizing properties of digestates from anaerobic digestion through a comparative study with digested sludge and compost. Chemosphere 81(5), 577-583.

Angelidaki, I., Karakashev, D., Batstone, D.J., Plugge, C.M. and Stams, A.J. (2011a) Methods in enzymology, pp. 327-351, Elsevier.

Karube, I., Kuriyama, S., Matsunaga, T. and Suzuki, S. (1980) Methane production from wastewaters by immobilized methanogenic bacteria. Biotechnology and Bioengineering 22(4), 847-857.

Lin, L., Xu, F., Ge, X. and Li, Y. (2019) Advances in Bioenergy. Li, Y. and Ge, X. (eds), pp. 121-181, Elsevier.
Uçkun Kiran, E., Stamatelatou, K., Antonopoulou, G. and Lyberatos, G. (2016) Handbook of Biofuels Production (Second Edition). Luque, R., Lin, C.S.K., Wilson, K. and Clark, J. (eds), pp. 259-301, Woodhead Publishing.
Chen, Y., Cheng, J.J. and Creamer, K.S. (2008) Inhibition of anaerobic digestion process: a review. Bioresource technology 99(10), 4044-4064.
Ponsá, S., Ferrer, I., Vázquez, F. and Font, X. (2008) Optimization of the hydrolytic–acidogenic anaerobic digestion stage (55 C) of sewage sludge: Influence of pH and solid content. Water research 42(14), 3972-3980.
Campanaro, S., Treu, L., Kougias, P.G., Luo, G. and Angelidaki, I. (2018) Metagenomic binning reveals the functional roles of core abundant microorganisms in twelve full-scale biogas plants. Water research 140, 123-134.
Angelidaki, I., Karakashev, D., Batstone, D.J., Plugge, C.M. and Stams, A.J. (2011b) Biomethanation and its potential. Methods Enzymol 494, 327-351.
Wilson, D.B. (2011) Microbial diversity of cellulose hydrolysis. Current opinion in microbiology 14(3), 259-263.
Dimock, R. and Morgenroth, E. (2006) The influence of particle size on microbial hydrolysis of protein particles in activated sludge. Water research 40(10), 2064-2074.
Chen, H. and Chang, S. (2017) Impact of temperatures on microbial community structures of sewage sludge biological hydrolysis. Bioresource technology 245, 502-510.
Cazier, E.A., Trably, E., Steyer, J.-P. and Escudie, R. (2019) Reversibility of hydrolysis inhibition at high hydrogen partial pressure in dry anaerobic digestion processes fed with wheat straw and inoculated with anaerobic granular sludge. Waste Management 85, 498-505.
Myint, M., Nirmalakhandan, N. and Speece, R. (2007) Anaerobic fermentation of cattle manure: Modeling of hydrolysis and acidogenesis. Water research 41(2), 323-332.
Zhu, X., Campanaro, S., Treu, L., Kougias, P.G. and Angelidaki, I. (2019) Novel ecological insights and functional roles during anaerobic digestion of saccharides unveiled by genome-centric metagenomics. Water research 151, 271-279.
Zhou, M., Yan, B., Wong, J.W. and Zhang, Y. (2018a) Enhanced volatile fatty acids production from anaerobic fermentation of food waste: a mini-review focusing on acidogenic metabolic pathways. Bioresource technology 248, 68-78.
Tian, H., Yan, M., Treu, L., Angelidaki, I. and Fotidis, I.A. (2019a) Hydrogenotrophic methanogens are the key for a successful bioaugmentation to alleviate ammonia inhibition in thermophilic anaerobic digesters. Bioresource technology, 122070.

Chen, S., Dong, B., Dai, X., Wang, H., Li, N. and Yang, D. (2019) Effects of thermal hydrolysis on the metabolism of amino acids in sewage sludge in anaerobic digestion. Waste Management 88, 309-318.
Tezel, U., Tandukar, M. and Pavlostathis, S.G. (2011) Comprehensive Biotechnology (Second Edition). Moo-Young, M. (ed), pp. 447-461, Academic Press, Burlington.
Tian, H., Karachalios, P., Angelidaki, I. and Fotidis, I.A. (2018a) A proposed mechanism for the ammonia-LCFA synergetic co-inhibition effect on anaerobic digestion process. Chemical Engineering Journal 349, 574-580.
Ziels, R.M., Beck, D.A. and Stensel, H.D. (2017) Long-chain fatty acid feeding frequency in anaerobic codigestion impacts syntrophic community structure and biokinetics. Water research 117, 218-229.
Zhou, M., Yan, B., Wong, J.W.C. and Zhang, Y. (2018b) Enhanced volatile fatty acids production from anaerobic fermentation of food waste: A mini-review focusing on acidogenic metabolic pathways. Bioresource technology 248, 68-78.
Hao, L., Bize, A., Conteau, D., Chapleur, O., Courtois, S., Kroff, P., Desmond-Le Quéméner, E., Bouchez, T. and Mazéas, L. (2016) New insights into the key microbial phylotypes of anaerobic sludge digesters under different operational conditions. Water research 102, 158-169.
Alves, M., Vieira, J.M., Pereira, R.A., Pereira, M. and Mota, M. (2001) Effects of lipids and oleic acid on biomass development in anaerobic fixed-bed reactors. Part II: Oleic acid toxicity and biodegradability. Water research 35(1), 264-270.
Xu, Z., Shi, Z. and Jiang, L. (2011) Comprehensive Biotechnology (Second Edition). Moo-Young, M. (ed), pp. 189-199, Academic Press, Burlington.
Diekert, G. and Wohlfarth, G. (1994) METABOLISM OF HOMOACETOGENS. Antonie Van Leeuwenhoek International Journal of General and Molecular Microbiology 66(1-3), 209-221.
Borja, R. (2011) Comprehensive Biotechnology (Second Edition). Moo-Young, M. (ed), pp. 785-798, Academic Press, Burlington.
Westerholm, M., Moestedt, J. and Schnürer, A. (2016) Biogas production through syntrophic acetate oxidation and deliberate operating strategies for improved digester performance. Applied energy 179, 124-135.
Borja, R. and Rincón, B. (2017) Reference Module in Life Sciences, Elsevier.
Vanwonterghem, I., Evans, P.N., Parks, D.H., Jensen, P.D., Woodcroft, B.J., Hugenholtz, P. and Tyson, G.W. (2016) Methylotrophic methanogenesis discovered in the archaeal phylum Verstraetearchaeota. Nature microbiology 1(12), 1-9.
Lyu, Z., Shao, N., Akinyemi, T. and Whitman, W.B. (2018) Methanogenesis. Current Biology 28(13), R727-R732.
Chen, S., Cheng, H., Liu, J., Hazen, T.C., Huang, V. and He, Q. (2017) Unexpected competitiveness of Methanosaeta populations at elevated

acetate concentrations in methanogenic treatment of animal wastewater. Applied Microbiology and Biotechnology 101(4), 1729-1738.
Dyksma, S., Jansen, L. and Gallert, C. (2020) Syntrophic acetate oxidation replaces acetoclastic methanogenesis during thermophilic digestion of biowaste. Microbiome 8(1), 105.
Smith, K.S. and Ingram-Smith, C. (2007) Methanosaeta, the forgotten methanogen? Trends in microbiology 15(4), 150-155.
Rotaru, A.-E., Shrestha, P.M., Liu, F., Shrestha, M., Shrestha, D., Embree, M., Zengler, K., Wardman, C., Nevin, K.P. and Lovley, D.R. (2014) A new model for electron flow during anaerobic digestion: direct interspecies electron transfer to Methanosaeta for the reduction of carbon dioxide to methane. Energy & Environmental Science 7(1), 408-415.
Capson-Tojo, G., Moscoviz, R., Astals, S., Robles, Á. and Steyer, J.-P. (2020) Unraveling the literature chaos around free ammonia inhibition in anaerobic digestion. Renewable and Sustainable Energy Reviews 117, 109487.
Zabranska, J. and Pokorna, D. (2018) Bioconversion of carbon dioxide to methane using hydrogen and hydrogenotrophic methanogens. Biotechnology Advances 36(3), 707-720.
Watkins, A.J., Roussel, E.G., Webster, G., Parkes, R.J. and Sass, H. (2012) Choline and N, N-dimethylethanolamine as direct substrates for methanogens. Applied and Environmental Microbiology 78(23), 8298-8303.
Tian, H., Mancini, E., Treu, L., Angelidaki, I. and Fotidis, I.A. (2019b) Bioaugmentation strategy for overcoming ammonia inhibition during biomethanation of a protein-rich substrate. Chemosphere 231, 415-422.
Zhang, C.-J., Chen, Y.-L., Pan, J., Wang, Y.-M. and Li, M. (2020) Spatial and seasonal variation of methanogenic community in a river-bay system in South China. Applied Microbiology and Biotechnology, 1-11.
Morris, B.E., Henneberger, R., Huber, H. and Moissl-Eichinger, C. (2013) Microbial syntrophy: interaction for the common good. FEMS microbiology reviews 37(3), 384-406.
Stams, A.J. and Plugge, C.M. (2009) Electron transfer in syntrophic communities of anaerobic bacteria and archaea. Nature Reviews Microbiology 7(8), 568-577.
Jiang, Y., McAdam, E., Zhang, Y., Heaven, S., Banks, C. and Longhurst, P. (2019) Ammonia inhibition and toxicity in anaerobic digestion: A critical review. Journal of Water Process Engineering 32, 100899.
Rajagopal, R., Massé, D.I. and Singh, G. (2013) A critical review on inhibition of anaerobic digestion process by excess ammonia. Bioresource technology 143, 632-641.
Wittmann, C., Zeng, A.-P. and Deckwer, W.-D. (1995) Growth inhibition by ammonia and use of a pH-controlled feeding strategy for the effective

cultivation of Mycobacterium chlorophenolicum. Applied Microbiology and Biotechnology 44(3-4), 519-525.
Kadam, P.C. and Boone, D.R. (1996) Influence of pH on Ammonia Accumulation and Toxicity in Halophilic, Methylotrophic Methanogens. Applied and Environmental Microbiology 62(12), 4486-4492.
Chang, H., Hu, R., Zou, Y., Quan, X., Zhong, N., Zhao, S. and Sun, Y. (2020) Highly efficient reverse osmosis concentrate remediation by microalgae for biolipid production assisted with electrooxidation. Water research 174, 115642.
Engelhardt, H. (2007) Mechanism of osmoprotection by archaeal S-layers: a theoretical study. Journal of structural biology 160(2), 190-199.
Yang, Z., Wang, W., Liu, C., Zhang, R. and Liu, G. (2019) Mitigation of ammonia inhibition through bioaugmentation with different microorganisms during anaerobic digestion: Selection of strains and reactor performance evaluation. Water research 155, 214-224.
Fotidis, I.A., Karakashev, D., Kotsopoulos, T.A., Martzopoulos, G.G. and Angelidaki, I. (2013) Effect of ammonium and acetate on methanogenic pathway and methanogenic community composition. FEMS Microbiology Ecology 83(1), 38-48.
Worm, P., Müller, N., Plugge, C.M., Stams, A.J. and Schink, B. (2010) (Endo) symbiotic methanogenic archaea, pp. 143-173, Springer.
Chen, S., He, J., Wang, H., Dong, B., Li, N. and Dai, X. (2018) Microbial responses and metabolic pathways reveal the recovery mechanism of an anaerobic digestion system subjected to progressive inhibition by ammonia. Chemical Engineering Journal 350, 312-323.
Dai, X., Hu, C., Zhang, D., Dai, L. and Duan, N. (2017) Impact of a high ammonia-ammonium-pH system on methane-producing archaea and sulfate-reducing bacteria in mesophilic anaerobic digestion. Bioresource technology 245, 598-605.
Liu, F., Rotaru, A.-E., Shrestha, P.M., Malvankar, N.S., Nevin, K.P. and Lovley, D.R. (2012) Promoting direct interspecies electron transfer with activated carbon. Energy & Environmental Science 5(10), 8982-8989.
Wang, T., Zhang, D., Dai, L., Dong, B. and Dai, X. (2018) Magnetite triggering enhanced direct interspecies electron transfer: a scavenger for the blockage of electron transfer in anaerobic digestion of high-solids sewage sludge. Environmental science & technology 52(12), 7160-7169.
Yabu, H., Sakai, C., Fujiwara, T., Nishio, N. and Nakashimada, Y. (2011) Thermophilic two-stage dry anaerobic digestion of model garbage with ammonia stripping. Journal of bioscience and bioengineering 111(3), 312-319.
Ho, L. and Ho, G. (2012) Mitigating ammonia inhibition of thermophilic anaerobic treatment of digested piggery wastewater: use of pH reduction, zeolite, biomass and humic acid. Water research 46(14), 4339-4350.

Lauterböck, B., Ortner, M., Haider, R. and Fuchs, W. (2012) Counteracting ammonia inhibition in anaerobic digestion by removal with a hollow fiber membrane contactor. Water research 46(15), 4861-4869.

Saha, S., Jeon, B.-H., Kurade, M.B., Chatterjee, P.K., Chang, S.W., Markkandan, K., Salama, E.-S., Govindwar, S.P. and Roh, H.-S. (2019) Microbial acclimatization to lipidic-waste facilitates the efficacy of acidogenic fermentation. Chemical Engineering Journal 358, 188-196.

Kurade, M.B., Saha, S., Kim, J.R., Roh, H.-S. and Jeon, B.-H. (2020) Microbial community acclimatization for enhancement in the methane productivity of anaerobic co-digestion of fats, oil, and grease. Bioresource technology 296, 122294.

Bhakta, J.N. (2016) Toxicity and Waste Management Using Bioremediation, pp. 75-96, IGI Global.

Tian, H., Fotidis, I.A., Kissas, K. and Angelidaki, I. (2018b) Effect of different ammonia sources on aceticlastic and hydrogenotrophic methanogens. Bioresource technology 250, 390-397.

Tian, H., Treu, L., Konstantopoulos, K., Fotidis, I.A. and Angelidaki, I. (2019c) 16s rRNA gene sequencing and radioisotopic analysis reveal the composition of ammonia acclimatized methanogenic consortia. Bioresource technology 272, 54-62.

Jing, Y., Wan, J., Angelidaki, I., Zhang, S. and Luo, G. (2017) iTRAQ quantitative proteomic analysis reveals the pathways for methanation of propionate facilitated by magnetite. Water research 108, 212-221.

Qin, J., Li, R., Raes, J., Arumugam, M., Burgdorf, K.S., Manichanh, C., Nielsen, T., Pons, N., Levenez, F. and Yamada, T. (2010) A human gut microbial gene catalogue established by metagenomic sequencing. nature 464(7285), 59-65.

Forbes, J.D., Knox, N.C., Ronholm, J., Pagotto, F. and Reimer, A. (2017) Metagenomics: the next culture-independent game changer. Frontiers in Microbiology 8, 1069.

Campanaro, S., Treu, L., Rodriguez-R, L.M., Kovalovszki, A., Ziels, R.M., Maus, I., Zhu, X., Kougias, P.G., Basile, A. and Luo, G. (2019) The anaerobic digestion microbiome: a collection of 1600 metagenome-assembled genomes shows high species diversity related to methane production. bioRxiv, 680553.

Kremp, F., Poehlein, A., Daniel, R. and Müller, V. (2018) Methanol metabolism in the acetogenic bacterium Acetobacterium woodii. Environmental Microbiology 20(12), 4369-4384.

Lins, P., Schwarzenauer, T., Reitschuler, C., Wagner, A.O. and Illmer, P. (2012) Methanogenic potential of formate in thermophilic anaerobic digestion. Waste Management & Research 30(10), 1031-1040.

Imachi, H., Sekiguchi, Y., Kamagata, Y., Hanada, S., Ohashi, A. and Harada, H. (2002) Pelotomaculum thermopropionicum gen. nov., sp. nov., an anaerobic, thermophilic, syntrophic propionate-oxidizing bacterium.

International journal of systematic and evolutionary microbiology 52(5), 1729-1735.
Sudmalis, D., Millah, S.K., Gagliano, M.C., Butré, C.I., Plugge, C.M., Rijnaarts, H.H.M., Zeeman, G. and Temmink, H. (2018) The potential of osmolytes and their precursors to alleviate osmotic stress of anaerobic granular sludge. Water research 147, 142-151.
Kraegeloh, A., Amendt, B. and Kunte, H.J. (2005) Potassium transport in a halophilic member of the bacteria domain: identification and characterization of the K+ uptake systems TrkH and TrkI from Halomonas elongata DSM 2581T. Journal of bacteriology 187(3), 1036-1043.
Müller, V., Spanheimer, R. and Santos, H. (2005) Stress response by solute accumulation in archaea. Current opinion in microbiology 8(6), 729-736.
Zhu, X., Campanaro, S., Treu, L., Seshadri, R., Ivanova, N., Kougias, P.G., Kyrpides, N. and Angelidaki, I. (2020) Metabolic dependencies govern microbial syntrophies during methanogenesis in an anaerobic digestion ecosystem. Microbiome 8(1), 22.
Fotidis, I.A., Wang, H., Fiedel, N.R., Luo, G., Karakashev, D.B. and Angelidaki, I. (2014) Bioaugmentation as a solution to increase methane production from an ammonia-rich substrate. Environmental science & technology 48(13), 7669-7676.
Schauer-Gimenez, A.E., Zitomer, D.H., Maki, J.S. and Struble, C.A. (2010) Bioaugmentation for improved recovery of anaerobic digesters after toxicant exposure. Water Res 44(12), 3555-3564.
Town, J.R. and Dumonceaux, T.J. (2016) Laboratory-scale bioaugmentation relieves acetate accumulation and stimulates methane production in stalled anaerobic digesters. Applied Microbiology and Biotechnology 100(2), 1009-1017.
Li, Y., Zhang, Y., Sun, Y., Wu, S., Kong, X., Yuan, Z. and Dong, R. (2017) The performance efficiency of bioaugmentation to prevent anaerobic digestion failure from ammonia and propionate inhibition. Bioresource technology 231, 94-100.
Fotidis, I.A., Treu, L. and Angelidaki, I. (2017) Enriched ammonia-tolerant methanogenic cultures as bioaugmentation inocula in continuous biomethanation processes. Journal of Cleaner Production 166, 1305-1313.
Westerholm, M., Levén, L. and Schnürer, A. (2012) Bioaugmentation of syntrophic acetate-oxidizing culture in biogas reactors exposed to increasing levels of ammonia. Appl. Environ. Microbiol. 78(21), 7619-7625.
Meury, J. and Kohiyama, M. (1992) Potassium ions and changes in bacterial DNA supercoiling under osmotic stress. FEMS microbiology letters 99(2-3), 159-164.
Sapra, R., Bagramyan, K. and Adams, M.W. (2003) A simple energy-conserving system: proton reduction coupled to proton translocation. Proceedings of the National Academy of Sciences 100(13), 7545-7550.

Tian, H., Yan, M., Treu, L., Angelidaki, I. and Fotidis, I.A. (2019d) Hydrogenotrophic methanogens are the key for a successful bioaugmentation to alleviate ammonia inhibition in thermophilic anaerobic digesters. Bioresource technology 293, 122070.
Rincón, B., Borja, R., Martín, M. and Martín, A. (2010) Kinetic study of the methanogenic step of a two-stage anaerobic digestion process treating olive mill solid residue. Chemical Engineering Journal 160(1), 215-219.
Cheng, L., Qiu, T.-L., Li, X., Wang, W.-D., Deng, Y., Yin, X.-B. and Zhang, H. (2008) Isolation and characterization of Methanoculleus receptaculi sp. nov. from Shengli oil field, China. FEMS microbiology letters 285(1), 65-71.
Xue, Y., Zhang, X., Zhou, C., Zhao, Y., Cowan, D.A., Heaphy, S., Grant, W.D., Jones, B.E., Ventosa, A. and Ma, Y. (2006) Caldalkalibacillus thermarum gen. nov., sp. nov., a novel alkalithermophilic bacterium from a hot spring in China. International journal of systematic and evolutionary microbiology 56(6), 1217-1221.
Massalha, N., Brenner, A., Sheindorf, C. and Sabbah, I. (2015) Application of immobilized and granular dried anaerobic biomass for stabilizing and increasing anaerobic bio-systems tolerance for high organic loads and phenol shocks. Bioresource technology 197, 106-112.
Yarberry, A., Lansing, S., Luckarift, H., Diltz, R., Mulbry, W. and Yarwood, S. (2019) Effect of anaerobic digester inoculum preservation via lyophilization on methane recovery. Waste Management 87, 62-70.
Bhattad, U., Venkiteshwaran, K., Cherukuri, K., Maki, J.S. and Zitomer, D.H. (2017) Activity of methanogenic biomass after heat and freeze drying in air. Environmental Science: Water Research & Technology 3(3), 462-471.
Rothrock, M.J., Vanotti, M.B., Szögi, A.A., Gonzalez, M.C.G. and Fujii, T. (2011) Long-term preservation of anammox bacteria. Applied Microbiology and Biotechnology 92(1), 147.
Banu, J.R., Kannah, R.Y., Kumar, M.D., Gunasekaran, M., Sivagurunathan, P., Park, J.-H. and Kumar, G. (2018) Recent advances on biogranules formation in dark hydrogen fermentation system: Mechanism of formation and microbial characteristics. Bioresource technology 268, 787-796.
Iacobellis, N.S. and DeVay, J.E. (1986) Long-term storage of plant-pathogenic bacteria in sterile distilled water. Applied and Environmental Microbiology 52(2), 388-389.
Oliver, J.D. (2010) Recent findings on the viable but nonculturable state in pathogenic bacteria. FEMS microbiology reviews 34(4), 415-425.
Scherer, P., Kluge, M., Klein, J. and Sahm, H. (1981) Immobilization of the methanogenic bacterium Methanosarcina barkeri. Biotechnology and Bioengineering 23(5), 1057-1065.

9 Papers

I **Yan, M.,** Fotidis, I.A., Tian, H., Khoshnevisan, B., Treu, L., Tsapekos, P. and Angelidaki, I. (2019) Acclimatization contributes to stable anaerobic digestion of organic fraction of municipal solid waste under extreme ammonia levels: focusing on microbial community dynamics. Bioresource technology 286, 121376. **(IF=7.5)**

II **Yan, M**, Treu, L., Zhu, X., Tian, H., B, Arianna, Fotidis, I A, Campanaro, S and Angelidaki, I. (2020) Insights into ammonia adaptation and methanogenic precursor oxidation by genome-centric analysis. Environmental Science & Technology. **(IF=7.9)**

III **Yan, M.,** Treu, L., Campanaro, S., Tian, H., Zhu, X., Khoshnevisan, B., Tsapekos, P., Angelidaki, I. and Fotidis, I.A. (2020) Effect of ammonia on anaerobic digestion of municipal solid waste: inhibitory performance, bioaugmentation and microbiome functional reconstruction. Chemical Engineering Journal, 126159. **(IF=10.7)**

IV **Yan, M**., Fotidis, I.A., Jéglot, A., Treu, L., Tian, H., Palomo, A., Zhu, X. and Angelidaki, I. (2020b) Long-term preserved and rapidly revived methanogenic cultures: Microbial dynamics and preservation mechanisms. Journal of Cleaner Production, 121577. **(IF=7.24)**

In this online version of the thesis, **papers I-IV** are not included but can be obtained from electronic article databases e.g. via www.orbit.dtu.dk or on request from:

DTU Environment
Technical University of Denmark
Bygningstorvet, Building 115
2800 Kgs. Lyngby
Denmark
info@env.dtu.dk.

I

Acclimatization contributes to stable anaerobic digestion of organic fraction of municipal solid waste under extreme ammonia levels: focusing on microbial community dynamics

Miao Yan, Ioannis A. Fotidis, Hailin Tian, Benyamin Khoshnevisan, Laura Treu, Panagiotis Tsapekos, Irini Angelidaki

Bioresource Technology, 2019, 286, 121376.

https://doi.org/10.1016/j.biortech.2019.121376

Bioresource Technology 286 (2019) 121376

Contents lists available at ScienceDirect

Bioresource Technology

journal homepage: www.elsevier.com/locate/biortech

Acclimatization contributes to stable anaerobic digestion of organic fraction of municipal solid waste under extreme ammonia levels: Focusing on microbial community dynamics

Miao Yan[a], Ioannis A. Fotidis[a,*], Hailin Tian[a], Benyamin Khoshnevisan[a], Laura Treu[b], Panagiotis Tsapekos[a], Irini Angelidaki[a]

[a] Department of Environmental Engineering, Technical University of Denmark, Bygningstorvet Bygning 115, DK-2800 Kgs. Lyngby, Denmark
[b] Department of Biology, University of Padova, Via U. Bassi 58/b, 35121 Padova, Italy

ARTICLE INFO

Keywords:
Ammonia acclimatization
Hydrogenotrophic pathway
Aceticlastic pathway
Metabolic pathway shift
Methanosarcina soligelidi

ABSTRACT

The organic fraction of municipal solid waste (OFMSW) is an abundant and sustainable substrate for the anaerobic digestion (AD) process, yet ammonia released during OFMSW hydrolysis could result in suboptimal biogas production. Acclimatized ammonia tolerant microorganisms offer an efficient way to alleviate ammonia inhibition during AD. This study aimed to achieve an efficient AD of OFMSW under extreme ammonia levels and elucidate the dynamics of the acclimatized microbial community. Thus, two mesophilic continuous stirred tank reactors (CSTR), fed only with OFMSW, were successfully acclimatized up to 8.5 g NH_4^+-N/L, and their methane yields fluctuated < 10%, compared to the methane yields without ammonia addition. Microbiological analyses showed that *Methanosaeta concilii* and *Methanosarcina soligelidi* were the dominant methanogens at low and high ammonia levels, respectively. Whilst, a unique metabolic pathway shift, from aceticlastic to hydrogenotrophic methanogenesis, of *M. soligelidi* was identified during the acclimatization process.

1. Introduction

The increasing global need for natural resources and consumer goods leads to vast amounts of municipal solid waste (MSW). In 2018, more than 2.5 Mt of MSW were generated in the European Union (Eurostat, 2018), with 46% of them been organic (OFMSW: organic fraction of MSW) (Hoornweg and Bhada-Tata, 2012). Improper treatment methods of OFMSW can cause environmental and health issues (Fisher, 2006). Currently, most of the MSW is treated in one of the four ways: landfilling (24%), incineration (28%), recycling (29%), and composting (16%) (Eurostat, 2018). Landfilling and incineration methods do not take advantage of the organic faction and the nutrients of OFMSW and can lead to extra greenhouse gas emissions (Fisher, 2006; Eurostat, 2018). At the same time, huge consumption and shortage of fossil fuels motivate researchers to find alternative energy sources. Thus, new treatment technologies must be developed to not only offset the use of fossil fuels but also maximize the reuse of the vast amounts of the OFMSW and thereby maintain and recycle the useful nutrient back to agriculture.

Anaerobic digestion (AD) is a process that can convert organic waste into sustainable energy (biogas), via a series of interrelated microbial metabolisms (Campanaro et al., 2018). The AD process is divided in four steps (i.e. hydrolysis, acidogenesis, acetogenesis and methanogenesis), which are mediated primarily by bacteria and archaea (Angelidaki et al., 2011). In addition, the liquid product of the AD process (digestate) contains high levels of nitrogen and phosphorus, which can be potentially reused as biofertilizer or after extraction, as supplement for fermentation processes. In spite of these benefits, the degradation of OFMSW produces ammonia, a by-product from the catabolism of proteins, which can be toxic to the AD process, resulting in poor operational stability and reduced methane production efficiency (Tian et al., 2018b).

Total ammonia (TAN) is the sum of ammonium ions (NH_4^+) and free ammonia (FAN, NH_3), while FAN exists in an equilibrium defined by the pH and the temperature (Tian et al., 2017). As Koster and Lettinga (1988) reported, when ammonia concentrations ranged from 4 to 5.7 g NH_4^+-N/L, more than 56% of the methanogenic activity was inhibited in a granular sludge reactor. The reason is that FAN is freely membrane-permeable and hence, decreases methanogenic activity by interfering with the natural intracellular biological pathways of the methanogens (e.g. inhibiting specific methane synthesizing enzyme reaction) (Sprott and Patel, 1986). It is generally accepted that

* Corresponding author.
E-mail address: ioanf@env.dtu.dk (I.A. Fotidis).

https://doi.org/10.1016/j.biortech.2019.121376
Received 22 March 2019; Received in revised form 19 April 2019; Accepted 20 April 2019
Available online 22 April 2019
0960-8524/

acetoclastic methanogens are more sensitive to ammonia toxicity compared to hydrogenotrophic methanogens (Schnürer and Nordberg, 2008). For example, hydrogenotrophic methanogenic pathway (coupled with syntrophic acetate oxidation) became dominant (by replacing the acetoclastic pathway) in a semi-continuous lab-scale anaerobic digester, when ammonia exceeded 3 NH_4^+-N g/L (Wiegant and Zeeman, 1986). However, there is conflicting information in the literature about the sensitivity of acetoclastic methanogens to ammonia, with few researchers reporting that different members of the acetoclastic *Methanosarcina* spp. could develop tolerance to ammonia toxicity.

Overall, the ammonia inhibition levels are case sensitive and are defined by the nature of substrate, the inoculum, the reactor type, the operating parameters (pH and temperature), the mixing and the acclimatization period. For example, 50% inhibition was observed at 3.9 and 5.6 g NH_4^+-N/L in mesophilic and thermophilic batch reactors, respectively that were digesting OFMSW (Liu et al., 2015). While another study found that 1 g NH_4^+-N/L in MSW's leachate was enough to inhibit the methane production with 25% loss in a mesophilic expanded granular sludge bed reactor (Nielsen and Angelidaki, 2008). Stepwise acclimatization to high ammonia levels is a common method used to increase ammonia tolerance in the AD microbiome (Akindele and Sartaj, 2018; Tian et al., 2018a). In such a process, mesophilic methanogenic consortia were successfully acclimatized to 5 g NH_4^+-N/L (at pH 7.50) in batch reactors, with OFMSW as substrate (Tian et al., 2018b). However, acclimatization in continuous reactors to overcome ammonia inhibition and improve methane production efficiency of OFMSW has never been reported.

Therefore, the preliminary aim of the present study was to achieve an efficient and stable continuous anaerobic degradation of OFMSW under extreme ammonia levels (greater than7 g NH_4^+-N/L). While, the main aim of the study was to elucidate the dynamics of the microbial community under different ammonia levels. To realize these aims, two continuous stirred tank reactors (CSTR) were fed with OFMSW, while a stepwise ammonia acclimatization process was followed.

2. Material and methods

2.1. Inoculum and feedstock

The inoculum used to start up the two CSTR reactors originated from the mesophilic (37 °C) anaerobic digesters, which run for 4 months fed with OFMSW. The substrate used in this study was OFMSW treated with the biopulping process to increase the biodegradability by Gemidan Ecogi A/S. The substrate was kept at −20 °C until use, when thawed at room temperature and diluted with distilled water to a fixed TS content of 60 g VS/kg. The characteristics of the inoculum and the biopulp are presented in Table 1.

Table 1
Characteristics of inoculum and substrate.

Parameter	Unit	Inoculum (SD)	Biopulp (SD)
Total solids (TS)	g/kg	38.61 (0.34)	60.52 (0.52)
Volatile solids (VS)	g/kg	24.07 (0.35)	52.11 (0.55)
pH	–	8.38	3.90
Total ammonia nitrogen (TAN)	g NH_4^+-N/L	3.80 (0.01)	0.40 (0.01)
Free ammonia nitrogen (FAN)	g NH_3-N/L	0.896 (0.01)	0.004 (0.01)
Total Kjeldahl Nitrogen (TKN)	g N/L	5.38 (0.25)	1.70 (0.03)

*SD: standard deviation.

2.2. Experimental setup

Two CSTR reactors (i.e. R1 and R2), with total and working volume of 4.5 and 3 L, respectively, were fed with OFMSW for 159 days with an organic loading rate of 2.5 g VS/L/day where timer was used to control feeding peristaltic pump to inject 75 mL OFMSW per 12 h. Each reactor was equipped with an influent and an effluent bottle, and a feeding peristaltic pump. Electrical heating jackets maintained the reactors' temperature at 37 °C and intermittent stirring with the rate of 30 s/min was applied for mixing the reactor content (worked 34 sec every 56 sec). Water-displacement gas meters were used to measure biogas production. The TAN levels of the influent and the reactor content were increased stepwise from 1.1 to 9.5 g NH_4^+-N/L with the addition of urea ($CO(NH_2)_2$) and ammonium chloride (NH_4Cl). To be more specific, every increase of TAN (1–1.5 g NH_4^+-N/L^{-1} each step) both inside the reactor and the feedstock in the influent bottle was implemented when there were no significant decrease (more than 85% of methane yield during the baseline period (P1)). The whole experiment was divided into seven phases as presented in Table 2.

Table 2
The CSTR reactors experimental design.

Phase	Days	TAN	Extra added ammonia	
		(g NH_4^+-N/L)	$CO(NH_2)_2$ (g NH_4^+-N/L)	NH_4Cl (g NH_4^+-N/L)
P1	0–30	1.1	0	0
P2	31–51	4	1	1.9
P3	52–66	5	2	1.9
P4	67–74	6	2	2.9
P5	75–89	7	3	2.9
P6	90–127	8.5	4	3.4
P7	128–159	9.5	4.5	3.9

2.3. Analyses

2.3.1. Chemical analyses

Methane concentration was measured with the gas chromatography as described by APHA (2005). VFA levels were analysed with gas chromatograph (TRACE 1300 from Thermo Scientific) equipped with flame ionization detector and a DB-FFAP fused silica capillary column. PHM99 LAB pH meter (RadiometerTM) was used to measure the pH. TS, VS, TAN and TKN, were determined according to Angelidaki and Ahring (1993a).

2.3.2. Microbial analysis

Five triplicate samples were taken from both reactors on days 33 (P1), 55 (P2), 77 (P3), 92 (P5) and 162 (P7) and analysed using 16S rRNA gene sequencing technique to elucidate the microbial community shift. After cleaning step with Phenol:Chloroform: Isoamyl Alcohol (25: 24: 1), genomic DNA were extracted using DNeasy PowerSoil® (QIAGEN GmbH, Hilden, Germany). PCR amplification using universal primers 515F/806R was performed on the V4 region of 16S rRNA gene and the amplicons were sequenced using MiSeq desktop sequencer at Ramaciotti Centre for Genomics (Sydney, Australia. Raw reads were deposited in Sequence Read Archive (SRA) database (http://www.ncbi.nlm.nih.gov/sra) with the name of SUB5320995.

The raw data were processed using CLC Workbench software (11.0.1) with the Microbial genomics module plugin. A trimming procedure was used to low-quality reads according to default parameters provided by the software and paired sequences were merged. Chimera crossover filter was also applied. Operational taxonomic units' (OTUs) clustering percent was set at 97%, with threshold for de novo OTUs creation set at 80% and minimum reads occurrence at five. Alpha diversity was calculated based on the number of OTUs and Chao 1 bias-corrected. Beta diversity (Principal Component Analysis) was calculated by Bray-Curtis matrix.

2.4. Calculations and statistics

2.4.1. Free ammonia

Free ammonia concertation was calculated with Eq. (1):

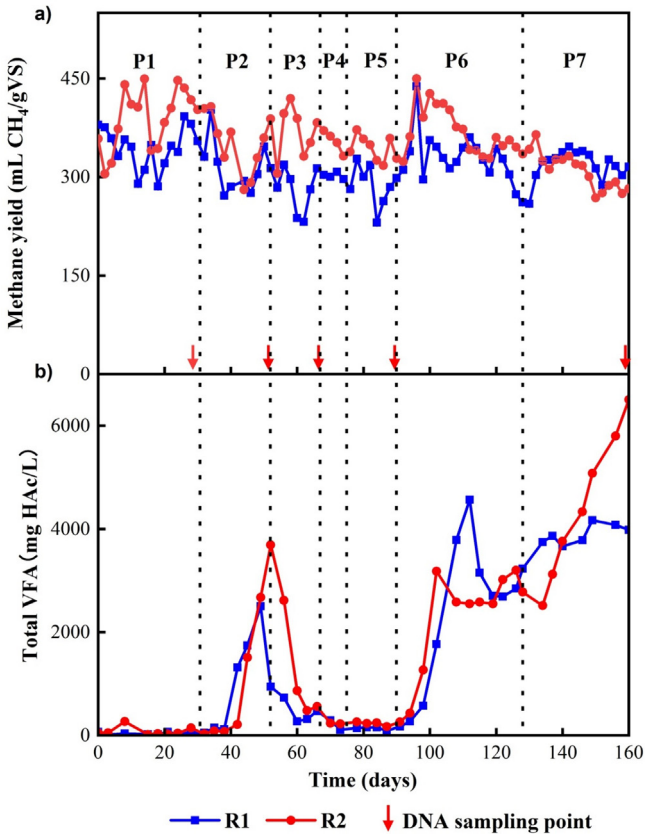

Fig. 1. a) CH_4 production, and b) VFA variation throughout the experimental period.

$$FAN = TAN/(1 + 10^{-pH}/K_a) \quad (1)$$

where K_a is the dissociation constant with the value of 1.29×10^{-9} at 37 °C.

2.4.2. Statistical analysis

All statistics and figures were performed using the Origin software (OriginLab Corporation, USA). Descriptive statistics were carried out for all variables, mean values and standard deviations were calculated. Pearson correlation and hierarchical clustering analyses were carried out using Multiexperiment viewer (MeV4.9.0).

3. Results and discussion

3.1. Reactors' performance

P1, where an average methane yield of 345 ± 40 and 391 ± 59 mL CH_4/g VS was observed for R1 and R2, respectively, was used as baseline phase (no ammonia addition) to evaluate the reactors' performance in the following ammonia acclimatization phases (P2-P7). During P2 to P5, both reactors experienced inhibition with an average loss of 15% of the methane yield compared to P1 (Fig. 1a). While at P6 (8.5 g NH_4^+-N/L) the methane production of both reactors, recovered with methane yields constantly above 94% compared to P1. Specifically, during P6 the average methane production yields did not change significantly and were 332 ± 37 and 369 ± 41 mL CH_4/g VS for R1 and R2, respectively. However, when ammonia was increased to 9.5 g NH_4^+-N/L (P7), both reactors' yields were reduced by more than 15% and the AD process operated under an "inhibited steady state". This stable but suboptimal steady-state is known as an ammonia induced "inhibited steady-state" and is a typical characteristic of many full-scale reactors that operate under high ammonia levels (Benabdallah El Hadj et al., 2009). Even though, there was a clear reduction of methane production at P7, it was significantly less than expected compared to previous studies. For example, Moestedt et al. (2016) have reported a 50% decrease could be observed in methane production of a mesophilic reactor when TAN exceeded 3.9 g NH_4^+-N/L.

The VFA accumulation in the two reactors was evolved mostly as expected, based on the methane production (Fig. 1b). Specifically, the VFA levels raised up to 4000 mg HAc/L at the end of P2, but decreased rapidly at the beginning of P3 due to the acclimatization (Tian et al., 2018a) and remained at low levels until P6. Stepwise ammonia acclimatization has been demonstrated before in co-digestions of manure and protein-rich substrates such as microalgae (Angelidaki and Ahring, 1993a). However, this was the first time that continuous AD reactors could acclimatize to this extreme ammonia levels (7 g NH_4^+-N/L) while mono-digesting the OFMSW.

During P6, despite the fact that methane production was stable and above 94% compared to P1, the VFA levels increased and remained above the defined threshold of 1500 mg HAc/L for a "healthy" AD process in CSTR reactors (De Vrieze et al., 2017). It appears that the 8.5 g NH_4^+-N/L (P6) was the threshold to the acclimatization process, which could be attributed to the FAN attained at this period (greater than800 mg NH_3-N/L and 8.0 ± 0.2, respectively, Fig. 2a). It is generally accepted that FAN is the most toxic form of ammonia, which has positive correlation with pH (Fig. 2b) (Angelidaki and Ahring, 1993b). Thus, despite that both reactors were acclimatised to more than tenfold higher FAN levels (P1 to P5, < 50 to greater than 500 mg NH_3-N/L, respectively), FAN concentrations above 700 mg NH_3-N/L were found to be very toxic for AD processes (Xu et al., 2014).

Finally, the VFA accumulation during P7 was severe and both reactors exceeded 4000 mg HAc/L, which is a clear indicator of an AD process failure (Lv et al., 2018). Interestingly, even at these extremely high ammonia levels, the acclimatized microbiome of the reactors was able to perform at high efficiency levels (methane production around

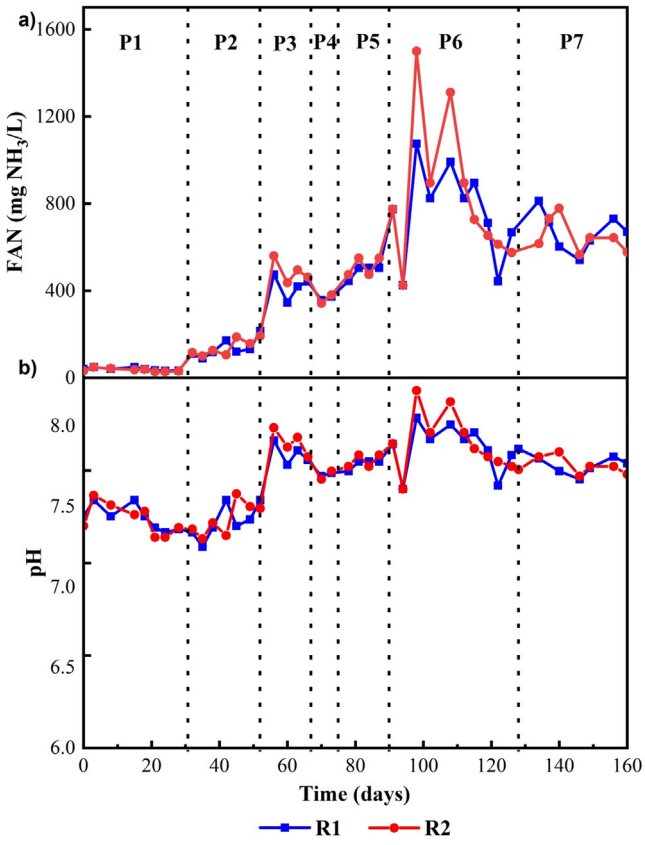

Fig. 2. a) FAN, b) pH throughout the experimental period.

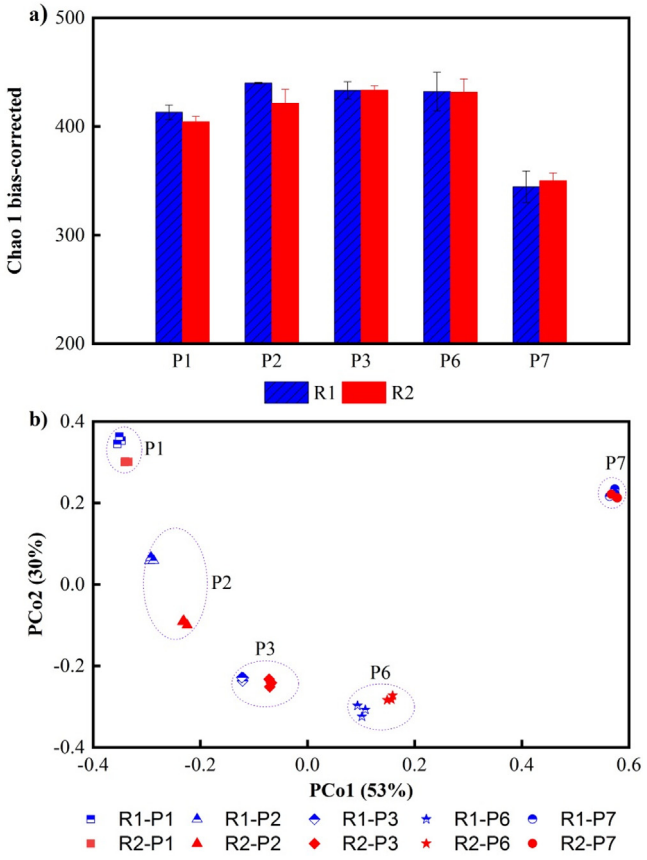

Fig. 3. Alpha Diversity a) based on Chao 1 bias-corrected index; b) Beta diversity of the triplicate samples in R1 and R2. Principal components (PC) 1 and 2 explained 53% and 30% of community variation, respectively.

85% compared to P1).

3.2. Global microbial dynamics

16S rRNA sequencing was used to elucidate the responses of the microbial community to the increased ammonia concentrations. Alpha diversity based on Chao 1 bias-corrected index (Fig. 3a) showed slight increase at P2 and stable trend alongside the increase of ammonia levels until P6. Afterwards, a sharp decrease of their alpha diversity was observed at P7, which indicated that ammonia increase from 8.5 to 9.5 g NH_4^+-N/L, was enough to washout approximately 12.5% of the microbial species from the reactors based on Chao 1 bias-corrected index. At the same time, Beta diversity (Fig. 3b) showed a clear microbial dynamic trend throughout the experimental process. Specifically, longest matrix distances were found between P1 and P7 for both reactors, followed by the one between P6 and P7. This indicated that when ammonia concentration exceeded 8.5 g NH_4^+-N/L, it drove the microbiome clustering shift (De Vrieze et al., 2017). According to De Vrieze (2017), high diversity and redundancy of microbial community (i.e. as detected from P1 to P6) was considered an effective strategy as buffer against ammonia inhibition, ensuring continuation of methane production, maintaining functionality or metabolic flexibility (Steinhaus et al., 2007). The sudden decrease of alpha diversity from P6 to P7 could have contributed rendering the reactors to become vulnerable to ammonia toxicity. Inhibition was confirmed by the accumulation of VFA (greater than4000 mg HAc/L) and decrease of methane production (< 312 mL CH_4/g VS) during P7. Therefore it is clear that the toxicity threshold of the two CSTR reactors, based on production performance and microbial activity, for this specific ammonia acclimatization process was 8.5 g NH_4^+-N/L.

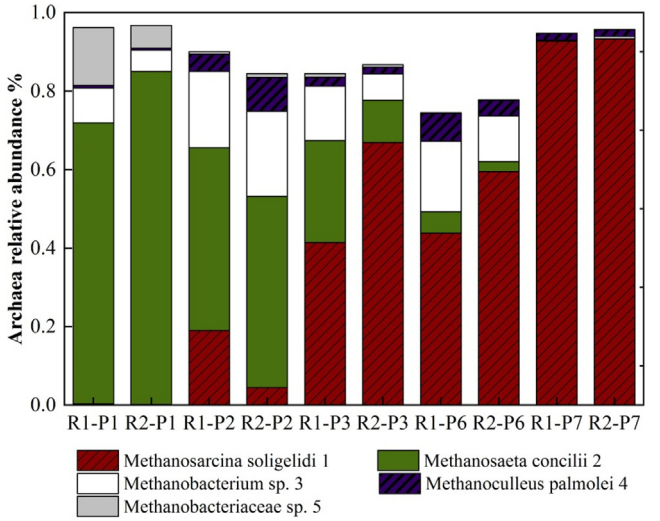

Fig. 4. Archaeal relative abundance (%) in different phases of reactor R1 and R2 at species level.

3.2.1. Shift in archaea dominance

Among the archaea, two interesting methanogens changed significantly its abundance from P1 to P7 (Fig. 4), indicating different tolerance capability in respect to ammonia. At P1, the main methanogen was *Methanosaeta concilii* 2, as a specialist species that uses only acetate, which accounted for more than 70% of total archaea population in both reactors (Fig. 4). Considering its abundance levels (still higher than 50% during P2), the dominant role in the archaeal community was well pronounced at medium-low levels of ammonia (< 5 g NH_4^+-N/L). During P3-7, the relative abundance of *M. concilii* 2 decreased alongside the increasing ammonia levels, dropping to 21% (P3), 5% (P6) and 0% (P7). It is explained by two reasons: on the one hand, *M. concilii* 2 can use acetate at concentration levels at the range of 5–20 μM, however acetate level at P6 was far higher than the optimum range. On the other hand, *M. concilii* 2 was found to be the most ammonia-sensitive methanogen, which was completely inhibited at 0.56 g NH_4^+-N/L, primarily due to ammonia's effect on intracellular ion exchange (Ince et al., 2011). Hence, results indicated that there is a negative impact of increasing acetate and ammonia concentrations on *M. concilii* 2 (Tian et al., 2018a).

Conversely, the relative abundance of *Methanosarcina soligelidi* 1 strongly increased from < 0.4% up to more than 94% in both reactors from P1 to P7. Remarkably, *M. soligelidi* 1 was found to be the most ammonia tolerant methanogen in this study. This finding was in accordance with a previous study, where *M. soligelidi* 1 was the dominant acetoclastic methanogens at extreme ammonia levels (greater than7 g NH_4^+-N/L) (Taubner et al., 2015). The dominant role of *M. soligelidi* 1 could be justified by several factors. Firstly, it is known that *M. soligelidi* 1 could form clusters of cells in order to reduce the toxicity of ammonia since this formation creates an ammonium gradient from the bulk ammonia concentration at the surface along the inner part of the aggregate and thereby lessen the ammonia concentration at the inner core of the sphere (Conklin et al., 2006; Wagner et al., 2013). Secondly, *M. soligelidi* 1 show remarkable capability of environmental stress tolerance (e.g. freezing, aerobic or dry condition) owning to its intact membrane lipids (Wagner et al., 2013). Thirdly, *M. soligelidi* 1 is metabolically more versatile (i.e. able to generate CH_4 from H_2/CO_2, methanol and acetate) than other acetoclastic and hydrogenotrophic methanogens (who are restricted with only carbon substrate) (Li et al., 2017). Additionally, despite the fact that, in many cases, *Methanosarcina* spp. were found to be more sensitive to ammonia compared to hydrogenotrophic methanogens (Wang et al., 2015; Li et al., 2017; Akindele and Sartaj, 2018); in this study, *M. soligelidi* 1 was able to

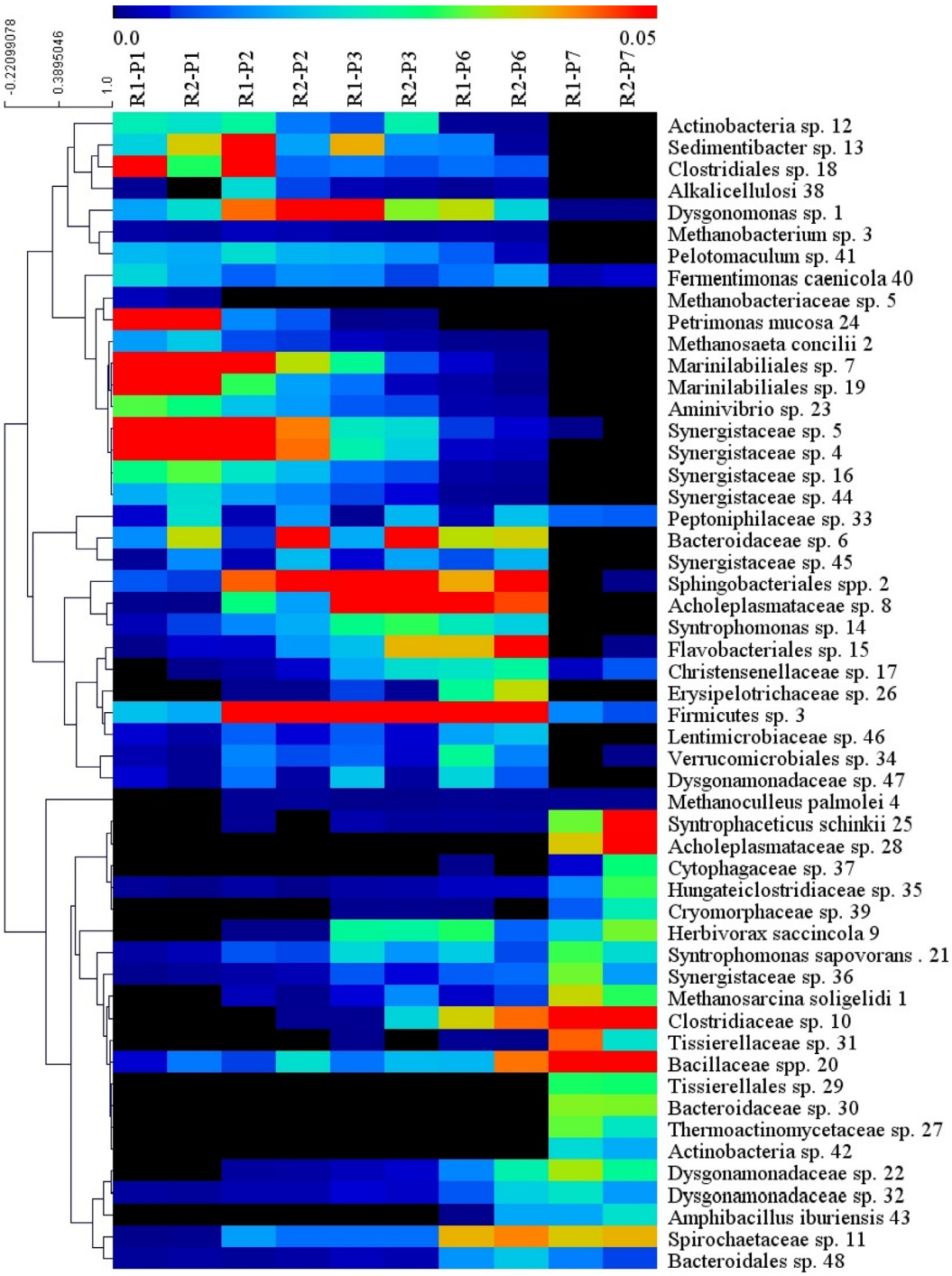

Fig. 5. Hierarchical cluster analysis of interesting bacteria and archaea in R1 and R2 at the different ammonia level.

become the dominant methanogen. Conversely, the hydrogenotrophic methanogens were found at extremely low abundance. Specifically, the relative abundance of *Methanobacterium* sp. 3 accounted for 7% at P1 increased to 18% at P6, but completely disappeared at P7, which was similar to the relative abundance of *Methanobacteriaceae* sp. 5. *Methanoculleus palmolei* 4 was the only hydrogenotrophic methanogen present at P7, although at low relative abundance (2% of archaeal community).

Considering the dominant ammonia tolerant methanogens are different in previous studies, it seems that dominant methanogens could be different at the same ammonia levels due to the different operating conditions (e.g. substrate, HRT, OLR, pH etc.) (Wang et al., 2015; Akindele and Sartaj, 2018; Capson-Tojo et al., 2018). Based on that (Akindele and Sartaj, 2018) have proposed that the initial archaeal composition of the inoculum plays an important role during the reactor start-up in order to achieve a stable AD process at high ammonia levels. Hence, we can infer that ammonia is the major but not the only driving force to shape the methanogenic communities of the AD processes, the other factors determining the methanogens dominance in digesters need further investigation.

3.2.2. Trends in bacterial populations

From P1 to P7, the addition of ammonia resulted in a dramatic change of the bacterial community (Fig. 5). To be more specific, at P1, the predominant phylum was *Bacteroidetes* with around 41.80% of

relative abundance, followed by the *Synergistetes* (24.78%) and *Firmicutes* (21.99%). As the ammonia levels increased, *Firmicutes* became the most dominant phylum with a relative abundance of 69.12% at P7. *Firmicutes* spp., which mediates the acidogenesis step of the AD process, have a recorded robustness to high TAN concentrations (Frank et al., 2016; Chen et al., 2018). On contrary, *Bacteroidetes* spp. and *Synergistetes* spp. abundances declined to 15.20% and < 1%, respectively, at P7; which indicated that both *Synergistetes* and *Bacteroidetes* phyla members were vulnerable to the elevated ammonia levels despite the stepwise acclimatization process.

At species-level, the relative abundance of *Bacillaceae* sp. 20 and *Syntrophaceticus schinkii* 25 showed a dramatic increase from undetectable levels (prior to P5) to 12% (P7). *Bacillaceae* sp. 20 was found to be similar to novel uncultured phylotype of syntrophic acetate oxidizing bacteria (SAOB) with 100% identity (Westerholm et al., 2010); while, *Syntrophaceticus schinkii* 25 was proposed to be syntrophic partner of a hydrogenotrophic methanogen (e.g. *Methanoculleus* sp.4), to perform methanogenesis by interspecies hydrogen transfer (Wagner et al., 2013). Thus, the extreme low abundance of strictly hydrogen-utilizing methanogens did not match the increased abundance of these two acetate oxidizing bacteria (SAOB). At the same time, *M. soligelidi* was found to have a faster growth rate on H_2/CO_2 compared to acetate (Örlygsson et al., 1996). Thus, it seems that *M. soligelidi* utilised H_2/CO_2 to perform methanogenesis in synergy with *Bacillaceae* sp. 20 and *Syntrophaceticus schinkii* 25 (SAOBs). Specifically, the low abundance of these two SAOBs at P1 to P5 was due to the lack of H_2 consumers between P1-P5; therefore, when *M. soligelidi* shifted to a hydrogenotrophic metabolism, the growth of these two SAOBs was stimulated.

Consequently, other acidogenic bacteria, *Clostridiaceae* sp. 10 (92% similarity with *Clostridium acetireducens*), which exclusively uses acetate during degradation of the branched-chain amino acids and alanine to produce butyrate and H_2 (Vartoukian et al., 2007), became the most dominant OTU with relative abundance of 15.5% at P7. The dominance of this species can be attributed to the unique composition of the reactors, containing both VFA and protein-rich substrates. In addition, two other OTUs with higher ammonia tolerance, i.e. *Tissierellales* sp. 30 (3%) and *Bacteroidaceae* sp. 31 (3.4%), were observed with high relative abundance at P7. *Tissierellales* sp. 30 and *Bacteroidaceae* sp. 31 (90% and 92% identity to *Sporanaerobacter acetigenes* and *Bacteroides propionicifaciens*, respectively (Wojcieszak et al., 2017)), were reported to be important acetate and H_2-producing bacteria (Xia et al., 2014; Wojcieszak et al., 2017). The dominancy of these H_2-producing bacteria (e.g. *Clostridiaceae* sp. 10, *Bacillaceae* sp. 20 and *Syntrophaceticus schinkii* 25, *Tissierellales* sp. 30, *Bacteroidaceae* sp. 31) was the result of the potential hydrogenotrophic pathway shift of *M. soligelidi*.

Overall, this microbial community redundancy and versatile metabolic pathway were the major reasons to maintain efficient and stable methane production, without loss of functionality or metabolic flexibility during ammonia acclimatization from 1.1 to 7 g NH_4^+-N/L. Clearly, 8.5 g NH_4^+-N/L was a threshold that introduced a suboptimal AD process and subsequently lead to the sharp drop of the microbial diversity at 9.5 g NH_4^+-N/L.

4. Conclusions

This study demonstrated a successful stepwise acclimatization up to 8.5 g NH_4^+-N/L during AD of the OFMSW. Microbiological analyses showed that ammonia load was identified as the main factor to shape microbial composition. The influence were characterized by a shift from hydrogenotrophic methanogens (e.g. *Methanobacterium* sp.5) and acetoclastic methanogens (*M. concilii*, only low-acetate affinity microorganisms) that prevailed in the initial inoculum samples at P1, to the dominance of metabolically more versatile and ammonia more tolerant acetoclastic methanogens (*M. soligelidi*) at extreme ammonia levels. The archaeal shift was essential to keep high biomethanation efficiency.

Acknowledgements

This work was supported by Energinet.dk under the project framework ForskEL “MicrobStopNH3-Innovative bioaugmentation strategies to tackle ammonia inhibition in anaerobic digestion process” (program no. 2015-12327). We acknowledge financial support from MUDP project “VARGA - VAnd Ressource Genvindings Anlægget”. Miao Yan would like to thank for the financial support from China Scholarship Council.

References

Akindele, A.A., Sartaj, M., 2018. The toxicity effects of ammonia on anaerobic digestion of organic fraction of municipal solid waste. Waste Manag 71, 757–766.
Angelidaki, I., Ahring, B., 1993. Thermophilic anaerobic digestion of livestock waste: the effect of ammonia. Appl Microbiol Biotechnol 38, 560–564.
Angelidaki, I., Karakashev, D., Batstone, D.J., Plugge, C.M., Stams, A.J., 2011. Biomethanation and its potential. MethodsEnzymol 494, 327–351.
APHA, 2005. Standard Methods for the Examination of Water and Wastewater. American Public Health Association, Washington, DC.
Benabdallah El Hadj, T., Astals, S., Gali, A., Mace, S., Mata-Alvarez, J., 2009. Ammonia influence in anaerobic digestion of OFMSW. Water Sci.Technol 59, 1153–1158.
Campanaro, S., Treu, L., Kougias, P.G., Luo, G., Angelidaki, I., 2018. Metagenomic binning reveals the functional roles of core abundant microorganisms in twelve full-scale biogas plants. Water Res. 140, 123–134.
Capson-Tojo, G., Trably, E., Rouez, M., Crest, M., Bernet, N., Steyer, J.P., Delgenes, J.P., Escudie, R., 2018. Methanosarcina plays a main role during methanogenesis of high-solids food waste and cardboard. Waste Manag 76, 423–430.
Chen, S., He, J., Wang, H., Dong, B., Li, N., Dai, X., 2018. Microbial responses and metabolic pathways reveal the recovery mechanism of an anaerobic digestion system subjected to progressive inhibition by ammonia. Chem. Eng. J. 350, 312–323.
Conklin, A., Stensel, H.D., Ferguson, J., 2006. Growth Kinetics and Competition Between Methanosarcina and Methanosaeta in Mesophilic Anaerobic Digestion. Water Environ. Res. 78, 486–496.
De Vrieze, J., Christiaens, M.E.R., Walraedt, D., Devooght, A., Ijaz, U.Z., Boon, N., 2017. Microbial community redundancy in anaerobic digestion drives process recovery after salinity exposure. Water Res. 111, 109–117.
Eurostat, 2018. Municipal waste generation. https://ec.europa.eu/eurostat/statistics-explained/index.php/Municipal_waste_statistics#Municipal_waste_generation.
Fisher, K., 2006. Impact of energy from waste and recycling policy on UK greenhouse gas emissions. Environment Resource Management for Department of Environment, Food and Rural Affairs. Prieiga per internetą: http://randd. defra. gov. uk/Document. aspx.
Frank, J.A., Arntzen, M.O., Sun, L., Hagen, L.H., McHardy, A.C., Horn, S.J., Eijsink, V.G., Schnurer, A., Pope, P.B., 2016. Novel Syntrophic Populations Dominate an Ammonia-Tolerant Methanogenic Microbiome. mSystems 1.
Hoornweg, D., Bhada-Tata, P., 2012. What a waste: a global review of solid waste management. World Bank, Washington, DC.
Ince, B., Koksel, G., Cetecioglu, Z., Oz, N.A., Coban, H., Ince, O., 2011. Inhibition effect of isopropanol on acetyl-CoA synthetase expression level of acetoclastic methanogen, Methanosaeta concilii. J. Biotechnol. 156, 95–99.
Koster, I.W., Lettinga, G., 1988. Anaerobic digestion at extreme ammonia concentrations. Biol. Wastes 25, 51–59.
Li, N., Xue, Y., Chen, S., Takahashi, J., Dai, L., Dai, X., 2017. Methanogenic population dynamics regulated by bacterial community responses to protein-rich organic wastes in a high solid anaerobic digester. Chem. Eng. J. 317, 444–453.
Liu, Z., Dang, Y., Li, C., Sun, D., 2015. Inhibitory effect of high NH4 + –N concentration on anaerobic biotreatment of fresh leachate from a municipal solid waste incineration plant. Waste Manage. 43, 188–195.
Lv, Z., Leite, A.F., Harms, H., Glaser, K., Liebetrau, J., Kleinsteuber, S., Nikolausz, M., 2018. Microbial community shifts in biogas reactors upon complete or partial ammonia inhibition. Appl Microbiol Biotechnol.
Moestedt, J., Muller, B., Westerholm, M., Schnurer, A., 2016. Ammonia threshold for inhibition of anaerobic digestion of thin stillage and the importance of organic loading rate. Microb Biotechnol 9, 180–194.
Nielsen, H.B., Angelidaki, I., 2008. Strategies for optimizing recovery of the biogas process following ammonia inhibition. Bioresour Technol 99, 7995–8001.
Schnürer, A., Nordberg, Å., 2008. Ammonia, a selective agent for methane production by syntrophic acetate oxidation at mesophilic temperature. Water Sci.Technol 57, 735–740.
Sprott, G.D., Patel, G.B., 1986. Ammonia toxicity in pure cultures of methanogenic bacteria. Syst Appl Microbiol 7, 358–363.
Steinhaus, B., Garcia, M.L., Shen, A.Q., Angenent, L.T., 2007. A Portable Anaerobic Microbioreactor Reveals Optimum Growth Conditions for the Methanogen < em > Methanosaeta concilii < /em&gt. Appl Environ Microbiol 73, 1653.
Taubner, R.-S., Schleper, C., Firneis, M.G., Rittmann, S.K.M.R., 2015. Assessing the Ecophysiology of Methanogens in the Context of Recent Astrobiological and Planetological Studies. Life (Basel, Switzerland) 5, 1652–1686.
Tian, H., Fotidis, I.A., Mancini, E., Angelidaki, I., 2017. Different cultivation methods to acclimatise ammonia-tolerant methanogenic consortia. Bioresour Technol 232, 1–9.
Tian, H., Fotidis, I.A., Mancini, E., Treu, L., Mahdy, A., Ballesteros, M., Gonzalez-Fernandez, C., Angelidaki, I., 2018a. Acclimation to extremely high ammonia levels

in continuous biomethanation process and the associated microbial community dynamics. Bioresour Technol 247, 616–623.
Tian, H., Karachalios, P., Angelidaki, I., Fotidis, I.A., 2018b. A proposed mechanism for the ammonia-LCFA synergetic co-inhibition effect on anaerobic digestion process. Chem. Eng. J. 349, 574–580.
Vartoukian, S.R., Palmer, R.M., Wade, W.G., 2007. The division "Synergistes". Anaerobe 13, 99–106.
Wagner, D., Schirmack, J., Ganzert, L., Morozova, D., Mangelsdorf, K., 2013. Methanosarcina soligelidi sp. nov., a desiccation- and freeze-thaw-resistant methanogenic archaeon from a Siberian permafrost-affected soil. Int J Syst Evol Microbiol 63, 2986–2991.
Wang, H., Fotidis, I.A., Angelidaki, I., 2015. Ammonia effect on hydrogenotrophic methanogens and syntrophic acetate-oxidizing bacteria. FEMS Microbiol. Ecol. 91.
Westerholm, M., Roos, S., Schnurer, A., 2010. Syntrophaceticus schinkii gen. nov., sp. nov., an anaerobic, syntrophic acetate-oxidizing bacterium isolated from a mesophilic anaerobic filter. FEMS Microbiol. Lett. 309, 100–104.
Wiegant, W.M., Zeeman, G., 1986. The mechanism of ammonia inhibition in the thermophilic digestion of livestock wastes. Agric. Wastes 16, 243–253.
Wojcieszak, M., Pyzik, A., Poszytek, K., Krawczyk, P.S., Sobczak, A., Lipinski, L., Roubinek, O., Palige, J., Sklodowska, A., Drewniak, L., 2017. Adaptation of Methanogenic Inocula to Anaerobic Digestion of Maize Silage. Front. Microbiol. 8.
Xia, A., Cheng, J., Ding, L., Lin, R., Song, W., Zhou, J., Cen, K., 2014. Effects of changes in microbial community on the fermentative production of hydrogen and soluble metabolites from Chlorella pyrenoidosa biomass in semi-continuous operation. Energy 68, 982–988.
Xu, Z., Zhao, M., Miao, H., Huang, Z., Gao, S., Ruan, W., 2014. In situ volatile fatty acids influence biogas generation from kitchen wastes by anaerobic digestion. Bioresour Technol 163, 186–192.
Örlygsson, J., Krooneman, J., Collins, M.D., Pascual, C., Gottschall, J.C., 1996. Clostridium acetireducens sp. nov., a Novel Amino Acid-Oxidizing, Acetate-Reducing Anaerobic Bacterium. Int J Syst Evol Microbiol 46, 454–459.

II

Insights into ammonia adaptation and methanogenic precursor oxidation by genome-centric analysis

Miao Yan, Laura Treu, Xinyu Zhu, Hailin Tian, Arianna Basile, Ioannis A. Fotidis, Stefano Campanaro, and Irini Angelidaki

Environmental Science & Technology, 2020.

https://doi.org/10.1021/acs.est.0c01945

Environmental Science & Technology

pubs.acs.org/est

Article

Insights into Ammonia Adaptation and Methanogenic Precursor Oxidation by Genome-Centric Analysis

Miao Yan, Laura Treu,* Xinyu Zhu, Hailin Tian, Arianna Basile, Ioannis A. Fotidis, Stefano Campanaro,# and Irini Angelidaki#

Cite This: https://dx.doi.org/10.1021/acs.est.0c01945

Read Online

ACCESS | Metrics & More | Article Recommendations | Supporting Information

ABSTRACT: Ammonia released from the degradation of protein and/or urea usually leads to suboptimal anaerobic digestion (AD) when N-rich organic waste is used. However, the insights behind the differential ammonia tolerance of anaerobic microbiomes remain an enigma. In this study, the cultivation in synthetic medium with different carbon sources (acetate, methanol, formate, and H_2/CO_2) shaped a common initial inoculum into four unique ammonia-tolerant syntrophic populations. Specifically, various levels of ammonia tolerance were observed: consortia fed with methanol and H_2/CO_2 could grow at ammonia levels up to 7.25 g NH^+-N/L, whereas the other two groups (formate and acetate) only thrived at 5.25 and 4.25 g NH^+-N/L, respectively. Metabolic reconstruction highlighted that this divergent microbiome might be achieved by complementary metabolisms to maximize biomethane recovery from carbon sources, thus indicating the importance of the syntrophic community in the AD of N-rich substrates. Besides, sodium/proton antiporter operon, osmoprotectant/K^+ regulator, and osmoprotectant synthesis operon may function as the main drivers of adaptation to the ammonia stress. Moreover, energy from the substrate-level phosphorylation and multiple energy-converting hydrogenases (*e.g.*, Ech and Eha) could aid methanogens to balance the energy request for anabolic activities and contribute to thriving when exposed to high ammonia levels.

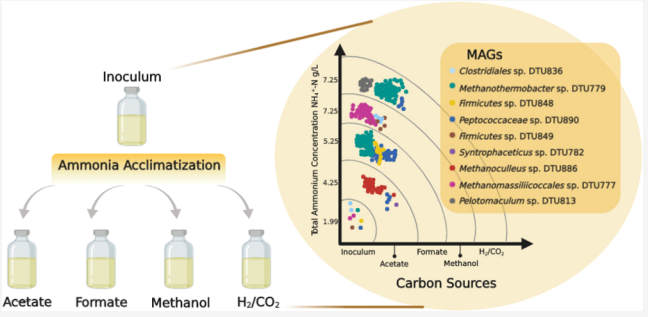

1. INTRODUCTION

The amount of nitrogen-rich organic waste generated worldwide is increasing significantly because of urbanization and population growth, which is becoming a major issue for the environment.[1] The application of anaerobic digestion (AD) can convert nitrogen-rich organic waste into a sustainable fuel.[2,3] However, free ammonia nitrogen (FAN) released from the degradation of protein or urea, once exceeding the threshold concentration, is a key parameter leading to low methane yield and process instability in AD.[4] Moreover, methanogens are more vulnerable to ammonia compared to the other AD microbes because of their weak cell wall structure lacking peptidoglycan.[5] FAN that permeates into cells can be converted to ammonium by protonation,[6] resulting in temporary proton imbalance, potassium deficiency, and strong osmotic stress.[7,8] Therefore, K^+ uptake is important for the microbial cells to overcome ammonia inhibition.[9,10] Meanwhile, the synthesis or transport of osmoprotectants such as glutamate, glutamine, phosphate, N^{ε}-acetyl-L-lysine, and glycine betaine has been reported to achieve osmotic balance and counteract ammonia inhibition.[10−12] These compatible solutes allow the survival at high osmolarity and the colonization of ecological niches in environmental conditions.[13,14] Therefore, more energy is needed for regulating the proton balance or potassium/osmoprotectant uptake during biosynthesis maintenance.[6,7] The electron-bifurcating flavoprotein complexes in *Bacteria* contribute to energy conservation through the energy-converting reductase complex (Rnf) or the energy-converting ferredoxin-dependent hydrogenase complex (Ech).[15] Specifically, Rnf catalyzes the reduction of NAD^+ with ferredoxin, thereby conserving the free-energy change in an electrochemical proton potential.[16] Likewise, HdrABC or Nuo present in methanogens is indicative of flavin-based electron bifurcation,[15] which contributes to obtaining energy from methanogenesis.[17] Additionally, Eha/b and Ech hydrogenases show high sequence similarity to the subunits of complex I, a protein pump, where they deposited NADH and reduced ferredoxin for the buildup of the proton motive force, suggesting an important role in adenosine triphosphate (ATP) synthesis.[18,19] Finally, the energy compensation to maintain the cation- and

Received: March 28, 2020
Revised: August 22, 2020
Accepted: August 27, 2020
Published: August 27, 2020

Table 1. Standard Gibbs Free Energy of Relevant Reactions in the AD Process

reactions	$\Delta G^{\circ\prime}$ (kJ/reaction)	reference
4 methanol → $3CH_4 + CO_2 + 2H_2O$	−315	20
acetate → $CH_4 + HCO^- + H^+$	−36	21
4 formate + $H^+ + H_2O \rightarrow CH_4 + 3HCO^-$	−130.4	22
$4H_2 + HCO^- + H^+ \rightarrow CH + 3HO$	−135.6	22
acetate + $HCO^- + H^+ + 3H \rightarrow$ propionate + 3HO	−76.1	23
4 methanol + $2CO_2 \rightarrow$ 3 acetate + $3H^+ + 2H_2O$	−71	24

osmobalance against ammonia stress can be obtained from substrate-level phosphorylation (Table 1). The more exergonic the reaction is, the higher ammonia level they can possibly tolerate.

Different tolerance levels to the ammonia of AD microbiome have been previously observed; for example, anaerobic glucose degradation in batch reactors was inhibited by about 70% at 3.5 g NH^+-N/L concentration and at a pH of 8.0.[25] Yan *et al.* found that *Methanosaeta concilii* and *Methanosarcina soligelidi* were the dominant methanogens at low (less than 3 g NH^+-N/L) and high ammonia levels (5−9 g NH^+-N/L), respectively, when degrading municipal solid waste.[26] Further, high ammonia levels suppressed acetoclastic methanogenesis and enhanced the hydrogenotrophic pathway, as evidenced by the increase of the relative abundance of *Methanoculleus* spp. co-digesting cattle slurry and microalgae.[4] Westerholm *et al.* also discovered the strong impact of ammonia on the occurrence of syntrophic acetate-oxidizing bacteria and the increased abundance of hydrogenotrophic methanogens.[27] The last was generally proved to be more resistant to ammonia than acetoclastic methanogens in many cases.[28]

However, all methanogens mentioned above mainly grow on acetate and/or CO_2/H_2, whereas the capability of ammonia tolerance of other methanogens dependent on methanol and formate (two other important precursors of methanogenesis) was infrequently reported.[29] Obviously, the substrate, together with the concentrations of ammonia, could drive different complete and balanced microbiome formation, leading to variable capabilities of microbes to tolerate ammonia. Deciphering the metabolic pathway of ammonia-tolerant microbiome would improve our understanding of the dynamics and the molecular mechanisms determining stress resistance, which is necessary to unravel the black box of AD microbial ecology.

Until now, only part of the AD microbiome and its interactions have been uncovered because of the difficulty in exploring such complexity with traditional cultivation-based approaches and techniques (*e.g.*, 16S rRNA sequencing) because of the limited taxonomic assignment and the presence of unknown metabolisms. Metagenomics have been recently applied to analyze the known and novel physiological, metabolic, and genetic features.[16,30] So far, most AD metagenomic studies focus on communities shaped by real feedstocks such as manure, wastewater, industrial by-products, and municipal solid waste containing various carbon sources.[31,32] Accordingly, extremely diverse communities composed of thousands of metagenome-assembled genomes (MAGs) and complex metabolic activities adapted to mixed substrate degradation were found.[30,33,34] These findings raise the possibility that specific interactions of ammonia-tolerant microbial members fed with single and simple carbon sources (the common precursors, *i.e.*, acetate, formate, H_2-CO_2, and methanol) and their functionalities await discovery.

This study provides novel insights into ammonia-tolerant methanogenic communities grown using four different carbon sources in a synthetic basal anaerobic (BA) medium. Specifically, a common initial microbiome was simplified with a stepwise increase of ammonia levels and meanwhile by providing single chemically defined substrates as an energy source: acetate, formate, H_2-CO_2, and methanol, individually. Genome-centric metagenomics was applied to unravel the methanogenesis pathways occurring in the four trophic groups. Moreover, the first look into the metabolism of the four microbiomes shaped by specific carbon sources showed how metabolic interactions occur among microbes at high ammonia levels.

2. MATERIALS AND METHODS

2.1. Experimental Setup. The samples for microbial analysis were collected from four lab-scale methanogenic batch reactors with a 1.15 L total volume. The four reactors were initially inoculated with the same digestate obtained from a lab-scale continuous-stirring tank reactor fed with cattle manure at 55 °C. The total solids and volatile solids of the digestate were 30.51 ± 0.20 and 19.76 ± 1.30 g/kg, respectively. The feedstock used in each period was a BA medium[35] ($NaHCO_3$ was used as the buffer solution) supplemented with ammonia chloride and one of the four different carbon sources (acetate, methanol, formate, and H_2/CO_2), and thus the same buffering capacity was achieved (Table S1). Furthermore, the pH was maintained at the level of 8.00 ± 0.10 by NaOH solution (4 mol/L) adjustment throughout the whole acclimatization process (Table S1).

Several successive cultivations were performed under thermophilic conditions (55 ± 1 °C) in order to adapt the microbial community to the specific substrate and the increased ammonia levels. Specifically, once methane production reached 80% of its maximal theoretical yield during each generation, inocula samples were harvested to an increased ammonia level. The process was repeated in the four groups, and the ammonia level was increased stepwise by 1 g NH^+-N/L in each increment until the microbial community could not grow anymore. The specific experimental conditions for consortia cultivation and acclimatization are listed in Table S1.

Methane yields, volatile fatty acid (VFA) concentrations, and pH values in the reactor were recorded in order to evaluate the acclimatization process. The biogas production was analyzed by a gas chromatograph (Mikrolab, Aarhus A/S, Denmark), equipped with a thermal conductivity detector. VFA concentrations derived from the intermediate steps of degradation of the carbon source were measured using a gas chromatograph (Shimadzu GC-2010 AF, Kyoto, Japan), equipped with a flame ionization detector. Finally, the pH was measured by a PHM99 LAB pH meter (RadiometerTM).

2.2. DNA Extraction and Sequencing. According to the specific carbon source used, the metagenomic DNA was

https://dx.doi.org/10.1021/acs.est.0c01945
Environ. Sci. Technol. XXXX, XXX, XXX−XXX

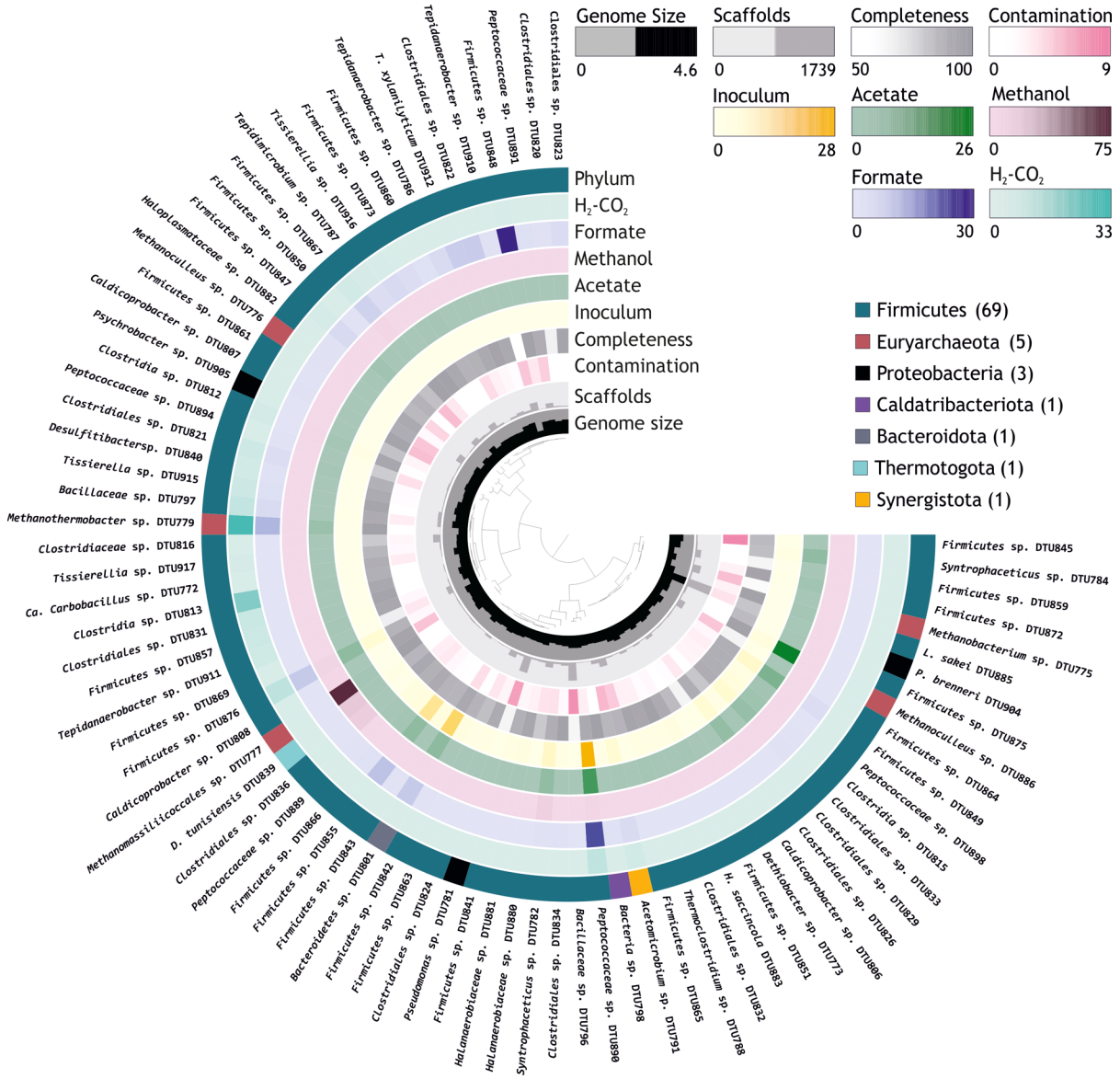

Figure 1. Microbial samples collected from five points of the batch reactors: $G_{methanol}$, $G_{formate}$, $G_{inoculum}$, $G_{acetate}$, and G_{H_2/CO_2}. The characteristics (coverage, quality, and taxonomic assignment) of 81 MAGs comprising the microbiome are reported. The outer layer represents the taxonomy at the phylum level. The five middle layers report the relative abundance of each MAG in the different microbiomes (% of relative abundance). The completeness (%), contamination (%), number of scaffolds, and genome size (Mbp) are colored in green, red, gray, and black, respectively. The middle phylogenetic tree represents the Pearson clustering of MAGs based on the relative abundances.

collected from five sampling points: $G_{inocula}$, an initial microbial community without additional ammonia and fed with cow manure (2.25 g NH^+-N/L); G, a methanol-degrading community (7.25 g NH^+-N/L); G, an acetate-degrading community (4.25 g NH^+-N/L); $G_{formate}$, a formate-degrading community (5.25 g NH^+-N/L); and G, a H/CO-degrading community (7.25 g NH^+-N/L) (Table S1). PowerSoil DNA Isolation Kit (QIAGEN, Germany) was used for genomic DNA extraction, and an additional phenol-cleaning step was performed in order to increase DNA purification.[36] Nanodrop 2000 (ThermoFisher Scientific, Waltham, MA) was used to evaluate the quality of the extracted DNA.

2.3. Genome-Centric Metagenomics and Statistics. A sequencing strategy including both Illumina and Oxford Nanopore MinION single-molecule sequencers was chosen. Library preparation was performed using the Nextera DNA Flex Library Prep Kit (Illumina Inc., San Diego CA) and the SQK rapid sequencing kit (Oxford Nanopore Technologies, Oxford, UK); libraries were sequenced with the Illumina NextSeq 500 platform (Illumina Inc., San Diego CA) with a paired-end and FLO-MIN106 R9 flow cell on a MinION device (Oxford Nanopore Technologies, Oxford, UK) at the CRIBI Biotechnology Center sequencing facility (University of Padova, Italy). Raw sequences were uploaded to the Sequence Read Archive (NCBI) under the project PRJNA613371. Oxford Nanopore Technologies base-calling for translating raw electrical signals to nucleotide sequences was performed using Guppy (v2.3.7 + e041753).[37] The total raw data provided 426,815,859 bases of sequence. Illumina reads with low-quality or ambiguous bases were filtered with Trimmomatic (v0.39). High-quality reads were independently assembled with three software, namely Spades (v3.13.0),[38]

https://dx.doi.org/10.1021/acs.est.0c01945
Environ. Sci. Technol. XXXX, XXX, XXX−XXX

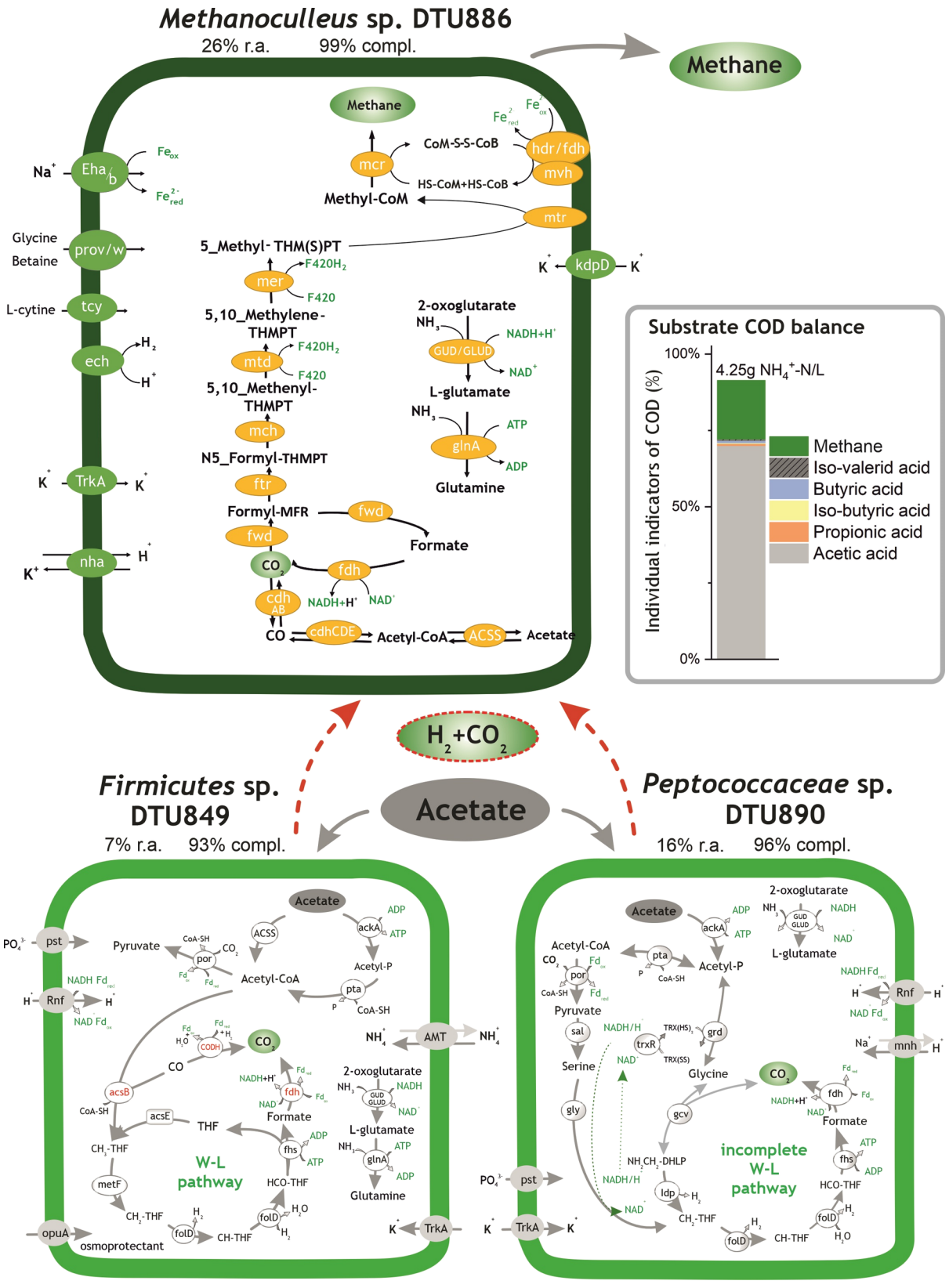

Figure 2. Histogram on the right side represents the substrate digestion profile (COD flow) measured in $G_{acetate}$. Obligate syntrophic acetate degradation pathway proposed in *Methanoculleus* sp. DTU886, *Firmicutes* sp. DTU849, and *Peptococcaceae* sp. DTU890. "R.a." and "compl." are abbreviations of the terms "relative abundance" and "completeness", respectively. The red dotted arrows represent the syntrophic intake of H_2/CO_2 by methanogens. All the relevant genes used for metabolic reconstruction can be found in Table S6.

OPERA-MS,[39] and Unicycler (v0.4.8-beta).[37] The assembly process was applied to Illumina reads alone and also to Illumina reads combined with Nanopore data using MEGAHIT (V1.2.4beta) software.[40] After the assembly, all the

https://dx.doi.org/10.1021/acs.est.0c01945
Environ. Sci. Technol. XXXX, XXX, XXX−XXX

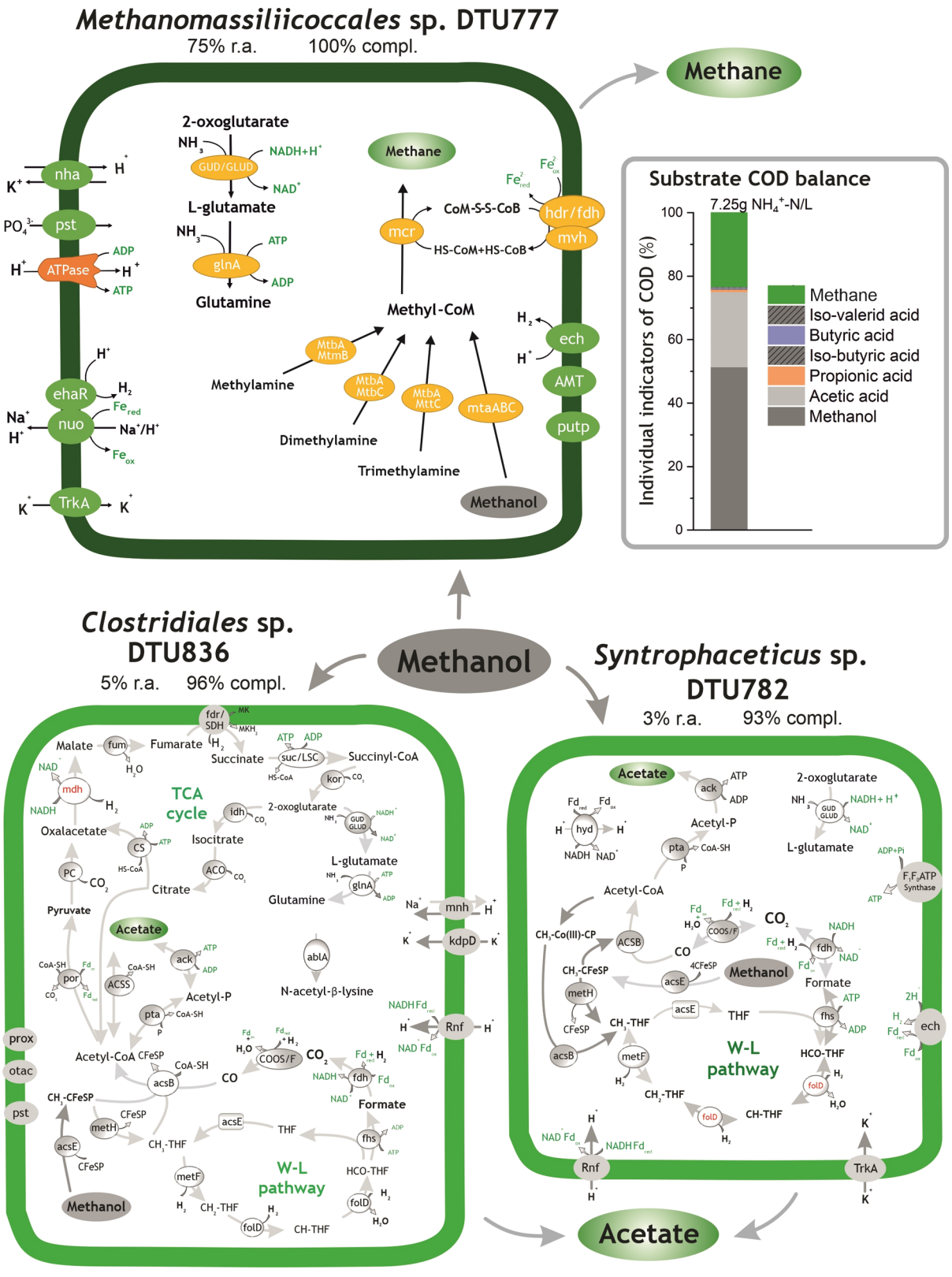

Figure 3. Histogram on the right side represents the substrate digestion profile (COD flow) measured in $G_{methanol}$. Methanol degradation pathways identified in *Methanomassiliicoccales* sp. DTU777, *Syntrophaceticus* sp. DTU782, and *Clostridiales* sp. DTU836. "R.a." and "compl." are abbreviations of the terms "relative abundance" and "completeness", respectively. All the relevant genes used for metabolic reconstruction can be found in Table S6.

scaffolds shorter than 1 kb were removed, and the statistics of the assemblies were determined using Quality Assessment Tool for Genome Assemblies (QUAST, V4.1).[41] The scaffolds' coverage was determined by aligning the reads of each sample back to the assembly with Bowtie 2 (v2.2.4)[42] and converting the output SAM files to BAM format using SAMtools (v1.9).[43]

https://dx.doi.org/10.1021/acs.est.0c01945
Environ. Sci. Technol. XXXX, XXX, XXX−XXX

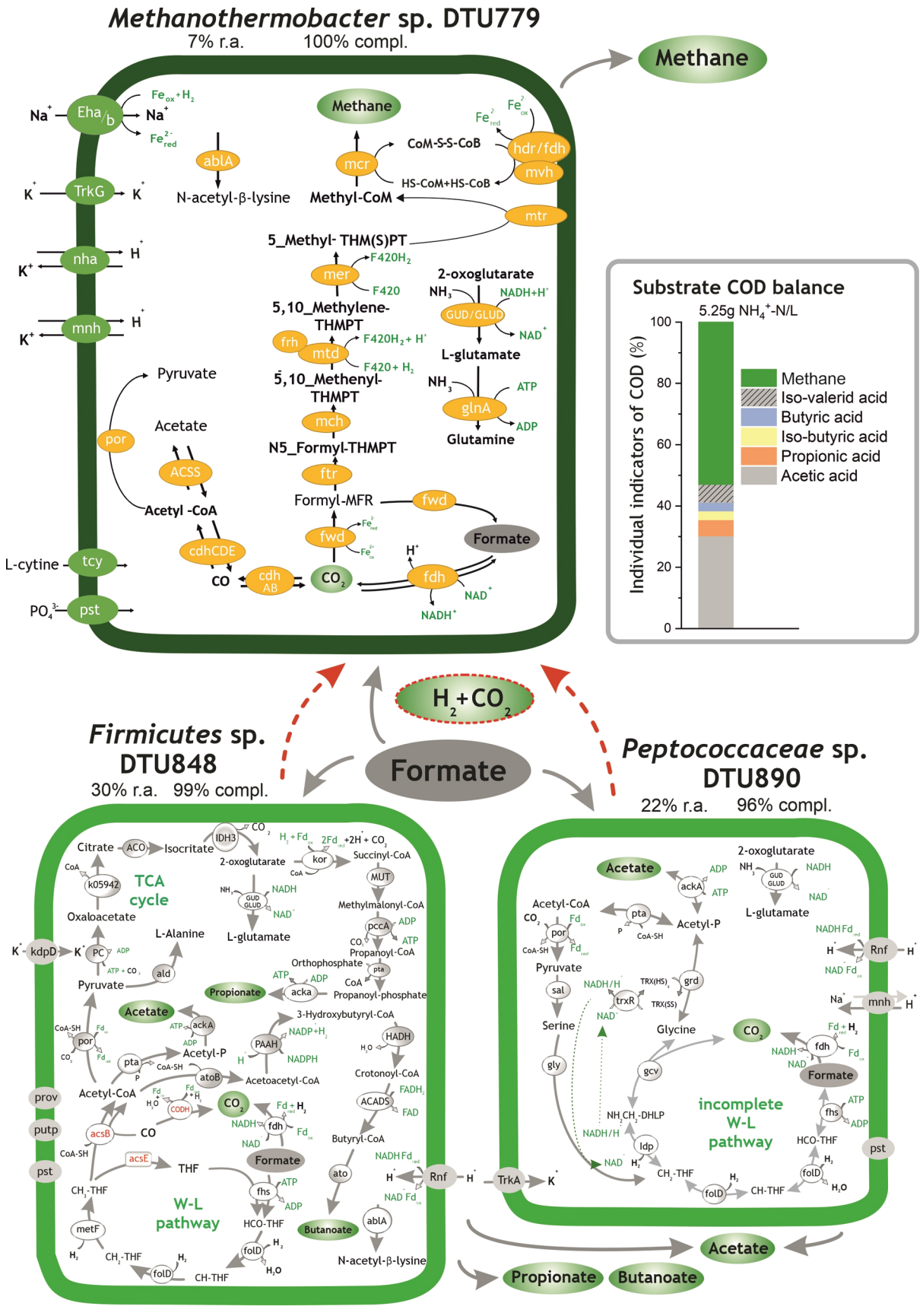

Figure 4. Histogram on the right side represents the substrate digestion profile (COD flow) measured in $G_{formate}$. Formate degradation pathways identified in *Methanothermobacter* sp. DTU779, *Peptococcaceae* sp. DTU890, and *Firmicutes* sp. DTU848. "R.a." and "compl." are the abbreviations of the terms "relative abundance" and "completeness", respectively. The red dotted arrows represent the syntrophic intake of H_2/CO_2 by *Bacteria*. All the relevant genes used for metabolic reconstruction can be found in Table S6.

https://dx.doi.org/10.1021/acs.est.0c01945
Environ. Sci. Technol. XXXX, XXX, XXX−XXX

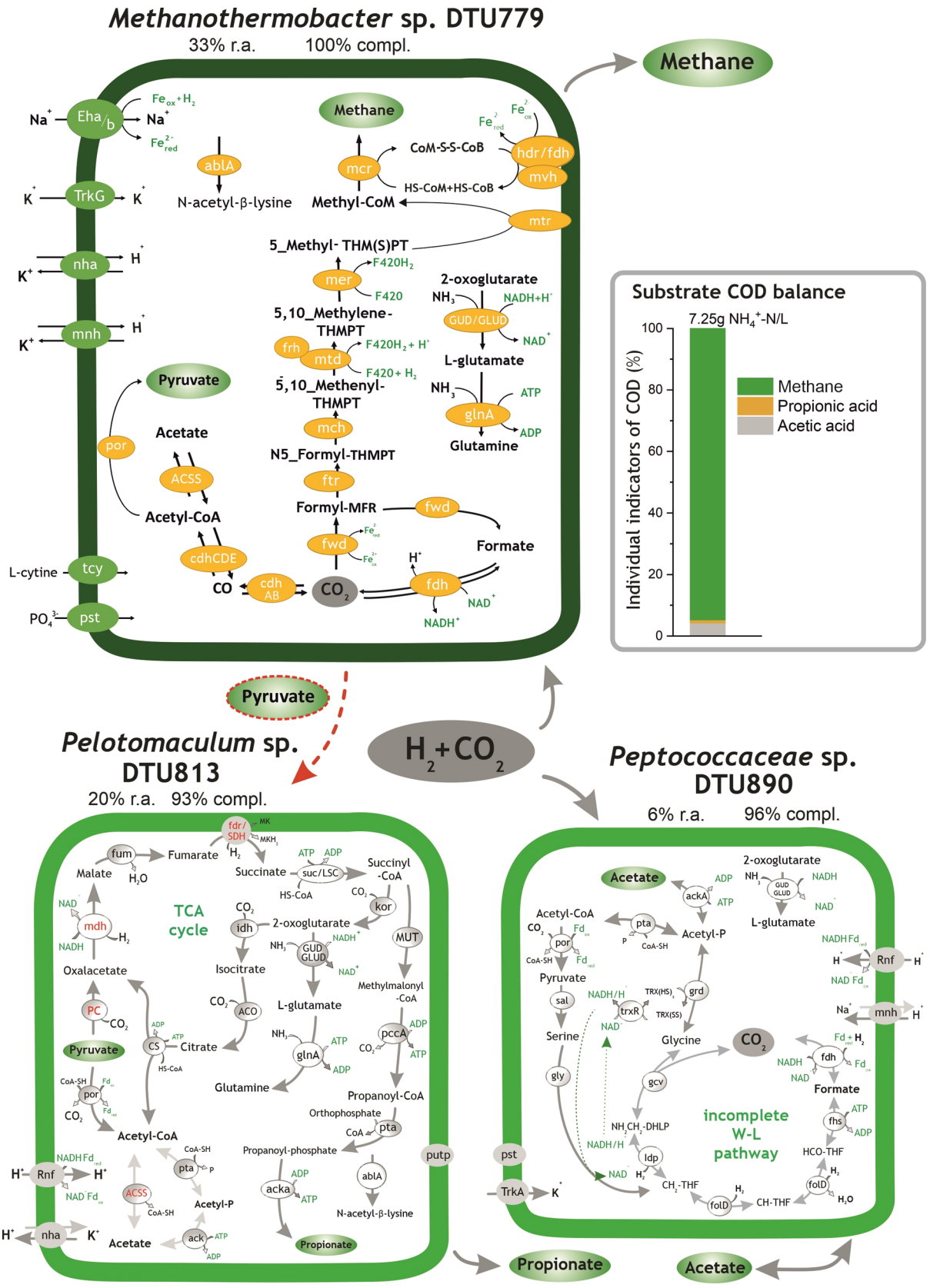

Figure 5. Histogram on the right side represents the substrate digestion profile (COD flow) measured in G_{H_2/CO_2}. H_2/CO_2 degradation pathways identified in *Methanothermobacter* sp. DTU779, *Peptococcaceae* sp. DTU890, and *Pelotomaculum* sp. DTU813. "R.a." and "compl." are the abbreviations of the terms "relative abundance" and "completeness", respectively. The red dotted arrows represent the syntrophic intake of pyruvate by methanogens. All the relevant genes used for metabolic reconstruction can be found in Table S6.

https://dx.doi.org/10.1021/acs.est.0c01945
Environ. Sci. Technol. XXXX, XXX, XXX−XXX

Metagenomic binning was performed using MetaWRAP software[45] which implements Metabat2 (v2.12.1) and MaxBin2 (v2.2.6).[44] Among the recovered MAGs, 143 were obtained from metaspades, 136 were from OPERA-MS, and 105 were from unicycler; the final selection was obtained by removing the redundancy and keeping the highest quality MAGs.

The completeness, contamination, and genome properties of the final MAGs were determined using CheckM (v1.0.3), and details can be found in Table S2. The relative abundance of microbes on each sample was obtained by aligning the reads to the assembly and subsequently using "BAM" files to calculate the final values using CheckM coverage (v1.0.3).The diversity index for each sample was measured from the unassembled Illumina reads using Nonpareil v3.303 with default parameters.[45]

Similarity with publicly available genomes was calculated by means of average nucleotide identity (ANI),[46] and the results are reported in Table S3. Taxonomical assignment and functional analysis were performed using GTDB-Tk[47] and CAT.[48] Protein-encoding genes were predicted using Prodigal (v2.6.2)[49] run in normal mode and associated with KEGG IDs using Diamond (v0.9.22.123).[50] The KEGG IDs were associated with modules to determine completeness using the KEGG mapper-reconstruct pathway tool, as previously described.[51] The functional visualization of MAG metabolism was performed using GhostKOALA.[52] Hierarchical clustering of the binned MAGs across five samples was constructed using the MultiExperiment viewer (v4.9.0) with the Pearson distance metric and visualized by Anvi'o.[53]

Simultaneously, MAGs were used for genome-scale metabolic reconstruction and the subsequent analysis of interactions within a flux balance analysis framework, adopting CarveMe (v. 1.2.1)[54] for the genome-scale metabolic reconstruction and a revised version of MMinte software (v.1.0.3)[55] for the inspection of interactions, following the pipeline developed by Basile and colleagues (https://github.com/arianccbasile/ADinteractions). Literature-guided metabolic reconstruction was manually performed based on the genes and pathways present in the most abundant MAGs for each microbiome.

Four genomes of ammonia-sensitive *Methanosaeta* spp. were downloaded from public databases of NCBI to compare the energy-converting mechanism. The GenBank assembly accession numbers of these four genomes were GCA_012729025.1; GCA_012798255.1; GCA_012798025.1; and GCA_012516895.1.

3. RESULTS AND DISCUSSION

3.1. Ammonia-Tolerant Reactor Performance Using Different Carbon Sources. The microbial consortia were cultivated in batch reactors fed with specific carbon sources, namely acetate, methanol, formate, and H_2/CO_2. After five to six consecutive generations of cultivation under stepwise ammonia increase, the microbial species present in each group showed different capabilities of resistance to ammonia (Figures 1−5). Specifically, in comparison to other groups, the community in $G_{methanol}$ and G_{H_2/CO_2} showed higher resistance to ammonia inhibition and were able to grow up to 7.25 g NH^+-N/L. Additionally, the highest methane yield (up to 91%) could be observed in G_{H_2/CO_2} at 7.25 g NH^+-N/L (Figure 5). On the contrary, the lowest methane yield (19%) was found in $G_{acetate}$ at 4.25 g NH^+-N/L (Figure 2). VFAs (*i.e.* acetate, propionate, iso-butyrate, butyrate, and iso-valerate) were detected as an important indicator of chemical oxygen demand (COD) flow from the substrate during the metabolic degradation driven by the microbial community. Trace amounts of VFAs were present in $G_{acetate}$ and G_{H_2/CO_2} (Figures 2 and 5); more than 20% of acetate (COD ratio of acetate to the added carbon source) was found in $G_{methanol}$ and $G_{formate}$, suggesting that acetate is a key intermediate during carbon degradation at high ammonia levels. To clearly decipher the main metabolic pathways that occurred during the different substrate degradations, the methane production and the intermediate accumulation (*e.g.*, VFAs) were expressed as the percentage (%) of the overall COD content to highlight the transformation processes and directly couple them with the metagenomic data. Besides, the methane yield is reported in Figure S1.

3.2. Microbial Community Composition and Activities. The assembly and binning process resulted in a total of 81 MAGs based on sequence mapping, and these microbial species accounted for 62.5−91.8% of the entire community, depending on the sample (Table S2 and Table S4). These MAGs represented the most abundant members of the microbiome; 52 out of 81 MAGs were of high quality (more than 90% completeness and lower than 5% contamination), whereas the remaining 29 MAGs were of medium quality (completeness from 50 to 90% and contamination from 5 to 10%) according to the minimum information about the metagenome-assembled genome (MIMAG)[56] (Figure 1 and Table S4). The 81 MAGs were taxonomically assigned into seven phyla, namely *Firmicutes*, *Proteobacteria*, *Thermotogae*, *Actinobacteria*, *Chloroflexi*, *Bacteroidetes*, and *Euryarchaeota* (Figure 1).

The different carbon sources (methanol, formate, acetate, and H_2/CO_2) used in this study, as well as the stepwise increased ammonia levels, worked as selecting pressure that shaped the microbial communities inducing considerable distinction in terms of diversity. In particular, attention was focused on the dominant members in each microbiome (Figures 1−5) and on the corresponding metabolic maps that were reconstructed using KEGG modules (Table S5), as well as individual gene's annotation and literature-based information. Hydrogenotrophic methanogenesis using H_2 or formate as electron donors was observed as the only methane-producing pathway in $G_{formate}$, G_{H_2/CO_2}, and $G_{acetate}$. Meanwhile, methylotrophic methanogenesis was solely observed in $G_{methanol}$, as revealed by the presence of methanol transferase and methyl-CoM reductase in *Methanomassiliicoccales* sp. DTU777.

The presence of acetate in each reactor was indicative of acetogenesis, performed *via* the conventional Wood−Ljungdahl (WL) pathway, methanol oxidation, and glycine cleavage system (Figure 3 and Table S6). The assumption is evidenced by the presence of these pathways in *Firmicutes* sp. DTU848, *Clostridiales* sp. DTU836, and *Peptococcaceae* sp. DTU890. In addition, a novel propionate synthesis pathway was reconstructed in *Firmicutes* sp. DTU848 based on the gene presence (*e.g.*, k05942, *kor*, and *acka*) using KEGG and the analysis of residual metabolites present in the medium (*e.g.*, acetate, propionate, and methane), growing in $G_{formate}$ (Figure 4 and Table S6). The following sections focus on how interspecies

https://dx.doi.org/10.1021/acs.est.0c01945
Environ. Sci. Technol. XXXX, XXX, XXX−XXX

interactions were established in a syntrophic consortium and the resistance mechanism to high ammonia levels.

3.2.1. Microbiome in the Original Inoculum. In $G_{inocula}$, *Bacteria* dominated the microbial community with a relative abundance of 98% of the binned microbiome (this value refers to the percent of reads aligned on the binned scaffolds), which accounted for 63.1% of the entire community, whereas *Archaea* were quite rare. Specifically, sugar-converting microbes (identified by the presence of Embden−Meyerhof pathway) represented the dominant MAGs consisting of *Peptococcaceae* sp. DTU890, *Bacteroidetes* sp. DTU801, *Firmicutes* sp. DTU855, and *Firmicutes* sp. DTU849 with 27.8, 16.6 10.7, and 3.8% of relative abundance, respectively (Figure 1 and Table S5). Results from ANI evaluation indicated that *Peptococcaceae* sp. DTU890 was 99.8% similar to *Clostridiales* sp. DTU010 and to other MAGs previously identified in different AD systems (Table S3).[57] According to the pathways present in these *Bacteria*, they are capable of performing a complete fermentation, converting glucose to acetate *via* the Embden−Meyerhof pathway and pyruvate oxidation (Table S5). These results show consistency with previous findings which suggested the main driving forces expanding the complexity and stability of the AD microbiome.[58] Meanwhile, *Peptococcaceae* sp. DTU890 was also involved in acetogenesis using a novel glycine cleavage system and the phosphate acetyltransferase−acetate kinase pathway (Figure 3). The other two MAGs, namely, *Syntrophaceticus* sp. DTU782 (4.3%) and *Acetomicrobium* sp. DTU791 (2.9%), were predicted to show the acetate-oxidizing ability that may work in syntrophy with hydrogenotrophic methanogens for methane production. The five identified *Euryarchaeota* sp. represented only 1.28% of the whole microbial community; among these, the most dominant MAG was *Methanoculleus* sp. DTU886 with 1.2% of relative abundance, followed by *Methanothermobacter* sp. DTU779 and *Methanomassiliicoccales* sp. DTU777, with 0.05 and 0.03%, respectively. Methanogenesis was performed by these three archaeal MAGs, having different metabolic traits of performing hydrogenotrophic and methylotrophic methanogenesis. Interestingly, no acetoclastic methanogens have been identified in the initial inoculum. The possible explanation is that the total ammonia level in $G_{inocula}$ was 2.25 g NH^+-N/L, which possibly suppressed the abundance of acetoclastic methanogens. This result also agrees with the microbial community of inocula (collected not on the same day but under the same operating conditions with our initial inocula) analyzed by 16S sRNA gene amplicon sequencing in our previous research.[59]

3.2.2. Ammonia-Tolerant Microbiome in the Acetate-Based Medium. In $G_{acetate}$, the microbiome shifted markedly, as evidenced by the change in the relative abundance of dominant MAGs when compared with the initial inoculum. In fact, the population evolved into a more simplified and specialized community, as confirmed by the diversity indexes (Table S7). $G_{acetate}$ was dominated by *Methanoculleus* sp. DTU886, *Firmicutes* sp. DTU849, and *Peptococcaceae* sp. DTU890 (Figure 2), with a cumulative relative abundance of 48% (Table S4).

More specifically, *Methanoculleus* sp. DTU886 had 99.6% ANI when compared with Candidatus *Methanoculleus thermohydrogenotrophicum*.[60] The archaeon dominated the microbiome with 26% of relative abundance and was the only methanogen present in the community. It was previously reported that *Methanoculleus* sp. could perform methanogenesis from H_2/CO_2 or formate but not acetate.[61] Interestingly, *Methanoculleus* sp. DTU886 in this study was found to harbor a series of genes for the conversion of acetate to CH_4 as well as the genes for H_2/CO_2 oxidation to CH_4 (Figure 2). Furthermore, the genomes of *Firmicutes* sp. DTU849 (7%) and *Peptococcaceae* sp. DTU890 (16%) encoded proteins involved in H_2 and CO_2 generation, suggesting the presence of a syntrophic interaction occurring between these two species and the methanogen. The presence of such interplay was confirmed by flux balance analysis revealing that *Methanoculleus* sp. DTU886 is favored by the interaction within both couples (Table S8). Specifically, *Firmicutes* sp. DTU849 possesses an incomplete gene set involved in the conventional syntrophic acetate oxidation pathway for H_2/CO_2 generation through the reverse WL pathway, whereas *CODH*, *acsB*, and *fdh* were not identified. According to the reconstructed pathway, acetate was possibly converted to pyruvate through the inverse phosphotransacetylase−acetate kinase pathway and acyl-CoA synthetase pathway (ACS). The genes encoded in *Peptococcaceae* sp. DTU890 suggested the use of an alternative glycine cleavage system for acetate oxidation (Figure 2). Specifically, the glycine cleavage system was combined with a partial WL pathway to convert acetate to CO_2/H_2, supporting the syntrophic activity with hydrogenotrophic methanogens.[62] Both syntrophic *Bacteria* possess the Rnf complex, which is involved in proton motive force-driven reverse electron transport from NADH to Fd_{ox}, where Fd_{red} was produced as a high-energy-electron carrier to facilitate H_2 generation. Regarding energy metabolism, *Methanoculleus* sp. DTU886 encodes a set of energy-conserving hydrogenases (Eha/b, Ech, and Fdh) contributing to the proton motive force by coupling proton translocation across the membrane to Fe_{red}; the same set of proteins can also be used for CO_2 reduction (Figure 2). Furthermore, methyl-THMPT HS-COM methyltransferase (Mtr), the membrane-bound enzyme complex, extruded Na^+/H^+ out of the cell, creating a Na^+/H^+-based ion motive force used for both ATP generation and methanogenesis.

3.2.3. Ammonia-Tolerant Microbiome in the Methanol-Based Medium. In $G_{methanol}$, the dominant *Methanomassiliicoccales* sp. DTU777 (75% of relative abundance) was the main player that was responsible for methane generation from methanol (Figure 3). The complete methanogenic pathway from methanol and methylamine was found in the genome (Figure 3 and Table S6). Additionally, the presence of membrane-bound NADH-ubiquinone oxidoreductase (Nuo) suggested the formation of a Fpo-like complex, capable of reoxidizing the reduced ferredoxin, with the concomitant translocation of protons or sodium ions across the membrane (Figure 3 and Table S6). The proton gradient generated by the complex mentioned above facilitated the ATP synthesis, employing the energy-conserving hydrogenase (Ech) complex, thereby coupling methane generation with energy conservation and enabling internal hydrogen cycling.[12,63]

D. tunisiensis DTU839, *Syntrophaceticus* sp. DTU782, and *Clostridiales* sp. DTU836 accounted for 7.3, 3, and 5% of relative abundance, respectively, and *Syntrophaceticus* sp. DTU782 and *Clostridiales* sp. DTU836 were chosen as the representatives of the whole bacterial community because of their high genome completeness and relative abundance. The flux balance analysis revealed a parasitic interaction between these two microbes, with *Clostridiales* sp. DTU836 taking advantage of the coexistence with *Syntrophaceticus* sp. DTU782 (Table S8). The presence of acetate in $G_{methanol}$ suggested that

https://dx.doi.org/10.1021/acs.est.0c01945
Environ. Sci. Technol. XXXX, XXX, XXX−XXX

acetogenic methanol degradation was performed as reported in the following description. According to the metabolic reconstruction, the methylic group was probably transferred to the methyl acceptor−−corrinoid Fe−S protein (CFeSP) into CH_3−CFeSP−−and followed two possible pathways of CH_3−CFeSP oxidation. First, a part of CH_3−CFeSP was converted into acetate *via* the acetate kinase pathway; second, the rest of CH_3−CFeSP was oxidized through the WL pathway, with a concomitant reduction of CO_2 into acetate. The reduction of ferredoxin and ATP for energy conservation for the above two pathways would occur following previously proposed mechanisms.[24,64] *Syntrophaceticus* sp. DTU782 had the potential to perform the first pathway using methyltransferase and acetyl synthase (ACSE and ACSB); these genes can activate and transfer the methyl group to a corrinoid Fe−S protein and oxidize it to acetyl-CoA *via* ACSB (Figure 3 and Table S6).

Meanwhile, *Clostridiales* sp. DTU836 harbored the two complete gene complexes related to acetate generation from methanol (Figure 3 and Table S6). The excess of ATP derived from the first pathway (the oxidation of one methanol to acetate) might be sacrificed to drive the endergonic oxidation of 2-methyltetrahydrofuran to 5,10-methylenetetrahydrofolate, which is in consistence with the previous study.[64]

3.2.4. Ammonia-Tolerant Microbiome in the Formate-Based Medium. The microbiome of $G_{formate}$ was mainly composed of two highly abundant *Bacteria*, *Peptococcaceae* sp. DTU890 and *Firmicutes* sp. DTU848, and one *Archaea*, *Methanothermobacter* sp. DTU779, with an aggregate relative abundance of 59% (Figure 5 and Table S4). The analyses of flux balance revealed that the growth rate of *Methanothermobacter* sp. DTU779 is positively influenced by the presence of *Firmicutes* sp. DTU848 (Table S8).

In *Methanothermobacter* sp. DTU779, the reduction of CO_2 to formyl-MFR using H_2 was driven by the electrochemical sodium ion potential (Nha and Mnh) (Figure 4 and Table S6). Furthermore, methyl-COM reduction to methane could proceed *via* the MvhADG/HdrABC complex and was coupled to ferredoxin (Fd) reduction.[65,66] Two sets of energy-conserving hydrogenases, Eha and Ehb, were found in the genome of *Methanothermobacter* sp. DTU779 (Table S6). These genes were shown to be critical for the refilling of methanogenesis intermediates (*e.g.*, H_2) and for CO_2 assimilation.[17] *Firmicutes* sp. DTU848 harbored the genes involved in the conversion of formate to acetate *via* the partial reverse WL pathway, which can explain the presence of acetate in $G_{formate}$. According to the metabolic reconstruction, propionate could be generated through a novel pathway, which involves the oxidation of acetyl-CoA into pyruvate *via* pyruvate ferredoxin oxidoreductase and the final step of amination to form citrate. Similarly, isocitrate could be transformed from citrate catalyzed into oxoglutarate, then oxidized into succinyl-CoA, and further into methylmalonyl-CoA (Figure 4 and Table S6). Finally, methylmalonyl-CoA can be converted into propionate *via* propionyl-CoA carboxylase and phosphate acetyltransferase, as previously described by Bar-Even *et al.*[67] Thereby, the sodium pumping pathway coupled with the decarboxylation of methylmalonyl-CoA derived from succinate-CoA to propionyl-CoA with the pumping of two Na^+ across the cell membrane, leading to a net energy gain.[68] Therefore, the clear carbon flow from formate conversion to propionate generation and the reductive citric acid (rTCA) cycle found in *Firmicutes* sp. DTU848 for energy conservation[69] confirmed that the bacterium could outcompete *Methanothermobacter* sp. DTU779 (30−7% of relative abundance) for formate utilization. As mentioned before, the absence of acetyl-CoA synthetase in the genome of *Peptococcaceae* sp. DTU890 indicated that an alternative glycine cleavage system was possibly employed for acetate oxidation. Additionally, both *Peptococcaceae* sp. DTU890 and *Firmicutes* sp. DTU848 encoded a sodium-ion pump (Rnf) that coupled the electron transfer for H_2 generation and ATP synthesis (Figure 4 and Table S6).

3.2.5. Ammonia-Tolerant Microbiome in the H_2/CO_2-Based Medium. In the G_{H_2/CO_2} microbiome adapted to 7.25 g NH^+-N/L, *Methanothermobacter* sp. DTU779 reached a remarkable relative abundance of 33% (5 times more than that in $G_{formate}$) (Figure 5). This finding indicated that, in the presence of formate, hydrogenotrophic methanogenesis was the main pathway. However, it can be assumed from these results that *Methanothermobacter* sp. DTU779 prefers H_2 as an electron donor for autotrophic growth, when compared to formate. Additionally, according to similarity results, DTU779 was found to have 99.8% of ANI with *Methanothermobacter wolfeii* and with other MAGs identified in previous studies[70,71] (Table S3). Interestingly, it is evidenced by Lins *et al.* that by replacing formate with H_2 in the feed, the doubling time of *M. wolfeii* can decrease to 7.65 h.[72]

The bacterial community in G_{H_2/CO_2} is mainly represented by *Pelotomaculum* sp. DTU813 and *Peptococcaceae* sp. DTU890 (26% of aggregate relative abundance). Although *Pelotomaculum* spp. are known syntrophic propionate-oxidizing *Bacteria*,[73] no propionate was provided in the feed of the H_2/CO_2-fed reactor. The metabolic reconstruction indicated that *Methanothermobacter* sp. DTU779 could produce pyruvate, suggesting a survival strategy of *Pelotomaculum* sp. DTU813, based on a parasitic relationship with *Archaea* in this specific condition. The flux balance analysis performed on this reactor actually revealed that the couple has a commensalistic behavior, with *Pelotomaculum* sp. DTU813 being favored by the coexistence. *Methanothermobacter* sp. DTU779 is not indeed negatively influenced by the coexistence, thus explaining its high abundance in the community (Table S8). This hypothesis, based on the gene content and metabolites presence, was also supported by previous literature. In fact, *Pelotomaculum thermopropionicum* is known for fermenting pyruvate into acetate and propionate (3:1 molar ratio)[73] and the same products were measured in the reactor (Figure 5). Finally, acetate, potentially produced by *Pelotomaculum* sp. DTU813, could be further utilized by *Peptococcaceae* sp. DTU890 for biomass production, with the consequent CO_2/H_2 generation. However, *Peptococcaceae* sp. DTU890 seems to have a versatile metabolism that can alternatively produce or consume different carbon sources (*i.e.*, acetate and CO_2/H_2) depending on the metabolites' concentrations in the medium.

3.3. Proposed Mechanisms for Ammonia Acclimatization. The adaptation of microbiome to ammonia through the strategy of single and simple carbon source cultivation under stepwise increased ammonia levels achieved the specialized and simplified microbiome discussed above. Most importantly, it also clarified some aspects of the mechanisms involved in ammonia resistance by identifying the metabolic pathways involved in the adaptation and unraveling the trophic niches occupied by each MAG. The variable capabilities of different microbiomes to tolerate ammonia seemed to be

https://dx.doi.org/10.1021/acs.est.0c01945
Environ. Sci. Technol. XXXX, XXX, XXX−XXX

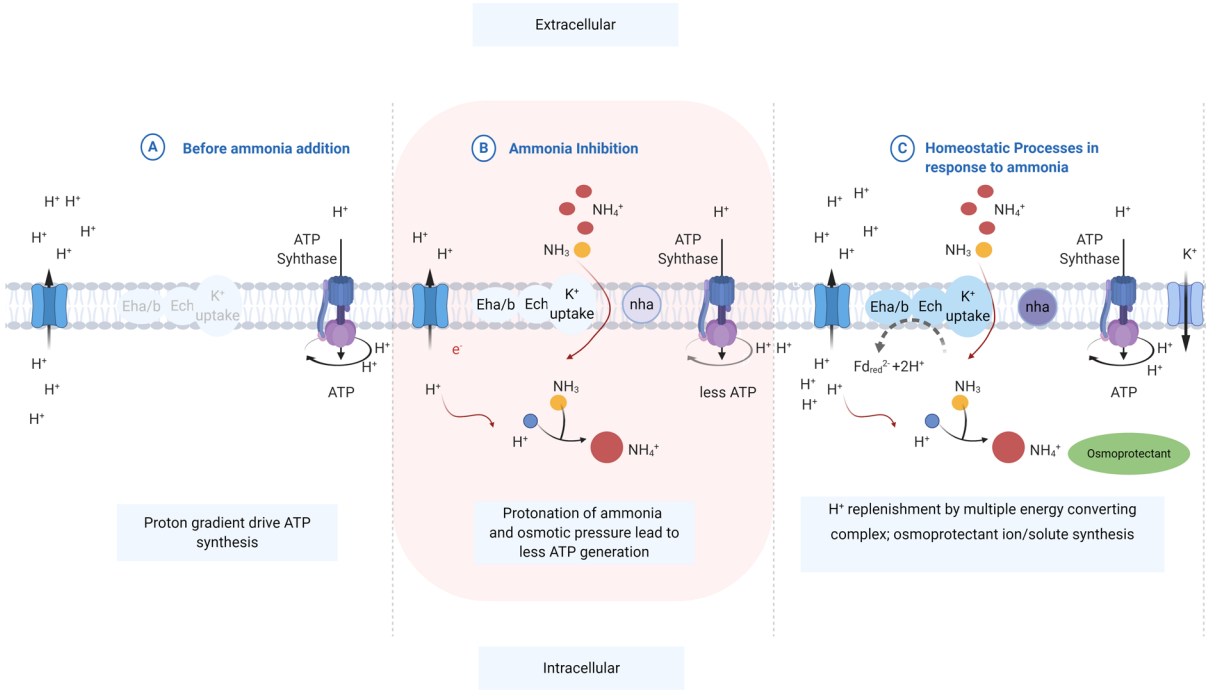

Figure 6. Proposed response of methanogen in different situations. (a) Before ammonia inhibition. (b) During ammonia inhibition, the protonation of ammonia and osmotic pressure lead to less ATP generation. (c) Homeostatic regulation in response to ammonia by following strategies: H^+ replenishment by multiple energy-converting complexes, osmoprotectant ion/solute synthesis, and H^+ binding by pumping K^+ into the cell for cation balance.

connected with the homeostatic system, energy conservation strategies, and different ATP generation *via* substrate-level phosphorylation (Table S6).

From the homeostatic perspective, the presence of the potassium or sodium/proton antiporter (nha) system and the K^+ uptake system (TrKA) had the potential to top-up intracellular protons and K^+ for homeostatic processes, including the regulation of the turgor pressure and maintenance of cytoplasmic pH in response to the protonation of ammonia (Figures 2−6 and Table S6). As a confirmation of this process, Kraegeloh *et al.* revealed a process in which the loss of TrKA abolished any K^+ uptake activity leading to osmotic sensitivity.[7] Considering the osmotic stress induced by ammonium, a possible resistance mechanism of the MAGs identified in the current study could be related to the activity of glutamate dehydrogenase, glutamine, glycine betaine, and N^{ε}-acetyl-L-lysine synthase. These enzymes can synthesize known osmoprotectants such as glutamate, glutamine, glycine betaine, and N^{ε}-acetyl-L-lysine, which contribute to the survival of the cells at high osmotic stress and allow the colonization of ecological niches in severe environmental conditions. It seemed that the co-occurrence of the two systems (*i.e.*, osmoprotectant generation and potassium uptake) was a necessity against ammonia stress. This finding was in agreement with previous studies, highlighting that the synthesis of glutamate requires a stable level of K^+.[74−76]

To regulate proton balance, potassium uptake, and biosynthesis maintenance, extra energy is needed. Thus, the raised question is how energy conservation can be achieved in order to survive during ammonia inhibition. The metabolic reconstruction provided novel insights regarding membrane-bound NADH-ubiquinone oxidoreductase (Nuo) in *Methanomassiliicoccales* sp. DTU777. In fact, the presence of a Fpo-like complex capable of reoxidizing the reduced ferredoxin, with simultaneous translocation of protons or sodium ions across the membrane, can generate the proton gradient needed for the ATP synthesis, as previously reported.[12,64] Similarly, Hdr, Fwd, and Fdh present in *Methanothermobacter* sp. DTU779 were described to support the assembly of a bifurcating multienzyme complex, and Mnh was employed as an electrochemical potential-driven transporter (Figure 5 and Table S6).

Additionally, the coexistence of Eha/b and Ech complexes, in the presence of optimized energy conservation in DTU779, could be a reason for its extraordinary adaption to ammonia-inhibiting conditions (Figure 5). This hypothesis may be supported by the ability of *Methanothermobacter* sp. to outcompete other methanogens for establishing a syntrophic relationship with fatty acid-oxidizing *Bacteria*.[16] Interestingly, the genome comparison of three identified *Archaea* in this study (*Methanoculleus* sp. DTU886, *Methanomassiliicoccales* sp. DTU777, and *Methanothermobacter* sp. DTU779) with the four ammonia-sensitive *Methanosaeta* spp. (downloaded from public databases) verified that the Eha/b and Ech energy-converting system was only present in the former three methanogens.

Obviously, when exposed to ammonia stress, methanogens with the multiple energy-converting hydrogenases mentioned above could become more energy-efficient and thereafter thrive easier than methanogens without these complexes (Figure 6). Additionally, the number of genes responsible for energy conservation in *Methanothermobacter* sp. DTU779 (n:25) was much higher than in *Methanomassiliicoccales* sp. DTU777 (n:18) and *Methanoculleus* sp. DTU886 (n:13), which is consistent with the variable capability of ammonia tolerance of each methanogen (Table S6).

Differential tolerance to ammonia might also be attributed to variable Gibbs free energies obtained by the different

https://dx.doi.org/10.1021/acs.est.0c01945
Environ. Sci. Technol. XXXX, XXX, XXX−XXX

microbes from substrate-level phosphorylation. According to previous studies (listed in Table 1), the energy for cell maintenance could be obtained *via* methanogenesis from methanol (−315 kJ/per reaction),[20] H_2/CO_2 (−135.6 kJ/per reaction),[77] formate (−130.4 kJ/per reaction),[77] and acetate (−36 kJ/per reaction).[21] Obviously, methanogenesis from methanol and H_2/CO_2 is far more exergonic compared to the other methanogenic processes, which might lead to the higher ammonia tolerance of *Methanomassiliicoccales* sp. DTU777 in $G_{methanol}$ and *Methanothermobacter* sp. DTU779 in G_{H_2/CO_2} than *Methanoculleus* sp. DTU886 in $G_{acetate}$. In particular, it is known from the literature that the conversion of 1 mol methanol to acetate in *Clostridiales* sp. and *Syntrophaceticus* sp. could release 0.625 ATP (the highest ATP gain identified for acetogens so far), with efficient sustained cell growth at energy-limited situations.[24,64] Interestingly, in $G_{formate}$, *Methanothermobacter* sp. DTU779 could only grow at an ammonia level up to 5.25 $N-NH^+$ g/L, whereas it could stand up to 7.25 $N-NH^+$ g/L in H/CO feeding, aided by the cooperative interaction with *Pelotomaculum* sp. DTU813. Furthermore, the presence of other intermediate metabolites (*e.g.*, acetate and propionate) in the four reactors indicated that alternative exergonic pathways were occurring. Specifically, the energy released from the conversion of acetate to propionate (−76.1 kJ/mol)[23] and methanol to acetate (−71 kJ/mol)[24] might support the growth of the whole consortium. Thus, ATP derived from *Archaea* and *Bacteria via* substrate-level phosphorylation might play a crucial role in overcoming bioenergetic barriers induced by ammonia inhibition and in driving thermodynamically unfavorable reactions. Besides, the difference in net ATP gain among the four microbial groups ($G_{acetate}$, $G_{methanol}$, $G_{formate}$, and G_{H_2/CO_2}) might determine the variable capabilities of ammonia tolerance.

■ ASSOCIATED CONTENT

Supporting Information

The Supporting Information is available free of charge at https://pubs.acs.org/doi/10.1021/acs.est.0c01945.

BA medium composition, characteristics of the reactors, and methane yields in the four groups; details and statistics for the total MAGs; average nucleotide identity comparison with previous projects; statistics and relative abundances of the MAGs selected according to MIMAG quality; KO terms used in KEGG mapper to visualize the metabolic pathways per MAG; metabolic reconstruction of the dominant MAGs; diversity indexes calculated for each sample using Nonpareil; results of pairwise interactivity in the microbiome of the four reactors characterized by different carbon sources (XLSX)

■ AUTHOR INFORMATION

Corresponding Author

Laura Treu − *Department of Biology, University of Padova, 35121 Padova, Italy;* orcid.org/0000-0002-5053-4452; Phone: +390498276165; Email: laura.treu@unipd.it

Authors

Miao Yan − *Department of Environmental Engineering, Technical University of Denmark, DK-2800 Kongens Lyngby, Denmark*

Xinyu Zhu − *Department of Environmental Engineering, Technical University of Denmark, DK-2800 Kongens Lyngby, Denmark*

Hailin Tian − *Department of Environmental Engineering, Technical University of Denmark, DK-2800 Kongens Lyngby, Denmark; NUS Environmental Research Institute, National University of Singapore, 138602, Singapore*

Arianna Basile − *Department of Biology, University of Padova, 35121 Padova, Italy*

Ioannis A. Fotidis − *Department of Environmental Engineering, Technical University of Denmark, DK-2800 Kongens Lyngby, Denmark; School of Civil Engineering, Southeast University, 210096 Nanjing, China;* orcid.org/0000-0003-4587-3617

Stefano Campanaro − *Department of Biology, University of Padova, 35121 Padova, Italy; CRIBI Biotechnology Center, University of Padua, 35131 Padua, Italy*

Irini Angelidaki − *Department of Environmental Engineering, Technical University of Denmark, DK-2800 Kongens Lyngby, Denmark;* orcid.org/0000-0002-6357-578X

Complete contact information is available at: https://pubs.acs.org/10.1021/acs.est.0c01945

Author Contributions

#S.C. and I.A. equal contribution.

Notes

The authors declare no competing financial interest.

■ ACKNOWLEDGMENTS

This work was supported by Energinet.dk under the project framework ForskEL "MicrobStopNH3-Innovative bioaugmentation strategies to tackle ammonia inhibition in anaerobic digestion process" (program no. 2015-12327). The authors acknowledge the financial support from MUDP (Miljøstyrelsens) under the project framework VARGA (MST-141-01377). M.Y. appreciates the financial support from China Scholarship Council.

■ REFERENCES

(1) Korai, M. S.; Mahar, R. B.; Uqaili, M. A. The Feasibility of Municipal Solid Waste for Energy Generation and Its Existing Management Practices in Pakistan. *Renew. Sustain. Energy Rev.* **2017**, *72*, 338−353.

(2) Fotidis, I. A.; Wang, H.; Fiedel, N. R.; Luo, G.; Karakashev, D. B.; Angelidaki, I. Bioaugmentation as a Solution to Increase Methane Production from an Ammonia-Rich Substrate. *Environ. Sci. Technol.* **2014**, *48*, 7669−7676.

(3) Satchwell, A. J.; Scown, C. D.; Smith, S. J.; Amirebrahimi, J.; Jin, L.; Kirchstetter, T. W.; Brown, N. J.; Preble, C. V. Accelerating the Deployment of Anaerobic Digestion to Meet Zero Waste Goals. *Environ. Sci. Technol.* **2018**, *52*, 13663.

(4) Tian, H.; Fotidis, I. A.; Kissas, K.; Angelidaki, I. Effect of Different Ammonia Sources on Aceticlastic and Hydrogenotrophic Methanogens. *Bioresour. Technol.* **2018**, *250*, 390−397.

(5) Capson-Tojo, G.; Moscoviz, R.; Astals, S.; Robles, Á.; Steyer, J.-P. Unraveling the Literature Chaos around Free Ammonia Inhibition in Anaerobic Digestion. *Renew. Sustain. Energy Rev.* **2020**, *117*, 109487.

(6) Kayhanian, M. Ammonia Inhibition in High-Solids Biogasification: An Overview and Practical Solutions. *Environ. Technol.* **1999**, *20*, 355−365.

(7) Kraegeloh, A.; Amendt, B.; Kunte, H. J. Potassium Transport in a Halophilic Member of the Bacteria Domain: Identification and Characterization of the K+ Uptake Systems TrkH and TrkI from Halomonas Elongata DSM 2581T. *J. Bacteriol.* **2005**, *187*, 1036.

https://dx.doi.org/10.1021/acs.est.0c01945
Environ. Sci. Technol. XXXX, XXX, XXX−XXX

(8) Liu, Y.; Yuan, Y.; Wang, W.; Wachemo, A. C.; Zou, D. Effects of Adding Osmoprotectant on Anaerobic Digestion of Kitchen Waste with High Level of Salinity. *J. Biosci. Bioeng.* **2019**, *128*, 723−732.
(9) Martin, D. D.; Ciulla, R. A.; Roberts, M. F. Osmoadaptation in Archaea. *Appl. Environ. Microbiol.* **1999**, *65*, 1815−1825.
(10) Vyrides, I.; Santos, H.; Mingote, A.; Ray, M. J.; Stuckey, D. C. Are Compatible Solutes Compatible with Biological Treatment of Saline Wastewater? Batch and Continuous Studies Using Submerged Anaerobic Membrane Bioreactors (SAMBRs). *Environ. Sci. Technol.* **2010**, *44*, 7437−7442.
(11) Grammann, K.; Volke, A.; Kunte, H. J. New Type of Osmoregulated Solute Transporter Identified in Halophilic Members of the Bacteria Domain: TRAP Transporter TeaABC Mediates Uptake of Ectoine and Hydroxyectoine in Halomonas Elongata DSM 2581T. *J. Bacteriol.* **2002**, *184*, 3078−3085.
(12) Vanwonterghem, I.; Evans, P. N.; Parks, D. H.; Jensen, P. D.; Woodcroft, B. J.; Hugenholtz, P.; Tyson, G. W. Methylotrophic Methanogenesis Discovered in the Archaeal Phylum Verstraetearchaeota. *Nat. Microbiol.* **2016**, *1*, 16170.
(13) Müller, V.; Spanheimer, R.; Santos, H. Stress Response by Solute Accumulation in Archaea. *Curr. Opin. Microbiol.* **2005**, *8*, 729−736.
(14) Kadam, P. C.; Boone, D. R. Influence of PH on Ammonia Accumulation and Toxicity in Halophilic, Methylotrophic Methanogens. *Appl. Environ. Microbiol.* **1996**, *62*, 4486−4492.
(15) Buckel, W.; Thauer, R. K. Flavin-Based Electron Bifurcation, Ferredoxin, Flavodoxin, and Anaerobic Respiration With Protons (Ech) or NAD+ (Rnf) as Electron Acceptors: A Historical Review. *Front. Microbiol.* **2018**, *9*, 401.
(16) Liu, P.; Lu, Y. Concerted Metabolic Shifts Give New Insights into the Syntrophic Mechanism between Propionate-Fermenting Pelotomaculum Thermopropionicum and Hydrogenotrophic Methanocella Conradii. *Front. Microbiol.* **2018**, *9*, 1551.
(17) Megaw, J.; Gilmore, B. F. Archaeal Persisters: Persister Cell Formation as a Stress Response in Haloferax Volcanii. *Front. Microbiol.* **2017**, *8*, 1589.
(18) Nobu, M. K.; Narihiro, T.; Rinke, C.; Kamagata, Y.; Tringe, S. G.; Woyke, T.; Liu, W.-T. Microbial Dark Matter Ecogenomics Reveals Complex Synergistic Networks in a Methanogenic Bioreactor. *ISME J.* **2015**, *9*, 1710. —Supplementary Information—35
(19) Lie, T. J.; Costa, K. C.; Lupa, B.; Korpole, S.; Whitman, W. B.; Leigh, J. A. Essential Anaplerotic Role for the Energy-Converting Hydrogenase Eha in Hydrogenotrophic Methanogenesis. *Proc. Natl. Acad. Sci.* **2012**, *109*, 15473−15478.
(20) Lovley, D. R.; Klug, M. J. Methanogenesis from Methanol and Methylamines and Acetogenesis from Hydrogen and Carbon Dioxide in the Sediments of a Eutrophic Lake †. *Appl. Environ. Microbiol.* **1983**, *45*, 1310−1315.
(21) Smith, M. R.; Mah, R. A. Growth and Methanogenesis by Methanosarcina Strain 227 on Acetate and Methanol. *Appl. Environ. Microbiol.* **1978**, *36*, 870−879.
(22) Schauer-Gimenez, A. E.; Zitomer, D. H.; Maki, J. S.; Struble, C. A. Bioaugmentation for Improved Recovery of Anaerobic Digesters after Toxicant Exposure. *Water Res.* **2010**, *44*, 3555−3564.
(23) Van Lier, J. B.; Grolle, K. C.; Frijters, C. T.; Stams, A. J.; Lettinga, G. Effects of Acetate, Propionate, and Butyrate on the Thermophilic Anaerobic Degradation of Propionate by Methanogenic Sludge and Defined Cultures. *Appl. Environ. Microbiol.* **1993**, *59*, 1003−1011.
(24) Keller, A.; Schink, B.; Müller, N. Alternative Pathways of Acetogenic Ethanol and Methanol Degradation in the Thermophilic Anaerobe Thermacetogenium Phaeum. *Front. Microbiol.* **2019**, *10*, 423.
(25) Fujishima, S.; Miyahara, T.; Noike, T. Effect of Moisture Content on Anaerobic Digestion of Dewatered Sludge: Ammonia Inhibition to Carbohydrate Removal and Methane Production. *Water Sci. Technol.* **2000**, *41*, 119−127.
(26) Yan, M.; Fotidis, I. A.; Tian, H.; Khoshnevisan, B.; Treu, L.; Tsapekos, P.; Angelidaki, I. Acclimatization Contributes to Stable Anaerobic Digestion of Organic Fraction of Municipal Solid Waste under Extreme Ammonia Levels: Focusing on Microbial Community Dynamics. *Bioresour. Technol.* **2019**, *286*, 121376.
(27) Westerholm, M.; Levén, L.; Schnürer, A. Bioaugmentation of Syntrophic Acetate-Oxidizing Culture in Biogas Reactors Exposed to Increasing Levels of Ammonia. *Appl. Environ. Microbiol.* **2012**, *78*, 7619−7625.
(28) Yang, Z.; Wang, W.; Liu, C.; Zhang, R.; Liu, G. Mitigation of Ammonia Inhibition through Bioaugmentation with Different Microorganisms during Anaerobic Digestion: Selection of Strains and Reactor Performance Evaluation. *Water Res.* **2019**, *155*, 214−224.
(29) Sorokin, D. Y.; Makarova, K. S.; Abbas, B.; Ferrer, M.; Golyshin, P. N.; Galinski, E. A.; Ciordia, S.; Mena, M. C.; Merkel, A. Y.; Wolf, Y. I.; van Loosdrecht, M. C. M.; Koonin, E. V. Discovery of Extremely Halophilic, Methyl-Reducing Euryarchaea Provides Insights into the Evolutionary Origin of Methanogenesis. *Nat. Microbiol.* **2017**, *2*, 17081.
(30) Wang, T.; Zhang, D.; Dai, L.; Dong, B.; Dai, X. Magnetite Triggering Enhanced Direct Interspecies Electron Transfer: A Scavenger for the Blockage of Electron Transfer in Anaerobic Digestion of High-Solids Sewage Sludge. *Environ. Sci. Technol.* **2018**, *52*, 7160−7169.
(31) Ruiz-Sánchez, J.; Campanaro, S.; Guivernau, M.; Fernández, B.; Prenafeta-Boldú, F. X. Effect of Ammonia on the Active Microbiome and Metagenome from Stable Full-Scale Digesters. *Bioresour. Technol.* **2018**, *250*, 513−522.
(32) Xia, Y.; Wang, Y.; Fang, H. H.; Jin, T.; Zhong, H.; Zhang, T. Thermophilic Microbial Cellulose Decomposition and Methanogenesis Pathways Recharacterized by Metatranscriptomic and Metagenomic Analysis. *Sci. Rep.* **2014**, *4*, 6708.
(33) Campanaro, S.; Treu, L.; Rodriguez-R, L. M.; Kovalovszki, A.; Ziels, R. M.; Maus, I.; Zhu, X.; Kougias, P. G.; Basile, A.; Luo, G. New Insights from the Biogas Microbiome by Comprehensive Genome-Resolved Metagenomics of Nearly 1600 Species Originating from Multiple Anaerobic Digesters. *Biotechnol. Biofuels* **2020**, *13*, 1−18.
(34) Liu, H.; Chen, Y. Enhanced Methane Production from Food Waste Using Cysteine To Increase Biotransformation ofl-Monosaccharide, Volatile Fatty Acids, and Biohydrogen. *Environ. Sci. Technol.* **2018**, *52*, 3777−3785.
(35) Tian, H.; Karachalios, P.; Angelidaki, I.; Fotidis, I. A. A Proposed Mechanism for the Ammonia-LCFA Synergetic Co-Inhibition Effect on Anaerobic Digestion Process. *Chem. Eng. J.* **2018**, *349*, 574−580.
(36) Treu, L.; Kougias, P. G.; de Diego-Díaz, B.; Campanaro, S.; Bassani, I.; Fernández-Rodríguez, J.; Angelidaki, I. Two-Year Microbial Adaptation during Hydrogen-Mediated Biogas Upgrading Process in a Serial Reactor Configuration. *Bioresour. Technol.* **2018**, *264*, 140−147.
(37) Wick, R. R.; Judd, L. M.; Holt, K. E. Performance of Neural Network Basecalling Tools for Oxford Nanopore Sequencing. *Genome Biol.* **2019**, *20*, 129.
(38) Bankevich, A.; Nurk, S.; Antipov, D.; Gurevich, A. A.; Dvorkin, M.; Kulikov, A. S.; Lesin, V. M.; Nikolenko, S. I.; Pham, S.; Prjibelski, A. D.; Pyshkin, A. V.; Sirotkin, A. V.; Vyahhi, N.; Tesler, G.; Alekseyev, M. A.; Pevzner, P. A. SPAdes: A New Genome Assembly Algorithm and Its Applications to Single-Cell Sequencing. *J. Comput. Biol.* **2012**, *19*, 455−477.
(39) Bertrand, D.; Shaw, J.; Kalathiyappan, M.; Ng, A. H. Q.; Kumar, M. S.; Li, C.; Dvornicic, M.; Soldo, J. P.; Koh, J. Y.; Tong, C.; Ng, O. T.; Barkham, T.; Young, B.; Marimuthu, K.; Chng, K. R.; Sikic, M.; Nagarajan, N. Hybrid Metagenomic Assembly Enables High-Resolution Analysis of Resistance Determinants and Mobile Elements in Human Microbiomes. *Nat. Biotechnol.* **2019**, *37*, 937−944.
(40) Li, D.; Liu, C.-M.; Luo, R.; Sadakane, K.; Lam, T.-W. MEGAHIT: An Ultra-Fast Single-Node Solution for Large and Complex Metagenomics Assembly via Succinct de Bruijn Graph. *Bioinformatics* **2015**, *31*, 1674−1676.

https://dx.doi.org/10.1021/acs.est.0c01945
Environ. Sci. Technol. XXXX, XXX, XXX−XXX

(41) Gurevich, A.; Saveliev, V.; Vyahhi, N.; Tesler, G. QUAST: Quality Assessment Tool for Genome Assemblies. *Bioinformatics* **2013**, *29*, 1072−1075.
(42) Langmead, B.; Salzberg, S. L. Fast Gapped-Read Alignment with Bowtie 2. *Nat. Methods* **2012**, *9*, 357.
(43) Li, H.; Handsaker, B.; Wysoker, A.; Fennell, T.; Ruan, J.; Homer, N.; Marth, G.; Abecasis, G.; Durbin, R. The Sequence Alignment/Map Format and SAMtools. *Bioinformatics* **2009**, *25*, 2078−2079.
(44) Tsuji, J. M.; Tran, N.; Schiff, S. L.; Venkiteswaran, J. J.; Molot, L. A.; Tank, M.; Hanada, S.; Neufeld, J. D. Genomic Potential for Photoferrotrophy in a Seasonally Anoxic Boreal Shield Lake. *bioRxiv* **2020**, 653014.
(45) Rodriguez-R, L. M.; Gunturu, S.; Tiedje, J. M.; Cole, J. R.; Konstantinidis, K. T. Nonpareil 3: Fast Estimation of Metagenomic Coverage and Sequence Diversity. *mSystems* **2018**, *3*, No. e00039.
(46) Varghese, N. J.; Mukherjee, S.; Ivanova, N.; Konstantinidis, K. T.; Mavrommatis, K.; Kyrpides, N. C.; Pati, A. Microbial Species Delineation Using Whole Genome Sequences. *Nucleic Acids Res.* **2015**, *43*, 6761−6771.
(47) Chaumeil, P.-A.; Mussig, A. J.; Hugenholtz, P.; Parks, D. H. GTDB-Tk: A Toolkit to Classify Genomes with the Genome Taxonomy Database. *Bioinformatics* **2020**, *36*, 1925−1927.
(48) von Meijenfeldt, F. A. B.; Arkhipova, K.; Cambuy, D. D.; Coutinho, F. H.; Dutilh, B. E. Robust Taxonomic Classification of Uncharted Microbial Sequences and Bins with CAT and BAT. *Genome Biol.* **2019**, *20*, 217.
(49) Hyatt, D.; Chen, G.-L.; LoCascio, P. F.; Land, M. L.; Larimer, F. W.; Hauser, L. J. Prodigal: Prokaryotic Gene Recognition and Translation Initiation Site Identification. *BMC Bioinf.* **2010**, *11*, 119.
(50) Buchfink, B.; Xie, C.; Huson, D. H. Fast and Sensitive Protein Alignment Using DIAMOND. *Nat. Methods* **2015**, *12*, 59−60.
(51) Treu, L.; Campanaro, S.; Kougias, P. G.; Sartori, C.; Bassani, I.; Angelidaki, I. Hydrogen-Fueled Microbial Pathways in Biogas Upgrading Systems Revealed by Genome-Centric Metagenomics. *Front. Microbiol.* **2018**, *9*, 1079.
(52) Kanehisa, M.; Sato, Y.; Morishima, K. BlastKOALA and GhostKOALA: KEGG Tools for Functional Characterization of Genome and Metagenome Sequences. *J. Mol. Biol.* **2016**, *428*, 726−731.
(53) Eren, A. M.; Esen, Ö. C.; Quince, C.; Vineis, J. H.; Morrison, H. G.; Sogin, M. L.; Delmont, T. O. Anvi'o: An Advanced Analysis and Visualization Platform for 'omics Data. *PeerJ* **2015**, *3*, No. e1319.
(54) Machado, D.; Andrejev, S.; Tramontano, M.; Patil, K. R. Fast Automated Reconstruction of Genome-Scale Metabolic Models for Microbial Species and Communities. *Nucleic Acids Res.* **2018**, *46*, 7542−7553.
(55) Mendes-Soares, H.; Mundy, M.; Soares, L. M.; Chia, N. MMinte: An Application for Predicting Metabolic Interactions among the Microbial Species in a Community. *BMC Bioinf.* **2016**, *17*, 343.
(56) Bowers, R. M.; Kyrpides, N. C.; Stepanauskas, R.; Harmon-Smith, M.; Doud, D.; Reddy, T. B. K.; Schulz, F.; Jarett, J.; Rivers, A. R.; Eloe-Fadrosh, E. A.; Tringe, S. G.; Ivanova, N. N.; Copeland, A.; Clum, A.; Becraft, E. D.; Malmstrom, R. R.; Birren, B.; Podar, M.; Bork, P.; Weinstock, G. M.; Garrity, G. M.; Dodsworth, J. A.; Yooseph, S.; Sutton, G.; Glöckner, F. O.; Gilbert, J. A.; Nelson, W. C.; Hallam, S. J.; Jungbluth, S. P.; Ettema, T. J. G.; Tighe, S.; Konstantinidis, K. T.; Liu, W.-T.; Baker, B. J.; Rattei, T.; Eisen, J. A.; Hedlund, B.; McMahon, K. D.; Fierer, N.; Knight, R.; Finn, R.; Cochrane, G.; Karsch-Mizrachi, I.; Tyson, G. W.; Rinke, C.; Lapidus, A.; Meyer, F.; Yilmaz, P.; Parks, D. H.; Murat Eren, A.; Schriml, L.; Banfield, J. F.; Hugenholtz, P.; Woyke, T. Minimum Information about a Single Amplified Genome (MISAG) and a Metagenome-Assembled Genome (MIMAG) of Bacteria and Archaea. *Nat. Biotechnol.* **2017**, *35*, 725−731.
(57) Campanaro, S.; Treu, L.; Kougias, P. G.; Luo, G.; Angelidaki, I. Metagenomic Binning Reveals the Functional Roles of Core Abundant Microorganisms in Twelve Full-Scale Biogas Plants. *Water Res.* **2018**, *140*, 123−134.
(58) Yan, M.; Treu, L.; Campanaro, S.; Tian, H.; Zhu, X.; Khoshnevisan, B.; Tsapekos, P.; Angelidaki, I.; Fotidis, I. A. Effect of Ammonia on Anaerobic Digestion of Municipal Solid Waste: Inhibitory Performance, Bioaugmentation and Microbiome Functional Reconstruction. *Chem. Eng. J.* **2020**, *401*, 126159.
(59) Tian, H.; Yan, M.; Treu, L.; Angelidaki, I.; Fotidis, I. A. Hydrogenotrophic Methanogens Are the Key for a Successful Bioaugmentation to Alleviate Ammonia Inhibition in Thermophilic Anaerobic Digesters. *Bioresour. Technol.* **2019**, *293*, 122070.
(60) Kougias, P. G.; Campanaro, S.; Treu, L.; Zhu, X.; Angelidaki, I. A Novel Archaeal Species Belonging to Methanoculleus Genus Identified via De-Novo Assembly and Metagenomic Binning Process in Biogas Reactors. *Anaerobe* **2017**, *46*, 23−32.
(61) Anderson, I. J.; Sieprawska-Lupa, M.; Lapidus, A.; Nolan, M.; Copeland, A.; Glavina Del Rio, T.; Tice, H.; Dalin, E.; Barry, K.; Saunders, E.; Han, C.; Brettin, T.; Detter, J. C.; Bruce, D.; Mikhailova, N.; Pitluck, S.; Hauser, L.; Land, M.; Lucas, S.; Richardson, P.; Whitman, W. B.; Kyrpides, N. C. Complete Genome Sequence of Methanoculleus Marisnigri Romesser et al. 1981 Type Strain JR1. *Stand. Genomic Sci.* **2009**, *1*, 189−196.
(62) Zhu, X.; Campanaro, S.; Treu, L.; Seshadri, R.; Ivanova, N.; Kougias, P. G.; Kyrpides, N.; Angelidaki, I. Metabolic Dependencies Govern Microbial Syntrophies during Methanogenesis in an Anaerobic Digestion Ecosystem. *Microbiome* **2020**, *8*, 22.
(63) Oehler, D.; Poehlein, A.; Leimbach, A.; Müller, N.; Daniel, R.; Gottschalk, G.; Schink, B. Genome-Guided Analysis of Physiological and Morphological Traits of the Fermentative Acetate Oxidizer Thermacetogenium Phaeum. *BMC Genom.* **2012**, *13*, 723.
(64) Kremp, F.; Poehlein, A.; Daniel, R.; Müller, V. Methanol Metabolism in the Acetogenic Bacterium Acetobacterium Woodii. *Environ. Microbiol.* **2018**, *20*, 4369−4384.
(65) Smith, S. G.; Rouvière, P. E. Purification and characterization of the reduced-nicotinamide-dependent 2,2′-dithiodiethanesulfonate reductase from Methanobacterium thermoautotrophicum delta H. *J. Bacteriol.* **1990**, *172*, 6435−6441.
(66) Kaster, A.-K.; Moll, J.; Parey, K.; Thauer, R. K. Coupling of Ferredoxin and Heterodisulfide Reduction via Electron Bifurcation in Hydrogenotrophic Methanogenic Archaea. *Proc. Natl. Acad. Sci.* **2011**, *108*, 2981−2986.
(67) Bar-Even, A.; Noor, E.; Milo, R. A Survey of Carbon Fixation Pathways through a Quantitative Lens. *J. Exp. Bot.* **2012**, *63*, 2325−2342.
(68) Hilpert, W.; Dimroth, P. On the Mechanism of Sodium Ion Translocation by Methylmalonyl-CoA Decarboxylase from Veillonella Alcalescens. *Eur. J. Biochem.* **1991**, *195*, 79−86.
(69) Springsteen, G.; Yerabolu, J. R.; Nelson, J.; Rhea, C. J.; Krishnamurthy, R. Linked Cycles of Oxidative Decarboxylation of Glyoxylate as Protometabolic Analogs of the Citric Acid Cycle. *Nat. Commun.* **2018**, *9*, 91.
(70) Fontana, A.; Kougias, P. G.; Treu, L.; Kovalovszki, A.; Valle, G.; Cappa, F.; Morelli, L.; Angelidaki, I.; Campanaro, S. Microbial Activity Response to Hydrogen Injection in Thermophilic Anaerobic Digesters Revealed by Genome-Centric Metatranscriptomics. *Microbiome* **2018**, *6*, 194.
(71) Kougias, P. G.; Campanaro, S.; Treu, L.; Tsapekos, P.; Armani, A.; Angelidaki, I. Spatial Distribution and Diverse Metabolic Functions of Lignocellulose-Degrading Uncultured Bacteria as Revealed by Genome-Centric Metagenomics. *Appl. Environ. Microbiol.* **2018**, *84*, No. e01244.
(72) Lins, P.; Schwarzenauer, T.; Reitschuler, C.; Wagner, A. O.; Illmer, P. Methanogenic Potential of Formate in Thermophilic Anaerobic Digestion. *Waste Manag. Res.* **2012**, *30*, 1031.
(73) Imachi, H. Pelotomaculum Thermopropionicum Gen. Nov., Sp. Nov., an Anaerobic, Thermophilic, Syntrophic Propionate-Oxidizing Bacterium. *Int. J. Syst. Evol. Microbiol.* **2002**, *52*, 1729−1735.
(74) Maus, I.; Wibberg, D.; Stantscheff, R.; Stolze, Y.; Blom, J.; Eikmeyer, F.-G.; Fracowiak, J.; König, H.; Pühler, A.; Schlüter, A. Insights into the annotated genome sequence of Methanoculleus

https://dx.doi.org/10.1021/acs.est.0c01945
Environ. Sci. Technol. XXXX, XXX, XXX−XXX

bourgensis MS2T, related to dominant methanogens in biogas-producing plants. *J. Biotechnol.* **2015**, *201*, 43−53.
(75) Yan, D.; Ikeda, T. P.; Shauger, A. E.; Kustu, S. Glutamate Is Required to Maintain the Steady-State Potassium Pool in Salmonella Typhimurium. *Proc. Natl. Acad. Sci.* **1996**, *93*, 6527−6531.
(76) Manzoor, S.; Schnürer, A.; Bongcam-Rudloff, E.; Müller, B. Complete Genome Sequence of Methanoculleus Bourgensis Strain MAB1, the Syntrophic Partner of Mesophilic Acetate-Oxidising Bacteria (SAOB). *Stand. Genomic Sci.* **2016**, *11*, 80.
(77) Schauer, N. L.; Ferry, J. G. Metabolism of Formate in Methanobacterium Formicicum. *J. Bacteriol.* **1980**, *142*, 800−807.

https://dx.doi.org/10.1021/acs.est.0c01945
Environ. Sci. Technol. XXXX, XXX, XXX−XXX

Supplementary Material

Insights into ammonia adaptation and methanogenic precursor oxidation by genome-centric analysis

Miao Yan[a], Laura Treu[b]*, Xinyu Zhu[a], Hailin Tian[a,d], Arianna Basile[b], Ioannis Fotidis[a,c], Stefano Campanaro[b,e§], Irini Angelidaki[a§]

[a] Department of Environmental Engineering, Technical University of Denmark, Bygningstorvet Bygning 115, DK-2800 Kgs. Lyngby, Denmark

[b] Department of Biology, University of Padova, Via U. Bassi 58/b, 35121 Padova, Italy

[c] School of Civil Engineering Southeast University Nanjing, China

[d] NUS Environmental Research Institute, National University of Singapore, 1 Create Way, 138602, Singapore

[e] CRIBI Biotechnology Center, University of Padua, 35131, Padua, Italy

The supporting information includes:

Table S1 BA medium composition, characteristics of the reactors and methane yields in the four groups

Table S2 Details and statistics for the total MAGs

Table S3 Average nucleotide identity comparison with previous projects Genes name

Table S4 Statistics and relative abundances of the MAGs selected according to MIMAG quality

Table S5 KO terms used in KEGG mapper to visualize the metabolic pathways per each MAG

Table S6 Metabolic reconstruction of the dominant MAGs

Table S7 The diversity indexes calculated for each sample using Nonpareil

Table S8 Results of pairwise interactivity in the microbiome of four reactor characterized by different carbon sources

Table S1 BA medium composition

	stock solution		portion		Final concentration
	g/L		10	ml/L	g/L
A	NH_4Cl	100			1
	NaCl	10			0.1
	$MgCl_2·6H_2O$	10			0.1
	$CaCl_2·2H_2O$	5			0.05
	g/L		2	ml/L	g/L
B	$K_2HPO_4·3H_2O$	200			0.4
	mg/L		1	ml/L	mg/L
D	$FeCl_2·4H_2O$	2000			2
	H_3BO_3	50			0.05
	$ZnCl_2$	50			0.05
	$CuCl_2$	30			0.03
	$MnCl_2·4H_2O$	50			0.05
	$(NH_4)_6Mo_7O_{24}·4H_2O$	50			0.05
	$AlCl_3$	50			0.05
	$CoCl_2·6H_2O$	50			0.05
	$NiCl_2$	50			0.05
	EDTA	500			0.5
	H_2SeO_3	49			0.049
	g/L		50	ml/L	g/L
	$NaHCO_3$	52			2.6

Characteristics of the reactors

	Acetate	Formate	Methanol	H_2/CO_2	Organic loading g.VS/L
Original ammonia level $N\text{-}NH_4^+$ g/L	2.25±0.15				
pH	7.9±0.1	8.1±0.01	8.0±0.02	7.9 ±0.02	
Acclimatization process $N\text{-}NH_4^+$ g/L	2.25	2.25	2.25	2.25	1
	3.25	3.25	3.25	3.25	1
	4.25	4.25	4.25	4.25	1
		5.25	5.25	5.25	1-2.5
			6.25	6.25	1-2.5
			7.25	7.25	1.7-2

* pH was maintained by NaOH solution (4 mol/L)

Figure S1: Methane yields in the four groups: $G_{H2/CO2}$, H_2/CO_2 degrading community at 7.25 g NH_4^+-N/L, $G_{methanol}$, methanol degrading community at 7.25 g NH_4^+-N/L; $G_{acetate}$, acetate degrading community at 4.25 g NH_4^+-N/L; $G_{formate}$, formate degrading community at 5.25 g NH_4^+-N/L.

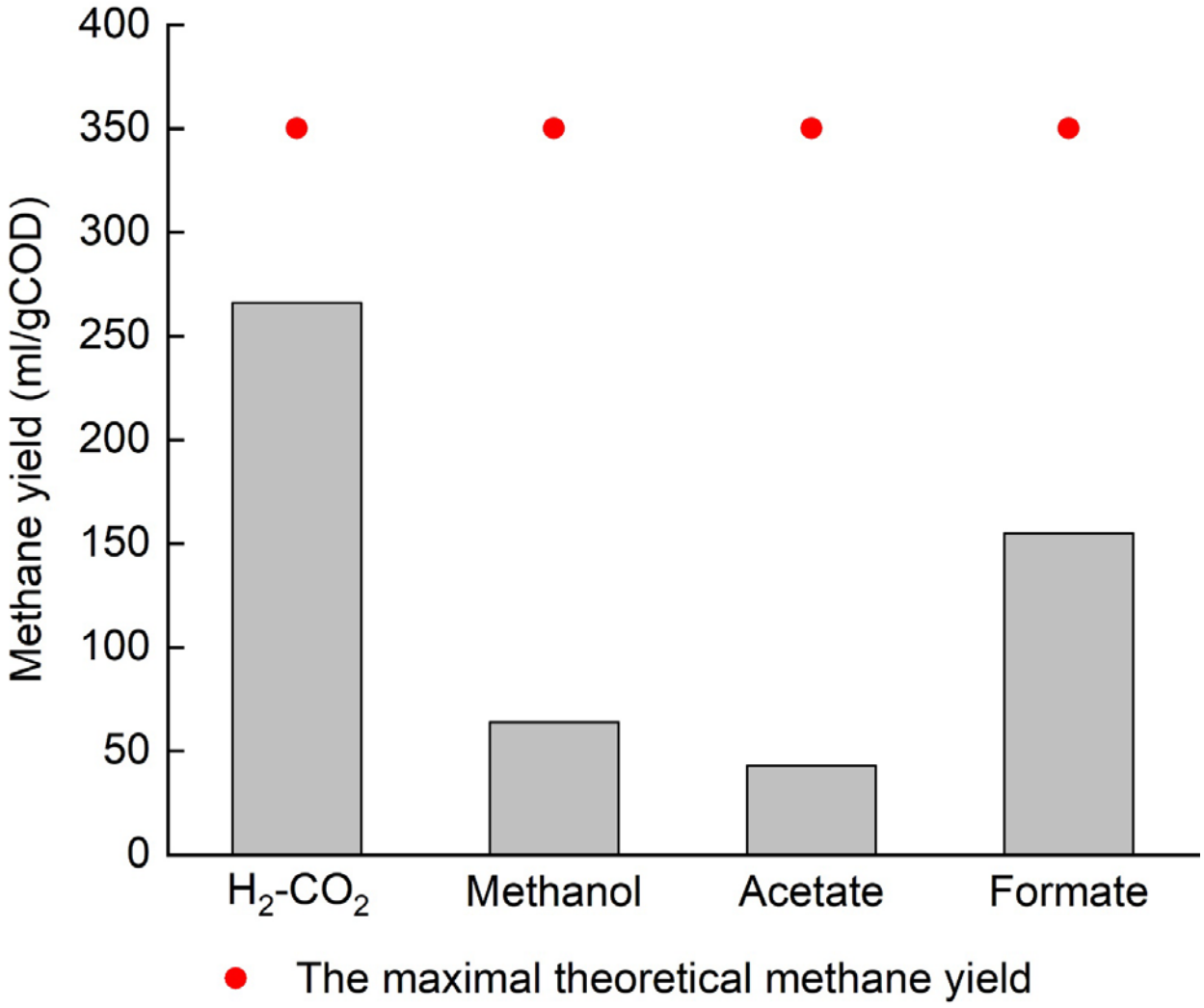

Table S2-8 contain mass of data, thus they are available online

https://pubs.acs.org/doi/10.1021/acs.est.0c01945?goto=supporting-info

III

Effect of ammonia on anaerobic digestion of municipal solid waste: inhibitory performance, bioaugmentation and microbiome functional reconstruction

Miao Yan, Laura Treu, Stefano Campanaro, Hailin Tian, Xinyu Zhu, Benyamin Khoshnevisan, Panagiotis Tsapekos, Irini Angelidaki, Ioannis A. Fotidis

Chemical Engineering Journal, 2020,126159.

https://doi.org/10.1016/j.cej.2020.126159

Chemical Engineering Journal 401 (2020) 126159

Contents lists available at ScienceDirect

Chemical Engineering Journal

journal homepage: www.elsevier.com/locate/cej

Effect of ammonia on anaerobic digestion of municipal solid waste: Inhibitory performance, bioaugmentation and microbiome functional reconstruction

Miao Yan[a], Laura Treu[b,*], Stefano Campanaro[b,c,*], Hailin Tian[a,d], Xinyu Zhu[a], Benyamin Khoshnevisan[a,e], Panagiotis Tsapekos[a], Irini Angelidaki[a,1], Ioannis A. Fotidis[a,f,1]

[a] Department of Environmental Engineering, Technical University of Denmark, Bygningstorvet Bygning 115, DK-2800 Kgs. Lyngby, DK, Italy
[b] Department of Biology, University of Padova, Via U. Bassi 58/b, 35121 Padova, Italy
[c] CRIBI Biotechnology Center, University of Padua, 35131 Padua, Italy
[d] NUS Environmental Research Institute, National University of Singapore, 1 Create Way, 138602, Singapore
[e] Key Laboratory of Non-point Source Pollution Control, Ministry of Agriculture, Institute of Agricultural Resources and Regional Planning, Chinese Academy of Agricultural Sciences, Beijing 100081, China
[f] School of Civil Engineering Southeast University Nanjing, 210096, China

HIGHLIGHTS

- The bioaugmentation with *Methanoculleus* sp. culture remarkably enhanced the methane yield by 21%
- The volatile fatty acids were decreased by 10% compared to the period before bioaugmentation.
- *Peptococcaceae* and *Tissierellales* were dominating the microbiome as glucose degraders.
- *Syntrophaceticus* was the key acetate oxidizer under the extremely high level of 13.5 NH_4^+-N/L.
- Multiple glucose/acetate metabolism were reconstructed by metagenomic approach.

GRAPHICAL ABSTRACT

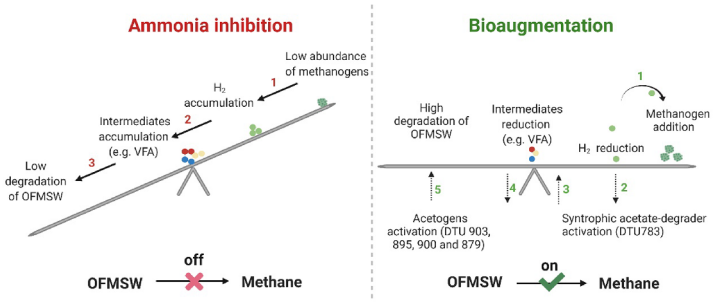

ARTICLE INFO

Keywords:
Bioaugmentation
Metagenomics
Ammonia tolerance
Energy-converting mechanisms
Interspecies interaction
Metabolic reconstruction

ABSTRACT

The bioaugmentation is crucial to improve the energy-efficient process for anaerobic digestion of organic wastes at high ammonia levels. Genomic insights into the intricate microbial networks at a high ammonia level remain underexplored. The present study showed that the addition of *Methanoculleus* sp. DTU887 remarkably enhanced the methane production yield of organic fraction of municipal solid waste by 21% and decreased the volatile fatty acids by 10% when compared to the period before bioaugmentation. Genome-centric metagenomics reports the functional contribution of microbial members during organic waste degradation under the extremely high level of 13.5 g NH_4^+-N/L. Specifically, metabolic reconstruction revealed that these organisms have the potential to perform fermentative and acetogenic catabolism, a process facilitated by energy conservation-related with H_2/CO_2 metabolism. *Peptococcaceae* spp. (DTU903, DTU900, and DTU895). and *Tissierellales* sp. DTU879 could degrade the organic waste hydrolysis product, i.e., glucose to acetate and H_2. *Tissierellales* sp. DTU879 and *Syntrophaceticus* sp. DTU783 could degrade the derived acetate. The H_2 scavenging *Methanoculleus* sp. DTU887

* Corresponding authors at: Department of Biology, University of Padova, Via U. Bassi 58/b, 35121 Padova, Italy.
E-mail addresses: laura.treu@unipd.it (L. Treu), stefano.campanaro@unipd.it (S. Campanaro).
[1] Authors are equally contributing.

https://doi.org/10.1016/j.cej.2020.126159
Received 7 May 2020; Received in revised form 29 June 2020; Accepted 30 June 2020
Available online 05 July 2020
1385-8947/

performs complementary metabolic reactions with *Peptococcaceae* spp., *Tissierellales* sp. and *Syntrophaceticus* sp., indicating syntrophic glucose and acetate degradation. This research offers the first insight that the key organisms form a syntrophy-supported food web in response to the bioaugmentation with ammonia tolerant methanogens performed in an AD system subjected to severe ammonia inhibition.

1. Introduction

The increasing amount of organic waste and its consequent disposal has been a major worldwide environmental and economic problem [1]. Inappropriate treatment, such as landfill, leads to greenhouse gas emissions, odors, and sanitary concerns [2]. To reach the United Nations' Sustainable Development Goals (SDGs) by 2030, organic waste should be integrated into a circular economy concept including nutrients recovery and bioenergy production [3,4]. Therefore the focus has been given to anaerobic digestion (AD) as a key technology, which treats residual biomasses properly and produces renewable energy (i.e., biogas). The biogas can substitute fossil fuels in heat production, electricity generation and transportation and, at the same time, preserve nutrients which can be retrieved for soil applications [5]. The efficient conversion of organic waste into biogas requires a well-balanced microbiome performing syntrophic interactions among four main steps of the AD process (i.e. hydrolysis, acidogenesis, acetogenesis, methanogenesis) This syntrophic association may contribute to (i) maintain the microbiome balance [6], (ii) prevent volatile fatty acids (VFA) and hydrogen accumulation, and (iii) convert intermediate compounds (acetate, H_2, CO_2) to methane [7]. Moreover, the energy potential of the current worldwide organic waste is estimated between 10,100 and 14,000 TWh equivalent to 26–37% of the current natural gas consumed globally (World Biogas Association 2019); therefore even small improvements in biogas production may be extremely relevant [8].

However, degradation of N-rich organic wastes, especially effluents from many industries, aquaculture production units, food processing plants, etc., can represent a major challenge in maintaining a balanced process [9]. Specifically, when the concentration of ammonia exceeds a certain limit (approximately 1.5 g NH_4^+-N /L during AD), it becomes toxic for the microbial consortium [10]. To be noticed, the methanogenic archaea are directly responsible for biogas production and more susceptible to ammonia compared to bacteria, excluding syntrophic acetate oxidizers (SAOB) [11–13]. The reduced methanogenic activity induces inefficient hydrogen/formate removal, and as a consequence, SAOB does not harvest enough energy to support self-growth at high H_2 concentrations. Besides, accumulation of additional intermediate compounds (e.g. VFA, H_2) happens because the reduction in the activity of bacteria doesn't occur to the same degree as that of methanogens [14,15]. This accumulation further inhibits methanogenesis lowering methane production rates, and can eventually lead to AD failure.

The supplementation of ammonia tolerant methanogens is one of the key strategies applied for the recovery from ammonia inhibition. This can be achieved by bioaugmentation, i.e. introducing specific acclimatized pure strain or enriched cultures into an under-performing anaerobic digester [16,17]. Additionally, another advantage of using the bioaugmentation is that the microbial cultures incorporated in the digestate can be directly used as a soil amendment or fertilizer [18]. In fact, other ammonia alleviation strategies, such as magnetite or zeolite addition, require extra separation steps before discharge [19,20]. The syntrophic mechanisms occurring due to bioaugmentation imply that the addition of specific microbes enhances the removal of self-limiting products (e.g. H_2 or acetate), which are used by archaea as electron donors/acceptors during methanogenesis [21]. The removal of these intermediates stimulates the growth of bacteria, improving the substrate consumption rates and funneling the substrate fermentation toward methane production [7]. Yang et al. (2019) have proved that the bioaugmentation performed with the simultaneous addition of *Methanobrevibacter smithii* and *Syntrophaceticu schinkii* could efficiently improve methane production by 71% at 4 g NH_4^+-N/L. To pinpoint the key role of specific consortia in the AD process [17], Westerholm et al. (2012) proved that the addition of SAOB cultures alone couldn't improve the performance at an ammonia load of 11 g NH_4^+-N/L [22]. However, bioaugmentation with hydrogenotrophic methanogens alone could dramatically stimulate the growth of SAOB, rapidly alleviating the acetate-ammonia co-inhibitory effect in thermophilic and mesophilic reactors [23,24]. Despite this, the metabolic pathways and microbial interactions induced by bioaugmentation and being responsible for improving methane production remain unknown. Recently, the metagenomics approach has been applied to unravel genomic information for diverse unknown microorganisms in AD microbiomes and offer insights into their potential functions creating a global reference database [12,25,26]. However genomic insight into interconnected networks of effective microbes growing at high ammonia level is still lacking.

The present study aimed to decipher holistic AD syntrophic interactions in response to the bioaugmentation with ammonia tolerant methanogen performed in an AD system subjected to severe ammonia stress. To achieve that, the bioaugmentation strategy was employed in an inhibited continuously stirred anaerobic reactor (CSTR) fed with organic fraction municipal solid waste (OFMSW) at 13.5 g NH_4^+-N/L. Specifically, bioaugmentation was performed with a pure culture of one ammonia-tolerant *Methanoculleus bourgensis*, belonging to a well-known resistant methanogenic genus [25]. An in-depth analysis of the microbial responses was performed by metagenomics and the metabolic pathways encoded by the most abundant taxa were reconstructed in detail.

2. Material and methods

2.1. Inoculum and feedstock

The inoculum used to start two CSTRs obtained from a mesophilic (37 °C) anaerobic digester used for OFMSW degradation at total ammonia nitrogen (TAN) of 9.5 g NH_4^+-N/L, which had been operated stably for 10 months [27]. The OFMSW, collected from Gemidan Ecogi A/S, was used as substrate after treated with the bio pulping process [28]. The substrate was preserved at −20 °C and thawed at 4 °C before use, then diluted with distilled water to reach a fixed total solid (TS) content of 80 g VS/kg. The characteristics of the inoculum and of the substrate are presented in Table 1.

2.2. Bioaugmentation culture

M. bourgensis MS2 culture (DSM 3045) was purchased from Leibniz Institute DSMZ-German Collection of Microorganisms and Cell Cultures, and routinely maintained for more than five years in the Bioenergy laboratory at Denmark Technical University. The sequential cultivation was done obtaining sub generation from previous seed generation at the exponential growth phase. Prior to bioaugmentation, the culture was acclimatized to 14 g NH_4^+-N/L (increment with 2 g NH_4^+-N/L each step) at 37 °C. The characteristics of the cultivation medium (CM) and growth curve for *M. bourgensis* are shown in Table S1.

2.3. Experimental setup

The experiment was performed in two identical mesophilic CSTR

Nomenclature

AD	Anaerobic Digestion
VFA	volatile fatty acids
OFMSW	organic fraction municipal solid waste
CSTR	continuously stirred anaerobic reactor
TAN	total ammonia nitrogen
TS	total solid
VS	Volatile solids
CM	cultivation medium
FAN	Free ammonia nitrogen
TKN	Total Kjeldahl Nitrogen
HRT	hydraulic retention time
MAG	Metagenome assembled genome
PTA-ACKA	phosphotransacetylase-acetate kinase pathway
ACS	forming acyl-CoA synthetase
acs	acyl-CoA synthetase gene
ack	acetate kinase gene
mcrA	methyl coenzyme M reductase gene
mta, *mtb*	coenzyme M methyltransferase genes
coo	carbon monoxide dehydrogenase gene
gcv	glycine decarboxylase genes
grd	glycine reductase gene
Vho	methanophenazine-reducing hydrogenase
Frh	coenzyme F_{420}-reducing hydrogenase
Ech	energy converting hydrogenase
Fpo	$F_{420}H_2$ dehydrogenase
hdr	membrane-bound heterodisulfide reductase gene
Ehb	energy-conserving hydrogenase B
WL	Wood-Ljungdahl
Rnf	Rhodobacter nitrogen fixation complex
EMP pathway	Embdene Meyerhofe Parnas pathway

reactors with a total and working volume of 4.5 and 3 L, respectively (Fig. 1). R_{bio} and R_{con} represent high ammonia loaded reactors with bioaugmentation (addition of *M. bourgensis*) and abiotic augmentation (without the addition of *M. bourgensis*), respectively. With a hydraulic retention time (HRT) of 20 days, the two reactors were fed with OFMSW at an organic loading rate of 3.4 g VS/L/day for 135 days. The whole experiment was divided into five periods (P1-P5) as presented in Table 2. During P1 to P3, the TAN levels of the influent and the reactor content were increased concurrently from 9.5 to 13.5 g NH_4^+-N/L (increment with 2 g NH_4^+-N/L each step) with the addition of urea ($CO(NH_2)_2$) and ammonium chloride (NH_4Cl). The ammonia load of 13.5 g NH_4^+-N/L was kept for all the remaining periods (P4-P5). The bioaugmentation with *M. bourgensis* resuspended in CM for R_{bio} was performed for four consecutive days at P4. Specifically, 240 ml of culture (volatile suspended solids (VSS): 67 mg/L) were centrifuged at 4000 rpm (37 °C) for 10 min; afterward, the 180 ml of supernatant was removed under nitrogen gas. The pellet was resuspended by vortexing in 60 ml of residual CM and was injected in the reactors with a sterile syringe. Meanwhile, the same volume of CM containing 14 g NH_4^+-N/L was introduced to R_{con} as abiotic augmentation. The mixing in CSTR reactors was stopped for 4 h after each injection to allow the culture to settle in the reactor. Besides, the substrate feeding was stopped during P4, avoiding any washout of the injected microbial culture.

2.4. Chemical analyses

Methane concentration and VFA were measured twice per week using two different gas chromatographs as previously described by Yan et al. (2019) [27]. pH was measured with PHM99 LAB pH meter (RadiometerTM). TS, Volatile solid, VSS, and TAN were measured according to the standard methods [29].

2.5. Microbial analysis

To explain how the bioaugmentation inocula affected the microbiome both immediately and steady-state after bioaugmentation, the sludge samples for genomic DNA extraction were collected from R_{bio} on days 31 (P3), 56 (P4), and 91 (P5) and were used for metagenomic analysis. A first step was added to the regular DNA extraction where Phenol:Chloroform: Isoamyl Alcohol (25: 24: 1) was used to further improve the quality of the DNA, afterward the samples were extracted using DNeasy PowerSoil® (QIAGEN GmbH, Hilden, Germany) with minor modification [30]. Finally, DNA concentration and purity were checked using NanoDrop (Thermo Fisher Scientific, Waltham, MA, USA) and Qubit fluorometer (Thermo Fisher Scientific, Waltham, MA, USA).

2.6. Metagenomic sequencing and binning analysis

A sequencing platform including both Oxford Nanopore MinION single-molecule and Illumina sequencers was performed. Nextera DNA Flex Library Prep Kit (Illumina Inc., San Diego CA) and SQK-RBK004 rapid sequencing kit (Oxford Nanopore Technologies, Oxford, UK) were applied for library preparation. Libraries sequencing was performed with FLO-MIN106 R9 flow cell on a MinION device (Oxford Nanopore Technologies, Oxford, UK) and Illumina NextSeq 500 platform (Illumina Inc., San Diego CA) with paired-end at the CRIBI biotechnology center sequencing facility (University of Padova, Italy). The total raw data includes 26997584, 25494946, and 21,089,120 filtered reads for P3, P4, and P5 respectively. Trimmomatic (v0.39) was used to filter Illumina reads with low quality or ambiguous bases [31]. Spades (v3.13.0) [32], Unicycler (v0.4.8-beta) [33] and OPERA-MS [34] were independently used for high-quality reads assembly. Illumina reads alone and Illumina reads bound with Nanopore data via MEGAHIT (V1.2.4beta) software [35], were utilized during the assembly process. Afterwards, all the scaffolds longer than 1 kb were kept and Quality Assessment Tool (QUAST_1, V4.1) was used for the binning [36]. The alignment of the reads per each sample back to the assembly was performed using Bowtie 2 (v2.2.4) [37] to determine scaffolds' coverage. Metagenomic binning was achieved using MaxBin2 (v2.2.6) and Metabat2 (v2.12.1) software [38]. The best MAGs among the different assemblies and binning results were chosen using metaWRAP [39] and finally 26, 21 and 20 MAGs were obtained from metaspades, OPERA-MS and unicycler, respectively. The basic metrics, contamination, and completeness of the final MAGs were evaluated using CheckM (v1.0.3). GTDB-Tk [40] and CAT [41] provided taxonomical assignment and functional analysis. The identification of protein-encoding genes was achieved using Prodigal (v2.6.2) [42,43] in normal mode and connected with KEGG IDs with Diamond (v0.9.22.123) [44]. Protein sequences predicted using Prodigal (v2.6.3) were annotated by similarity

Table 1
Characteristics of inoculum and substrate.

Parameter	Unit	Inoculum (SD)	Biopulp (SD)
Total solids (TS)	g/kg	49.04 (0.92)	79.39 (0.51)
Volatile solids (VS)	g/kg	39.75 (0.71)	67.66 (0.21)
pH	–	7.8(0.01)	3.9 (0.1)
Total ammonia nitrogen (TAN)	g NH_4^+-N/L	9.50 (0.01)	1.10 (0.01)
Free ammonia nitrogen (FAN)	g NH_3-N/L	0.896 (0.01)	0.10 (0.00)
Total Kjeldahl Nitrogen (TKN)	g N/L	5.38 (0.25)	NM
Total Carbohydrate	g/L	NM	42.1 (1.58)
Total protein	g/L	NM	12.11 (0.45)
Total lipid	g/L	NM	10.49 (0.39)

* NM: Not Measured.

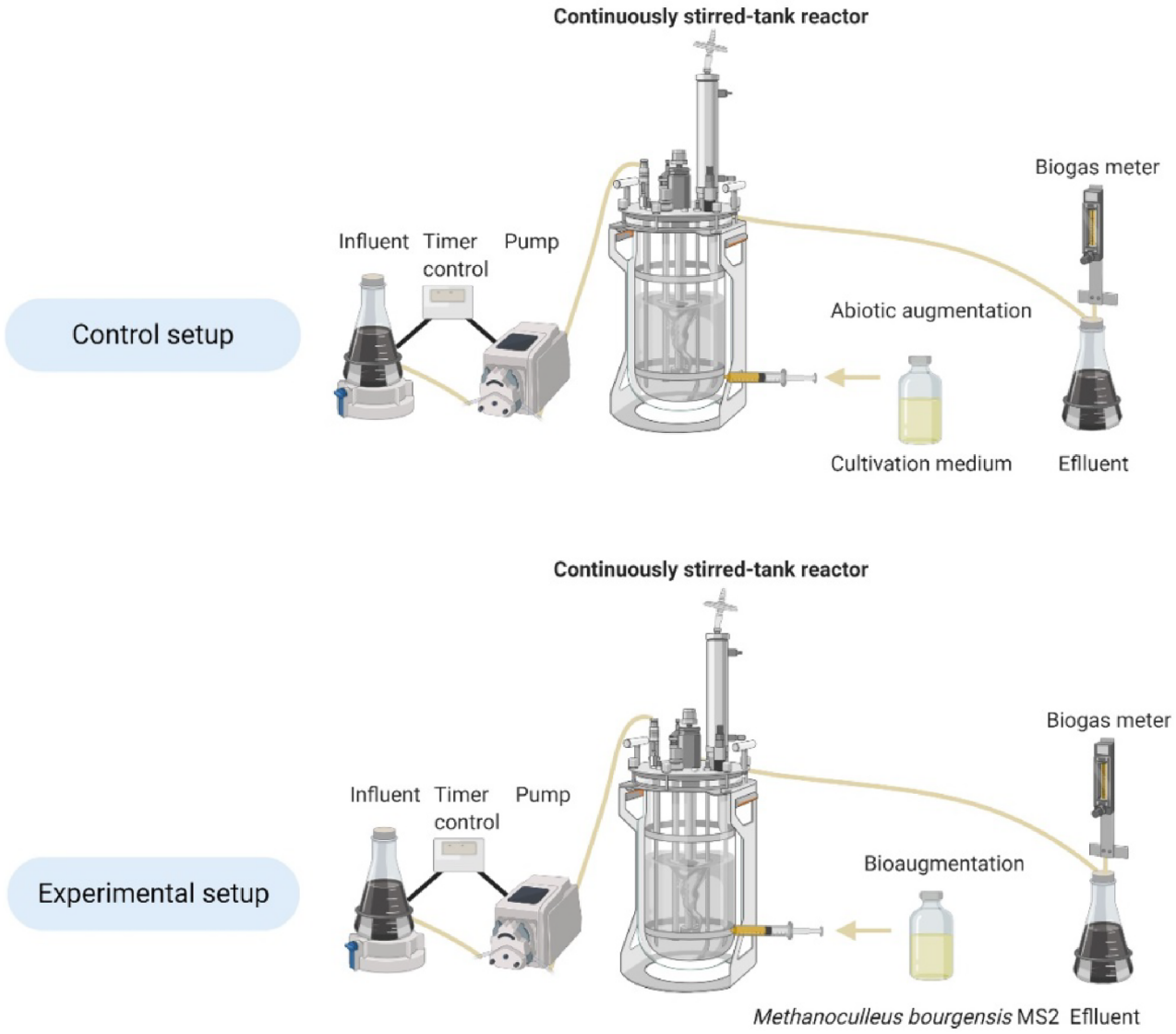

Fig. 1. Schematic diagram of the continuously stirring tank reactors.

Table 2
The CSTR reactors experimental design.

Phase	Days	TAN	Extra added ammonia	
		(g NH_4^+-N/L)	$CO(NH_2)_2$ (g NH_4^+-N/L)	NH_4Cl (g NH_4^+-N/L)
P1	0–5	9.5	4.5	3.9
P2	6–22	11.5	5.5	4.9
P3	23–50	13.5	6.5	5.9
P4 (Bioaugmentation)	51–54	13.5	–	–
P5	55–120	13.5	6.5	5.9

* "–": No extra ammonia addition.

search on COG and Pfam databases using RPS-BLAST (v2.2.26) using self-written perl scripts as previously described [45]. Functional completeness based on KEGG IDs was assessed using the KEGG mapper-reconstruct pathway. Hierarchical clustering analyses were done with the Multiexperiment viewer (v4.9.0). The characteristic of the microbiome collected from each period was visualized using Anvi'o [46]. The details regarding metagenomic results are described in Table S2. Raw sequencing data have been uploaded to the NCBI Sequence Read Archive database under the Bioproject PRJNA613576, with specific SRA codes per sample: SRR11356280, SRR11356279, and SRR11356278.

2.7. Data analysis

All tests were measured in duplicate, and the significance of each result was determined by analyses of variance (ANOVAs) and Student's *t*-test. A p value < 0.05 means statistically significant.

3. Results and discussion

3.1. Reactors' performance

From P1 to the end of P3, both reactors experienced inhibition with an average methane production loss close to 25% compared to the results obtained from previous research (Fig. 2). The experiment was performed in the same reactor and operating conditions treating the same OFMSW under steady-state without ammonia addition with an average methane yield of 368 CH_4/g VS [27]. During bioaugmentation (P4), methane production yield in R_{bio} and R_{con} decreased slightly because of the discontinuity in substrate feeding. After bioaugmentation, the average methane production (from day 54 to 120) in R_{bio} reactor showed an increase by 21% compared to P3 (Fig. 2). Moreover, during the final steady-state of P5 (days 70–120), the R_{bio} had an average 11% ($p < 0.05$) higher methane yield than R_{con}. To our knowledge, this is the first time that bioaugmentation of ammonia tolerant methanogen

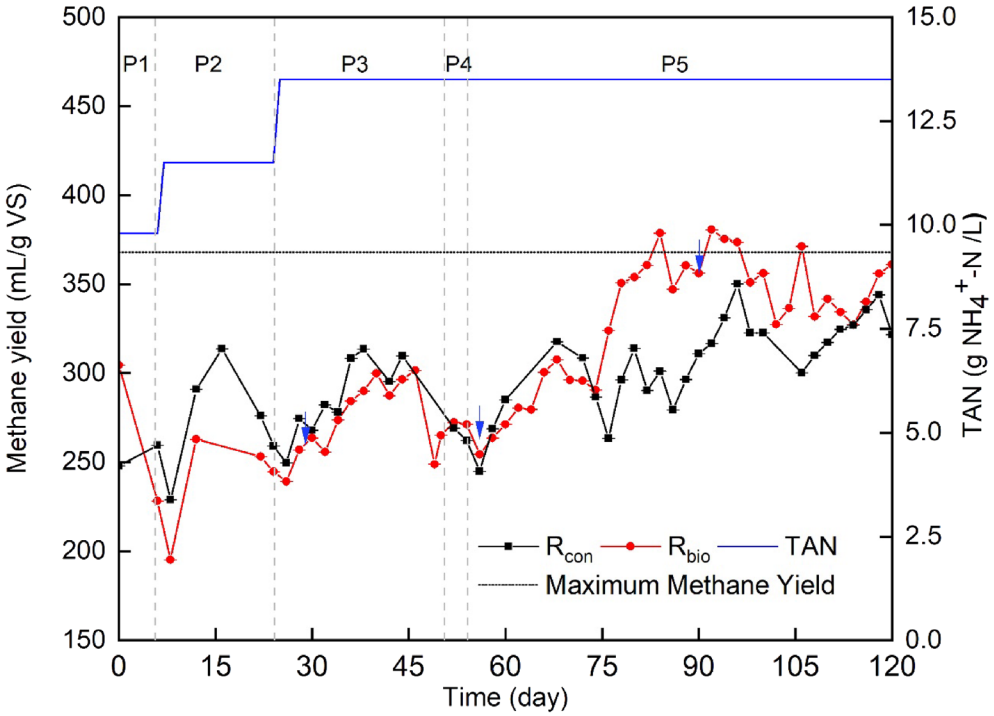

Fig. 2. CH_4 production in R_{con} and R_{bio}, and TAN levels throughout the experimental period. The maximum methane yield means average methane yield in a reactor treating the same OFMSW under the steady-state condition without ammonia addition. The arrow (blue) represents the sampling point for microbial analysis. Each point presents an average of two consecutive days. (For interpretation of the references to colour in this figure legend, the reader is referred to the web version of this article.)

significantly improved methane productivity of CSTR fed with OFMSW under the extremely high level of 13.5 g NH_4^+-N/L.

The gap in VFA concentrations between the two reactors, during the P5 at 13.5 g NH_4^+-N/L, was consistent with the different methane production (Fig. 2, Fig. 3). More specifically, the VFA levels in R_{bio} decreased continuously for over 50 days from 15,000 to 5398 mg/L. Each point (Figs. 2 and 3) presents the average of consecutive two days, thus the data points of 15,000 and 5398 are representative of the VFA reduction profile at P5. In particular, the acetate consumption indicated a faster degradation compared to propionate. On the contrary, VFA accumulation (above 7500 mg/L) in R_{con} progressed as expected in reactors exposed to ammonia (Fig. 3). Hence, the findings in this study confirmed that bioaugmentation of the ammonia tolerant inocula did successfully recover the methane yield and determined a decrease in VFA levels compared to R_{con}.

3.2. The microbiome composition dynamics

The role of the microbiome in reactor performance was determined using genome-centric metagenomics, which allowed the identification of 67 MAGs as the most abundant members (≥99.5% of cumulative relative abundance) of the microbiome (Tables S2 and S3). 42 out of 67 MAGs were of high-quality (completeness ≥ 90% and contamination ≤ 5%), while the remaining 25 MAGs were of medium quality (50% ≤ completeness ≥ 90% and 5% ≤ contamination ≤ 10%) referring to Genomic Standards Consortium about a Metagenome-Assembled Genome (MIMAG) [44] (Fig. 4; Table S2). The 67 MAGs were taxonomically assigned to five phyla, namely *Firmicutes*, *Actinobacteria*, *Cloacimonadota*, *Bacteroidetes* and *Euryarchaeota* (Fig. 4). The bioaugmentation process induced a marked change in the microbial composition throughout the P4 to P5 (Fig. 4; Table S3). During P3, within the *Firmicutes* phylum, *Peptococcaceae* spp. (DTU 903, DTU900, and DTU895), *Tissierellales* sp. DTU879 and *Syntrophaceticus* sp. DTU783 (55%, 3.7% and 4.4% of cumulative relative abundance, respectively) were the most relevant members identified (Fig. 4; Table S3). In the archaeal community, *Methanoculleus* spp. DTU887, DTU888 and *Methanomassiliicoccales* sp. DTU778 were present at low relative abundance (0.42%, 0.23% and 0.27%) and were assumed to pull OFMSW degradation through methanation of intermediate compounds derived from fermentation (i.e. H_2 and methanol). The low abundance of methanogens was the main cause of the under-performing AD process (e.g. low methane production) during the inhibited P3. Afterwards, the bioaugmented culture triggered the whole microbiome shift during the transition from P3 to P4 (Fig. 4, Fig. 5). Specifically, an increment of *Tissierellales* sp. DTU879 (3.3 fold when compared to P3) was observed after bioaugmentation, suggesting that positive interactions were established among these microbes (Fig. 5; Table S3). During P5, the relative abundance of *Methanoculleus* sp. DTU887 was 6.1 fold higher than P3, indicating a successful establishment of the exogenous archaea (*M. bourgensis*) in the endemic community of R_{bio} (Fig. 5; Table S3). Correspondingly, *Peptococcaceae* spp. (DTU 903, DTU900, and DTU895), *Syntrophaceticus* sp. DTU 783 and *Tissierellales* sp. DTU879 increased in abundance by 4.7, 2.4 and 1.5 fold, respectively, when compared to P3 (Fig. 5; Table S3).

3.3. Species interactions among key microorganisms

The functional role of individual MAGs was determined based on the information of their metabolic potential combined with relative abundances in the different conditions. In this way, a network of metabolic interactions occurring in the microbiome at high ammonia levels was manually reconstructed (Fig. 6; Table S4). After substrate hydrolysis, amino acids, fatty acids and sugars are generally degraded into acetate, H_2, and CO_2, which are the main feed sources for SAOB and methanogens. The roles of microbes involved in the key metabolic pathways related to acetate and H_2 formation/ oxidation were established.

3.3.1. Acetogenic-related related community

The cumulative relative abundance of dominant bacteria (*Peptococcaceae* sp. DTU903, *Peptococcaceae* sp. DTU895, *Peptococcaceae* sp. DTU900, and *Tissierellales* sp. DTU879) accounted for more than 50% through the entire period (Fig. 4; Table S3), suggesting their major role in degrading OFMSW. The high content of carbohydrates (65%) [28] in OFMSW and the presence of two distinct glucose metabolic pathways in these dominant bacteria reveals that glucose is a necessary intermediate

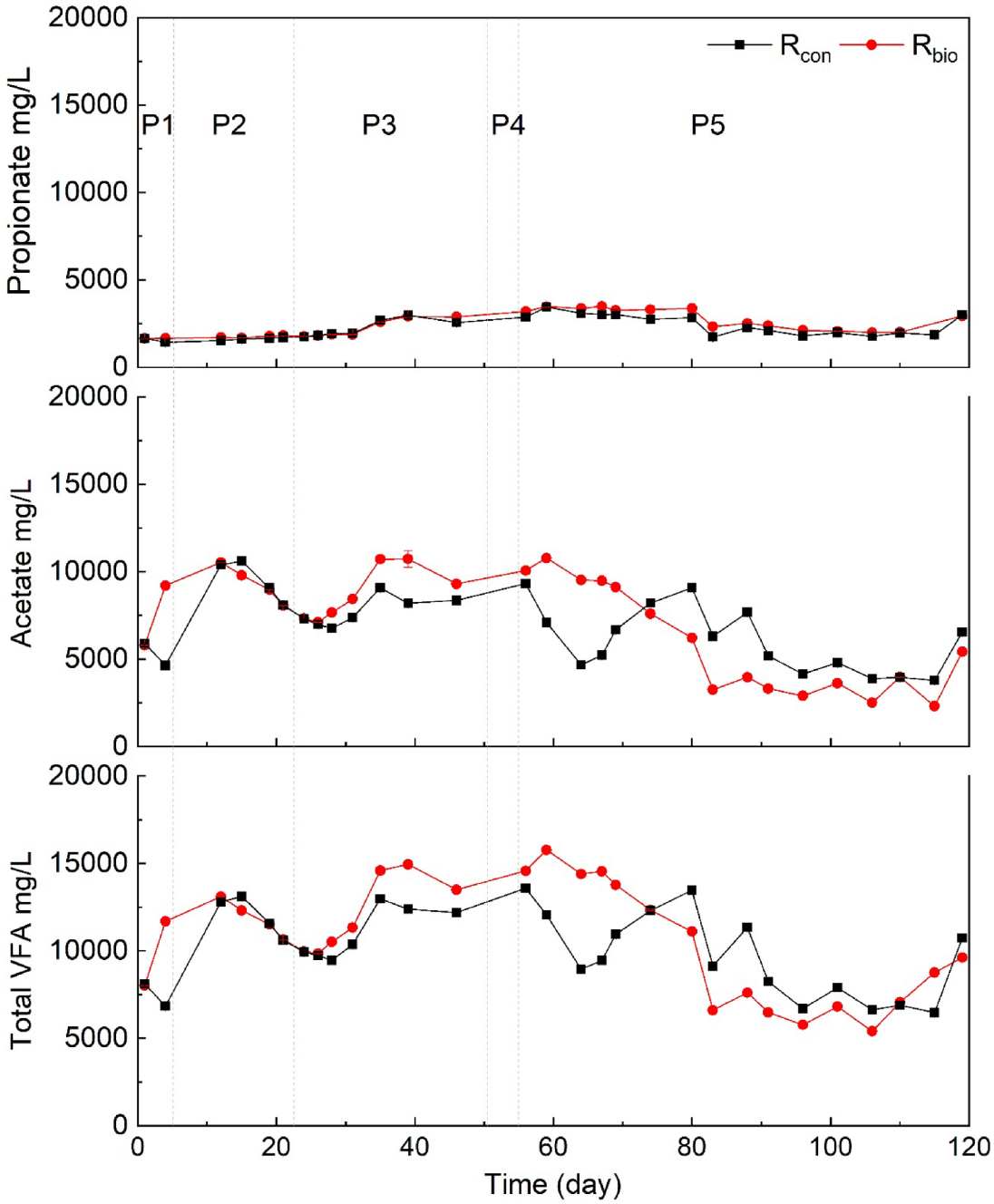

Fig. 3. Concentration of propionate, acetate, total VFAs determined during the entire experimental period. Each point presents an average of two consecutive days.

product during organic waste catabolism (Fig. 6; Tables S4 and S5). More specifically, in the first glucose degradation pathway (identified as complete only in *Tissierellales* sp. DTU879) (Fig. 6; Table S4), pyruvate produced through the Embden-Meyerhof-Parnas (EMP) process was directly converted to H_2/CO_2 via the glycine cleavage system and tetrahydrofolate pathways, as previously reported [26]. The incomplete pathway in *Peptococcaceae* spp. (DTU895, DTU900 and DTU903) intriguingly suggests a possible interspecies exchange of nutrients and intermediates products occurring during glucose degradation. The second glucose degradation pathway starts from pyruvate production through the EMP process, and follows with acetate and H_2 as the end products (Fig. 6; Table S4). The genes of rhodobacter nitrogen fixation complex (*rnf*) harbored in *Peptococcaceae* spp. and *Tissierellales* sp. DTU879 had the potential to produce reduced ferredoxin. The utilization of these high-energy electron carriers is essential to achieve the endergonic electron transfer in AD systems, specifically facilitating the reactions of NAD^+ reduction to NADH, H^+ reduction to H_2 and pyruvate reduction to acetyl-CoA (Fig. 6; Table S4). It is consistent with previous finding of the key role of reduced ferredoxin for driving redox reactions [47]. The presence of *rnf* potentially supports the degradation of organic matter to acetate, H_2 and ATP, and possibly confers an advantage to the dominant bacteria (*Peptococcaceae* spp. related members, and *Tissierellales* sp. DTU879). However, both glucose conversion pathways are dependent from the low concentrations of H_2 and acetate, as previously reported by Zhu et al. (2019) [26]. More specifically, H_2 and NAD^+ should be always regenerated from NADH during the above processes; in fact, NAD^+ is an essential electron acceptor for the anaerobic degradation of sugars, amino acids, and fatty acids. Nevertheless, NAD^+ formation is impossible at a high H_2 partial pressure and thus the produced CO_2/H_2 needs to be scavenged by hydrogenotrophic methanogen for methanogenesis which thereby drives glucose degradation at real reactor

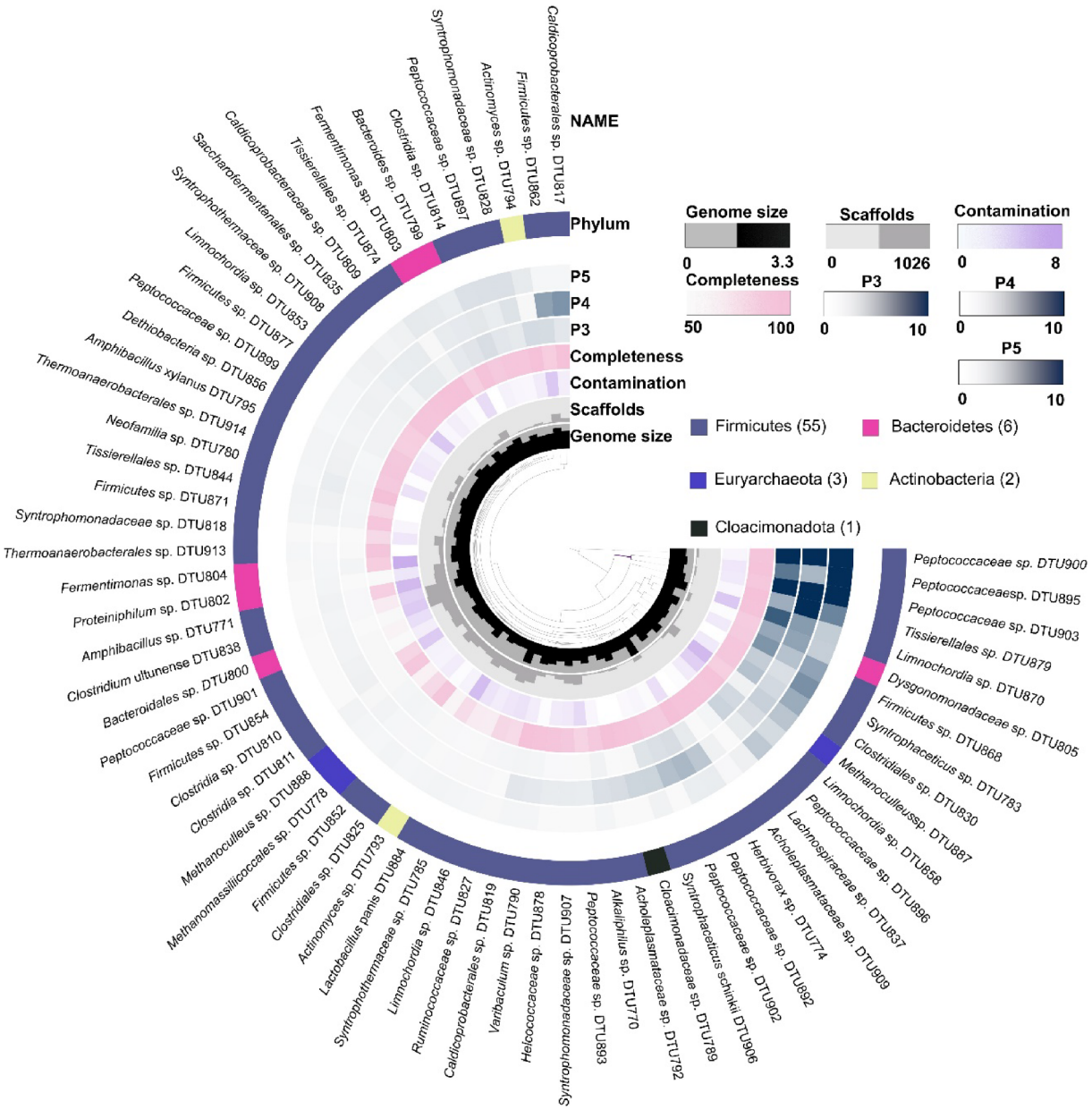

Fig. 4. Microbial samples collected from R_{bio} at different time points: on days 31 (P3), 56 (P4), and 91 (P5). The characteristics (taxonomic assignment, coverage and MIMAG values) of 67 MAGs composing the microbiome are presented. The outer layer represents the taxonomy at the phylum level. The four middle layers represent the relative abundance (%) of each MAG in the different phases. The four inner layers represent completeness (%), contamination (%), number of scaffolds, and genome size (Mbp) colored in pink, purple, grey and black, respectively. The middle tree represents the euclidean clustering of MAGs based on their relative abundances. (For interpretation of the references to colour in this figure legend, the reader is referred to the web version of this article.)

conditions [48]. In the present study, MAGs reconstruction provides evidence of cooperation between *Tissierellales* sp. DTU879/*Peptococcaceae* spp. and *Methanoculleus* sp. DTU887 (Fig. 4, Fig. 6), which is consistent with previous findings [26,27]. Thereby, syntrophic glucose degrading-communities exploited possible thermodynamic reactions to conserve the maximum amount of energy.

Additionally, *Syntrophomonadaceae* and *Syntrophothermaceae* groups might participate in the syntrophic butyrate and propionate oxidation. Functional annotation of MAGs assigned to *Syntrophaceticus* and *Syntrophomonadaceae* revealed a partially complete butyrate/propionate degradation pathways, probably due to the incompleteness of some genomes (Table S5). As evidenced by a previous study, *Syntrophomonas* related members were obligate syntrophic bacteria able to utilize various fatty acids, especially butyrate [49]. However, in the present study, their low abundance (< 2%) suggests a minor role in the global community, and the scarce butyrate detected in the reactor suggests a negligible contribution to OFMSW degradation.

3.3.2. Acetate degraders

The extremely high concentrations of acetate throughout P1 to P3 (Fig. 3) indicates that acetate degraders were less active than fermenting bacteria. Acetogenic microbes are assumed to play an important role in the AD system, scavenging the acetate produced during fermentation, which pulls the degradation of glucose/VFA and alleviates acetate-ammonia synergistic inhibition [50,51]. For example, *Syntrophaceticus* sp. DTU783 encodes two complete gene sets involved in the reversed Wood-Ljungdahl pathway and the alternative acetate degradation through the glycine cleavage system (Fig. 6; Table S4). The hydrogenase involved in energy conservation in these two pathways was different. Specifically, during acetate degradation through glycine

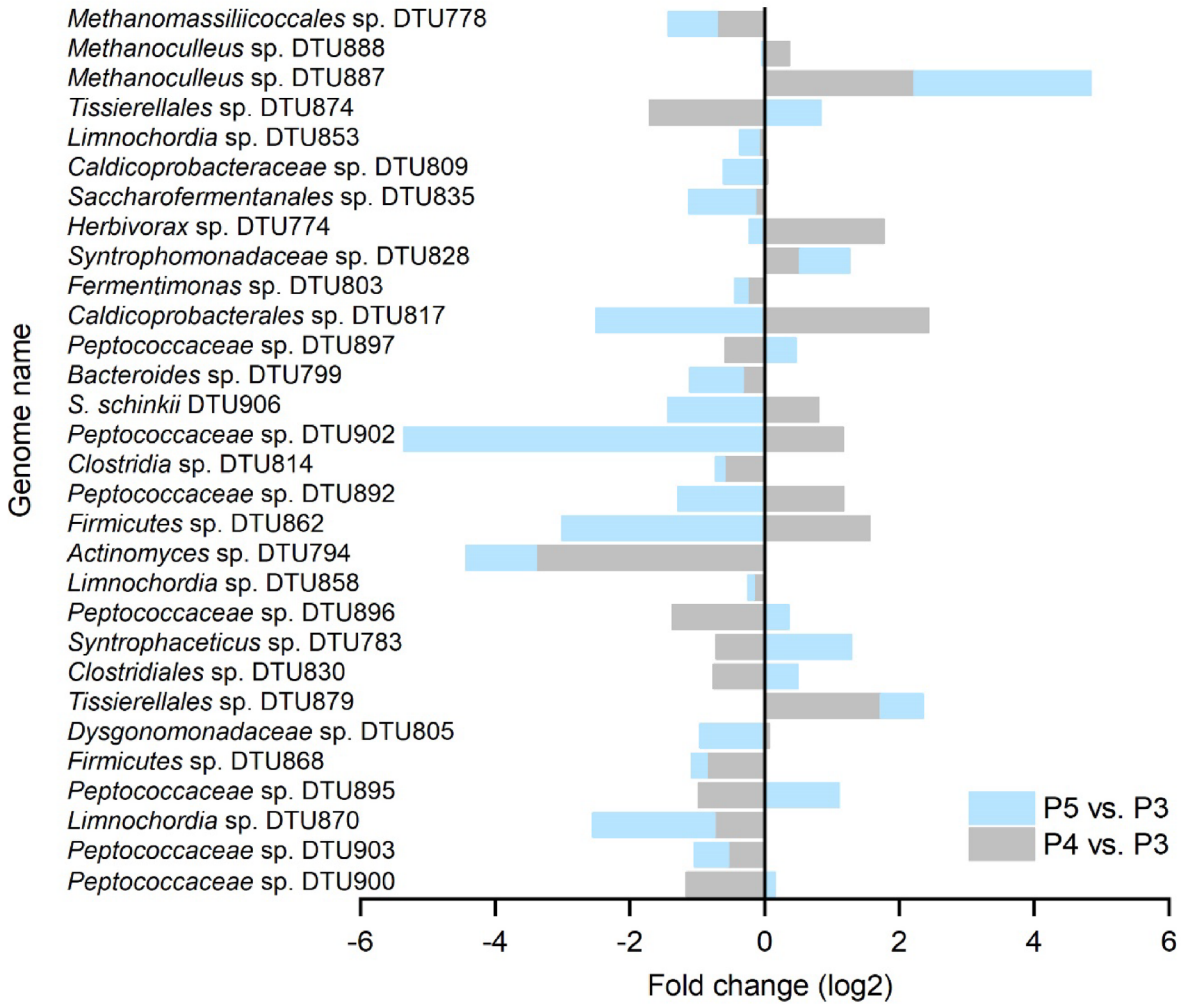

Fig. 5. The specific variation trends of dominant MAGs was obtained by calculating the fold change (log_2) between the different periods.

cleavage system, 1 Fd_{red} was employed for electron transport, instead of NADH, thus 1 more ATP was generated per each molecule of acetate compared to that of the reversed Wood-Ljungdahl pathway.

During the P5, the increased relative abundance of *Syntrophaceticus* sp. DTU783 (2.4 fold when compared with P3), occurring in response to bioaugmentation, greatly lowered the acetate concentration (Fig. 3, Fig. 5; Table S3). This reduction subsequently promoted VFAs and/or glucose degradation due to reactions equilibrium, which is consistent with previous findings [52]. As evidenced by the negative correlation between the abundance of *Syntrophaceticus* sp. DTU783 and acetate concentration (Fig. S2), we proposed DTU783 as the key acetate metabolizer in the system, possibly acting in syntrophy with the bioaugmented *Methanoculleus* sp. DTU887 (Fig. 6). This result highlights again that the exogenous addition of *Methanoculleus* sp. DTU887 represents a prime remedy to guarantee the optimized performance in ammonia-inhibited mesophilic processes. Interestingly, also the other dominant bacteria (*Tissierellales* sp. DTU879, *Peptococcaceae* spp.) harbored the genes for acetate degradation via glycine cleavage pathway (Fig. 6; Table S5). As Nobu et al. (2015) proposed, in comparison to the Wood-Ljungdahl pathway, there is no endergonic 5-methyl-THF oxidation in this alternative acetate degradation, whereby intermediates produced could be easily used for biosynthesis [47]. Therefore, acetate oxidation through the acetate-glycine pathway might be another biological solution to overcome the thermodynamic limitations, especially when hydrogenotrophic methanogens are present at low relative abundance [53,54]. The multiple strategies to degrade carbon sources and regulate energy conversions could be the winning strategy put in place by microbes to optimize their energy metabolism when a suitable partner is absent, or in response to varying environmental conditions.

3.3.3. Methanogenesis

Methanoculleus spp. are known to be involved in the utilization of hydrogen produced by syntrophic acetate-producing species or by fatty acid-oxidizing microorganisms [55,56]. The complete pathway for H_2-mediated reduction of CO_2 to CH_4 was identified in *Methanoculleus* sp. DTU887 (Fig. 6). The first step of this pathway is the reduction of CO_2 with H_2 to formyl-MFR, which is subsequently reduced to CH_4, in a process catalyzed by Fwd, Ftr, Mch, Mtd, Mer, Mtr and Mvh-Hdr respectively (Fig. 6; Table S4). The presence of methanol dehydrogenase (*mdh*) and its electron acceptor - a specific c-type cytochrome (Fig. 6; Table S4), is associated with the high affinity for H_2, which confirms the high growth yield on H_2 of *Methanoculleus* sp. found in the previous study [57].

Besides, the presence of genes encoding multiple energy regulating complexes performing H^+ and Na^+ translocation (*mtr*, hydrogenase subunits (*eha*), the energy-converting hydrogenase (*ech*), Na^+/H^+ antiporter (*mnh*) and V/A type ATP synthase) were proposed to contribute to *Methanoculleus* sp. DTU887 robustness (Fig. 6; Table S4). Specifically, Mtr, Eha hydrogenase subunits, and Na^+/H^+ antiporter are assumed to be sodium ion translocating, while Ech hydrogenase subunits, as well as the ion pump and V/A type ATP synthase, should be proton translocating [58]. Overall, the presence of multiple ion-translocating electron transfer complexes, and membrane-bound Fe-S proteins with connected heterodisulfide reductase in the genome of *Methanoculleus* sp. DTU887,

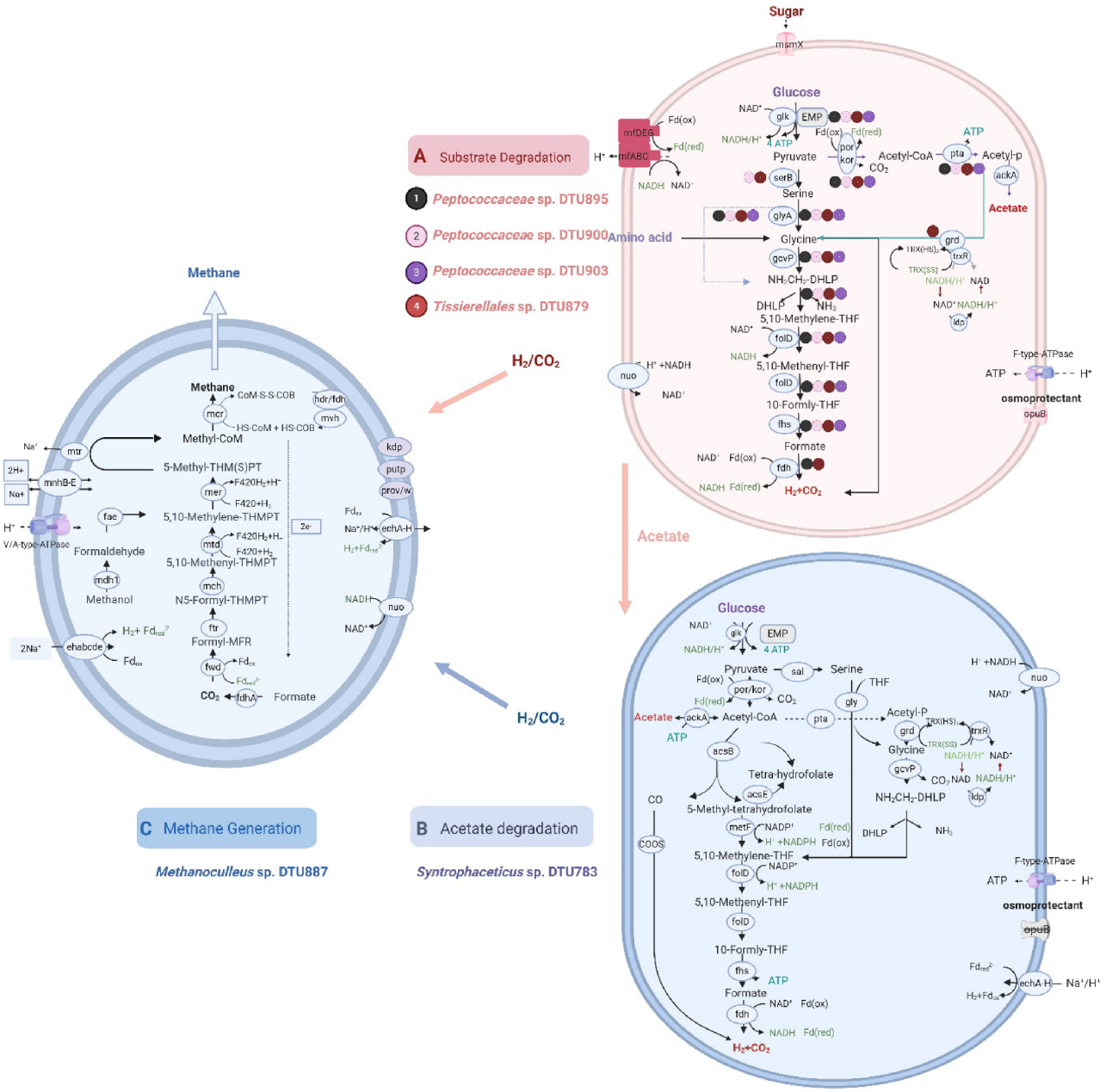

Fig. 6. Metabolic reconstruction of the OFMSW degrading syntrophic community. Metagenomic data revealed pathways involved in substrate degradation, in the utilization of intermediates compounds (H_2/CO_2, acetate) and in methanogenesis. All the relevant genes included can be found in Table S4.

can modulate the energy status of the cell in response to varying thermodynamic conditions. This confirms the previous observations of the flexible energy conversion approach, which is taking advantage of the positive energy margin [59,60]. Besides, *Methanoculleus* sp. DTU887 harbors genes potentially involved in osmolytes uptake system (*kdp*, *putp*, and *proW/V*), as well as the *mnhBCDE* complexes responsible for pH homeostasis and balancing external H^+/Na^+ ratios. These genetic characteristics of *Methanoculleus* sp. DTU887 (the bioaugmented culture) enable its high tolerance to extreme ammonia levels and drive the syntrophic substrate degradation in situations of ammonia stress.

Additionally, the increased abundance of *Methanoculleus* sp. DTU887 (from P4 to P5) decreased the inter-microbial distances occurring between H_2-producing bacteria and methanogens. As a consequence, the H_2 diffusion distance diminished, thus the interspecies transfer rate increased and methanogenic activity was enhanced. Hydrogen consumption by methanogens can lower the partial pressure, and enhance the rate of acetate degradation promptly [61,62]. Moreover, the addition of *Methanoculleus* sp. DTU887 perturbed the microbiome structure, triggering modification of the indigenous microbial community with the increase of hydrogenotrophic methanogens (Fig. 4), which finally resulted in a huge increase in methane yield (21%) (Fig. 2).

Hence, *Methanoculleus* sp. was critical to recovering the AD system from ammonia inhibition: its increase in abundance accelerated the consumption of VFA and other intermediates by strengthening the electron transfer between syntrophic microbes. Therefore, the resume of a complete chain of energetic electron transfer among the OFMSW-degrading microbiome renders the successful bioaugmentation.

4. Conclusions

This study is the first comprehensive investigation supported by

metagenomics analysis revealing the interconnected metabolic pathways induced by the addition of *Methanoculleus* sp. to AD of OFMSW. Implementation of cutting-edge technology based on microbial functional reconstruction and insights into the varying conditions of AD allowed a more clear investigation of the OFMSW-degrading community. This study proved the importance of a critical amount of methanogens for a fully-functional AD process. Additionally, it also provided evidence for the occurrence of important interactions among different microbiome members by revealing the presence of the genes (e.g. *gcvp, metF* and *ackA*) related to glucose and acetate degradation pathways. The presence of multiple pathways might provide enough flexibility to some species, such as *Peptococcaceae* spp., *Tissierellales* sp. DTU879, and *Syntrophaceticus* sp. DTU783, to recover the AD efficiency under extremely high ammonia levels. This study provides strong evidence regarding the importance of *Methanoculleus* sp. to enhance the ability of the anaerobic reactor to withstand the shock determined by VFA overload and ammonia inhibition.

Declaration of Competing Interest

The authors declare that they have no known competing financial interests or personal relationships that could have appeared to influence the work reported in this paper.

Acknowledgments

This work was supported by Energinet.dk under the project framework ForskEL "MicrobStopNH3-Innovative bioaugmentation strategies to tackle ammonia inhibition in anaerobic digestion process" (program no. 2015-12327). Authors appreciate financial support from MUDP (Miljøstyrelsens) under the project framework FUBAF project (MST-117-00508) and VARGA project (MST-141-01377); and also by EUDP (Energistyrelsen) under the project EFUEL (64018-0559). Miao Yan acknowledges the financial support from China Scholarship Council. Prof. Stefano Campanaro acknowledges the support from Consorzio Interuniversitario Biotecnologie (CIB).

Appendix A. Supplementary data

Supplementary data to this article can be found online at https://doi.org/10.1016/j.cej.2020.126159.

References

[1] R. Campuzano, S. González-Martínez, Characteristics of the organic fraction of municipal solid waste and methane production: a review, Waste Manage. 54 (2016) 3–12.
[2] A. Minelgaitė, G. Liobikienė, Waste problem in European Union and its influence on waste management behaviours, Sci. Total Environ. 667 (2019) 86–93.
[3] P. Schroeder, K. Anggraeni, U. Weber, The relevance of circular economy practices to the sustainable development goals, J. Ind. Ecol. 23 (2019) 77–95.
[4] L. Favaro, T. Jansen, W.H. van Zyl, Exploring industrial and natural *Saccharomyces cerevisiae* strains for the bio-based economy from biomass: the case of bioethanol, Crit. Rev. Biotechnol. 39 (2019) 800–816.
[5] A. Nielfa, R. Cano, M. Fdz-Polanco, Theoretical methane production generated by the co-digestion of organic fraction municipal solid waste and biological sludge, Biotechnol. Rep. 5 (2015) 14–21.
[6] L. Awhangbo, R. Bendoula, J. Roger, F. Béline, Detection of early imbalances in semi-continuous anaerobic co-digestion process based on instantaneous biogas production rate, Water Res. 171 (2020) 115444.
[7] T.P.N. Bui, H.A. Schols, M. Jonathan, A.J. Stams, W.M. de Vos, C.M. Plugge, Mutual metabolic interactions in co-cultures of the intestinal *Anaerostipes rhamnosivorans* with an acetogen, methanogen, or pectin-degrader affecting butyrate production, Front. Microbiol. 10 (2019) 2449.
[8] S.G. Center, Basic data on biogas, Available Online, Accessed January (2012).
[9] C.E. Boyd, Nitrogen, Water Quality, Springer, 2020, pp. 269–290.
[10] G. Capson-Tojo, R. Moscoviz, S. Astals, Á. Robles, J.-P. Steyer, Unraveling the literature chaos around free ammonia inhibition in anaerobic digestion, Renew. Sustain. Energy Rev. 117 (2020) 109487.
[11] J. Ruiz-Sánchez, S. Campanaro, M. Guivernau, B. Fernández, F. Prenafeta-Boldú, Effect of ammonia on the active microbiome and metagenome from stable full-scale digesters, Bioresour. Technol. 250 (2018) 513–522.
[12] S. Campanaro, L. Treu, L.M. Rodriguez-R, A. Kovalovszki, R.M. Ziels, I. Maus, X. Zhu, P.G. Kougias, A. Basile, G. Luo, New insights from the biogas microbiome by comprehensive genome-resolved metagenomics of nearly 1600 species originating from multiple anaerobic digesters, Biotechnol. Biofuels 13 (2020) 1–18.
[13] A.G. Hashimoto, Ammonia inhibition of methanogenesis from cattle wastes, Agric. Wastes 17 (1986) 241–261.
[14] H. Tian, L. Treu, K. Konstantopoulos, I.A. Fotidis, I. Angelidaki, 16s rRNA gene sequencing and radioisotopic analysis reveal the composition of ammonia acclimatized methanogenic consortia, Bioresour. Technol. 272 (2019) 54–62.
[15] M. Kayhanian, Ammonia inhibition in high-solids biogasification: an overview and practical solutions, Environ. Technol. 20 (1999) 355–365.
[16] H. Tian, M. Yan, L. Treu, I. Angelidaki, I.A. Fotidis, Hydrogenotrophic methanogens are the key for a successful bioaugmentation to alleviate ammonia inhibition in thermophilic anaerobic digesters, Bioresour. Technol. 122070 (2019).
[17] Z. Yang, W. Wang, C. Liu, R. Zhang, G. Liu, Mitigation of ammonia inhibition through bioaugmentation with different microorganisms during anaerobic digestion: Selection of strains and reactor performance evaluation, Water Res. 155 (2019) 214–224.
[18] E. Tampio, S. Marttinen, J. Rintala, Liquid fertilizer products from anaerobic digestion of food waste: mass, nutrient and energy balance of four digestate liquid treatment systems, J. Cleaner Prod. 125 (2016) 22–32.
[19] F. Lü, C. Luo, L. Shao, P. He, Biochar alleviates combined stress of ammonium and acids by firstly enriching *Methanosaeta* and then *Methanosarcina*, Water Res. 90 (2016) 34–43.
[20] T. Wang, D. Zhang, L. Dai, B. Dong, X. Dai, Magnetite triggering enhanced direct interspecies electron transfer: a scavenger for the blockage of electron transfer in anaerobic digestion of high-solids sewage sludge, Environ. Sci. Technol. 52 (2018) 7160–7169.
[21] J. Megaw, B.F. Gilmore, Archaeal Persisters: Persister Cell Formation as a Stress Response in Haloferax volcanii, Front. Microbiol. 8 (2017).
[22] M. Westerholm, L. Levén, A. Schnürer, Bioaugmentation of syntrophic acetate-oxidizing culture in biogas reactors exposed to increasing levels of ammonia, Appl. Environ. Microbiol. 78 (2012) 7619–7625.
[23] I.A. Fotidis, H. Wang, N.R. Fiedel, G. Luo, D.B. Karakashev, I. Angelidaki, Bioaugmentation as a solution to increase methane production from an ammonia-rich substrate, Environ. Sci. Technol. 48 (2014) 7669–7676.
[24] H. Tian, E. Mancini, L. Treu, I. Angelidaki, I.A. Fotidis, Bioaugmentation strategy for overcoming ammonia inhibition during biomethanation of a protein-rich substrate, Chemosphere 231 (2019) 415–422.
[25] A. Bremges, I. Maus, P. Belmann, F. Eikmeyer, A. Winkler, A. Albersmeier, A. Pühler, A. Schlüter, A. Sczyrba, Deeply sequenced metagenome and metatranscriptome of a biogas-producing microbial community from an agricultural production-scale biogas plant, GigaSci 4 (1) (2015), https://doi.org/10.1186/s13742-015-0073-6.
[26] X. Zhu, S. Campanaro, L. Treu, P.G. Kougias, I. Angelidaki, Novel ecological insights and functional roles during anaerobic digestion of saccharides unveiled by genome-centric metagenomics, Water Res. 151 (2019) 271–279.
[27] M. Yan, I.A. Fotidis, H. Tian, B. Khoshnevisan, L. Treu, P. Tsapekos, I. Angelidaki, Acclimatization contributes to stable anaerobic digestion of organic fraction of municipal solid waste under extreme ammonia levels: focusing on microbial community dynamics, Bioresour. Technol. 286 (2019) 121376.
[28] B. Khoshnevisan, P. Tsapekos, M. Alvarado-Morales, I. Angelidaki, Process performance and modelling of anaerobic digestion using source-sorted organic household waste, Bioresour. Technol. 247 (2018) 486–495.
[29] A. Apha, AWWA (2005) Standard methods for the examination of water and wastewater, American Public Health Association, Washington, DC, 2005.
[30] L. Treu, P. Tsapekos, M. Peprah, S. Campanaro, A. Giacomini, V. Corich, P.G. Kougias, I. Angelidaki, Microbial profiling during anaerobic digestion of cheese whey in reactors operated at different conditions, Bioresour. Technol. 275 (2019) 375–385.
[31] A.M. Bolger, M. Lohse, B. Usadel, Trimmomatic: a flexible trimmer for Illumina sequence data, Bioinformatics 30 (2014) 2114–2120.
[32] A. Bankevich, S. Nurk, D. Antipov, A.A. Gurevich, M. Dvorkin, A.S. Kulikov, V.M. Lesin, S.I. Nikolenko, S. Pham, A.D. Prjibelski, SPAdes: a new genome assembly algorithm and its applications to single-cell sequencing, J. Comput. Biol. 19 (2012) 455–477.
[33] R.R. Wick, L.M. Judd, C.L. Gorrie, K.E. Holt, Unicycler: resolving bacterial genome assemblies from short and long sequencing reads, PLoS Comput. Biol. 13 (2017) e1005595.
[34] D. Bertrand, J. Shaw, M. Kalathiyappan, A.H.Q. Ng, M.S. Kumar, C. Li, M. Dvornicic, J.P. Soldo, J.Y. Koh, C. Tong, Hybrid metagenomic assembly enables high-resolution analysis of resistance determinants and mobile elements in human microbiomes, Nat. Biotechnol. 37 (2019) 937–944.
[35] D. Li, C.-M. Liu, R. Luo, K. Sadakane, T.-W. Lam, MEGAHIT: an ultra-fast single-node solution for large and complex metagenomics assembly via succinct de Bruijn graph, Bioinformatics 31 (2015) 1674–1676.
[36] A. Gurevich, V. Saveliev, N. Vyahhi, G. Tesler, QUAST: quality assessment tool for genome assemblies, Bioinformatics 29 (2013) 1072–1075.
[37] H. Li, B. Handsaker, A. Wysoker, T. Fennell, J. Ruan, N. Homer, G. Marth, G. Abecasis, R. Durbin, The sequence alignment/map format and SAMtools, Bioinformatics 25 (2009) 2078–2079.
[38] J. Tsuji, N. Tran, S. Schiff, J. Venkiteswaran, L. Molot, J. Neufeld, Supplementary information Genomic potential for photoferrotrophy in a seasonally anoxic Boreal Shield lake.
[39] G.V. Uritskiy, J. DiRuggiero, J. Taylor, MetaWRAP—a flexible pipeline for genome-resolved metagenomic data analysis, Microbiome 6 (2018) 1–13.

[40] P.-A. Chaumeil, A.J. Mussig, P. Hugenholtz, D.H. Parks, GTDB-Tk: a toolkit to classify genomes with the Genome Taxonomy Database, Bioinformatics (2018).
[41] F.B. von Meijenfeldt, K. Arkhipova, D.D. Cambuy, F.H. Coutinho, B.E. Dutilh, Robust taxonomic classification of uncharted microbial sequences and bins with CAT and BAT, bioRxiv (2019) 530188.
[42] D. Hyatt, G.-L. Chen, P.F. LoCascio, M.L. Land, F.W. Larimer, L.J. Hauser, Prodigal: prokaryotic gene recognition and translation initiation site identification, BMC Bioinf. 11 (2010) 119.
[43] M. Kanehisa, Y. Sato, K. Morishima, BlastKOALA and GhostKOALA: KEGG tools for functional characterization of genome and metagenome sequences, J. Mol. Biol. 428 (2016) 726–731.
[44] B. Buchfink, C. Xie, D.H. Huson, Fast and sensitive protein alignment using DIAMOND, Nat. Methods 12 (2015) 59.
[45] S. Campanaro, L. Treu, P.G. Kougias, G. Luo, I. Angelidaki, Metagenomic binning reveals the functional roles of core abundant microorganisms in twelve full-scale biogas plants, Water Res. 140 (2018) 123–134.
[46] A.M. Eren, Ö.C. Esen, C. Quince, J.H. Vineis, H.G. Morrison, M.L. Sogin, T.O. Delmont, Anvi'o: an advanced analysis and visualization platform for 'omics data, PeerJ 3 (2015) e1319.
[47] M.K. Nobu, T. Narihiro, C. Rinke, Y. Kamagata, S.G. Tringe, T. Woyke, W.-T. Liu, Microbial dark matter ecogenomics reveals complex synergistic networks in a methanogenic bioreactor, ISME J. 9 (2015) 1710.
[48] A.J. Stams, Metabolic interactions between anaerobic bacteria in methanogenic environments, Antonie Van Leeuwenhoek 66 (1994) 271–294.
[49] H. Imachi, Y. Sekiguchi, Y. Kamagata, S. Hanada, A. Ohashi, H. Harada, *Pelotomaculum thermopropionicum* gen. nov., sp. nov., an anaerobic, thermophilic, syntrophic propionate-oxidizing bacterium, Int. J. Syst. Evol. Microbiol. 52 (2002) 1729–1735.
[50] B.M. Van der Zaan, F.T. Saia, A.J. Stams, C.M. Plugge, W.M. de Vos, H. Smidt, A.A. Langenhoff, J. Gerritse, Anaerobic benzene degradation under denitrifying conditions: *Peptococcaceae* as dominant benzene degraders and evidence for a syntrophic process, Environ. Microbiol. 14 (2012) 1171–1181.
[51] N. Sakai, F. Kurisu, O. Yagi, F. Nakajima, K. Yamamoto, Identification of putative benzene-degrading bacteria in methanogenic enrichment cultures, J. Biosci. Bioeng. 108 (2009) 501–507.
[52] P. Worm, N. Müller, C.M. Plugge, A.J. Stams, B. Schink, Syntrophy in methanogenic degradation, (Endo) symbiotic methanogenic archaea, Springer, 2010, pp. 143–173.
[53] H. Latif, A.A. Zeidan, A.T. Nielsen, K. Zengler, Trash to treasure: production of biofuels and commodity chemicals via syngas fermenting microorganisms, Curr. Opin. Biotechnol. 27 (2014) 79–87.
[54] A. Bar-Even, E. Noor, R. Milo, A survey of carbon fixation pathways through a quantitative lens, J. Exp. Bot. 63 (2012) 2325–2342.
[55] S. Manzoor, A. Schnürer, E. Bongcam-Rudloff, B. Müller, Complete genome sequence of *Methanoculleus bourgensis* strain MAB1, the syntrophic partner of mesophilic acetate-oxidising bacteria (SAOB), Standards Genom. Sci. 11 (2016) 80.
[56] L. Treu, S. Campanaro, P.G. Kougias, C. Sartori, I. Bassani, I. Angelidaki, Hydrogen-fueled microbial pathways in biogas upgrading systems revealed by genome-centric metagenomics, Front. Microbiol. 9 (2018).
[57] C. Anthony, P. Williams, The structure and mechanism of methanol dehydrogenase, Biochimica et Biophysica, Acta (BBA) – Proteins and Proteomics 1647 (2003) 18–23.
[58] R. Sapra, K. Bagramyan, M.W. Adams, A simple energy-conserving system: proton reduction coupled to proton translocation, Proc. Natl. Acad. Sci. 100 (2003) 7545–7550.
[59] D.E. Holmes, T. Ueki, H.-Y. Tang, J. Zhou, J.A. Smith, G. Chaput, D.R. Lovley, A membrane-bound cytochrome enables *Methanosarcina acetivorans* to conserve energy from extracellular electron transfer, MBio 10 (2019) e00789–00719.
[60] R.K. Thauer, A.-K. Kaster, M. Goenrich, M. Schick, T. Hiromoto, S. Shima, Hydrogenases from methanogenic archaea, nickel, a novel cofactor, and H_2 storage, Annu. Rev. Biochem. 79 (2010) 507–536.
[61] S. Hattori, Syntrophic acetate-oxidizing microbes in methanogenic environments, Microbes Environ. 23 (2008) 118–127.
[62] B. Schink, A.J. Stams, Syntrophism among prokaryotes, Prokaryotes 2 (2006) 309–335.

Supplementary Material

Effect of ammonia on anaerobic digestion of municipal solid waste: inhibitory performance, bioaugmentation and microbiome functional reconstruction

Miao Yan[a], Laura Treu[b,*], Stefano Campanaro[b,c,*], Hailin Tian[a,d], Xinyu Zhu[a], Benyamin Khoshnevisan[a,e], Panagiotis Tsapekos[a], Irini Angelidaki[a,§], Ioannis A. Fotidis[a,f,§]

[a] Department of Environmental Engineering, Technical University of Denmark, Bygningstorvet Bygning 115, DK-2800 Kgs. Lyngby, DK

[b] Department of Biology, University of Padova, Via U. Bassi 58/b, 35121 Padova, Italy

[c] CRIBI Biotechnology Center, University of Padua, 35131, Padua, Italy

[d] NUS Environmental Research Institute, National University of Singapore, 1 Create Way, 138602, Singapore

[e] Key Laboratory of Non-point Source Pollution Control, Ministry of Agriculture, Institute of Agricultural Resources and Regional Planning, Chinese Academy of Agricultural Sciences, Beijing 100081, China

[f] School of Civil Engineering Southeast University Nanjing, China 210096

[*]Corresponding authors: Laura Treu laura.treu@unipd.it, Stefano Campanaro stefano.campanaro@unipd.it

[§]equally contributing

Table of content

Table S2-S5 contain mass of data, thus they are available online

https://doi.org/10.1016/j.cej.2020.126159

Table S1 the characteristics of the cultivation medium (CM) for *M. bourgensis MS2*

***Methanoculleus bourgensis* MS2 cultivation medium (CM)**			
		Value	Unit
1	NH_4Cl	1	g
2	K_2HPO_4 x 3 H_2O	0.4	g
3	$MgCl_2$ x 6 H_2O	0.1	g
4	Na-formate	5	g
5	Na-acetate	1	g
6	Trypticase peptone (BD BBL)	1	g
7	Yeast extract (OXOID)	1	g
8	Resazurin solution (0.1% w/v)	1	ml
9	L-Cysteine-HCl x H_2O	0.5	g
10	Na_2CO_3	1.5	g
11	Na_2S x 9 H_2O	0.2	g
12	Distilled water	1000	ml

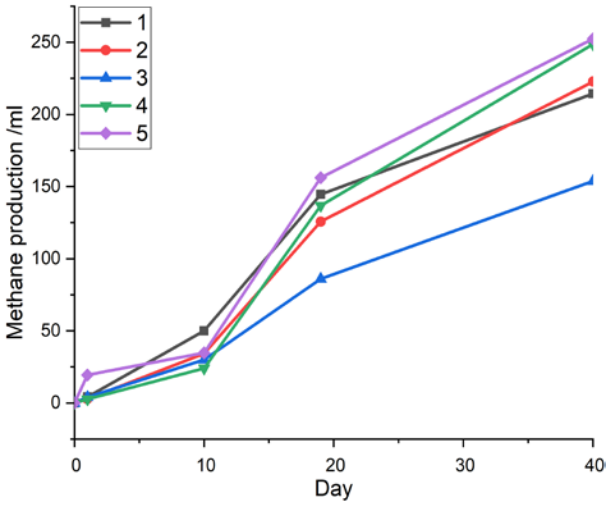

Figure S1. *M. burgensis* culture growth curve at 14 g NH_4^+-N/L.

IV

Long-term preserved and rapidly revived methanogenic cultures: Microbial dynamics and preservation mechanisms

Yan, M., Fotidis, I. A., Jéglot, A., Treu, L., Tian, H., Palomo, A., Angelidaki, I.

Journal of Cleaner Production, 2020, 121577.

https://doi.org/10.1016/j.jclepro.2020.121577

Journal of Cleaner Production 263 (2020) 121577

Contents lists available at ScienceDirect

Journal of Cleaner Production

journal homepage: www.elsevier.com/locate/jclepro

Long-term preserved and rapidly revived methanogenic cultures: Microbial dynamics and preservation mechanisms

Miao Yan [a], Ioannis A. Fotidis [a, b, *], Arnaud Jéglot [a], Laura Treu [c], Hailin Tian [a], Alejandro Palomo [a], Xinyu Zhu [a], Irini Angelidaki [a]

[a] Department of Environmental Engineering, Technical University of Denmark, Bygningstorvet Bygning 115, DK-2800, Kgs. Lyngby, Denmark
[b] School of Civil Engineering Southeast University Nanjing, 210096, China
[c] Department of Biology, University of Padova, Via U. Bassi 58/b, 35121, Padova, Italy

ARTICLE INFO

Article history:
Received 17 February 2020
Received in revised form
1 April 2020
Accepted 6 April 2020
Available online 11 April 2020

Handling Editor: H Mikulcic

Keywords:
Ammonia tolerant
Revival rate
Cell entrapment
Gel preservation
Methanosarcina soligelidi

ABSTRACT

Bioaugmentation with specialized inocula has been proven a feasible way to remediate underperforming anaerobic digestion (AD) processes. However, a major bottleneck for successful and cost-effective bioaugmentation is the lack of ready-to-use, specialized methanogenic cultures when required. The reason is the slow growth of the anaerobic consortia and the high cost of maintaining them active in the necessary amounts for successful bioaugmentation applications. This study offers an effective procedure where customized AD inocula could be preserved and used on-demand for remediation of ammonia inhibited AD reactors. Additionally, it introduces the biological and physicochemical mechanisms that render the long-term preservation of the AD inocula possible. Specifically, two different preservation carriers (i.e. agar gel and liquid basic anaerobic medium) were assessed at two different temperatures (i.e. 4 °C and 24 °C) using an ammonia tolerant methanogenic consortium. The results from methane production, lag-phase, maximum methane production rate and cell viability indicate that the consortium preserved for 168 days in agar gel at 24 °C performed best compared to the other tested preservation conditions. Meanwhile, 16S rRNA sequencing analysis indicated that *Methanosarcina soligelidi* and *Methanoculleus palmolei* shown a high revival rate and metabolic activity after long-term preservation. Thus, this successful long-term preservation method of ready-to-use AD consortia could render the successful bioaugmentation in full-scale biogas reactors economically possible in the near future.

1. Introduction

Treating organic waste in a biogas plant can reduce the disposal cost (Alibardi et al., 2017) and generate renewable energy simultaneously (Woon and Lo, 2016). The application of Anaerobic digestion (AD) complies with the policy of greenhouse gas (GHG) emission reduction and the target of increasing renewable energy production, thus plays an important role in the circular economy (Vinois, 2017). Hence, it has become economically, environmentally and socially pivotal to divert the organic waste disposal from conventional landfills and incineration towards AD. It is predicted that biomethane would account for 20% of the European indigenous energy production by the year 2020 (Gil-Carrera et al., 2019). However, the efficiency of AD process is easily affected by a lot of parameters, among which high ammonia levels are a common one when N-rich organic waste is used as feedstock (Fotidis et al., 2013).

Bioaugmentation, the addition of specific microorganisms into a biological system to achieve a specific purpose by changing the indigenous microbial community and catabolic ability, has been widely used to enhance AD efficiency (Fotidis et al., 2014). As previously reported, bioaugmentation increased methane production by more than 31.3% from ammonia-rich substrate (Tian et al., 2019c), decreased the recovery time of AD process from ammonia inhibition (Town and Dumonceaux, 2016) and accelerated the volatile fatty acids (VFA) degradation (Groboillot et al., 1994). However many archaea with specific functions are slow-growing, bioaugmentation of ready-to-use inocula is proposed as an alternative technology for successful applications to achieve increased

* Corresponding author. Department of Environmental Engineering, Technical University of Denmark, Bygningstorvet Bygning 115, DK-2800, Kgs. Lyngby, Denmark.
E-mail address: ioanf@env.dtu.dk (I.A. Fotidis).

https://doi.org/10.1016/j.jclepro.2020.121577
0959-6526/

Abbreviations

AD	Anaerobic digestion
GHG	greenhouse gas
VFA	volatile fatty acids
BA	basal anaerobic medium
TS	Total solid
VS	Volatile solid
TAN	Total ammonia
PCA	principal component analysis

methane yields (Tian et al., 2019c). For full-scale reactors, this could significantly increase efficiencies in the treatment of organic waste and yield of energy which reduce economical loss from ammonia inhibition.

To date, few bioaugmentation studies with preserved inocula have been done for digester start-up and restabilization (Massalha et al., 2015). Therefore, it is essential to explore a fast and cost-effective procedure where customized inocula could be preserved and used on-demand in underperforming AD processes.

Previous studies have evaluated inoculum preservation with mixed success via the following strategies. 1) refrigeration and freezing: Rothrock et al. (2011) proved that *Planctomycetes* strains could be successfully preserved by liquid nitrogen storage. The disadvantage of this method is the difficult and expensive transportation of large cultures stored in liquid nitrogen. 2) Freeze-drying: Castro et al. (2002) determined that the CH_4 recovery of freeze-dried inoculum in trehalose or glucose was only less than 17%, while the specific freezing parameter (protective agents, rehydration, etc.) varied from different strains, which require specific exploration and validation (Morgan et al., 2006). Likewise, Bhattad et al. (2017) evaluated the survivability of methanogenic archaea after the heat-drying preservation in ambient atmosphere, respectively, where long lag phases (>42d) were observed. 3) compare with methods above, gel or appropriate growth media was proved as a more suitable preservation strategy because it is easy to operate and efficiently keep microbial activity at low cost.

For example, Barbabietola et al. (2016) proved that the use of gel for entrapping living cells in its pores matrix significantly minimises the detrimental effects from environment. Likewise, the agar gel could work as a protective layer for microorganisms from ammonia inhibition (Banu et al., 2018). Moreover, Iacobellis and DeVay (1986) found that after 20 or 24 years of storage in medium, 90–92% of *Pseudomonas syringae* tested were still alive.

However, the ability of agar gel and the liquid medium as long-term preservation carriers for the methanogenic community has selodom been evaluated to date. Therefore, the major challenge of developing long-term preservation strategies for methanogenic archaea is to ensure that the inocula are not only easily and cost-effectively preserved, but also revived at a high proportion.

Based on previous developments, this study aims to evaluate the appropriateness of the agar gel and the liquid medium as long-term preservation carriers of ammonia-tolerant methanogenic consortia. To achieve this aim, a known ammonia-tolerant consortia cultivated with acetate (Tian et al., 2019b), was tested with different preservation strategies: two different carriers (i.e. agar gel and liquid-original cultivation media) under two different storage temperatures (4 °C and 24 °C) and seven different preservation time frames (0, 1, 7, 14, 28, 84 and 168 days). The efficiency of the different preservation strategies was evaluated using five parameters: methane production, lag-phase, maximum methane production rate, cell viability, and microbiome composition.

2. Materials and methods

2.1. The initial seed inoculum

The microbial community of the seed methanogenic consortium was analysed by (Tian et al., 2019b), where three dominant methanogenic species were found: *Methanomassiliicoccus luminyensis* (relative abundance of 17.4% to the total community) *Methanosarcina soligelidi* (12%) *Methanoculleus* sp. (0.6%).

Prior to the preservation, the consortium was cultivated with 4 g/L acetate as a carbon source in basal anaerobic medium (BA) (Angelidaki et al., 1990) according to the aforementioned study. When the methane production was close to the maximal theoretical yield (i.e. 373.33 mL CH_4/g VS), the inoculum was used in the following preservation experiments. The characteristics of inoculum are shown in Table 1.

2.2. Experimental setup

2.2.1. Preservation strategies

Four different preservation strategies (Table 2) were applied in this study with different preservation times (1, 7, 14, 28, 84 and 168 days): preservation in agar gel at 24 °C ($PSG_{(24°C)}$), preservation in agar gel at 4 °C ($PSG_{(4°C)}$), preservation in liquid at 24 °C ($PSL_{(24°C)}$) and preservation in liquid at 4 °C ($PSL_{(4°C)}$). The serum bottles with a total volume of 118 mL were used for preservation. Prior to the preservation, the bottles were rinsed with distilled water, closed with rubber stoppers and metal rings, flushed with 100% nitrogen gas for 3 min and finally autoclaved at 120 °C for 20 min. Afterward, for strategy $PSL_{(24°C)}$ and $PSL_{(4°C)}$, 5 mL methanogenic consortium cultivated in section 2.1 were directly injected into each bottle by sterilized syringe. Whereas for $PSG_{(24°C)}$ and $PSG_{(4°C)}$, besides the injected 5 mL methanogenic consortium, 2 mL prepared agar solution (10 g/L) was also injected to entrap the microorganisms when the agar solidified into the gel. The agar solution was prepared as follows: adding agar powder (Sigma-Aldrich) into BA medium and heating the mixed solution to 90 °C to dissolve the agar powder and achieve an agar concentration of 10 g/L. It must be mentioned that the injection of agar solution into the bottles only happened when the solution cooled down to around 50 °C. Afterward, all the bottles were placed at their corresponding storage temperature, i.e. 24 °C and 4 °C, according to the set preservation time. For each preservation strategy, eight bottles were preserved based on the following reactivation test experiment.

2.2.2. Revival test

At the end of each preservation period, a revival test was performed for the preserved consortium (Table 2, Fig. 1). Specifically, the above mentioned eight bottles for each preservation strategy were divided into two groups: three bottles as the negative control (without extra substrate) and five bottles for methane productivity test (with acetate as extra substrate). For the negative control group, only ammonia-adjusted BA medium was added into the

Table 1
The characteristics of the initial inoculum and the substrate.

Parameter	Inoculum	Substrate
TS (g/L)	0.08[b] ± 0.02[a]	4.00 ± 0.00
VS (g/L)	0.07[c] ±0.02	4.00 ± 0.00
TAN (g NH_4^+-N/L)	9.00	9.00
pH	8.00 ± 0.10	8.00 ± 0.10

[a] Standard deviation.
[b] TSS.
[c] VSS.

Table 2
Experimental setup.

Strategy	Preservation medium	Preservation temperature °C	Reactivation
$PSG_{(24°C)}$	5 mL Inoculum + 2 mL Agar solution	24	33 mL BA medium+ 4g HAc/L+ 9.00 g NH_4^+-N/L
$PSG_{(4°C)}$	5 mL Inoculum + 2 mL Agar solution	4	33 mL BA medium+ 4g HAc/L+ 9.00 g NH_4^+-N/L
$PSL_{(24°C)}$	5 mL Inoculum	24	35 mL BA medium+ 3.77g HAc/L + 9.0 g NH_4^+-N/L
$PSL_{(4°C)}$	5 mL Inoculum	4	35 mL BA medium+ 3.77 g HAc/L+ 9.00 g NH_4^+-N/L

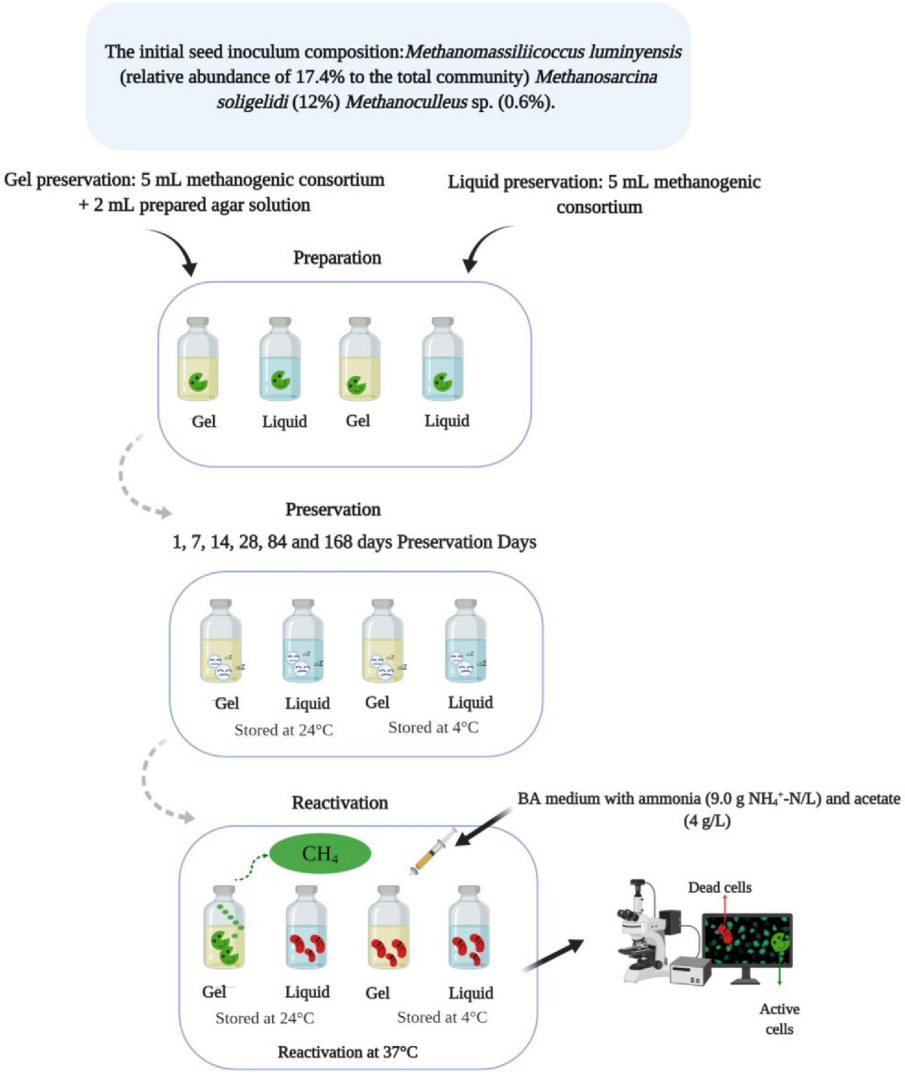

Fig. 1. Flow chart of the overall methodology.

bottles; while for the methane productivity test bottles, BA medium with ammonia and acetate adjustment was added to control the same ammonia (9.0 g NH_4^+-N/L) and acetate (4 g/L) level of all groups. As a result, all the bottles had a 40 mL working volume. Afterward, all the bottles were incubated at 37 ± 1 °C. The efficiencies of different preservation strategies were assessed by the accumulative methane production, lag-phase, maximum methane production rate, cell viability, and microbiome composition.

2.3. Analytical methods

2.3.1. Physicochemical analyses

The methane content in the headspace of batch reactors was determined using a gas chromatograph (GC Thermo Fischer scientific 1310) with a flame ionization detector. VFA concentrations were measured with gas chromatographer (TRACE 1300 from Thermo Scientific) equipped with a flame ionization detector and an FFAP (Free fatty acid phase) fused silica capillary column. The pH was measured by PHM99 LAB pH meter. The following parameters: volatile suspended solids (VSS), total suspended solids (TSS) (APHA, 2005), and total ammonia nitrogen were measured following Tian et al. (2019a).

2.3.2. Microbial analysis

2.3.2.1. Live and dead cell staining. A Live/Dead BacLight viability kit (L7012; Molecular Probes/Invitrogen, USA) was used, to stain

500 μL samples which were collected after two weeks of stationary phase. Stained samples were observed with a confocal laser scanning microscope ([CLSM] TCS SP5; Leica, Germany) equipped with an Ar laser (488 nm), with 20 × and 64 × objectives. DNA in dead and damaged bacterial or archaea cell walls/membranes were stained with red fluorescence; DNA in alive bacterial or archaea cell walls/membranes were stained with green fluorescence.

2.3.2.2. 16S rRNA gene sequencing. To decipher microbial community shift upon different preservation conditions and times, microbial samples were taken in triplicates from the bottles: 1) $PSG_{(24°C)}$-14 (inoculum preserved in gel at 24 °C for 14 days); 2) $PSL_{(24°C)}$-28 (inoculum preserved in liquid at 24 °C for 28 days); 3) $PSL_{(4°C)}$-14 (inoculum preserved in liquid at 4 °C for 14 days); 4) $PSL_{(24°C)}$-84 (inoculum preserved in liquid at 24 °C for 84 days) 5) $PSG_{(24°C)}$-168 (inoculum preserved in gel at 24 °C for 168 days).

All samples were analysed using 16S rRNA gene sequencing to elucidate the microbial diversity in response to different preservation strategies. Most importantly, the 16S rRNA gene sequencing results of the seed consortium, which the raw data can be found in (Tian et al., 2019b) and were also integrated into the discussion part. The DNA extraction was performed using the DNeasy PowerSoil Kit (QIAGEN, Germany) according to standardized procedures described in a previous study (Treu et al., 2018). The amplicon of the V4 hypervariable region amplified with universal primers (515F/806R) followed by Illumina MiSeq sequencing was performed at BMR Genomics S.r.l. (Padua, Italy). CLC Workbench software (V.8.0.2) with Microbial genomics module plugin (QIAGEN Bioinformatics, Germany) was used for reads data filtering and processing as previously described (Treu et al., 2018) The consensus sequences of the most interesting OTUs were manually checked with BLAST (16S ribosomal RNA database). Heat maps and hierarchical clustering analyses were done using Multi experiment viewer software (MeV 4.9.0). Two groups comparison *t*-test (equal variance) was chosen to evaluate the significance of changes in abundance between samples (p-value < 0.05). Statistical analysis and Beta diversity (Principal Component Analysis) were estimated using STAMP software. Meanwhile, Alpha diversity was analysed considering the number of OTUs and Chao 1 bias-corrected. PC1 and PC2 stand for principal components 1 and 2, which explain 59.9% and 21.0% of the community variation, respectively.

Raw reads were deposited in the Sequence Read Archive (SRA) database (http://www.ncbi.nlm.nih.gov/sra) with the name of SUB6374518.

2.3.3. Calculations and statistics

The accumulative methane yield of the productivity test group was calculated by subtracting the value obtained from the corresponding negative control assay. Statistical analysis and figures were conducted with the OriginLab program (OriginLab Corporation, Northampton, Massachusetts) and Microsoft Excel 2010 (Microsoft Corporation).

2.3.3.1. Maximum methane production. The theoretical biomethane potential ($B_{o,th}$, unit: CH_4 mL/g VS) of the carbon source (acetate) used in the activation experiment was calculated based on stoichiometric balance, assuming complete conversion of organic matter to CH_4 and CO_2 through Eq. (1) and Eq. (2).

$$CnHaOb + \left(n - \frac{a}{4} - \frac{b}{2}\right)H2O \rightarrow \left(\frac{n}{2} + \frac{a}{8} - \frac{b}{4}\right)CH4 + \left(\frac{n}{2} - \frac{a}{8} + \frac{b}{4}\right)CO2 \quad (1)$$

$$\mathbf{Bo,th} = \frac{\left(\frac{n}{2} + \frac{a}{8} + \frac{b}{4}\right)22.4}{12n + a + 16b} \quad (2)$$

2.3.3.2. Lag phase and methane production rate. To compare the lag phase and the methane production rate under different preservation strategies, the experimental data were fitted by the modified Gompertz model, Eq. (3) (Lü et al., 2016):

$$\mathbf{M(t)} = P^{*}\mathbf{e}\left(-\exp\left(\frac{R\,max}{P}(\lambda - t) + 1\right)\right) \quad (3)$$

where M(t) is the cumulative CH_4 production (mL CH_4/g VS) at time t; P is the maximum CH_4 potential (mL CH_4/g VS) at the end of incubation; t is the time (d); R_{max} is the maximum CH_4 production rate (mL CH_4/g VS/d); λ is the lag phase (d), and e is 2.71828.

3. Results and discussion

3.1. Revival performance

Focusing on the long preservation period, $PSG_{(24°C)}$ showed advantage compared to other preservation strategies. The results clearly showed that the $PSG_{(24°C)}$ group could produce methane even after 168 days of preservation with less than 25 days of lag-phase (Fig. 2 and Table 3). On the contrary, $PSL_{(4°C)}$, $PSL_{(24°C)}$ and $PSG_{(4°C)}$ showed no methane activity after 168 days of preservation. At the same time, the consortia entrapped in $PSL_{(24°C)}$ and $PSG_{(4°C)}$ were revived successfully after 84 days of preservation (Fig. 2). These results indicated better recovery than previous studies assessing the viability and the biosynthetic activity of entrapped methanogens in agar gel for 90 days (Flickinger, 2010).

Nevertheless, when the preservation time was less than 14 days, $PSL_{(24°C)}$ had shorter lag phases (≤18 days) and higher maximum methane production rates (ranging from 20.7 to 34.7 CH_4 mL/g VS/d) compared to $PSG_{(24°C)}$. Opposite behaviour in $PSL_{(24°C)}$ with longer lag phases (>40 days) and slower methanogenic activity (17.94 and 0.84 CH_4 mL/g VS/d with 84 and 168 days preservation, respectively) was observed when the preservation time was above 14 days at 24 °C, This finding was also confirmed by other study where immobilized methanogenic cells in gel were found to be more active after a long period (more than 30 days) than suspended cells (Yang, 2011). This phenomenon could be explained by an energy conservation theory hypothesizing that gel-immobilized cells were alive but inactive and could minimize their energy consumption during preservation, which was evidenced by the higher DNA content but lower double-stranded RNA content in gel-preserved cells compared to liquid ones (Zhu, 2007).

Surprisingly, the 4 °C preserved cultures were completely inactive after just 28 days of preservation for both gel and liquid media. Specifically, effective preservation was only achieved when preservation time was less than 14 days, where long lag phases (>54 days) were observed during reactivation (Fig. 2c and d and Table 3). Furthermore, when the preservation time exceeded 28 days both the gel and liquid preserved inocula had very low methanogenic activities (<7 CH_4 mL/g VS/day) and extremely long lag phases (>75 days) (Fig. 2c and d; Table 3).

Overall, the preservation of methanogens at 24 °C in both carriers was found to be more effective. Specifically, the liquid strategy was more applicable for short time preservation (≤14 days) compared to the gel strategy, based on the higher methane

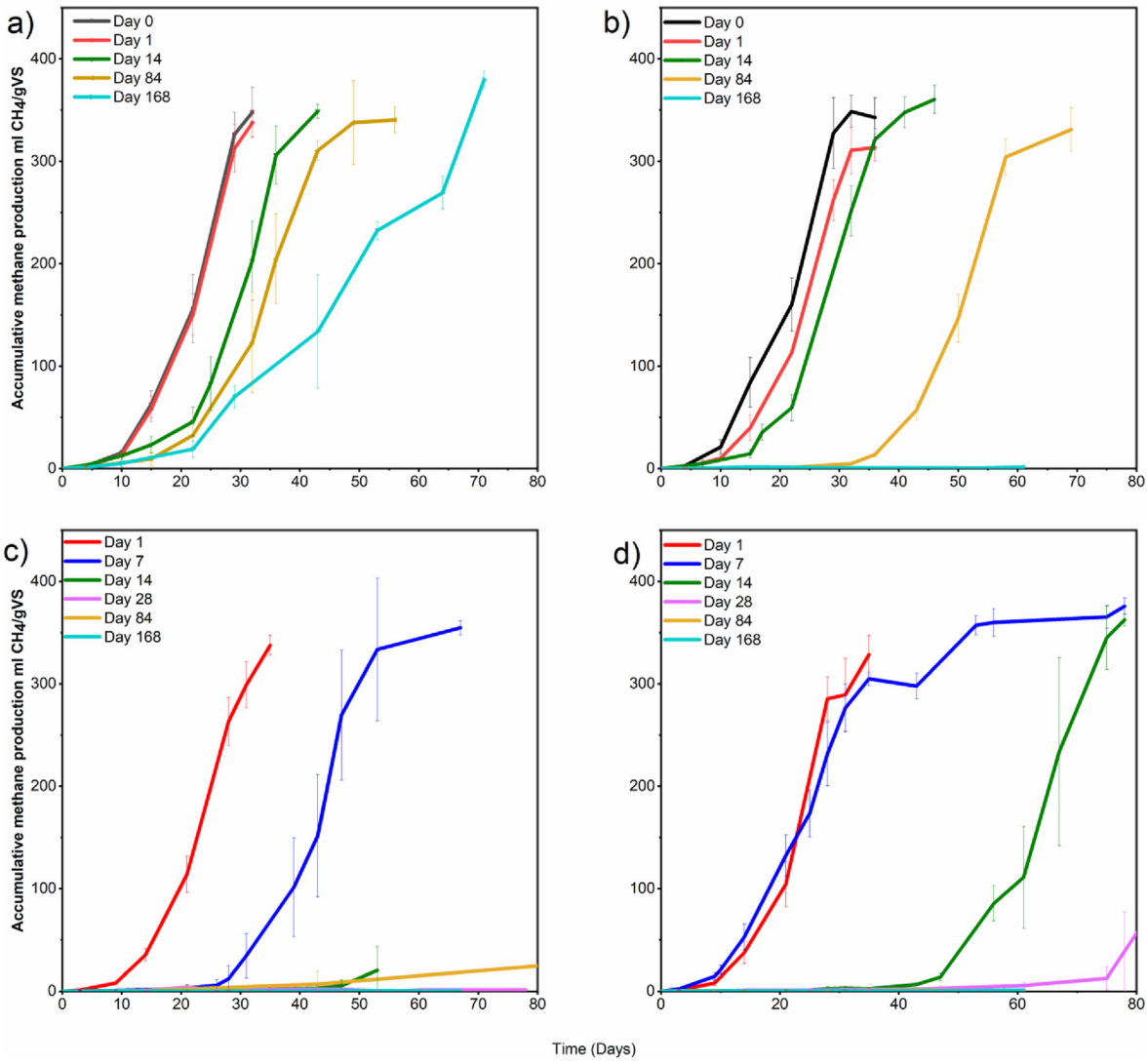

Fig. 2. Accumulative methane production of the preserved ammonia-tolerant methanogenic culture in reactivation experiment: a) $PSG_{(24°C)}$; b) $PSL_{(24°C)}$; c) $PSG_{(4°C)}$; d) $PSL_{(4°C)}$.

Table 3
Growth parameters obtained using the modified Gompertz equation for methanogenesis under different conditions.

Different conditions	Preservation time (days) days	Lag phase λ (days)	Maximum CH_4 production rate R_{max} (mL/g VS/d)	R^2
$PSG_{(24°C)}$	0	13.95 ± 1.44	23.67 ± 3.76	0.98
	1	14.07 ± 1.26	22.63 ± 3.02	0.98
	14	21.14 ± 0.89	21.40 ± 2.11	0.98
	84	24.52 ± 1.26	18.11 ± 1.95	0.99
	168	24.85 ± 3.70	8.44 ± 1.30	0.97
$PSL_{(24°C)}$	0	12.09 ± 1.50	20.67 ± 3.00	0.98
	1	18.08 ± 1.40	34.26 ± 7.60	0.97
	14	18.26 ± 0.60	21.39 ± 1.48	0.99
	84	40.79 ± 1.21	17.94 ± 2.05	0.99
	168	176.88 ± 46.41	0.84 ± 0.32	0.76
$PSG_{(4°C)}$	1	13.03 ± 0.74	19.29 ± 1.55	0.99
	7	34.92 ± 1.04	22.23 ± 2.63	0.99
	14	54.24 ± 0.31	7.87 ± 0.68	0.98
	28	381.62 ± 141.78	0.30 ± 0.13	0.35
$PSL_{(4°C)}$	1	15.56 ± 1.13	22.40 ± 2.53	0.99
	7	12.19 ± 0.56	14.15 ± 0.57	0.99
	14	57.09 ± 0.75	26.38 ± 2.50	0.99
	28	75.05 ± 0.34	6.99 ± 0.29	0.99

production rate (>20 CH_4 mL/g VS/d) or shorter lag phase (<18 days). Meanwhile, inocula were more preferable for long-term preservation (>14 days) due to the shorter lag phase (less than 25 days) upon reactivation (Table 3).

3.2. Live and dead cells

The results of the alive/dead differential staining coupled with direct microscopic examination agreed with the above reactor performance. The alive cells (preserved at 24 °C) were only observed in the gel for 168 days of preservation (Fig. 4a). As evidenced by the microscopic examination, the 168 days of liquid preserved cells were dead, which was confirmed by the absence of methane production in $PSL_{(24°C)}$-168 (Fig. 2b). On contrary, both in $PSG_{(24°C)}$-84 and $PSL_{(24°C)}$-84 similar clusters of alive cells were observed (Fig. 3a and b), which, in conjunction with the maximum CH_4 production rate of 18 mL CH_4/g VS/day, suggested that the cells retained the activity required for survival. The preservation temperature of 4 °C was proven to be not suitable for maintaining microbes' viability with only dead cells been identified in $PSG_{(4°C)}$ and $PSL_{(4°C)}$, after both 84 and 168 days of preservation (Fig. 3c, d, and Fig. 4c, d). This result was consistent with previous studies showing that at a low temperature (5 °C), after 28 days and up to 150 days of preservation, the rate of methanogenesis and methanogenic community structure could not be stimulated with the addition of acetate (Scherer et al., 1981). Overall, preservation temperature had a greater impact on microbial activity than preservation carriers, to be more specific, 24 °C was the more efficient method for long term storage of methanogenic inocula, compared to 4 °C.

3.3. Proposed mechanism of long-term preservation in gel

The reasons that allowed methanogens to be preserved in the gel for more than 168 days are still not clear and additional research is required to pinpoint the exact mechanism that contributes to successful preservation. However, based on results obtained in the current study combined with previously published researches, some potential explanations can be proposed.

Specifically, during preservation, the gel could immobilize cells (Partovinia and Rasekh, 2018), thereby preventing the motility of the cells, which decreased the energy consumption (Cassidy et al., 1996). Additionally, the composition of the gel (unbranched polysaccharide), had a potential to form a supporting structure in the cell walls that improved cell viability by slowing down the cell wall lysis process (Shen et al., 2003). Furthermore, gel polysaccharides seemed to act as an outer membrane to the cell envelope (similar to bacterial capsule) and thus created the conditions for a process similar to dormancy (Shen et al., 2003). When in dormancy, microorganisms reduce their energy consumption (Megaw and Gilmore, 2017), which allows them to maximize their long-term viability (Jones and Lennon, 2010). The slow-release mechanism that the dissolving of the gel had during the reactivation process, exposed the microbes slowly to the substrate and ammonia and thus protected them from a direct inhibitory shock (Zhu, 2007).

3.4. Microbial community analysis

3.4.1. The alpha and beta diversity of the microbial community

Alpha diversity based on Chao 1 bias-corrected index (Fig. 5a) showed similar microbial richness among the five samples analysed. The results demonstrated that the different preservation strategies were highly useful for intact microbiome preservation.

However, Beta diversity based on principal component analysis (PCA) showed a clear distinction of the microbial community under different preservation conditions (Fig. 5b). Specifically, it seems that the preservation time drove the microbiome shifting significantly. This is evidenced by the observation that the microbial community of $PSG_{(24°C)}$ −14, $PSL_{(24°C)}$ −28 and $PSL_{(24°C)}$ −84 clustered together indicating high microbial community similarity of these two groups. However, the longest matrix distances were found between $PSL_{24°C}$ −84 and $PSG_{24°C}$ −168, followed by the one between $PSL_{4°C}$ −14 and $PSG_{24°C}$ −168. Overall, preservation may change beta diversity by imposing more stringent environmental filters (Chase, 2007) and alter local evenness by favouring the group of disturbance tolerant specialists (Kimbro and Grosholz, 2006). It

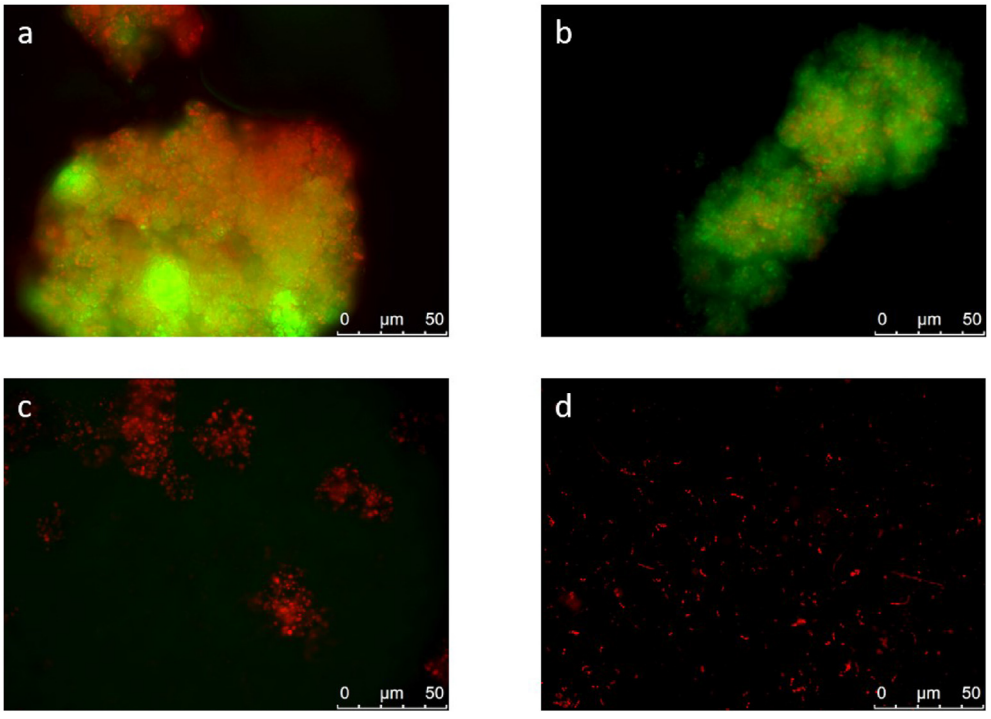

Fig. 3. Spatial distribution of microorganisms in different preservation conditions: a) $PSG_{(24°C)}$; b) $PSL_{(24°C)}$; c) $PSG_{(4°C)}$; d) $PSL_{(4°C)}$ after 84 days preservation.

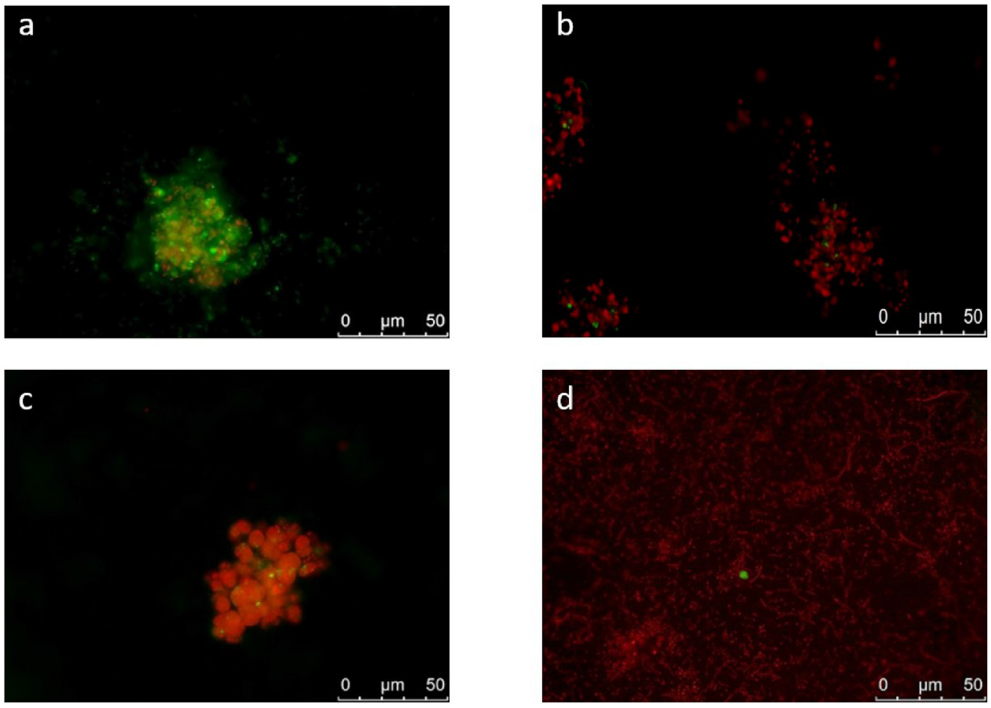

Fig. 4. Spatial distribution of microorganisms in different preservation conditions a) $PSG_{(24°C)}$; b) $PSL_{(24°C)}$; c) $PSG_{(4°C)}$; d) $PSL_{(4°C)}$ after 168 days preservation.

was clear that different preservation strategies affected more beta diversity than alpha diversity.

3.4.2. The microbial community characteristics

The microbial community of the seed methanogenic consortium had three dominant methanogens (*M. luminyensis*, *M. soligelidi* and *Methanoculleus* sp. with 17.4%, 12% and 0.6% relative abundance, respectively) (Tian et al., 2019b); after preservation and reactivation, a significant decrease of *Methanomassiliicoccus luminyensis* was observed in all samples with a relative abundance of less than 3% of the total community, suggesting a high sensitivity of *M. luminyensis* in response to the preservation process. On the contrary, *M. soligelidi* was dominant in all samples (Fig. 6), ranging from 21.6% to 33.7% of relative abundance, reflecting the versatile nature of this species (Yan et al., 2019), with the ability to adapt to a broader range of environments, compared with the more limited capabilities of *M. luminyensi* (Serrano et al., 2015). Specifically, *M. soligelidi* is known for its exceptional resistance against osmotic stress (Alawi et al., 2015), long-term freezing (Wagner et al., 2013) and starvation, which could contribute to high survival capability with the broad adaptive potential to the long-term preservation (Zhang et al., 2012). In addition, the preservation process resulted in the higher microbial relative abundance of *M. soligelidi*. It could be the competitive advantage of facilitating easier quorum sensing for regulating and coordinating microbial behaviours of the entire community via signal exchange among microbes (Waters and Bassler, 2005). Thus it would contribute to organisms to avoid, tolerate or defend themselves against the stressful environment (Miller and Bassler, 2001). Other studies also confirmed that the initial relative abundance of microorganisms played a role in the survival and preservation of microbial populations (Kim et al., 2018).

The second dominant methanogenic species was *Methanoculleus palmolei* OTU12, accounting for more than 0.3% relative abundance of total microorganisms in all samples. It is worth noting that the relative abundance of *M. palmolei* OTU12, especially

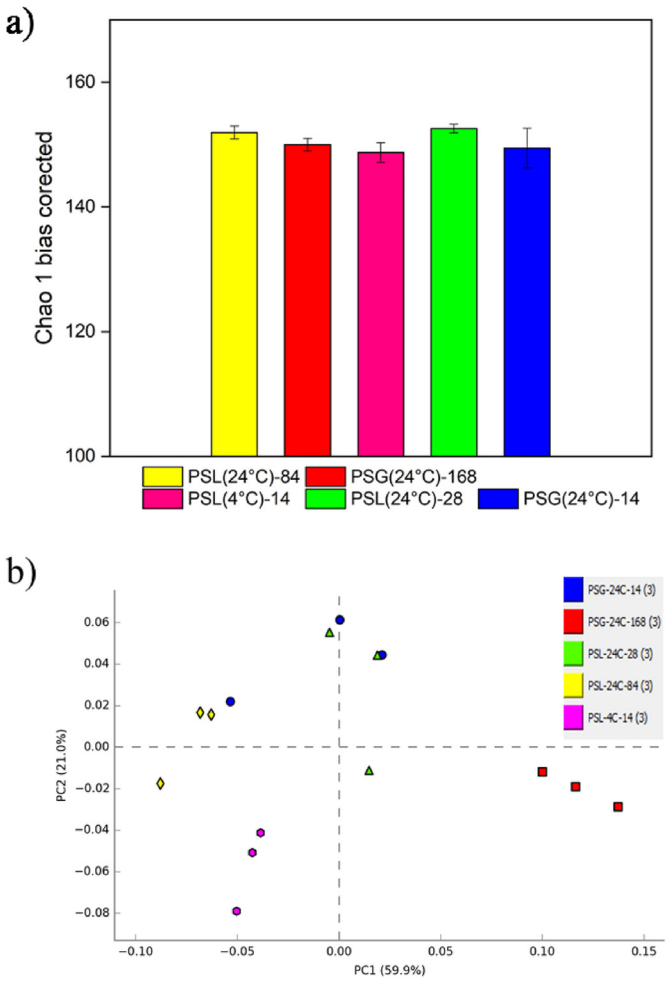

Fig. 5. Alpha Diversity a) based on Chao 1 bias-corrected index; b) Principal component analysis of the triplicate samples after preservation.

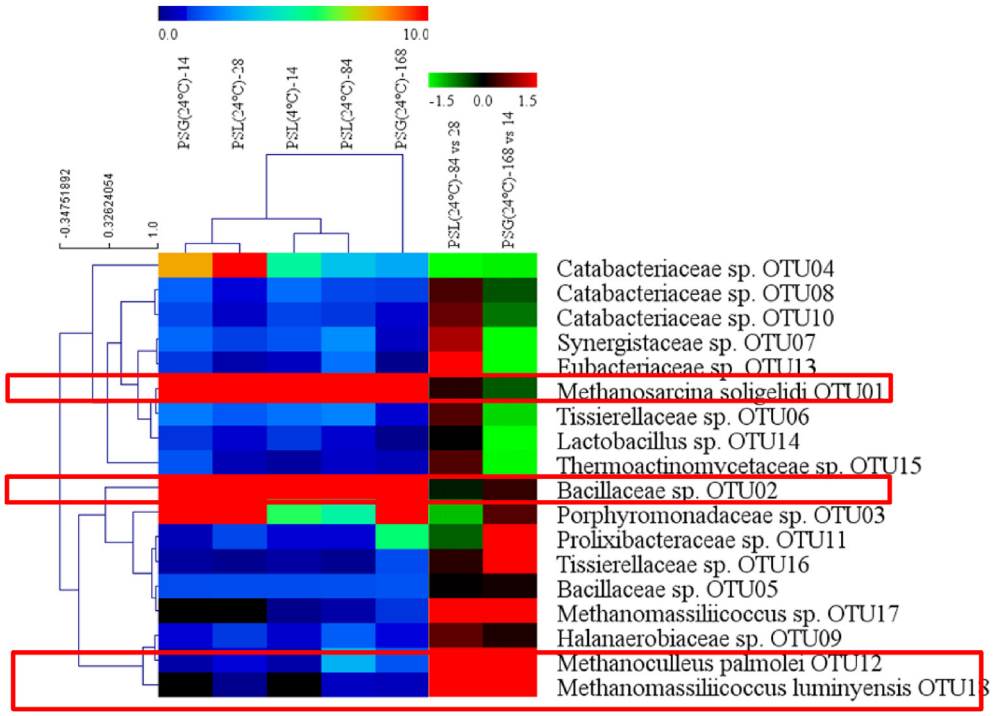

Fig. 6. Hierarchical cluster analysis of the 18 most abundant bacteria and archaea found after preservation. Values of two right columns representing the specific variation trend for each OTU were obtained calculating the fold change (log2) between the two periods.

in $PSL_{(24°C)}$-84 and $PSG_{(24°C)}$-168, was more than 4.5 fold higher ($P \leq 0.05$), than the initial relative abundance in seed consortium (0.6%), suggesting that *M. palmolei* OTU12 were resilient to long-term preservation. However, *M. palmolei* OTU12 only grown on H_2/CO_2 or sodium formate (Cheng et al., 2008). The low relative abundance around 1%–2% of *Tissierellaceae* sp. OUT06 (assigned to *Clostridium ultunense* with 95% identity), was correlated with the low abundant *M. palmolei* OTU12. It indicated the limitation of *M. palmolei* OTU12 to thrive during activation when grown on acetate (Mosbæk et al., 2016). Therefore, *M. palmolei* OTU12 possibly be abundant if it is activated by H_2 and CO_2 specific.

Bacillaceae sp. OTU02 was found to be the most dominant bacteria with around 25%–33% of relative abundance. This species was identified to be *Caldalkalibacillus thermarum* with 91% identity, which is a carbohydrate and VFA degrader commonly found in anaerobic digesters (Xue et al., 2006).

Overall, the first field evaluation of the microbial community characteristics indicated that *M. soligelidi*, *Methanoculleus* sp. and *Bacillaceae* sp. OTU02 are suitable for long-term preservation strategy, employing agar-gel carriers. The well-maintenance of functionality and viability of the consortia above promises advantages for a successful bioaugmentation process.

4. Conclusions

This study provides the first technical insight and mechanism analysis of customized methanogenic consortia preservation. The results showed that the agar gel carrier acted as a protective layer, methanogenic inocula could be efficiently preserved long-term at 24 °C. Specifically, it is successful to reactivate the preserved methanogens and maintain high methanogenic activity after 168 days of preservation. On the contrary, it was not possible to maintain high methanogenic activity and cell viability rates for more than seven days of preservation at 4 °C. *M. soligelidi* and *M. palmolei* were the most dominant methanogens after long-term preservation, indicating that they were robust enough to withstand the temperature and starvation shock. This developed process offers a successful preservation strategy of ammonia-tolerant methanogenic cultures and paves the way forward to the scaling up of full-scale reactors' start-up and bioaugmentation technologies. In the future work, the investigation is required on the response of different phases of the microorganism to different preservation approaches and optimization of original cell densities for preservation to provide high viability.

Declaration of competing interest

The authors declare that they have no known competing financial interests or personal relationships that could have appeared to influence the work reported in this paper.

CRediT authorship contribution statement

Miao Yan: Writing - original draft, Writing - review & editing, Conceptualization. **Ioannis A. Fotidis:** Writing - review & editing, Conceptualization, Funding acquisition. **Arnaud Jéglot:** Methodology, Writing - review & editing. **Laura Treu:** Writing - review & editing. **Hailin Tian:** Writing - review & editing, Conceptualization. **Alejandro Palomo:** Methodology, Writing - review & editing. **Xinyu Zhu:** Writing - review & editing. **Irini Angelidaki:** Funding acquisition.

Acknowledgements

This work was supported by Energinet.dk under the project framework ForskEL "MicrobStopNH_3-Innovative bioaugmentation strategies to tackle ammonia inhibition in anaerobic digestion process" (program no. 2015-12327). This study was financially supported by MUDP project "VARGA - VAnd Resource Genvindings Anlægget". Miao Yan would like to appreciate the financial support from China Scholarship Council.

References

Alawi, M., Shapiro, N., Woyke, T., Horn, F., Bakermans, C., Wagner, D., 2015. Genome sequence of Methanosarcina soligelidi SMA-21, isolated from Siberian permafrost-affected soil. Genome Announc. 3 (2) e00270-00215.

Alibardi, L., Green, K., Favaro, L., Vale, P., Soares, A., Cartmell, E., Fernández, Y.B., 2017. Performance and stability of sewage sludge digestion under CO2 enrichment: a pilot study. Bioresour. Technol. 245, 581–589.

Angelidaki, I., Petersen, S.P., Ahring, B.K., 1990. Effects of lipids on thermophilic anaerobic digestion and reduction of lipid inhibition upon addition of bentonite. Appl. Microbiol. Biotechnol. 33 (4), 469–472.

Apha, A., 2005. AWWA (2005) Standard Methods for the Examination of Water and Wastewater. American Public Health Association, Washington, DC.

Banu, J.R., Yukesh Kannah, R., Dinesh Kumar, M., Gunasekaran, M., Sivagurunathan, P., Park, J.-H., Kumar, G., 2018. Recent advances on biogranules formation in dark hydrogen fermentation system: mechanism of formation and microbial characteristics. Bioresour. Technol. 268, 787–796.

Barbabietola, N., Tasso, F., Alisi, C., Marconi, P., Perito, B., Pasquariello, G., Sprocati, A.R., 2016. A safe microbe-based procedure for a gentle removal of aged animal glues from ancient paper. Int. Biodeterior. Biodegrad. 109, 53–60.

Bhattad, U., Venkiteshwaran, K., Cherukuri, K., Maki, J.S., Zitomer, D.H., 2017. Activity of methanogenic biomass after heat and freeze drying in air. Environ. Sci.: Water Res. Technol. 3 (3), 462–471.

Cassidy, M.B., Lee, H., Trevors, J.T., 1996. Environmental applications of immobilized microbial cells: a review. J. Ind. Microbiol. 16 (2), 79–101.

Castro, H., Queirolo, M., Quevedo, M., Muxi, L., 2002. Preservation methods for the storage of anaerobic sludges. Biotechnol. Lett. 24 (4), 329–333.

Chase, J.M., 2007. Drought mediates the importance of stochastic community assembly. Proc. Natl. Acad. Sci. Unit. States Am. 104 (44), 17430–17434.

Cheng, L., Qiu, T.-L., Li, X., Wang, W.-D., Deng, Y., Yin, X.-B., Zhang, H., 2008. Isolation and characterization of Methanoculleus receptaculi sp. nov. from Shengli oil field, China. FEMS Microbiol. Lett. 285 (1), 65–71.

Flickinger, M.C., 2010. Encyclopedia of Industrial Biotechnology: Bioprocess, Bioseparation, and Cell Technology, vol. 7. John Wiley & Sons. Volume Set.

Fotidis, I.A., Karakashev, D., Angelidaki, I., 2013. Bioaugmentation with an acetate-oxidising consortium as a tool to tackle ammonia inhibition of anaerobic digestion. Bioresour. Technol. 146, 57–62.

Fotidis, I.A., Wang, H., Fiedel, N.R., Luo, G., Karakashev, D.B., Angelidaki, I., 2014. Bioaugmentation as a solution to increase methane production from an ammonia-rich substrate. Environ. Sci. Technol. 48 (13), 7669–7676.

Gil-Carrera, L., Browne, J.D., Kilgallon, I., Murphy, J.D., 2019. Feasibility study of an off-grid biomethane mobile solution for agri-waste. Appl. Energy 239, 471–481.

Groboillot, A., Boadi, D.K., Poncelet, D., Neufeld, R.J., 1994. Immobilization of cells for application in the food industry. Crit. Rev. Biotechnol. 14 (2), 75–107.

Iacobellis, N.S., DeVay, J.E., 1986. Long-term storage of plant-pathogenic bacteria in sterile distilled water. Appl. Environ. Microbiol. 52 (2), 388–389.

Jones, S.E., Lennon, J.T., 2010. Dormancy contributes to the maintenance of microbial diversity. Proc. Natl. Acad. Sci. Unit. States Am. 107 (13), 5881–5886.

Kim, J.-S., Chowdhury, N., Yamasaki, R., Wood, T.K., 2018. Viable but non-culturable and persistence describe the same bacterial stress state. Environ. Microbiol. 20 (6), 2038–2048.

Kimbro, D.L., Grosholz, E.D., 2006. Disturbance influences oyster community richness and evenness, but not diversity. Ecology 87 (9), 2378–2388.

Lü, F., Luo, C., Shao, L., He, P., 2016. Biochar alleviates combined stress of ammonium and acids by firstly enriching Methanosaeta and then Methanosarcina. Water Res. 90, 34–43.

Massalha, N., Brenner, A., Sheindorf, C., Sabbah, I., 2015. Application of immobilized and granular dried anaerobic biomass for stabilizing and increasing anaerobic bio-systems tolerance for high organic loads and phenol shocks. Bioresour. Technol. 197, 106–112.

Megaw, J., Gilmore, B.F., 2017. Archaeal persisters: persister cell formation as a stress response in haloferax volcanii. Front. Microbiol. 8 (1589).

Miller, M.B., Bassler, B.L., 2001. Quorum sensing in bacteria. Annu. Rev. Microbiol. 55 (1), 165–199.

Morgan, C.A., Herman, N., White, P.A., Vesey, G., 2006. Preservation of micro-organisms by drying; A review. J. Microbiol. Methods 66 (2), 183–193.

Mosbæk, F., Kjeldal, H., Mulat, D.G., Albertsen, M., Ward, A.J., Feilberg, A., Nielsen, J.L., 2016. Identification of syntrophic acetate-oxidizing bacteria in anaerobic digesters by combined protein-based stable isotope probing and metagenomics. ISME J. 10 (10), 2405–2418.

Partovinia, A., Rasekh, B., 2018. Review of the immobilized microbial cell systems for bioremediation of petroleum hydrocarbons polluted environments. Crit. Rev. Environ. Sci. Technol. 48 (1), 1–38.

Rothrock, M.J., Vanotti, M.B., Szögi, A.A., Gonzalez, M.C.G., Fujii, T., 2011. Long-term preservation of anammox bacteria. Appl. Microbiol. Biotechnol. 92 (1), 147.

Scherer, P., Kluge, M., Klein, J., Sahm, H., 1981. Immobilization of the methanogenic bacterium Methanosarcina barkeri. Biotechnol. Bioeng. 23 (5), 1057–1065.

Serrano, P., Hermelink, A., Lasch, P., de Vera, J.-P., König, N., Burckhardt, O., Wagner, D., 2015. Confocal Raman microspectroscopy reveals a convergence of the chemical composition in methanogenic archaea from a Siberian permafrost-affected soil. FEMS (Fed. Eur. Microbiol. Soc.) Microbiol. Ecol. 91 (12).

Shen, H.-Y., Moonjai, N., Verstrepen, K., Delvaux, F., 2003. Impact of attachment immobilization on yeast physiology and fermentation performance. J. Am. Soc. Brew. Chem. 61 (2), 79–87.

Tian, H., Mancini, E., Treu, L., Angelidaki, I., Fotidis, I.A., 2019a. Bioaugmentation strategy for overcoming ammonia inhibition during biomethanation of a protein-rich substrate. Chemosphere 231, 415–422.

Tian, H., Treu, L., Konstantopoulos, K., Fotidis, I.A., Angelidaki, I., 2019b. 16s rRNA gene sequencing and radioisotopic analysis reveal the composition of ammonia acclimatized methanogenic consortia. Bioresour. Technol. 272, 54–62.

Tian, H., Yan, M., Treu, L., Angelidaki, I., Fotidis, I.A., 2019c. Hydrogenotrophic Methanogens Are the Key for a Successful Bioaugmentation to Alleviate Ammonia Inhibition in Thermophilic Anaerobic Digesters. Bioresource technology, 122070.

Town, J.R., Dumonceaux, T.J., 2016. Laboratory-scale bioaugmentation relieves acetate accumulation and stimulates methane production in stalled anaerobic digesters. Appl. Microbiol. Biotechnol. 100 (2), 1009–1017.

Treu, L., Kougias, P., de Diego-Díaz, B., Campanaro, S., Bassani, I., Fernández-Rodríguez, J., Angelidaki, I., 2018. Two-year microbial adaptation during hydrogen-mediated biogas upgrading process in a serial reactor configuration. Bioresour. Technol. 264, 140–147.

Vinois, J.-A., 2017. The Road to Energy Union. Springer, Energy Union, pp. 27–50.

Wagner, D., Schirmack, J., Ganzert, L., Morozova, D., Mangelsdorf, K., 2013. Methanosarcinasoligelidi sp. nov., a desiccation-and freeze-thaw-resistant methanogenic archaeon from a Siberian permafrost-affected soil. Int. J. Syst. Evol. Microbiol. 63 (8), 2986–2991.

Waters, C.M., Bassler, B.L., 2005. Quorum sensing: cell-to-cell communication in bacteria. Annu. Rev. Cell Dev. Biol. 21 (1), 319–346.

Woon, K.S., Lo, I.M.C., 2016. A proposed framework of food waste collection and recycling for renewable biogas fuel production in Hong Kong. Waste Manag. 47, 3–10.

Xue, Y., Zhang, X., Zhou, C., Zhao, Y., Cowan, D.A., Heaphy, S., Grant, W.D., Jones, B.E., Ventosa, A., Ma, Y., 2006. Caldalkalibacillus thermarum gen. nov., sp. nov., a novel alkalithermophilic bacterium from a hot spring in China. Int. J. Syst. Evol. Microbiol. 56 (6), 1217–1221.

Yan, M., Fotidis, I.A., Tian, H., Khoshnevisan, B., Treu, L., Tsapekos, P., Angelidaki, I., 2019. Acclimatization contributes to stable anaerobic digestion of organic fraction of municipal solid waste under extreme ammonia levels: focusing on microbial community dynamics. Bioresour. Technol. 286, 121376.

Yang, S.-T., 2011. Bioprocessing for Value-Added Products from Renewable Resources: New Technologies and Applications. Elsevier.

Zhang, G., Zhang, F., Ding, G., Li, J., Guo, X., Zhu, J., Zhou, L., Cai, S., Liu, X., Luo, Y., Zhang, G., Shi, W., Dong, X., 2012. Acyl homoserine lactone-based quorum sensing in a methanogenic archaeon. ISME J. 6, 1336.

Zhu, Y., 2007. Chapter 14 - immobilized cell fermentation for production of chemicals and fuels. In: Yang, S.-T. (Ed.), Bioprocessing for Value-Added Products from Renewable Resources. Elsevier, Amsterdam, pp. 373–396.

The Department of Environmental Engineering (DTU Environment) conducts science based engineering research within five sections: Air, Land & Water Resources, Urban Water Systems, Water Technology, Residual Resource Engineering, Environmental Fate and Effect of Chemicals. The department dates back to 1865, when Ludvig August Colding gave the first lecture on sanitary engineering.

Department of Environmental Engineering

Bygningstorvet, Building 115
2800 Kgs. Lyngby
Tel. +45 4525 1600
Fax +45 4593 2850

www.env.dtu.dk